Effect of the interface geometry on the structural integrity of the ceramic crown-tooth complex

Academic Unit of Restorative Dentistry

School of Clinical Dentistry

The University of Sheffield

A PhD thesis submitted by

Raad Al Marza

February 2015

Dedication

I would like to dedicate this work to **my parents** who have meant and continue to mean so much to me.

A special feeling of gratitude to my lovely wife **Soolav** for her endless love, support and encouragement.

……..Thanks Soolav to be in my live.

To whom I am greatly in debt, my lovely children **Saif, Ahmed** & **Yara** who without their incredible patience, this thesis might not have been written.

Yara, you have been always asking “close the computer and let’s play daddy" …. Im coming back so let’s start our life again honey.

Acknowledgments

I would like to express my sincere gratitude to my supervisor, **Professor Nicolas Martin** for his unwavering support, dedicated guidance and precious time he provided. It was because his guidance that I could bring this project to its present form.

I would like to thank my co-supervisors: **Dr. Shirin Shahrbaf** and **Dr. Elaheh Ghassemieh** for their advice and support throughout this project. Special thanks for **Professor Richard van Noort** for the valuable recommendations in this project.

Many special thanks to my wife, **Dr. Soolav Ahmad** for her advice in the statistical analysis and the thesis formatting.

I would also acknowledge the help and the support of **Dr. Robert Moorehead** throughout my project from the begging till the last day. I would also like to thank **Mr. Karl Deakin** for his help in my practical work. I would like to acknowledge **Dr. Les Coulton** for his help and for training me on Micro CT Scan. Thanks for **Dr. Duncan Wood** for his help in the laboratory work. Thanks for **(Materialise Co., Ltd)** for providing us with the Mimics software licence throughout this project's work. Many thanks to the following manufacturers: **3M ESPE, Ivoclar/Vivadent** for the donation of e.max blocks, ingots and the Variolink II resin cement used in this study.

I would like to thank my siblings, and especially my brother **Ahmed Al-Marza** for helping me to fulfil my continuous commitments in Iraq.

Finally, I would like to thank all my friends and staff in the Academic Unit of Restorative Dentistry for being so friendly and helpful.

Table of contents

1 Introduction 1

1.1 Research questions 9

2 Literature review 11

2.1 The need for tooth restoration 11

2.2 Materials and technique of tooth restoration 12

2.3 Stress distribution 16

2.3.1 Nature of stress distribution in sound tooth structures 16

2.3.2 Nature of stress distribution in the restored tooth structures 18

2.3.3 Role of the cement interface on the stress distribution in restored tooth 21

2.4 Effect of a dental restoration on the tooth structures 23

2.4.1 The effect of the inlay (intra-coronal restoration) on the tooth 23

2.4.2 The effect of the onlay (extra coronal restoration) on the tooth 26

2.5 Physical and mechanical properties of the materials 27

2.6 Terms of physical properties 27

2.6.1 Force: 27

2.6.2 Stress: 27

2.6.3 Strain 28

2.6.4 Fracture 28
2.6.5 Strength 28
2.6.6 Fracture Strength 29
2.6.7 Stiffness 29
2.6.8 Toughness 29
2.6.9 Fracture toughness 29
2.6.10 Crack 29
2.6.11 Compressive strength 30
2.6.12 Yield strength 30
2.6.13 Ultimate strength 30
2.6.14 Fatigue 31
2.6.15 Fatigue limit 31
2.6.16 Fatigue life 31
2.6.17 Brittle fracture 31
2.6.18 Ductile fracture 32
2.6.19 Elastic Modulus 32
2.7 Performance of the tooth-ceramic-crown system 33
2.7.1 Tooth 33
2.7.2 Interface 37

2.7.3 Ceramics.....59

2.7.4 CAD/CAM in dentistry.....75

2.7.5 Development of CEREC machines.....76

2.7.6 Single (monolithic) and Bi-layer (two-layer) All-ceramic crown...78

2.8 Technical fabrication parameters.....82

2.8.1 Capture of the preparation.....82

2.8.2 Physical: (conventional impression).....82

2.8.3 Optical: (the effect of the scanning powder).....83

2.8.4 Configuration of the spacer.....83

2.8.5 Fabrication of the crown.....85

2.9 Performance of Ceramic systems.....86

2.9.1 Failure of ceramics.....86

2.10 Structural integrity.....90

2.10.1 Conventional full coverage crown restoration of the posterior teeth…….....…….93

2.11 Fracture mechanics of dental ceramic structure.....97

2.12 Fractography of the dental ceramic.....103

2.13 Types of experiments for measuring stress distribution.....105

2.13.1 Mechanical destructive testing approach.....106

2.14 Computational non-destructive test approach 115

2.14.1 Aspects of FEA 120

2.14.2 Types of structural FE analysis (linear and nonlinear analysis) 128

2.14.3 Types of FEA stress 130

3 Aims& objectives 133

3.1 Aims of the study 133

3.2 Objectives 133

3.3 Hypothesis 134

4 Generation of a digital model of the restored tooth 136

4.1 Introduction 136

4.2 Aim 138

4.3 Objectives 138

4.4 Null Hypothesis 139

4.5 Materials and method 139

4.5.1 Physical model creation 139

4.5.2 Digital scanning of the Physical model 140

4.5.3 3D Modelling 141

4.5.4 Modelling PDL and Bone with FreeForm® haptic technology 147

4.6 Discussion 155

4.7 Conclusion 158

5 Interface measurement 160

5.1 Introduction 160

5.2 Aims 164

5.3 Objectives 165

5.4 The hypothesis 166

5.5 Materials and method 166

5.5.1 Developing the novel technique for interface measurement 166

5.5.2 Influence of Barium Sulphate on the viscosity of the cement 166

5.5.3 3D Model creation 168

5.5.4 Validation of the measurement technique 176

5.5.5 Development of a new technique for creating a uniform thickness interface for pressed ceramic crowns 180

5.5.6 Measurement of the crown-tooth interface width. 182

5.6 Results 197

5.6.1 Viscosity of cement with the addition of Barium Sulphate (BaSO4)… 197

5.6.2 Validation of the measuring technique 198

5.6.3 Evaluation of the cement interface geometry: I - Mesio-distal 199

5.6.4 Evaluation of the cement interface geometry: II- Bucco-lingual……203

5.7 Discussion.....207

5.8 Conclusions 215

6 SEM evaluation 218

6.1 Introduction 218

6.2 Aims 222

6.3 Objectives.....222

6.4 The hypothesis.....222

6.5 Materials and method 222

6.5.1 Specimen creation.....222

6.5.2 Samples scan by Scanning Electron Microscope [SEM].....224

6.6 Results 224

6.6.1 Non-etched Pressed and Machined lithium disilicate crowns 224

6.6.2 Etched Pressed and Machined lithium disilicate crowns.....233

6.7 Discussion.....242

6.8 CONCLUSION 246

7 FEA of real VS virtual.....248

7.1 Introduction 248

7.2 Aim 250
7.3 Objectives 250
7.4 Null Hypothesis 250
7.5 Materials & Methods 251
7.5.1 3D model generation of the tooth-restoration complex 252
7.5.2 Sample selection and model preparation 252
7.5.3 3D model and FEA model generation 253
7.5.4 Generation of a 3D component of a uniform cement interface 259
7.5.5 Material properties 260
7.5.6 Boundary condition and load application 262
7.5.7 Convergence test analysis 264
7.6 Results 265
7.7 Discussion 272
7.8 Conclusions 280
8 Mechanical fatigue testing 282
8.1 Introduction 282
8.2 Aims 286
8.3 Objectives: 286
8.4 Null hypothesis 287

8.5 Materials and method 288
8.5.1 Sample preparation 288
8.5.2 Periodontal Ligament (PDL) simulation and samples mounting ..291
8.5.3 Mounting the specimen in the fatigue testing machine 296
8.5.4 Load cell calibration..... 299
8.5.5 Fatigue limit experiment 302
8.5.6 Fatigue life experiment 303
8.5.7 Fracture mode..... 303
8.6 Results 304
8.6.1 Fatigue strength..... 304
8.6.2 Fracture mode analysis..... 311
8.7 Discussion..... 315
8.8 Conclusions 322
9 FEA of Pressed VS Machined crown 325
9.1 Introduction 325
9.2 Aim..... 329
9.3 Objective..... 329
9.4 Null hypothesis..... 329
9.5 Materials and methods..... 330

9.5.1 Physical model creation 330

9.5.2 Digitizing the Physical Model 331

9.5.3 3D FEA model creation 331

9.5.4 Materials properties.....332

9.5.5 Boundary condition and load application 333

9.5.6 Convergence analysis.....334

9.6 Results 336

9.6.1 The stress values in the (thin and uniform interface) model 336

9.6.2 The stress values in the machined (thick and non-uniform interface) model….....344

9.7 Discussion.....354

9.8 Conclusions 360

10 General discussion 362

11 General Conclusions.....380

11.1 Clinical Relevance.....382

12 Further studies.....384

13 References.....388

List of the abbreviations

Abbreviations	Meaning
2D	Two-dimension
3D	Three-dimension
%	Percentage
α	Alpha
β	Beta
µA	Micro Ampere
µm	Micrometer
°C	Celsius scale for temperature measurements
ANOVA	Analysis of variance
CAD/CAM	Computer Aided Design/Computer Aided Manufacturing
CT	Computerized Tomography
Micro-CT	Micro Computerized Tomography
E	Elastic modulus
F	Force
FEA	Finite Element Analysis
FPD	Fixed partial denture
GB	Giga bite
GPa	Giga Pascal
Kg	Kilogram
Kv	Kilovolt
max	Maximum
mini	Minimum
Mimics	Materialise Interactive Medical Image Control System
mm	Millimetre
MRI	Magnetic Resonance Image
N	Newton
PDL	Periodontal ligament
SD	Standard deviation
SEM	Scanning Electron Microscopy
STL	Standard Triangle Language (Stereolithography file)
W	Watt

List of Tables

Table 2-1: Evolution of the CEREC system(Mörmann, 2006) 77

Table 2-2: Suitable ceramic materials for use with CAD/CAM System.....81

Table 5-1: Preparation guidelines (adapted from Ivoclar/Vivadent website)...169

Table 5-2: Set up parameters of the micro CT scanner 171

Table 5-3: Measurement point abbreviation.....175

Table 5-4: Dependent and independent variables tested in this experiment 183

Table 5-5: Nomenclature of the experiment.....186

Table 5-6: Flowability of Variolink II with and without BaSO4 (Paired Samples Test).....197

Table 5-7: Mean values of cement thickness at each measured point cross the all the planes measured in mesio-distal direction [the measurement in µm]. 199

Table 5-8: The Minimum, Maximum and SD of the cement thickness for all samples in mesio-distal direction [in µm] 201

Table 5-9: ANOVA test to compare the thickness of the cement for all the groups in a mesio-distal direction.....202

Table 5-10: POST HOC test for comparing a pair of means between groups in mesio-distal direction.....202

Table 5-11: Mean values of cement thickness at each measured point cross the all planes measured in bucco-lingual direction [the measurement in µm].....203

Table 5-12: The Minimum, Maximum and SD of the cement thickness for all samples in a bucco-lingual direction [in µm] 205

Table 5-13: ANOVA test to compare the thickness of the cement for all the groups in a bucco-lingual direction.....206
Table 5-14: POST HOC test for comparing a pair of means between groups in bucco-lingual direction 206
Table 7-1: Materials properties according to the original study (Shahrbaf et al., 2013) 261
Table 7-2: The peak values of von-Mises stress (MPa) for each component for the modified (uniform cement interface) and original (non-uniform cement interface) models.....266
Table 7-3: The peak values of maximum principal stress (MPa) for each component for the modified(uniform cement interface) and original (non-uniform cement interface) models 270
Table 8-1: Physical properties of IPS e.max® Press and CAD ceramic [the data collected from Ivoclar/Vivadent websites].....291
Table 8-2: Load calibration.....301
Table 8-3: Burke's classification of codes of fracture 304
Table 8-4: The maximum and average of the survived cycles for all the groups 309
Table 8-5: ANOVA test for all the groups comparing the survival cycles 309
Table 8-6: Mode of fracture in the group samples.....311
Table 8-7: Kruskal-Wallis Test showing the mean rank of fracture mode for each group 313

Table 8-8: Kruskal Wallis test for the fracture mode for each group of samples 314
Table 9-1: Modulus of elasticity and Poisson's ratio of the materials 333
Table 9-2: Final number of elements and nodes in both models 335
Table 9-3: The peak values of von-Mises stress for the (thin and uniform interface) model 336
Table 9-4: The peak values of the maximum principal stress for the tooth restored with the (thin and uniform interface) crown 337
Table 9-5: The peak values of von-Mises stress for the tooth restored with the (thick and non-uniform interface) crown 344
Table 9-6: The peak values of the maximum principal stress for the tooth restored with the (thick and non-uniform interface) crown 345
Table 9-7: The peak values of von Mises stress for both models.....348
Table 9-8: The peak values of maximum principal stress for both models.....349

List of Figures

Figure 2-1: Types of stress.....28

Figure 2-2: Crack modes.....30

Figure 2-3: Flexural strength of the ceramic 68

Figure 2-4: Ceramic crack types 101

Figure 2-5: S-N curve [Wohler's curve].....111

Figure 2-6: Step stress testing profiles.....114

Figure 4-1: CTAn for pictures cropping (N Recon) 141

Figure 4-2: Identifying the image orientations of the planes.....142

Figure 4-3: Mimics default view: 142

Figure 4-4: Thresholding option 144

Figure 4-5: Masks generation 145

Figure 4-6: 3D calculation of the lute interface component 147

Figure 4-7: 3D calculation of the tooth component.....147

Figure 4-8: Import of STL files in FreeForm® 148

Figure 4-9: Offset step for generation of PDL-[A] original, [B] offset.....149

Figure 4-10: Drawing curved line to fit it on the surface 150

Figure 4-11: Generating the PDL by removing the coronal part of the offset .151

Figure 4-12: Perfect adaption of the PDL to the Tooth objects.....152

Figure 4-13: Automatic cube clay for bone simulation 153

Figure 4-14: Optimum adaption between the Bone-PDL-Tooth.....154

Figure 5-1: The cement interface before and after using Barium Sulphate.....167

Figure 5-2: Illustration of maximum tooth preparation.....168

Figure 5-3: Sky scan micro-CT scanner.....172

Figure 5-4: Mimics® default view and the standardise technique for cross-sections determination (novel technique).....174

Figure 5-5: Determination of Measurement Points.....174

Figure 5-6: Measuring same point in 2D and 3D.....175

Figure 5-7: The ceramic disk specimen.....176

Figure 5-8: Mimics measurement.....176

Figure 5-9: Laser micrometer assembly.....178

Figure 5-10: Laser beams scanning the ceramic disc.....178

Figure 5-11: Laser micrometer measurement.....179

Figure 5-12: Vacuum formed Isofolan® on die (A) and following removal from die (B). Biostar vacuum forming machine (C).....181

Figure 5-13: Experimental method steps for measuring the interface.....182

Figure 5-14: The experimental groups [n=3 crowns per group].....185

Figure 5-15: 3D wax printer.....189

Figure 5-16: CEREC InLab CAD/CAM machine.....191

Figure 5-17: Cementation technique by universal testing machine.....193

Figure 5-18: Alignment of the sample in the Micro CT scanner.....194

Figure 5-19: Replacing the sample in the mounting base.....194

Figure 5-20: Representative Mimics view for each group.....196

Figure 5-21: Flowability of Variolink II resin cement with and without $BaSO_4$ 197

Figure 5-22: Mean values of cement thickness for the samples' groups at all planes measured in mesio-distal direction [the measurement in µm]. 200

Figure 5-23: Mean values of cement thickness for the samples' groups at all planes measured in bucco-lingual-direction [the measurement in µm].....204

Figure 6-1: IPS e.max® CAD block.....223

Figure 6-2: IPS e.max® Press ingot.....223

Figure 6-3: SEM of e.max® pressed non-etched at 300x.....225

Figure 6-4: SEM of e.max® machined non-etched at 300x.....225

Figure 6-5: SEM of e.max® pressed non-etched at 600x.....226

Figure 6-6: SEM of e.max® machined non-etched at 600x.....226

Figure 6-7: SEM of e.max® pressed non-etched at 1200x.....227

Figure 6-8: SEM of e.max® machined non-etched at 1200x.....227

Figure 6-9: SEM of e.max® pressed non-etched at 2400x.....228

Figure 6-10: SEM of e.max® machined non-etched at 2400x.....228

Figure 6-11: SEM of e.max® pressed non-etched at 5000x.....229

Figure 6-12: SEM of e.max® machined non-etched at 5000x.....229

Figure 6-13: SEM of e.max® pressed non-etched at 10000x.....230

Figure 6-14: SEM of e.max® machined non-etched at10000x.....230

Figure 6-15: SEM of e.max® pressed non-etched at 20000x.....231

Figure 6-16: SEM of e.max® machined non-etched at 20000x.....231

Figure 6-17: SEM of e.max® pressed non-etched at 40000x 232
Figure 6-18: SEM of e.max® machined non-etched at 40000x 232
Figure 6-19: SEM of the etched e.max® pressed at 300x 234
Figure 6-20: SEM of the etched e.max® machined at 300x 234
Figure 6-21: SEM of etched e.max® pressed at 600x 235
Figure 6-22: SEM of etched e.max® machined at 600x 235
Figure 6-23: SEM of etched e.max® pressed at 1200x 236
Figure 6-24: SEM of etched e.max® machined at 1200x 236
Figure 6-25: SEM of etched e.max® pressed at 2400x 237
Figure 6-26: SEM of etched e.max® machined at 2400x 237
Figure 6-27: SEM of etched e.max® pressed at 5000x 238
Figure 6-28: SEM of etched e.max® machined at 5000x 238
Figure 6-29: SEM of etched e.max® pressed at 10000x 239
Figure 6-30: SEM of etched e.max® machined at 10000x 239
Figure 6-31: SEM of etched e.max® pressed at 20000x 240
Figure 6-32: SEM of etched e.max® machined at 20000x 240
Figure 6-33: SEM of etched e.max® pressed at 40000x 241
Figure 6-34: SEM of etched e.max® machined at 40000x 241
Figure 7-1: Flaw chart of the experiment steps 251
Figure 7-2: 3D volume mesh of the ceramic crown component 255
Figure 7-3: 3D volume mesh of the cement interface component 256
Figure 7-4: 3D volume mesh of tooth component.....256

Figure 7-5: 3D volume mesh of pulp component 257
Figure 7-6: 3D volume mesh of PDL component.....257
Figure 7-7: 3D volume mesh of cancellous bone component 258
Figure 7-8: 3D volume mesh of cortical bone component 258
Figure 7-9: Uniform VS non-uniform cement interface.....259
Figure 7-10: Boundary condition.....262
Figure 7-11: Load application on the two points of the crown.....263
Figure 7-12: load of 150N in each point to be 300N in total.....264
Figure 7-13: The peak values of von-Mises stress in each component for the non-uniform VS. Uniform interface models.....266
Figure 7-14: von-Mises stress pattern in the crown of the modified model.....267
Figure 7-15: von-Mises stress pattern in the cement of the modified model ...267
Figure 7-16: von-Mises stress pattern in the dentine of the modified model ...267
Figure 7-17: von-Mises stress pattern in the PDL of the modified model 268
Figure 7-18: von-Mises stress pattern in the Spongy bone of the modified model 268
Figure 7-19: von-Mises stress pattern in the Trabecular Bone of the modified model.....268
Figure 7-20: von-Mises stress pattern in the cement of the original model 269
Figure 7-21: von-Mises stress pattern in the crown of the original model.....269
Figure 7-22: von-Mises stress pattern in the PDL of the original model 269
Figure 7-23: von-Mises stress pattern in the dentine of the original model.....269

Figure 7-24: von-Mises stress pattern in the Trabecular Bone of the original model.....269
Figure 7-25: von-Mises stress pattern in the Spongy bone of the original model 269
Figure 7-26: The peak values of maximum principal stress in each component for the non-uniform VS. uniform interface models. 271
Figure 8-1: Mean (3D) and SD cement thickness of the test groups.....290
Figure 8-2: Alignment of the tooth in the dental surveyor 293
Figure 8-3: Covering the coronal part of the sample by the Dublisil 15 A and B material.....293
Figure 8-4: the metal base cylinder covered the root of the sample.....294
Figure 8-5: the mould of the ideal alignment of the samples 294
Figure 8-6: Actual sample in the base.....295
Figure 8-7: PDL simulation (tooth crown embedded in acrylic for this specimen to facilitate sectioning that enables visualisation of the tooth and PDL in cross-section) 296
Figure 8-8: Indenter design.....297
Figure 8-9: Fatigue machine tester 298
Figure 8-10: Diagrammatic representation of the occlusal contact points of the indenter on the tooth surface. 299
Figure 8-11: Load weight disc of 0.5 Kg.....300
Figure 8-12: Force sensor device.....300

Figure 8-13: Staircase for fatigue limit of CAD/CAD specimens.....302
Figure 8-15: The relation of β to α parameter in Weibull analysis 307
Figure 8-16: Weibull probability plot of the all the groups at 453N load.....307
Figure 8-17: Weibull maximum likelihood comparison of the all the groups .308
Figure 8-18: Number of cycles at failure (column refer to different specimen) 308
Figure 8-19: The mean values and SD of the survived cycles for all the groups 310
Figure 8-20: Fracture code 2.....312
Figure 8-21: Fracture code 3.....312
Figure 8-22: Fracture code 4.....312
Figure 9-1: Load application to the occlusal surface of the crown-tooth complex 334
Figure 9-2: The peak values of von-Mises stress for the tooth restored with the thin and uniform interface crown.....337
Figure 9-3: The peak values of the maximum principal stress for the tooth restored with the (thin and uniform interface) crown. 338
Figure 9-4: The peak values of von-Mises and the maximum principal stress for the tooth restored with the (thin and uniform interface) crown.....339
Figure 9-5: Max principal stress pattern in the crown of the (thin and uniform interface) model 340

Figure 9-6: Max principal stress pattern in the cement of the (thin and uniform interface) model 340
Figure 9-7: Max principal stress pattern in the dentin of the (thin and uniform interface) model 341
Figure 9-8: Max principal stress pattern in the PDL of the (thin and uniform interface) model 341
Figure 9-9: von Mises stress pattern in the crown of the (thin and uniform interface) model 342
Figure 9-10 : von Mises stress pattern in the cement of the (thin and uniform interface) model 342
Figure 9-11: von Mises stress pattern in the dentine of the (thin and uniform interface) model 343
Figure 9-12: von Mises stress pattern in the PDL of the (thin and uniform interface) model 343
Figure 9-13: The peak values of von-Mises stress for the tooth restored with the (thick and non-uniform interface) crown.....345
Figure 9-14: The peak values of the maximum principal stress for the tooth restored with the (thick and non-uniform interface) crown.....346
Figure 9-15: The peak values of von-Mises and the maximum principal stress for the tooth restored with the (thick and non-uniform interface) crown.....347
Figure 9-16: The peak values of von-Mises stress in the all components of both models 348

Figure 9-17: The peak values of the maximum principal stress in the all components of both models 349
Figure 9-18: Max principal stress pattern in the crown of the (thick and non-uniform interface) model 350
Figure 9-19: Max principal stress pattern in the cement of the (thick and non-uniform interface) model 350
Figure 9-20: Max principal stress pattern in the dentine of the (thick and non-uniform interface) model 351
Figure 9-21: Max principal stress pattern in the PDL of the (thick and non-uniform interface) model 351
Figure 9-22: von Mises stress pattern in the crown of the (thick and non-uniform interface) model 352
Figure 9-23: von Mises stress pattern in the cement of the (thick and non-uniform interface) model 352
Figure 9-24: von Mises stress pattern in the dentine of the (thick and non-uniform interface) model 353
Figure 9-25: von Mises stress pattern in the PDL of the (thick and non-uniform interface) model 353

Introduction

1 Introduction

Dental caries, dental trauma, tooth wear and developmental tooth defects are thought to be the major factors that cause teeth defects. In most cases, tooth defects require dental repair. Any change in the external shape of the tooth due to placement of a restoration can lead to changes in the main mechanical and physical characteristics of the tooth. Normally, when there is a load application such as a mastication load, deformation [strain] will be generated within the body of the tooth. It has been reported that the internal stress and strain distribution depend on the shape of the body and the stiffness distribution of the body structures (Habelitz et al., 2001).

In a sound tooth structure the load of mastication travels in a different way from that in a repaired tooth. Thus, the stress distribution pattern in a sound tooth structure is different from the pattern in the restored tooth structure (Kuroe et al., 2000).

The enamel structure in a sound tooth body shows intimate bonding to the dentine, which is not the case in the restored tooth, where the restoration is separated from the dentine by the cement material. This sequence of different layers between the sound and restored tooth structures gives rise to differences in the pattern of stress distribution between them (Suzuki et al., 2008).

Some structures, such as tooth enamel, have been classified as an anisotropic structure, which is a property of the material's mechanical behaviour being a directionally dependent, in contrast to isotropy property that show identical properties in all directions. The stress distribution through an anisotropic enamel structure is directed toward the more resilient dentine because the load path distribution follows the stiff direction of the prisms of the enamel, while within the isotropic structure of the restoration the load distribution is directed laterally (Spears et al., 1993).

Several factors affect the longevity of the restoration, according to Wang's findings; the fit or accuracy of the marginal and internal adaptation is valued as one of the most important requirements for achieving the best clinical quality and success of the fixed restorations (Wang et al, 2007). It has been verified that the stress development in the uneven cement layer varies and the strength of the adhesive cement might be reduced (Mou et al., 2002).

Non-uniform cement film thickness can affect the stress distribution and structural integrity of the tooth, as well as the bonding surface, by increasing the maximum shear stress to values exceeding the bond strength of the cement layer to the restoration and tooth walls. Thus, it is advisable to make the resin cement film thickness as uniform and as thin as possible (De Jager et al., 2005). However, there is still little knowledge concerning the effect of the uniform resin cement film thickness and bond value on the structural integrity of all-ceramic machined and pressed restorations (Abo-Hamar et al., 2005).

Restorative dentistry has in recent decades seen an increase in the use of adhesively cemented all-ceramic restorations and the introduction of CAD/CAM techniques (Sturdevant et al., 1999, Martin and Jedynakiewicz, 2000). The effect of the adhesive cement agent properties on the width of the marginal and internal gaps has also been the subject of debate (Addi et al., 2002).

Measuring the interface is very important as the interface is considered to be one of the most important factors in determining the longevity of the restoration. In measuring the interface of a restoration, many techniques implemented include restored tooth sectioning and replica technique. The former is destructive (Shearer et al., 1996), whilst the latter, replica technique, has been considered as a reliable and non-invasive method.

However, the replica technique has many disadvantages; for example, the measurements obtained from any section in any given plane may be different from those acquired in a different plane. Moreover, it is very difficult to create the same plane cross section on different specimens, and that renders comparisons between several samples slightly inaccurate.

Nowadays, with the introduction of micro CT scans and the capability to obtain images with high-resolution scale, the creation of a very accurate 3D replica of the real object has become possible. Generally, the more accurate the data and the 3D model, the more reliable results can be obtained.

More recently, and because Mimics® software is compatible with micro CT scan-based data, an effective alternative way for measuring the interface has been introduced. Any sample can be represented by an accurate 3D model created by Mimics® software (Materialise Interactive Medical Image Control System), which is developed by (Materialise Co., Ltd). Mimics® software is compatible with the data obtained from the CT and micro-CT scan for the hard tissue structures and MRI for the soft tissue structures. Using Mimics® software seems challenging, but through the option of thresholding and depending on the different scales of contrast properties between the restored tooth layers, the procedure of layers separation and measuring the lute interface in 3D can be achieved with reasonable ease. Thus, measurement of the thickness of the interface at any point at any section can be standardized for several samples by using Mimics® and the potential accuracy of the outcome can be ensured.

Among all types of tooth restoration currently in use, the machined and pressed ceramic are the most popular aesthetic restorations. Ceramic is a tooth coloured restoration and can be positioned via the indirect procedures (a solid structure that has been fabricated in the lab outside the oral cavity and then to be placed on/in a prepared tooth). Glass ceramic, which is one of the most popular ceramic types with a frequently used today, can be etched and retained on the tooth with the aid of adhesive resin cement (Jiang et al., 2010, Hill and Lott, 2011)

All-ceramic restorations with a strong core structure are still more brittle and less ductile compared with the metal restorations. As a consequence, for all-ceramic restorations the preparation procedure and the cementation technique are more critical than is the case with metal ceramic restorations. Fracture resistance of the all-ceramic restoration as well as the adhesion between the tooth and the restoration can be affected by the shape of the preparation and the shape of the cement layer (De Jager et al., 2005).

CAD/CAM or machined ceramic restorations have been criticized at the level of fitting and adaptation more than the other techniques (Mou et al., 2002). In the machined all-ceramic crowns the cement thickness is not uniform, with the occlusal gap being larger than marginal area and the gap distally is bigger than the gap in the mesial surface(Mou et al., 2002, Reich et al., 2011). Thus, stress development could vary in an uneven cement thickness which is more likely to reduce the support provided by tooth walls. Therefore the risk of ceramic restoration fracture and the failure of whole restored system will be increased(Mou et al., 2002). However, according to Yeo et al.'s investigation conducted in 2003, the marginal and internal fit of pressed ceramic show less discrepancy (Yeo et al., 2003).

More recently, by using the 3D wax printer, it has become possible to standardize the two techniques of ceramic fabrication (machined and pressed) through creating the interface for several crowns by pre-setting the interface parameters in a model created by using the related software. The 3D wax

printer has eliminated the variations in the thickness of the interface caused by using the die spacer and the brush. Thus, one wax pattern, created using the data from scanning the die, can be duplicated in several standard crowns by using the 3D wax printer.

Mechanical testing is a universal term used to describe a broad range of activities that are applied to determine the behaviour and properties of the materials. Typically, this covers a load application and measurement of the response. The load application may be either static or dynamic in nature and could be applied in a specific localized area or distributed at a single or multiple locations. The destructive mechanical tests for determination of fracture resistance and main mechanical properties of the materials are important means for assessing the behaviour of the tooth.

Generally, static tests in restorative dentistry are designed to examine the material in order to assess the structural integrity of the structure and whether it is affected by changes in the materials or the final design.

Dynamic testing allows a material to be tested under changeable rather than constant conditions to check the durability of the material or the design under determined conditions. In the case of dental material, the dynamic fatigue test is aimed at simulation of oral clinical conditions and examining the clinical performance of the restoration structure. Fatigue testing is used to determine a mode of failure whereby an object eventually fails after being repeatedly subjected to a load.

As a result of the *in vivo* condition's intricacy, the majority of the biomechanical studies of the intraoral environment for the stress analysis (such as: FEA, strain gauge or photo-elastic analysis) have been done *in vitro* (Pietrabissa et al., 2002, Assunção et al., 2009).

A sophisticated innovation in dentistry has been the development of a numerical method of analysing the stress distribution that is known as finite element analysis (FEA). Through FEA, it has become possible to consider the deformation of the various components of the restoration simultaneously.

The numerical analysis method (FEA) has been used successfully in many engineering and bioengineering fields since the 1950s and in dentistry since the 1970s. By using FEA, it has become possible to calculate the stress distribution in a complex three-dimensional structure by dividing a large structure into a number of small simple-shape parts called elements, whose ends meet to form nodes (Boschian Pest et al., 2006).

During the last decade, the use of FEA in dentistry has been substantially refined. Undoubtedly, the numerical approach to stress analysis has now become a most comprehensive *in vitro* examination method, particularly in restorative dentistry (Versluis et al., 2004, Versluis and Tantbirojn, 2009).

The stress distribution and structural integrity of the restored tooth maybe affected by the uniformity of the cement film thickness. A pressed all ceramic crown the interface shows less discrepancy than machined crown. Thus, stress distribution in a tooth adhesively restored with all-ceramic crown may vary according to the fabrication technique of the crown (machined or pressed). Moreover, there is still little, if any, precise information concerning the effect of the uniformity of the resin cement film thickness on the structural integrity of all-ceramic restorations, so it is of interest to investigate this. Novel FE computational models may complement current mechanical testing and improve our understanding of stress distribution in these compound complex restorative systems.

1.1 Research questions

1. Does the geometry (thickness and uniformity) of the cement interface influence the fracture resistance of a tooth restored with an adhesively cemented all-ceramic crown?

2. Does the measurement of the stress distribution by finite element analysis provide an effective complementary tool to determine the structural integrity of the restored tooth-crown complex?

Literature review

2 Literature review

2.1 The need for tooth restoration

A tooth can be subjected to multifactorial causes that can damage its structure. The main causes for tooth structure loss or destruction are trauma, bad oral hygiene and naturally occurring breakdowns such as dental caries and wear. Dental problems may cause difficulty in eating, tooth sensitivity, and other health problems. Patients tend to be very concerned to have their teeth restored, either to gain relief from the discomfort associated with the decay or because the patient desires to return the injured tooth to its previous appearance.

In all cases, the objectives of restoring the compromised tooth are:

- To eradicate the disease or structurally compromised tissue as necessary
- To restore the function of the damaged tooth
- To restore the aesthetic appearance of the distorted tooth
- To restore the structural integrity and performance of the compromised tooth

Restoration of a tooth includes a variety of techniques used by dentists to restore missing parts of a tooth or replace missing teeth. Damage to teeth caused by dental caries or fracture can be improved both structurally and cosmetically by a variety of treatment approaches, such as intra-coronal restorations, or full-coverage extra-coronal crowns designed to restore function, size, appearance, and strength. Full coverage restorations have been used widely to save teeth that

have been damaged by functional and para-functional wear processes, trauma and caries.

2.2 Materials and technique of tooth restoration

Dental materials that have been used as tooth restorations possess different physical properties. Some of them are classified as brittle materials, such as some types of cements, and the others as tough, such as metals. The techniques as well, vary between direct and indirect restoration, inlay or onlay (partial or full coverage restoration).

Different types of dental materials have been used for fabrication of a full coverage restoration, such as metal, acrylic, composite and ceramic. The natural appearance and the high durability of the chemical and optical properties of ceramic have made it a most popular type of restoration materials. The recent dental ceramics that have been introduced in the dental field have developed to the point where the strength and toughness fulfil the demands of use in fabrication of full coverage restoration (Kelly et al., 1996, Rizkalla and Jones, 2004, Ban, 2008). Veneering the zirconia core material with heat pressed glass ceramic shows a significantly higher fracture strength as well as a higher micro tensile bond strength between the zirconia core and glass ceramic veneer (Lin et al., 2012).

The idea of bonding a relatively thin cross section of ceramic to the tooth structure was developed particularly after it was found that the stress transferred

directly from the restoration to the tooth structures. *In vitro* investigation of load transference in resin-bonded veneer has shown a potential for successful transference of the load from the adhesively cemented all ceramic restoration to the underlying tooth structures (Burke et al., 1995, Qualtrough and Piddock, 1997, Fleming and Addison, 2009).

Regarding tooth strength, studies have shown that teeth restored with a resin bonded all ceramic inlay or onlay restorations demonstrate strength similar to that of a sound tooth (Jensen et al., 1989, Casson et al., 2001, Desai and Das, 2011). Moreover, *in vitro* studies that aimed to restoring natural incisors with laminated veneer have shown that the strength of the tooth has recovered to its original value(Andreasen et al., 1991, Stokes and Hood, 1993). Similarly, another study has shown that there is no statistical difference between the fracture resistance of a group of teeth restored with resin bonded crowns and a group of sound teeth (Qualtrough and Piddock, 1997).

A review of the literature has revealed that most of the researchers have examined several parameters that might have an impact on the mechanism of failure of the all-ceramic restoration. However, the cement geometry hasn't been taken into account in these studies as a contributor factor in the failure mechanism of the ceramic restoration. Thus, thoroughly understanding the effect of the cement geometry (thickness and uniformity) on the ceramic failure is essential.

Several clinical studies have reported the excellence of the long term success of adhesively cemented all-ceramic restorations, such as laminated veneer, inlay and onlay ceramic, adhesively bonded fixed partial dentures and all-ceramic crowns (Felden et al., 1998, Van Dijken et al., 1998, Friedman, 2001, Blatz et al., 2003, Krämer and Frankenberger, 2005, Lin et al., 2012). A study was done on 300 porcelain veneers in 30 patients (ten veneers per patient in the maxillary arch)in which the veneers were recalled at 1, 2 and 5 years (Aykor and Ozel, 2009). Criteria were utilized to evaluate the successful clinical performance in terms of marginal adaptation, postoperative sensitivity, marginal discolouration and secondary caries. The data showed no signs of failure.

Similarly, D'Arcangelo et al., have used the same criteria for evaluating the success of veneering porcelain as well as the additional criteria of cracks, fractures and debonding. This study has recorded a success rate of a 97.5% after 7 years of performance (D'Arcangelo et al., 2011). Regarding the inlay and onlay restorations made from machined feldspathic ceramic (Vitablocs Mark I and II) and from pressed leucite reinforce ceramic (IPS Empress Esthetic), the absence of fracture of restoration and long-term clinical survivability have been documented as 97% at 5 years and 90% at 10 years (Otto and De Nisco, 2002, Fasbinder, 2006).

Since single all-ceramic crown systems first became available in the market, the performance of these systems has been highlighted by many researchers. There are different types of all-ceramic systems used for fabrication of a single-unit

crown, such as leucite reinforced glass ceramic (IPS Empress), glass infiltrated ceramics (In-Ceram Spinell and In-Ceram Alumina, Vita Zahnfabrik) and polycrystalline alumina (Procera Alumina, Nobel Biocare, Göteborg, Sweden). Although ceramic systems have different composition, microstructure and processing techniques, most studies have recorded the survival rate as more than 90% in respect of the time in service. In these studies, the survival rate has been measured based on crack initiation in the ceramic, abutment of secondary caries and fracture of the crown (Pröbster, 1996, Odén et al., 1998, McLaren and White, 2000, Segal, 2001, Mörmann, 2002, Bindl and Mörmann, 2004, Walter et al., 2006, Gehrt et al., 2013).

Lithium disilicate glass ceramic has recorded a very high survival rate. Toksavul and Toman examined lithium disilicate-based glass ceramic crown restoration in terms of failure through fracture of the crown due to crack initiation and propagation; they reported a survival rate of 95% after 5 years of performance (Toksavul and Toman, 2007). Another study has recorded a 100% survival rate for the same period of performance as that of the Toksavul and Toman study (Marquardt and Strub, 2006). It is assumed that the high percentage of success of clinical performance of lithium disilicate is due to the rod-shape crystal in the ceramic, which may act as a crack stopper (Gehrt et al., 2013).

2.3 Stress distribution

2.3.1 Nature of stress distribution in sound tooth structures

Studying the stress distribution within tooth structures is very difficult as the tooth and its supporting tissues are a complex assemblage of different structures with different mechanical properties (Yettram et al., 1976). Generally, the stress distribution within any body depends on the shape and the stiffness distribution of the structure's material. Obviously, the enamel's elastic properties are anisotropic, which means they are not the same in all directions, and that is because the alignment of the microstructures of enamel is highly orientated (well-ordered) and that leads to anisotropy of the enamel's mechanical properties (Habelitz et al., 2001).

Spear et al. assumed that the enamel was isotropic under applied loads and compared that with the results of the enamel as anisotropic under the same situation. They found that the stress distribution within the isotropic enamel was significantly different from that when the enamel was anisotropic(Spears et al., 1993). The concept is that within the isotropic enamel structure the load distribution is directed toward the outer stiff enamel shell, while in an anisotropic enamel it is directed toward the dentine because the load path distribution follows the stiff direction of the prisms of the enamel (Spears et al., 1993).

The good arrangement of the stiff prisms of the enamel play an important role in effectively dissipating the occlusal force toward the more resilient dentine (Habelitz et al., 2001). Generally, the stress distribution pattern in anisotropic enamel serves the tooth better than when the enamel is isotropic because the occlusal force is not directed laterally but directed toward the more elastic dentine. The major function of the anisotropic properties of the enamel is to reduce compressive and tensile stress that would otherwise occur on the enamel. Thus, and because of these properties, there will be a reduced risk of enamel fracture (Spears et al., 1993).

Although the enamel is organically bonded to the dentine, they respond differently to the masticatory load. Despite the two structures supporting each other, they react independently to the stresses (Goel et al., 1990). Enamel is five times stiffer than dentine and resists wear but it is a brittle material and offers low resistance to crack propagation. However, dentine is four times tougher than enamel and the distribution of the stress can be in an isotropic pattern (Spears et al., 1993). In the normal tooth structure, the external load will be directed from the stiffer enamel to the more elastic dentine as compression. Within the normal chewing action of the oral cavity, the concentrated external loads that are exerted on the enamel are distributed over a large internal volume of the tooth structure (the dentine), as a result, the local stress will be less (Roberson et al., 2006). Accordingly, the stress can be more effectively distributed within dentine than enamel.

Under the normal conditions, the occlusal load, with the assistance of dentine, can transfer from enamel through dentine to the root and periodontal complex (Goel et al., 1991). Basically, the PDL structure is a fibre reinforced substance; it acts as a shock absorbent to reduce the impact of the chewing force on the entire tooth structure. It has been reported that the PDL can respond to the load in a nonlinear and viscoelastic manner. Therefore, the nature of the relationship between the external occlusal load and the amount of the PDL distortion is time dependent and not linear(Fill et al., 2011). It has been recorded that the deformation of the PDL can easily occur with a low functional load. However, the PDL is harder to deform with an excessive functional load (Suzuki et al., 2008).

2.3.2 Nature of stress distribution in the restored tooth structures

During the lifetime of the human being, the teeth are subjected to various changes, such as, caries, attrition, abrasion, trauma and some sorts of restorative procedures which can lead to deterioration in the integrity of the tooth structures and the general oral health conditions of the other oral hard and soft tissues (Goel et al., 1990, Roberson et al., 2006). Moreover, the lesion area in the tooth will undergo decomposition and a change in the shape and structure of the hydroxyapatite crystal.

The lesion's shape and dimensions govern the stress concentration severity. It has been found that the stress is more likely to concentrate in the apex of the

lesion than in any other area on the tooth structure when subjected to the load. Therefore, the stress distribution within the restored tooth structure is different from that in the sound tooth structure (Kuroe et al., 2000, Yunmao and Jukun, 2008). In natural teeth, there is no intermediate layer between enamel and dentine. However, to restore the tooth with any sort of crown, cement should be used as a luting layer to fix the crown. Thus, the changing in the sequence of the layers between the sound tooth and restored tooth gives rise to differences in stress distribution (Suzuki et al., 2008).

The transmission and distribution of the stress in a restored tooth is dependent on factors such as the properties of the restoration material, the design of the cavity or tooth preparation and the strength of the bond between the restoration and the dentine in the restoration-dentine interface (Goel et al., 1992).

It has been found that the resistance of the tooth to the intraoral force will reduce according to the amount of the tooth reduced by the disease or tooth preparation. The tooth's ability to resist occlusal force is directly related to the amount that remains of the coronal tooth structure (Reeh et al., 1989, St-Georges et al., 2003, Soares et al., 2008). During the intraoral load application, the elastic modulus of the luting material could be supposed to be one of the most important factors affecting the stress distribution and stress/strain correlation within the tooth-restoration complex (Sabbagh et al., 2002, Soares et al., 2008).

The pattern of stress distribution in sound tooth structures is different than that in a restored tooth because the transmission of the load differs in direction and effect as it passes through different structures. It has been found that when the structure is composed of dissimilar materials such as dentine structure and restoration material, the higher the elastic modulus of the luting and restoration material when the joint restoration/tooth is stressed, the lower the tooth structure deformation (Reeh et al., 1989, Magne and Belser, 2003, Roberson et al., 2006, Soares et al., 2008). A study by De Jager et al, has shown that the stress in the restored tooth and the luting cement are non-uniform; the stress distribution and structural integrity of the tooth can be affected and the stress can exceed the bonding strength, which leads to failure in the tooth restoration complex (De Jager et al., 2005).

The stress generated from the load on the restoration can be manifested in a form of compressive, tensile and shear stress throughout the interface between the restoration and the tooth, rather than just in the compression stress exerted on the sound tooth structure when subjected to the load (Mahler and Peyton, 1955, Farah et al., 1973, Roberson et al., 2006).

Generally, the structural design of the sound tooth is such that it can withstand the effect of the intraoral load more effectively. However, the distribution of the normal internal tooth stress will alter when the tooth structure is affected by the restoration. Therefore, the restored tooth cannot dissipate the stress in the same

way as a sound tooth, resulting in the formation of a high stress concentration area and, as a consequence, the fracture resistance of the tooth will be reduced (Mahler and Peyton, 1955, Pilo et al., 2002). It has been proved that the tooth preparation design and the restoration type and design can affect the stress distribution and fracture resistance of the restored tooth (Zarone et al., 2005a).

Reviewing the evidence of all-ceramic failure from the retrieved clinical data of the glass ceramic restorations failure have shown that more than 90% of all ceramic failure tend to start from flaws and stresses that generated at the interface surface rather than functional surface (Pagniano Jr et al., 2005, ElGuindy et al., 2010). Since, most of the evidences confirmed the fracture tendency of the inner surface of the all-ceramic restoration; the stress distribution and restoration durability could be substantially determined by the cement interface factor.

2.3.3 Role of the cement interface on the stress distribution in restored tooth

The cement material acts as a link between the tooth structure and the dental restoration, forming an interface complex. For retaining the indirect restorations on the prepared tooth and fully maintaining the integrity of the abutment, the luting material must fulfil some special mechanical requirements (Sumer and Deger, 2011).

The mechanical properties of the resin cement are the most important requirements that can affect the bonding force between the restoration complexes (ceramic crown- cement - tooth). These properties are; the elastic modulus (which is proposed as a good parameter to measure the ability to transfer / distribute the force to /through the tooth structures); resin resiliency (which is the amount of energy needed to deform the object permanently) and fracture toughness (which is the ability of the material to resist crack propagations) (De La Macorra and Pradíes, 2002).

Most of the acid-base reaction conventional dental cements, such as zinc phosphate, zinc polycarboxylate and glass ionomer are brittle materials and very vulnerable to tensile failure. Resin adhesive cement has a greater tensile strength and that makes it less vulnerable to tensile failure (White and Yu, 1993a). Several *in vitro* studies have compared the structural integrity of the tooth restored with conventional cement and the adhesive resin cement; most of them have found that the structural integrity is most likely to be restored by adhesively bonding ceramic to the tooth rather than using a conventional cement (Jensen et al., 1989, Qualtrough and Piddock, 1997).

A study carried out by Burke et al. (2002) demonstrated that the adhesive resin bonding helps in stress diffusion and precludes crack propogation in the internal surface of the ceramic restoration(Burke et al., 2002). Considering the effect of the aforementioned mechanical properties (elastic modulus, resiliency, fracture

toughness) on the restoration durability, the adhesive resin based dental cement can represents the best clinically used luting material (Krämer et al., 2000).

It has been documented that the nature of the implemented resin cement, considering the stress dissipation aspect, could effectively optimise the whole system's performance. The new generation of resin adhesive cements can increase the retention of the restoration to the underlining structure (enamel or dentine), reduce the marginal microleakage, improve the marginal adaptation and enhance the fracture strength of both the tooth and the restoration (Sorensen et al., 1991, El-Mowafy, 2001, Potiket et al., 2004).

Obtaining a desired stress distribution within the restored system, the modern restorative approaches often use the ceramic materials combined with the adhesive bonding cement. This combination would offer a restoration of the tooth's structural integrity with a wide range of remarkable aesthetic restoration options that can be used in the dental clinic today (Qualtrough and Piddock, 1997, Peumans et al., 2000, Blatz et al., 2003, Della Bona and Kelly, 2008).

2.4 Effect of a dental restoration on the tooth structures

2.4.1 The effect of the inlay (intra-coronal restoration) on the tooth

Any compromised tooth should be restored with either an inlay or onlay (intra or extra coronal restoration respectively). Inlay restoration, which can be either a direct placement material or a pre-fabricated restoration, does not completely

cover the external surface of the tooth and can be made of various types of materials such as amalgam, gold, composite and ceramic (Roberson et al., 2006).

In the case of huge destruction of tooth structure by dental caries, the normal procedure for restoring the tooth might necessitate removing a large part of the tooth. Tooth preparation can weaken the tooth structure by about 59% (St-Georges et al., 2003). It has been reported that the strength to resist tooth fracture can be reduced by approximately 54% of the original strength after mesio-occlusal-distal (MOD) cavity preparation (Hannig et al., 2005). The researchers found that removal of tooth structure can cause cuspal flexure and deformation directly proportional to the applied load (Assif et al., 1990).

Comparing the path of stress transmission within the structures in a sound tooth and a tooth restored with intra-coronal restoration, the stress will follow different paths. In sound tooth structures, the stress is directed from stiff enamel towards the more resilient dentine, while in a restored tooth it follows a different path through the enamel to the restoration and dentine. As the load is transformed through a mismatch of elastic properties of the attached materials in a restored tooth (enamel-restoration-dentine), the stress distribution is quite different from that in sound tooth structures (Ausiello et al., 2004).

Although dental amalgam has adequate strength in bulk, it is not tooth coloured and therefore is used only for posterior teeth. Moreover, the brittle nature of

dental amalgam restricts its use to the area in which tensile stress should be kept to a minimum (Kidd and Smith, 2003). The elastic modulus of the restoration plays an important role in load transformation within the tooth structure. Gold restorations have a high elastic modulus and cause the greatest stress concentration in the tooth when compared with other types of materials. However, resin composite restoration with low elastic modules, when compared with gold, shows a most favourable pattern of stress distribution in MOD cavity preparation (Jiang et al., 2010).

It has been reported that in class II MOD cavity preparation, the optimum stress magnitude and distribution are best served with low modulus cement and restorative materials (Ausiello et al., 2004).

For crown restoration, ceramic is the most popular aesthetic restoration material currently used. Ceramic is a tooth coloured means of restoration and can be put in place in indirect procedure. Most types of ceramic today can be held in place in the tooth with the aid of adhesive resin cement (Jiang et al., 2010). Restoration materials that just fill the cavity space within the prepared tooth without using adhesive resin cement, such as gold or amalgam, do not reinforce the weakened tooth structures (St-Georges et al., 2003). There is conflicting evidence in the dental literature as it has been found that there is no significant difference in fracture resistance between a tooth restored with the adhesively cemented restoration and a sound tooth. However, the adhesively bonded

restoration can reinforce the tooth structure, although it cannot restore the original tooth's strength (Bremer and Geurtsen, 2001, St-Georges et al., 2003, Dejak and Mlotkowski, 2008).

2.4.2 The effect of the onlay (extra coronal restoration) on the tooth

A restoration that covers the external part of the tooth is called extracoronal restoration and includes onlays and crowns. In this type of restoration, the pattern of load transmission is through the restoration to the supporting dentine. The tooth's structural integrity depends to a large extent on the amount of dentine remaining in the crown (Assif et al., 1990). Compared with the inlay restoration, an onlay could cover one or more cusps, resulting in a most favourable stress distribution pattern combined with a decrease in the fracture risk. Therefore, extracoronal restoration is often recommended for providing protection for an endodontically treated tooth.

Regarding the restoration's materials, it has been recorded that the all ceramic restorations (inlay/onlay) compared with the composite resin, transfer less stress to underlying substrate. Generally, it has been reported that a tooth restored with the extracoronal restoration shows a more favourable stress distribution pattern than one restored with the intracoronal restoration, regardless the types of restoration material and condition of the load application, especially in the cervical portion of the root (Yamanel et al., 2009, Jiang et al., 2010).

2.5 Physical and mechanical properties of the materials

Before delving deeply into factors that affect the structural integrity of the tooth restored with an adhesively cemented all-ceramic crown, it is important to define and give short notes about the main related physical and mechanical properties and their effect and roles in the behaviour of the materials.

2.6 Terms of physical properties

2.6.1 Force:

Any influence that causes a change of status in an object in terms, for example, of its position, speed, direction and geometry

2.6.2 Stress:

When there is an applied force, the stress is a measure of an internal average force per unit area (within the body which has been deformed) against the external force. This internal resistance is equal in value but opposite in direction to the external force.

2.6.2.1 Types of stress: Compression, tension and shear stress

The stress can be classified according to the direction of the application on the body (see figure 2-1).

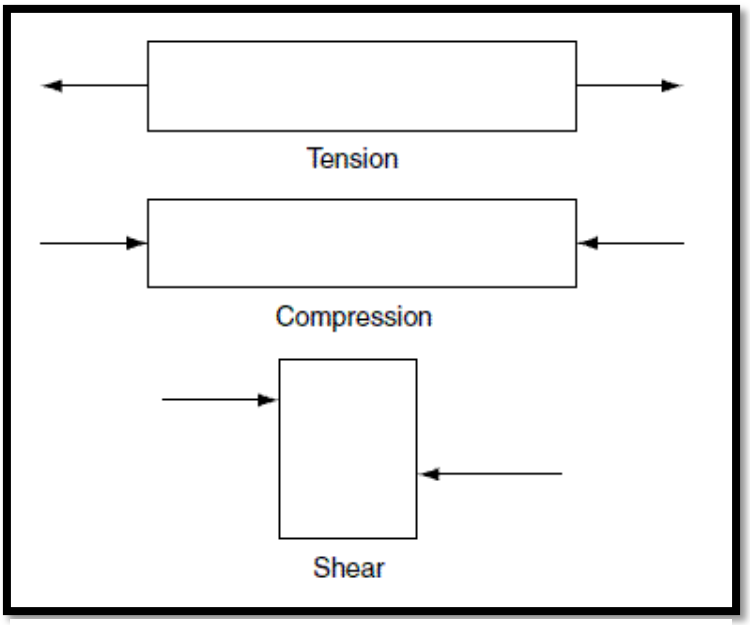

Figure 2-1: Types of stress

2.6.3 Strain

This is a fractional change in the object's dimensions when it is subjected to external force.

2.6.4 Fracture

This is a separation of the object or the material into two or more parts by the action of force.

2.6.5 Strength

This is the capability of the material to survive under any applied force without suffering failure or indicate the maximum amount of the force that the structure can support before get failure.

2.6.6 Fracture Strength

Sometimes called flexural strength, modulus of rupture, or bend strength, this is a stress at which the object fails due to fracture. It can be defined simply as the stress required for breaking the object. It is a mechanical parameter for brittle materials. Usually, a tensile test is used to determine the fracture strength of the given materials.

2.6.7 Stiffness

The property of material to resist deformation and keep its original shape when load is applied is call stiffness.

2.6.8 Toughness

This is the ability of the materials to resist fracturing when stressed. Toughness can measure the capability of the material to absorb the energy and plastically deform without fracturing.

2.6.9 Fracture toughness

It is the resistance of the material to crack propagation and failure.

2.6.10 Crack

This is a break in the body without a complete separation of its components (see figure 2-2).

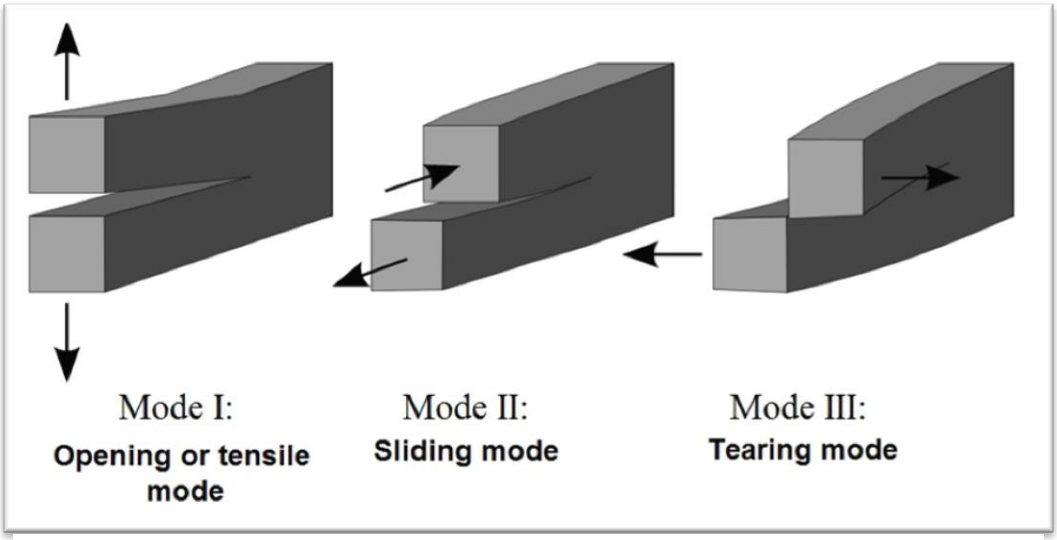

Figure 2-2: Crack modes

2.6.11 Compressive strength

This is the capacity of the material to resist or withstand axially directed force without suffering failure.

2.6.12 Yield strength

This is the stress at which a material undergoes a plastic deformation. Before this stage is reached, the material deformation is elastic and can return to its original shape when the applied force is removed.

2.6.13 Ultimate strength

This is the maximum resistance to the applied load that the body can develop before failure (or stress at the moment of rupture).

2.6.14 Fatigue

This term reflect the phenomenon that characterized by the localized and progressive structural damage to the material under a cyclic loading level below the fracture strength or under a constant condition over a time. This response can be an essential consideration in the way of comprehending and improving the clinical performance of dental restoration. The fatigue value of any material depends on several things, such as nature of the structure or the material, the nature of the applied stress, the environments of the test, the amplitude of the load, and the frequency of the stress cycle. In fatigue test, the load can be applied as an axial, bend, or torsion load.

2.6.15 Fatigue limit

Measuring of a load at which the material can withstand the fixed number of cycles.

2.6.16 Fatigue life

This is the number of cycles that the material can withstand of the determined load.

2.6.17 Brittle fracture

This is a fracture of the material (such as dental ceramic) without any noticeable deformation [before the fracture no any obvious plastic deformation will take place] and failure therein as a consequence of rapid crack propagation.

2.6.18 Ductile fracture

This is the ability of a material to plastically deform under a tensile stress before failure occurs. It is often characterized by the ability of the material to stretch into a wire.

2.6.19 Elastic Modulus

This is a numerical description of the object's elastic deformation tendency (non- permanent deformation) under load application. Simply, it is a measure of the elasticity of the subject. Sometimes it is called Young's modulus or modulus of elasticity. The stiffness of the material can be represented by the elastic modulus. The composition of the material plays an important role in determining the elastic property as the inter-atomic or inter-molecular force is responsible for determination of the elastic property of the material. Therefore, as the attraction force is strong, the elastic modulus value is higher in stiffer materials.

2.7 Performance of the tooth-ceramic-crown system

The components of the system are:

2.7.1 Tooth

2.7.1.1 Enamel

This is the outer layer covering the coronal part of the tooth. Enamel is the hardest and the most mineralised crystalline structure in the human body. It varies in thickness in different areas (graduating from the thickest area at the cusp to the thinnest at the cemento-enamel junction) and across different cusps (averaging from 2.0mm at incisal edge of the anterior teeth , to 2.3-2.5 at cusp tip of the premolar, and 2.5-3.0mm at cusp tip of molar).

Chemically, enamel is a highly mineralised crystalline structure and it is composed of from 95% to 98% inorganic matter by volume. The remaining constituents are 1-2% organic content and 4% water, which together approximately equate to 6% by volume. The primary mineral that makes up enamel is hydroxyapatite, in the form of a crystalline lattice, which is a crystalline calcium phosphate. Hydroxyapatite is the largest mineral crystal found in the enamel's structure, comprising 90%-92% by volume. Structurally, enamel rods or prisms are formed in their millions in the enamel's structure; enamel rods or prisms are the largest structural components and they contain millions of elongated apatite crystallites, which vary in size and shape. The

strength and structural properties of the enamel derive from the tight packing of the crystallites in a distinct pattern of orientation.

Enamel is an anisotropic structure, and more likely to be stiffer in a prism direction compared to a perpendicular direction (Spears et al., 1993, Habelitz et al., 2001, Roberson et al., 2006).

A study by Xu et al. has shown the effect of the tooth structure orientation on hardness. A combination of the Vickers indentation and scanning electron microscopy (SEM) demonstrated that the enamel's mechanical properties are anisotropic in nature (Xu et al., 1998). Enamel rods have a wavy arrangement within the enamel's structure. They run in a perpendicular direction from the dentino-enamel junction towards the enamel external surface (Spears et al., 1993). The hardness and Young's modulus are higher in an occlusal section compared with a longitudinal section (Habelitz et al., 2001). Thus, the enamel can tolerate a force directed vertically on the occlusal surface of the tooth more efficiently than a force that is directed horizontally.

2.7.1.2 Dentine

Dentine is the largest structure of the tooth. It is covered externally by the enamel layer in the anatomical crown and by cementum in the anatomical root. Internally, dentine covers the pulp and acts as the wall of the pulp in the main two portions of the pulp (pulp chamber and pulp canals).

Compared with the enamel, dentine is less mineralised than enamel but it is more mineralised than cementum and bone. The chemical composition of the dentine is inorganic material 75%, organic material 20%, 5% water by volume and some other materials.

Regarding its softness, dentine is significantly softer than enamel but harder than bone and cementum. Dentine's hardness is approximately one fifth of that of enamel. The hardness of the dentine near the dentino-enamel junction is three times greater than the hardness near the pulp (Roberson et al., 2006). The mineral composition of dentine is mainly hydroxyapatite crystallites which in turn form the basic composition of a tubular structure called dentinal tubules. Dentine crystallite is needle-like in shape near the pulp and it changes to a plate-like shape progressing towards the enamel (Kinney et al., 2003). Dentine crystallites are smaller than enamel crystallites and arranged in a less systematic arrangement or pattern than enamel crystallites. Basically, dentine is mineralised hard tissue but it is somewhat more flexible than enamel, with a modulus of elasticity of 18.6 GPa. Thus, dentine can absorb more load than enamel and can support the more brittle, non-resilient enamel (Roberson et al., 2006).

2.7.1.3 Periodontium

The hard and soft oral tissues that support the teeth are called periodontium. Periodontium is divided into two main parts, which are:

(1) The gingival part

(2) The attachment apparatus

Three parts make up this apparatus: the cementum, periodontal ligament, and alveolar process. The periodontal ligament (PDL) fixes the tooth to a bony socket structure (alveolus).The experimental and clinical evidences have shown a viscous and elastic response of the PDL during the load condition. The viscoelastic response of the PDL has a determinate effect on the dynamic behaviour of the teeth under any load (Sanctuary et al., 2005).

The PDL is a complex soft, connective tissue, which is rich with cells, blood vessels, nervous tissue and some extracellular substances. The extracellular substances consist of fibres, which are mainly collagen fibre, and the ground substances, which are protein and polysaccharide (Roberson et al., 2006). The main function of the PDL is to support the tooth in various ways: it has sensation properties, nutrition properties and, most importantly, homeostatic properties. There are bundles of collagen fibres within the PDL, known as the principal fibres, which provide attachment of the cementum to the alveolar bone. It has been found that the PDL plays a very important role in absorbing and distributing the occlusal force by acting as a cushion for supporting and suspending the tooth in the supporting bone (Rios et al., 2008).

2.7.2 Interface

2.7.2.1 Lute agent

The survival rate of dental fixed restoration is critically related to the retention, marginal seal, and the durability of the restoration, which, to a large extent, are influenced by the cement materials and cementation procedures (Piemjai et al., 2002, Vargas et al., 2011). Several studies evaluated the clinical failure of glass ceramic restoration have suggested that more than 90% of the ceramic failure has a tendency to start from the defect and stress that generating from the interface surface rather than from the outer serviceable surface (Kelly et al., 1990, Thompson et al., 1994).

The cement agent performs different functions through the tooth restoration complex. In general, the main functions of the cement can be described as:

1. To correctly fill the space between the prepared tooth and the inner surface of the restoration.
2. To establish or increase the retention of the dental prosthesis in place.
3. To properly transform the force from the restoration structure to the underlying dentine structure and maintain its integrity.

The cementation procedure is either non-adhesive (conventional cementation) or adhesive that uses adhesive cement. Adhesive cementation involves the use of bonding agent to enhance the bonding of the restorative material to the substrate, so it is a combination of chemically adhesive bonding and

micromechanical interlocking. On the other hand, a non-adhesive cementation procedure involves the use of the luting agent only to fill the space between the dental restoration and the tooth substrate, so it depends solely on micromechanical rotation (Pospiech, 2002, Thompson et al., 2011). Several factors determine whether adhesive or non-adhesive cementation is used.

Depending on factors such as the composition of the luting agent, type of the pre-treatment of the tooth and the type of indirect restoration, the attachment relationship between the tooth and the restoration could be chemical, mechanical or a combination of both (Piwowarczyk et al., 2001).

There are many luting agents in the market and each one is unique in terms of its composition, chemical and mechanical abilities, advantages and disadvantages, and handling characteristics. Choosing an appropriate cement agent for each clinical situation can be difficult and confusing. The long-term prognosis for a dental fixed prosthesis is largely dependent on the choice of luting agent, the durability of the luting agent and the content of adhesive bond (Diaz-Arnold et al., 1999, Piwowarczyk et al., 2004).

The indication of each cement type is dictated by cement composition, availability of tooth preparation for achieving retention and resistance form and the field control at the time of the cementation procedure (Zidan and Ferguson, 2003, Duarte et al., 2005). There is no ideal luting cement available in the market today that is suitable for all cementation situations. Nowadays, dentists

have several options for luting an indirect restoration to the abutment teeth, so specific selection criteria should be used (Vargas et al., 2011).

In general, there are five commercially available cement materials for long-term cementation of fixed dental restoration: water-based dental cements, such as Zinc phosphate, zinc polycarboxylate, glass ionomer, resin modified or "hybrid" glass ionomer, and polymer-based dental lutes, such as resin composite cements. The main difference between these two classes is their main setting mechanism; it is water-dependent in the case of cements while for the resin agents it is achieved through the polymerization reaction (Zorzin et al., 2012).

2.7.2.1.1 Zinc phosphate cement

This type of dental cement was introduced in the dentistry field more than a century ago and the formulation has since been refined through continuous use. In spite of well-documented drawbacks, such as low setting pH, high solubility, and lack of adhesion, zinc phosphate was extremely popular during most of the twentieth century. Therefore, it is often referred to as the gold standard material (Diaz-Arnold et al., 1999, Roberson et al., 2006).

This type comes in powder and liquid forms and is classified as a cement of an acid-base reaction. The reaction is initiated by mixing a powder, which is composed of 90% ZnO and 10% MgO, with an aqueous solution that consists of approximately 67% phosphoric acid buffered with aluminium and zinc. The mixing reaction is very critical and to develop optimal cement, the reaction

should be performed on a cool slab. The strength of the cement is mostly linearly dependent on the powder: liquid ratio; thus, the more powder the greater the strength. The compressive strength is (80 to 110 MPa) and tensile strength is (5 to 7 MPa) of the properly mixed zinc phosphate, which is adequate to resist masticatory load. Moreover, the completely set cement is extremely stiff and shows a high modulus of elasticity of 13 GPa, which allows the cement to resist the elastic deformation in areas of high masticatory force and in long span prostheses (Diaz-Arnold et al., 1999, Roberson et al., 2006, Pameijer, 2012).

The reaction of the powder with the liquid is a heat generation reaction (exothermic reaction) and the pH is 3.5 when the mixing is completed. During the reaction between the powder and the liquid, not all the liquid reacts with the powder, so unreacted phosphoric acid that has a low pH ±1.5 is exposed to the pulp, which is very irritating for the pulp due to its small molecular size and its ability to penetrate into the dentinal tubules. Thus, the pulp has to cope with heat as well as with high acidity (Pashley et al., 1998, Pameijer, 2012). The zinc phosphate cement does not bond chemically to the substrate, but rather, offers a retention seal to the substrate by mechanical means only. Therefore, the length, the taper, and the surface area of the prepared tooth are critical to its success(Diaz-Arnold et al., 1999).

2.7.2.1.2 Zinc polycarboxylate cement

Zinc polycarboxylate cement agent was developed in the 1960s in an effort to avoid potential problems in the pulp associated with the low pH of traditional cements (zinc phosphate cement). Through the replacing of the pulp-irritant phosphoric acid with a high molecular weight polyacrylic acid, zinc polycarboxylate cement has become biologically quite favourable as there is little or no irritation to the pulp(Roberson et al., 2006, Pameijer, 2012). It is believed that the long molecular chains and the larger molecular size of the polyacrylic acid prevent their penetration to the dentinal tubules (Pameijer, 2012). One of the polycarboxylate cement's disadvantages is its demonstration of an early and rapid increase in cement film thickness that may hinder the proper seating of a dental restoration. Moreover, after the completion of setting, it may exhibit significantly greater plastic deformation compared with the zinc phosphate cement. Thus, in an area of a high masticatory force or cementation of long span prostheses, zinc polycarboxylate cement is not well-suited for use (Diaz-Arnold et al., 1999). Zinc polycarboxylate cement also uses an acid-base reaction and it has lower compressive (55 to 85 MPa) but higher tensile (8 to 12 MPa) strength than zinc phosphate. The most important advantage of polycarboxylate cement is the ability of the cement to adhere to the tooth structure by chemical bonding through the reaction of the free carboxylic acid group with the calcium ions of the dental structure. This property of bonding to

the Ca ions is called chelation (Diaz-Arnold et al., 1999, Roberson et al., 2006, Pameijer, 2012).

2.7.2.1.3 Glass Ionomer Cements

Glass ionomer cements (GICs), which are also called glass polyalkenoate cements, are hybrids of silicate and polycarboxylate cements. This cement is a producer of an acid–base reaction between an aqueous polymer solution and a glass powder (Roberson et al., 2006, Tian et al., 2012). GIC were first invented in the late 1960s and were first used in dental clinics in the early 1970s. They are commonly used in dentistry, but also have been considered for use in the reconstruction of bone and ears as well as in veterinary sciences because of the good biocompatibility and bioactivity which the cements possess that stimulate tooth and bone remineralisation (Tian et al., 2012). Glass-ionomer cements are thought to have an ability to adhere to tooth structure by formation of ionic bonds at the tooth cement interface owing to the chelation reaction of the carboxyl groups in the acid with the calcium and/or phosphate ions in the hydroxyapatite crystals of enamel and dentine (Diaz-Arnold et al., 1999). Compared with polycarboxylate and zinc phosphate cements the compressive strength of GIC is higher. However, the modulus of elasticity of GIC is lower than that of zinc phosphate cements; therefore, there is potential for elastic deformation in regions of high masticatory load(Diaz-Arnold et al., 1999). GIC has considerable advantages, such as good chemical bonding to the tooth

enamel and dentine, translucency, biocompatibility, low value of thermal expansion, and anticariogenic ability through release of fluoride ions to possibly prevent the recurrence of caries. However, the major drawbacks of this type of cement are its susceptibility to moisture attack and the consequent solubility of the cement material on exposure to water during the initial setting period, leading to cohesive failure from microcrack formation. Moreover, it has been well- documented that the GIC has low ability to adhere to the ceramic structure (Gemalmaz et al., 1998, Moscovich et al., 1998, Diaz-Arnold et al., 1999, Moshaverinia et al., 2012).

As a result of the shortcomings of the acid-base reaction cements in terms of some mechanical properties, researchers have attempted to overcome the aforementioned drawbacks by producing new strong materials that can withstand a functional load over the lifetime of the dental prostheses; these newer materials include the resin modified glass ionomer and the adhesive resins (Gladys et al., 1997).

2.7.2.1.4 Resin Modified Glass Ionomer

Resin modified glass ionomer cements (RMGI) were produced in the late 1980s in an attempt to improve some of mechanical properties of the conventional glass ionomer cement in terms of tensile strength and fracture resistance. Simply, RMGI cement can be described as a hybrid of glass ionomer and a

composite resin. Thus, RMGI cement has an acid-base as well as polymerizable component (Berzins et al., 2010).

Comparing the mechanical properties of RMGI cement with other types of dental cements, RMGI cement has greater compressive and tensile strength than zinc phosphate, zinc polycarboxylate, and conventional glass ionomer cement, but less than resin composite cement (White and Yu, 1993b, Piwowarczyk et al., 2004).

In general, the ease of mixing and use as well as its production of a low film thickness, can be claimed as advantages of this type of cement (Kious et al., 2009). However, the hydrophilic nature of RMGI cement can be considered as a significant disadvantage. During the setting reaction, its hydrophilic nature leads to increased water sorption and subsequent plasticity and hygroscopic expansion (Zhao et al., 2009). Although the appropriate expansion of the RMGI cement can compensate for its polymerization shrinkage, excessive expansion of the RMGI cement can cause significant dimensional changes in the cement as well as creating radial pressure; so the excessive expansion can affect the strength of the cement and can damage the surrounding tooth structure. Thus, the explanation of a fracture tendency of the all ceramic restoration particularly the feldspathic –type ceramic that is cemented by a RMGI cement can be based on the concept of the hygroscopic expansion of this type of the dental cement (Leevailoj et al., 1998, Zhao et al., 2009, Sumer and Deger, 2011).

2.7.2.1.5 Adhesive Resin Luting Agents

Its poor adhesive properties and the desire to improve the clinical success of resin modified glass ionomer cement have led to advances in the development of resin-based luting agents, which in turn have resulted in the introduction of adhesive resin cements (Pameijer, 2012).

The applications of adhesive resin cement in dentistry have increased significantly over the last decade. This type of cement can be used for cementation of all-ceramic crowns, porcelain veneers, and indirect composite or ceramic restoration. The composition of adhesive resin cement is a variation of filled BIS-GMA resin and other methacrylates.

The development of the resin cement started with the producing of cement that has the ability to micromechanically interlocking to a conditioned enamel surface [to the hydroxyapatite crystals and prism treated by acid]. Owing to the polymerization shrinkage, a large stress on the interface and tooth were recorded, which my lead to break the two surfaces bonding. Adding the dentine bonding to the pre-etched porcelain and tooth surface has offered an ability to generate a chemical bond between the resin cement and porcelain/tooth respectively.

Thereafter, the adhesion quality has been included in the composition of some resin cement by adding 4-META (4-methacryloxyethyl trimellitate anhydride) and MDP (10-methacryloyloxydecyl dihydrogen phosphate) to the resin's

monomer to attribute with the main components as self-adhesive resin cement(Sumer and Deger, 2011).

For initiation of the polymerization reaction of the adhesive resin cement, three methods are available: auto polymerization, light polymerization, or a combination of both, which is called dual polymerization (Attar et al., 2003). The possibility of a reaction by chemical or photo initiation mechanisms has made the use of adhesive luting cement more prevalent in cementation of dental restorations than other cements (Piwowarczyk et al., 2004). However, the adhesive luting agent used in dual polymerizing is characterized by higher mechanical strength and much better aesthetic properties than those of the chemical or light polymerizing luting agents (Lia and White, 1999).

Recently, a new generation of dual-polymerizing universal resin cement, which is called self-adhesive resin cement, has been introduced. In this new type of resin cement, ease of manipulation (pre-treatment steps not required), favourable mechanical properties, good aesthetic quality, and good tooth adhesion of resin luting agent have been combined. Thus, proper bonding to the tooth surfaces can be achieved without performing common pre-treatment steps such as etching, priming, or bonding(Piwowarczyk et al., 2004).

In spite of the excellent properties of the adhesive resin cement, still the use of this cement is considered as technique-sensitive and it requires more careful handling/manipulation during bonding and removal of excess material, which may be difficult when the cement is completely set (Attar et al., 2003).

2.7.2.2 Adhesive resin mechanism

Adhesive cement systems have led to resin bonded ceramic crowns and resin bonded fixed partial dentures becoming more popular. The importance of the adhesive lute is reflected by its ability to adhere to metal, ceramic, enamel and dentine surfaces. This adhesion ability is accomplished by the intimate apposition of the adhesive cement to tooth structures (De La Macorra and Pradíes, 2002).

Traditionally, conventional cement materials (such as zinc phosphate or zinc polycarboxylate cement) were used for a long time to fix the metal restoration on the tooth.

Basically, the conventional cement acts as an intermediate to fill the space between the prepared tooth walls and the restoration, without offering any retention means to the restoration. For that reason, the restoration process is critical in a tooth that has exhibited extensive coronal destruction due to caries or trauma, as the retention depends mainly on the length and taper degree of the tooth walls; in addition, preparation would further undermine the remaining tooth structure.

The complete cast metal restoration was considered as the restoration of choice for posterior teeth that exhibited extensive coronal destruction due to caries or trauma. The complete cast crown demonstrated the best longevity of all fixed restorations, with maximum retention and resistance (Rosenstiel et al., 2006, Shillingburg et al., 2012).

Although, the all-ceramic crown was widely used for the areas of most aesthetic importance, the marginal integrity of ceramic restoration was not comparable to that of cast metallic restoration (Cho et al., 1998). With the conventional cements available at that time, it was difficult to enhance the marginal integrity of the ceramic, as the cement, as mentioned before, was not integrated chemically with the restoration, but only mechanically.

Studies of adhesive cements have shown that the all-ceramic restoration demonstrate a high marginal resistance to fracture when cemented with resin cement rather than conventional cement (Lia and White, 1999, Pagniano Jr et al., 2005, Bindl et al., 2006).

It has been reported that the adhesive cement materials have the best mechanical properties and exhibit superior retentive capabilities in bonding to the tooth and the restoration surfaces that provide a synergistic effect in their ability for retention (Attar et al., 2003, Sümer and Deger, 2011).

The application of a coupling silane agent to a glassy matrix ceramic that has been etched by means of hydrofluoric acid has a great effect on the adhesion between the adhesive lute agent and the ceramic surface. A strong link between adhesive resin cement and the etched glassy surface of the ceramic is registered (Appeldoorn et al., 1993, Wolf et al., 1993, Fleming and Addison, 2009).

For the oxide ceramic (alumina and zirconium) with no glassy matrix, sandblasting of the surface is an alternative procedure for conditioning the

surface and making the application of the silane agent more compatible (Wolf et al., 1993).

Several studies have reported the strength of the bond between the adhesive resin cement and other surfaces. It has been found that the strength of the bond of the adhesive cement to the ceramic surface may exceed the strength of the bond to the tooth surface, especially if a new generation dentine-bonding agent is used. Despite a significant improvement in the adhesive materials regarding their composition and performance, they still exhibit a considerable degree of polymerization shrinkage (De Gee et al., 1993).

Various factors can affect resin polymerization shrinkage, such as the chemical composition of the cement material, the thickness of the cement, the geometry of the cavity or surface preparation and the curing mode (Diaz-Arnold et al., 1999, Bouillaguet et al., 2003, Fleming and Addison, 2009).

The harmful effect of the resin polymerizing shrinkage is the generation of the contraction stresses, which can generate a tensile pre-load of the lute, the bond, and the adjacent structures, and that could potentially reduce the functional strength (Jongsma et al., 2012). The amount of the generated stresses is highly dependent on the c-factor, which can be defined as the ratio between bonded / un-bonded preparation's surface areas. The cohesive strength of some types of cement that are based on Bis-GMA (Bisphenol A diglycidyl methacrylate) and TEGDMA (Triethylene glycol dimethacrylate) monomers can be negatively affected be the high c-factor. These types of resin cement are stronger than the

other types of cement but subject more to the effect of the polymerization mode and c-factor. It has been shown that a high c-factor could reduce the efficiency of the resin flow to compensate the volume loss, as well as, reducing the flexural strength and the modulus of elasticity of the resin cement(Jongsma et al., 2012).

However, the action of resin polymerization shrinkage, astonishingly, creates a compressive stress within the ceramic structure that can increase the strength of the ceramic structure by two ways. Some studies that inspected the basic properties of the ceramic have shown that the ceramic has a high resistance to compressive stress rather than tensile stress. Thus, the compressive stress produced as a result of the polymerizing shrinkage can increase the fracture resistance of the all-ceramic crown (Magne et al., 1999b).

Another study has revealed the resin polymerisation shrinkage utilize a stabilising compressive stress on the surface defect population which may lead to an increase of the amount of the energy that required to initiate the ceramic failure through reaching the critical tensile stress of the ceramic(Fleming and Addison, 2009).

Regarding the general effect of the resin cement on the ceramic strength, Pagniano et al. have found by testing resin luting cement on hydrofluoric acid etched and silanated glass-ceramic surfaces, such as IPS Empress and IPS Empress2, that this potentially offers an important method for improving the fracture resistance of these types of ceramics(Pagniano et al., 2005). Another

study has recorded that a significantly increased load was required to initiate a fracture of an adhesively cemented castable glass ceramic crown when compared with cementing by zinc phosphate or glass ionomer cement. Thus, the low ceramic strength could be enhanced by using adhesive resin cement to be comparable to the high ceramic strength. (Bindl et al., 2006, Fleming and Addison, 2009).

More recently, it has been found that the strengthening quantity that achieved following the adhesive cementation of the all-ceramic restoration was not solely because of the improvement in the stress distribution to the underlying tooth structure. The strengthening mechanism could be attributed to the effect of crack healing through the cement coating that infiltrate the defect (Fleming and Addison, 2009).

Although, some studies have shown a valuable improvement in the fracture resistance of the ceramic crown cemented by resin cement that might be close to that of the sound tooth. However, regarding the cement interface, some of these experimental parameters are still unknown. As mentioned, the cement interface geometry can affect the ceramic restoration strength. Since, there is an experimental possibility of the tested samples had uniform interface geometry. Hence, the present study is aimed to investigate the role of the even cement thickness on the durability of the tooth adhesively cemented with an all ceramic crown.

Generally, the ability of the resin cement to adhere to the different types of ceramic substructures (glassy and polycrystalline ceramic), as well as its other properties, such as high strength, insolubility in the oral environment, and perfect shade matching, have made the resin cement the cement of choice for most aesthetic-type restorations. Such restorations include all-ceramic inlays or onlays, composite inlays or onlays, veneers, all- ceramic fixed partial dentures and the newly developed fibre reinforced composite restorations (Diaz-Arnold et al., 1999).

2.7.2.3 Ideal adhesive cement qualities

Due to the complexity of the restoration system (tooth-cement-restoration) and the variables of each component separately, the ideal mechanical properties of adhesive luting agents remain unidentified(Attar et al., 2003).

Adhesive resin cements are classified according to their initiation mode as photo activated (light activated), auto polymerizing (chemically activated) or dual-activated materials (Blatz et al., 2003).

No one type of cement can achieve ideal mechanical, biological and handling properties (Hill, 2007). However, cement should have the following properties:

1. It should provide a durable bond between dissimilar materials.
2. It should be bioinert (well adapted to the underlining dental tissues), have no pulp irritating toxic materials and have anticariogenic properties.

3. It should be of low viscosity, with the possibility for application in a thin film thickness to reach into the finest spaces between the tooth walls and the restoration.
4. It should be insoluble or have low-resolution ratios within the liquid of the oral cavity, with low microleakage.
5. It should have perfect light transparency.
6. It should offer the possibility of acting as heat insulation to protect the living dental tissue from thermal effects.
7. It should provide high wear resistance and sufficient strength against fracture by withstanding the mastication force and distributing the force evenly throughout the tooth surfaces.
8. It should have a high capability for bonding to the tooth hard tissues (less need for mechanical retention).
9. It should give sufficient working time and be easy to handle.
10. It should have a radiopacity greater than that of dentine, to make the diagnosis of recurrent caries or the detection of residual material and an open gingival margin easier.
11. It should have the lowest possible level of polymerization shrinkage.
12. It should have dimension stability.

However, most of the conventional dental cements, such as zinc phosphate, polycarboxylate, and glass ionomer, are brittle and they are susceptible to

tensile failure. The adhesive resin cements have less susceptibility to tensile failure because of their high tensile stress (White and Yu, 1993a).

Most the adhesive lute cements on the market today have most of the ideal qualities to some extent, but each one displays different physical attributes with respect to their own substance (Hill, 2007, Sumer and Deger, 2011).

2.7.2.4 Geometry of the interface

2.7.2.4.1 Lute interface thickness

All-ceramic restorations can be considered as aesthetically superior to metal fused porcelain restorations. However, their shortcomings regarding the poor fracture resistance and their brittle nature have raised concerns about the longevity of this form of restoration (Anusavice, 2012).

The exact cause of failure is usually difficult to ascertain. Failure can be produced by factors such as tooth preparation, crown design, ceramic thickness, load parameters (orientation, localization and magnitude). Various attempts have been made to improve the fracture resistance of ceramic restorations. One of the most important improvement approaches involved using adhesive resin cement with a high modulus of elasticity to place a ceramic restoration on the tooth (Eden and Kacicz, 1987, Scherrer et al., 1994).

In order to improve the long term performance of any dental material, factors inducing clinical failure should be thoroughly examined. The fracture strength of the all ceramic restoration is not the only factor that determined the failure load. The restoration design and geometry as well as flaws size and location could be considered as a contributor in the clinical failure (Pallis et al., 2004).

The failure behaviour of restoration made up from glass ceramic material has been investigating in several studies. Based on evaluating the retrieved clinical data, these studies have showed an essential role of the interface in failure inducing of the glass ceramic restorations. Based on the retrieved clinical data, more than 90% of failure originated from the flaws and stress generated along the bonded surface rather than the functional surface. The interface has been highlighted as an interested area to be given further examination. (Lawn et al., 2004, Pallis et al., 2004, Lüthy et al., 2005, Pagniano Jr et al., 2005).

The effect of resin cement thickness on the fracture resistance of all-ceramic restorations is not well established. Lizuka et al. have reported that the retention of the crown depends on the cement film thickness, with the retention reducing as the film thickness increases (Iizuka et al., 1987). It has been reported that the film thickness of the adhesive resin cement has an effect on the joint bend strength of the dentine-ceramic interface, showing the bend strength value to be significantly lower for the 20-μm film than for thicker film thicknesses (Molin et al., 1996). A study has been done to determine the fracture strength of ceramic plates loaded in compression, using a spherical

indenter. The fracture strength of the ceramic that was cemented with zinc phosphate cement was found by the study not to be dependent on the film thickness of the cement. However, when the resin cement was used, a slight decrease in the ceramic fracture resistance became significantly important when the film thickness was 300μm or more (Scherrer et al., 1994).

Large marginal thickness and discrepancy can lead to exposure of the cement material to the oral fluid, leading to further cement dissolution due to the action of the fluid and the chemo-mechanical forces. Cement seals might become weak and that can lead to trapping of food and bacteria. Consequently, the longevity of a restored tooth with an ill-fitted crown could be compromised by caries and periodontal problems (Felton et al., 1991, Qualtrough et al., 1993, Beschnidt and Strub, 2001, Beuer et al., 2009, Reich et al., 2011).

A number of methods for measuring and assessing the internal and marginal adaptation of the crown have been described. Some of these were performed *in vivo* to measure the marginal thickness and accuracy, using a mirror and probe or by radiography. The other methods were performed *in vitro* by using the restored sample for subsequent assessment by measuring the cement space in the sectioned specimens or by taking elastomeric impression wash replicas of the luting space. Several studies have shown the reliability of the replica technique in measuring the interface between the prepared teeth wall and the crown (Shearer et al., 1996, Karakaya et al., 2005, Tsitrou et al., 2007, Laurent et al., 2008, Reich et al., 2011). However, the use of replica techniques for

measuring the accuracy of fit of the crown restoration has been questioned by Qualtrough et al. They have found that the silicon impression material used for replicating the interface gap may not exactly replicate the behaviour of the cement in the real clinical situation (Qualtrough et al., 1993).

Two main factors can affect the cement film thickness, namely, the viscosity as a function of time and the amount of the load applied during the cementation procedure. Magne et al. reported that a veneer ceramic restoration can be provided with a favourable configuration, with regard to propensity to crack, when a sufficient and even ceramic thickness is combined with the minimal film thickness of the resin lute cement. They recommended that the thickness ratio of the ceramic and the lute cement to be above 3.0 (Magne et al., 1999a).

2.7.2.4.2 Lute interface uniformity

All-ceramic restorations have a low ability to plastically deform under a load with a history of being prone to brittle fracture, especially if placed in a stress bearing area such as the posterior area. Many attempts have been made to overcome the shortcoming of brittle fracture. Very strong core ceramic materials have been developed to support the weaker veneer ceramic materials. However, even ceramic restorations with a strong core structure are still more brittle and less ductile compared with metal restorations. As a consequence, in all-ceramic restorations the preparation procedure and the cementation

technique are more critical than in metal ceramic restoration. Fracture resistance of the all-ceramic restoration as well as the adhesion between the tooth and the restoration can be affected by the shape of the preparation and of the cement layer (De Jager et al., 2005). In the machined all-ceramic crowns the cement thickness is not uniform, with the occlusal gap being larger than the marginal area (Reich et al., 2005).

It has been verified that stress development in the uneven cement layer will vary and the incidence of the failure in the bond strength of the adhesive cement might be increased(Mou et al., 2002, De Jager et al., 2005). The non-uniform cement film thickness can affect the bonding surface by increasing the maximum shear stress to values exceeding the bond strength of the cement layer to restoration and preparation. Thus, it is advisable to make the resin cement film thickness as uniform and as thin as possible (De Jager et al., 2005). However, there is still little precise information concerning the effect of the non-uniform resin cement film thickness on the structural integrity of all-ceramic restorations, so it is of interest to assess this factor.

2.7.3 Ceramics

For 2,700 years, ceramic has been a main material used to produce domestic objects. It is a clay, formed of inorganic non-metallic based material that can easily be fabricated by firing. Recently, ceramic has undergone significant sophistication in terms of both structure and manufacturing. Due to an increase in the demand for aesthetic restoration, the gold covering crown material began to be replaced by porcelain, which is more translucent, through the introduction of porcelain jacket crowns to clinical dentistry. The porcelain jacket crown has shown inevitable defects in terms of contraction and cracking on its surface. These defects have led to the necessity of modifying ceramic structures and firing procedures to create a very hard structure, which has opened up the horizons to the production of new materials and research in this area.

2.7.3.1 Structure of ceramic

The dental porcelain that is used nowadays differs from that used in earlier days. The ceramic, which was used for producing early pottery, was composed of kaolin, quartz and feldspar. The first modification in household ceramics involved omitting the kaolin because it is an opaque material. The quartz has remained unchanged and it acts as a strengthening agent in a form of crystalline dispersion in a glassy phase of the feldspar. The feldspar composition is a mixture of different proportions of potassium alumina silicate and sodium

alumina silicate. Any change in the proportions of potash and soda will affect the fusion temperature or the viscosity of the feldspar(Van Noort, 2007).

The first use of porcelain in dentistry was for single tooth crowning. Later, when restorations were required to be more than just aesthetic and factors such as performance and covering long spans of missing tooth became important, pioneers like Mclean changed the structure of the feldspathic porcelain by adding (Al_2O_3) to improve its mechanical and physical properties. Before Mclean's endeavours, there was another effort to enhance the strength of the porcelain jacket crown by fusing the porcelain to metal core. However, clinical weaknesses such as ceramic low tensile strength, brittleness, crack propagation and marginal accuracy have limited the use of this technique. The clinical shortcomings of this technique have led to introduce a new technique that depend on the use of the zirconia and alumina rather than the metal as a core material (Nam et al., 2008).

2.7.3.2 All-ceramic

In restorative dentistry the general trend has been inclined toward replacing metal based restoration with ceramic restoration (Blatz et al., 2003). However, there are several factors which affect the mechanical properties of all-ceramic restoration, for instance, ceramic microstructure, fabrication technique and type and method of using luting agent that may affect the performance of the ceramic (Kelly, 1999). The technique of etching the ceramic with hydrofluoric acid

followed by silanation and cementing the crown with adhesive luting resin can provide the all-ceramic restoration with high fracture strength when compared with non-adhesive cementation techniques (Diaz-Arnold et al., 1999).

The brittleness of the ceramic requires a greater margin of safety in strength compared to using metal. Basically, dental ceramic materials fail at 0.1% strain. Thus, increasing the strength and toughness of dental ceramic is possible through increasing, for example, the elastic modules of the luting materials or treating the ceramic with an ion exchange method using a KNO_3 (Addison et al., 2007). Gradually, ceramic materials have come to demonstrate tensile strength and fracture toughness ten time greater than that of the ceramic which was used in the past, and for that reason all-ceramic restorations are preferred by both patients and dentists (Pospiech, 2002).

2.7.3.3 Classification of ceramics

Ceramics have been classified into different categories according to different divisional patterns. However , the most important categories are based on the microstructure and processing techniques (McLaren and Cao, 2009).

Regarding the microstructure level, ceramics can be divided according to the glass/crystalline ratio into:

1- Group 1/ Glass-based systems (mainly silica)
2- Group 2/ Glass-based systems (mainly silica) with fillers, usually crystalline (typically leucite or, more recently, lithium disilicate)
3- Group 3/ Crystalline-based systems with glass fillers (mainly alumina)
4- Group 4/ Polycrystalline solids (alumina and zirconia)

2.7.3.4 Glass based systems (Glass ceramic)

This type of ceramic consists mainly of silicon dioxide (also known as silica or quartz); this contains various amounts of alumina. Basically, alumina-silicates are found in nature, but with different ratios of sodium and potassium. The two components of alumina-silicate (sodium and potassium) are both feldspars.

Feldspars are modified synthetically in many ways to create the material used in dentistry known as ceramic.

The first used of glass-based ceramic was for producing denture teeth. This material is found in two forms: powder –liquid form and machinable (block ceramic) form. Machinable block ceramic, such as Vitablocs Mark II (Vident), is used with the CEREC®CAD/CAM system (Sirona Dental Systems, Charlotte, NC). For fabrication of inlays and onlays, it was found that this machinable block obtained the most clinically successful results, with studies showing a < 1% per year failure rate (Reiss and Walther, 2000). The most important benefit that can be gained from the pre-manufactured block is the absence of the

residual porosity that can make a weak point in the core of the final restoration and potentially lead to catastrophic failure.

The powder liquid form was produced for specific purposes, such as veneering of alumina-based core systems, e.g., In-Ceram® (Vita Zahnfabrik, distributed by Vident, Brea, CA) and Nobel Procera™ (Nobel Biocare, Yorba Linda, CA).

2.7.3.4.1 Glass-based systems (mainly silica) with fillers, usually crystalline

(Typically leucite or, more recently, lithium disilicate)

This group has a wide range of glass/crystalline ratios to the extent that they can be divided into three sub groups according to the amount of crystal or filler that they contain. Basically, the glass is of the same structure as the first group and the differences are only in the type and the amount of the crystal. The main crystals which are added to the glass ceramic are leucite, lithium disilicate and fluoroapatite.

2.7.3.4.2 Subdivision 1 - low to moderate leucite containing glass

In this group, the leucite is created by increasing the amount of potash K_2O to more than the amount that occurred originally in the glass ceramic, and this is called feldspathic porcelain. The amount of potassium oxide which is added to the glass ceramic depends on the core that will be used with it, such as metal or zirconia core. The leucite is added to glass ceramic to increase the coefficient of thermal expansion of the ceramic to make it suitable for applying to any type of

material core, such as metal or zirconia. Feldspathic porcelain is fairly random in size, arrangement and distribution of leucite. Therefore, due to this randomness, the material has low fracture resistance and abrasive properties (McLaren et al., 2003). More recently, after different attempts to improve the properties, a new generation has been introduced, which is called (VM 13, Vita). This type is composed of fine leucite crystals and has very even crystal distribution. It has higher flexural strength and fewer abrasive properties than the first generation (McLaren and Giordano, 2005).

2.7.3.4.3 Subdivision 2 - High leucite containing glass:

In this sort of ceramic, the amount of leucite by volume is equal to approximately 50% of the glass. This category of the glass material has been found in different forms, such as powder-liquid, block and pressable. This type of ceramic is produced by a process called controlled crystallization of glass, in which the crystalline phase is grown in a glass matrix, while in the feldspathic porcelain (subdivision 1) the crystalline leucite is added to a glass matrix. IPS Empress® (Ivoclar Vivadent, Amherst, NY) is the most popular type of this material.

Pressable and machinable high-leucite ceramics are used with both CEREC and E4D (D4D Technologies, LLC, Richardson, TX) and have showed clinically superb results when used for posterior inlays, onlays, anterior veneer and crown restorations (Wagner et al., 2003, McLaren and Giordano, 2005).

2.7.3.4.4 Subdivision 3 - Lithium disilicate glass ceramic

Lithium disilicate is created in dental ceramic by adding Li_2O to the aluminum silicate glass. It is developed in 1998 by Ivoclar company as IPS Empress®II, which is used for fabricating a three unit fixed bridge in the anterior region. Although IPS Empress®II demonstrating a high strength, veneering this material was inevitable because it is opaque material.

In 2007 the new generation of lithium disilicate (with higher strength and great scale of translucency) was launched on the market and known as (IPS e.max®). The IPS e.max® comes in two forms: pressable and machinable (e.max® press and e.max® cad respectively). The flexural strength and fracture toughness have been made twice as strong; this is due to the amount of the crystal in the material as a whole, which is equal to 2/3 of the material, and to the needle-like shape of the crystal (Albakry et al., 2003).

The shade and translucency of the dental materials could be considered as a major request for the esthetic demand. Lithium disilicate ceramic has been developed with a wide range of translucency which is sufficient for use as a full anatomical crown restoration without the need for veneering by other ceramic materials. In order to obtain a maximum aesthetic quality, sometimes lithium disilicate ceramic crown could be veneered with an apatite glass ceramic (McLaren and Cao, 2009).

2.7.3.5 Crystalline-based systems with glass fillers

The fracture strength of this type depends on the crystals' properties and types; in contrast to glass and leucite-based glass ceramics they are dependent on the processing technique rather than their crystals (Reiss and Walther, 2000, Van Dijken et al., 2001). The first such system was used in 1988 and was called In-Ceram. It was designed as an alternative material to ceramic fused to metal. It is partially sintered alumina; the strength of In-Ceram matches that of the conventional metal-ceramic crown and it demonstrate high clinical strength (Pröbster, 1993). In this system, because of the high temperature used in sintering, the crystalline particles are linked to each other by a special junction, unlike the process for glass ceramics, in which their matrix is embedded with crystals without a junction between the crystal particles. The high strength of this system is attributed to the needle-like shape of the crystals, and to the minimal glass content. Many studies that have been conducted to evaluate the use of In-Ceram as a single crown have reported a high rate of success for anterior teeth up to the first molar, except for one study which showed a high rate of failure in the second molar (McLaren and White, 2000). In-Ceram's crystalline phase can be alumina only, alumina and zirconia, or an alumina and magnesia (spinell). These types are created by a technique called slip casting, or can be created from a pre-sintered block of the same material as produced by slip casting. The crown framework consists of alumina or spinell infiltrated at high temperature by low viscosity lanthanum glass. Many studies have

demonstrated that the flexural strength of this sort of dental ceramic is three to four times superior to that of any other glass ceramic (Giordano II et al., 1995). In-Ceram alumina and alumina/zirconia are used mainly for molars because of their opacity. However, although alumina/magnesia (spinell) has strength about half that of the alumina/zirconia, it is used for anterior teeth because of its higher translucency (McLaren and Cao, 2009).

2.7.3.6 Polycrystalline Solids

This system is the strongest of the all-ceramic systems because of its solid sintering and monophase structure. Through sintering alumina- oxide or zirconia- oxide at a very high temperature, polycrystalline ceramic becomes a very hard structure because it is formed through an air free and glass free process. Despite the excellent properties of polycrystalline in terms of strength and toughness, it is a new invention in terms of fabrication of crowns and bridges because of the high temperatures used in firing and inevitable shrinkage. There are three types of polycrystalline ceramic fabrication; the first uses machining of the fully sintered block, but this is very expensive because it requires the use of special machinery due to the very hard structure. Procera is another technique, whereby an oversized die is used and slurry of alumina-oxide or zirconia- oxide are applied and then firing takes place. A more recent procedure is to machine oversized cope made from a block of partially sintered

zirconia–oxide then fire it at a high temperature to shrink and fit the die. Zirconia has special properties, which are not found in any other types of ceramic in terms of flexural strength and toughness, which are reported as 900 MPa to 1,100 MPa and 8 MPa to 10 MPa respectively. The unique properties of zirconia make it two times stronger and tougher than alumina based ceramic (see figure 2-3) (Van Dijken et al., 2001, Brochu and El-Mowafy, 2002, Albakry et al., 2003).

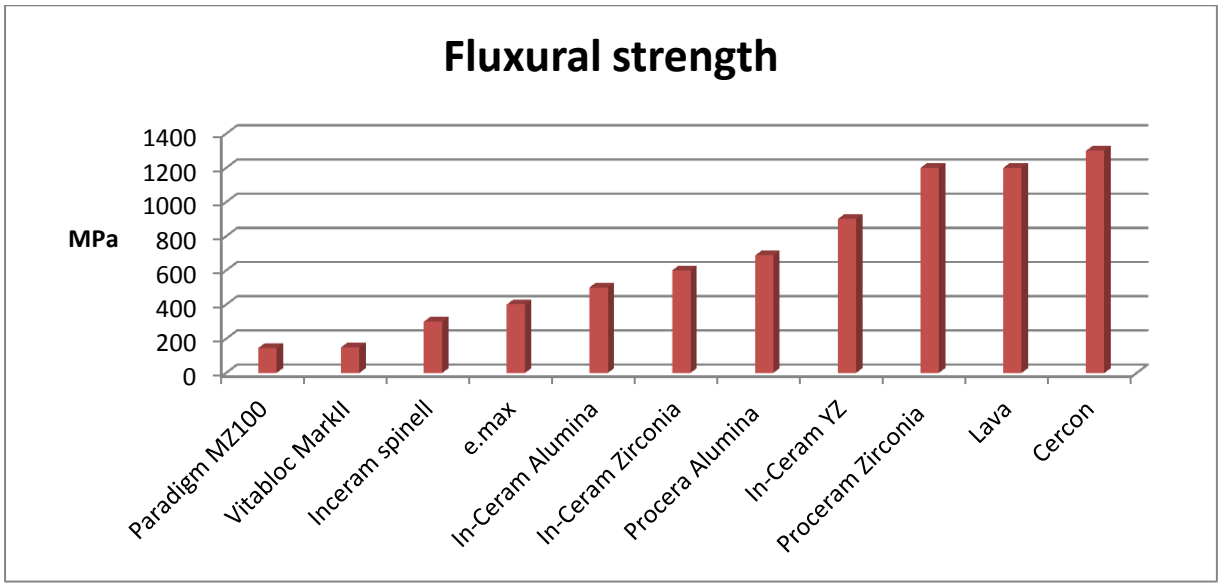

Figure 2-3: Flexural strength of the ceramic

The information was collected from brochures as detailed: Ivoclar/Vivadent (e-max), 3M ESPE (lava, Paradigm MZ100), DENTSPLY (cercon), Nobel Biocare (Procera Zirconia, Procera Alumina), and VITA (In-Ceram [YZ, zirconia, alumina, and Spinell]; Vitablocs Mark II.

The sources of the graph are:

e-max, Available from:
http://www.ivoclarvivadent.us/emaxchangeseverything/lithium-disilicate/index.php.
[Accessed 5th Dec 2012].
lava, Available from:
http://solutions.3m.com/wps/portal/3M/en_US/3M-ESPE-NA/dental-professionals/products/category/digital-materials/lava-plus-zirconia/.
[Accessed 5th Dec 2012].
ParadigmMZ100, Available from:
http://multimedia.3m.com/mws/mediawebserver?mwsId=66666UF6EVsSyXTtOxM_5x46EVtQEVs6EVs6EVs6E666666--.
[Accessed 5th Dec 2012].
Cercon, Available from:
http://www.dentsply.ca/media/800261%20Cercon%20Z%20ConsrvOptns.pdf.
[Accessed 5th Dec 2012].
Procera Zirconia, Available from:
http://www.nobelbiocare.com/Images/en/Q3_Crown_Zirconia_0.4_Product_Release_v2.5_tcm261-30070.pdf.
[Accessed 5th Dec 2012].
Procera Alumina, Available from:
http://www.dentsply.ca/media/800261%20Cercon%20Z%20ConsrvOptns.pdf.
[Accessed 5th Dec 2012].
In-Ceram , Available from:
http://vident.com/products/cadcam/vita-in-ceram-yz/.
[Accessed 5th Dec 2012].
Vitablocs Mark II. , Available from:
http://www.vita-zahnfabrik.com/resourcesvita/shop/en/en_3055534.pdf.
[Accessed 5th Dec 2012].

2.7.3.7 Ceramic fabrication techniques

There are many techniques for processing any material but for dental ceramics, there are only four techniques. Basically, dental ceramic is processed by means of the old technique (sintering) but, recently, to produce higher quality ceramic (glass ceramic), different techniques have been used, such as slip casting, heat-pressed and machined ceramic.

2.7.3.7.1 Sintering

This is the oldest technique for processing dental ceramic. Sintering can be defined generally as the transformation of a material from a porous compact phase to a denser and stronger phase. The most specific definition of sintering is that it is a process of complex steps of high temperature reaction above the softening level of dental porcelain, as a consequence of which, the glass matrix is partially melted, with coalescence of powder particles. Normally, during the increasing of temperature the density of the ceramic increases significantly but this is accompanied by 30-40% volume shrinkage (Denry, 1996). Only two types of all-ceramic are suited to the sintering procedure: Leucite reinforced feldspar and alumina reinforced feldspar.

The process of sintering falls into two types: liquid phase and solid phase sintering. Liquid phase sintering is used with leucite ceramics, whereas the solid phase sintering applies to application to alumina and zirconia after CAD/CAM processing for the last densification firing. After undergoing the sintering process, the dental ceramic becomes a structure of the crystalline phase surrounded by a glassy phase. The strength of dental ceramic can be modified according to the crystalline phase content (Raigrodski, 2005). Generally, the most important properties in ceramics are strength and translucency. The higher the crystalline constituent (up to 90% by volume), the better the mechanical properties, and the higher the glassy phase, the better the optical properties (Craig et al., 2006).

2.7.3.7.2 Hot-pressed "heat-pressed" ceramics

Hot-pressing is another high-technology ceramic processing technique used in dentistry. This process depends on the external application of pressure at a high temperature in order to achieve the sintering of the ceramic body. Large pores caused by non-uniform mixing can be avoided by the hot-pressing technique. Two types of ceramic can be used with heat-pressed ceramic processing techniques: Leucite reinforced ceramic and lithium disilicate reinforced ceramic. Since ceramic treated by heat-pressing technique can achieve a high density and small grain size arrangement, hence the mechanical properties can be improved (Denry, 1996, Gonzaga et al., 2008).

2.7.3.7.3 Slip casting

The slip casting processing procedure is used in dentistry to create great strength in ceramic core frameworks. Basically, this procedure depends on the use of an aqueous porcelain slip to be condensed on a refractory die. The water of the slip is absorbed by the capillary action of the porous surface of the die and will lead to condensing of the slip on the die. After that the piece has to be fired at a high temperature (1150° C). Normally, the die will shrink more than the porcelain, which makes the separation easier. This procedure produces a porous core, and then the fired porous core is glass infiltrated by a unique procedure of drawing molten glass into the pores by capillary action at high temperature. However, the lengthy time of processing is the main disadvantage

of this technique. The structure of the material which is produced by slip casting shows good properties in terms of low porosity and fewer defects than the structure of material that is produced by sintering processing technique. The alumina based ceramic (In-Ceram) that is produced by this procedure has three to four times greater strength than the earlier alumina core material. All-ceramic restorations depending on the use of Alumina-based, spinell-based and zirconia-based ceramics can be fabricated by using the slip-casting technique (Rosenstiel et al., 2006).

2.7.3.7.4 Machining ceramic (by CAD/CAM)

Factors that influence the clinical survival rate of ceramic dental restorations include the density, severity and location of flaws within the ceramic structure. The failure of the dental ceramic restoration can start from flaws such as cracks and voids even if they are only small structures. The stress raising effect of these flaws can lead to reduction of the strength of the structures and this is in turn leads to reduction in the durability of the ceramic restoration. As a consequence of the effect of load application, the corrosive nature of the oral fluid, and the residual stress, crack propagation is possible. Eventually, the resistance of the ceramic to fracture may decrease and that can lead to a fracture of the whole restoration under a normal load (Tinschert et al., 2000). Strength of the brittle material such as ceramic can be measured by a Weibull modulus. It is a parameter that is used to measure the strength of brittle materials depending

on the distribution of the physical flaws that present in the body or on the surface of the brittle specimen. If the flaws are few in number and evenly distributed, the ceramic is stronger and the value of Weibull modulus is higher (Klein, 2009). The ceramic restorations that are fabricated by following conventional laboratory methods have sizable flaws, which increase the failure rates. On the other hand, dental restorations fabricated from industrially produced ceramic have a minimum of cracks, voids, and flaws because the ceramic material is manufactured under controlled industrial conditions. The ceramic that is produced in this way has greater reliability and restorations using this type of ceramic are more homogenous and stronger (Tinschert et al., 2000, Jedynakiewicz and Martin, 2001). Data recorded by Tinschert et al. 2000, show that all-ceramic materials that are produced industrially are more structurally sound, as is demonstrated by the higher Weibull modulus values. Since, the structural reliability of the ceramic can be optimised when the restoration is manufactured by machining industrially fabricated ceramic block, the CAD/CAM technique for fabricating dental restoration can offer one solution to the manufacturing problem. However, it is still unclear what effects such a machining technique has on the fracture behaviour of the entire restoration (Tinschert et al., 2000).

2.7.3.8 All-ceramic forms

Ceramic can be classified according to the physical forms of the products that are found in the market, such as ceramic powder, ingot, and blocks.

2.7.3.8.1 Conventional powder

Slurry ceramic – This type of ceramic is supplied as a powder and the technician adds water to produce slurry. The final contour of the restoration is produced by building up layers of this slurry on the die material. The ceramic powder is available in different shades and translucencies, with the possibility of staining and glazing.

2.7.3.8.2 Castable ceramic

This type is supplied as solid ceramic ingots. A full crown or core can be fabricated by using the lost wax and centrifugal-casting technique of the castable ceramic. Usually, this type of ceramic comes in one shade and is covered by normal feldspathic porcelain later.

2.7.3.8.3 Pressable ceramic

This is also supplied as ingots, and the system is based on melting the material at high temperature and then pressing it into a mould that has already been created using the lost wax technique. This system can create either a full contour crown or substrates which can be covered by conventional porcelain build up.

2.7.3.8.4 Machinable ceramic

This system is supplied in the form of blocks of different shades and can be used with CAD/CAM. The final restoration can be stained or glazed.

2.7.4 CAD/CAM in dentistry

CAD/CAM is used in dentistry as a synonym referring to any restorations or prostheses that are produced by using milling technology**.** However, the exact meaning of CAD/CAM is Computer-aided design/computer-aided manufacturing technology, a term which was first used in dentistry back in 1985 (Mörmann, 2006, Beuer et al., 2008). CAD/CAM allows the use of materials in dentistry that could not be used in usual methods of dental processing. Despite the major drawback of CAD/CAM systems, namely the high investment necessary in machines that might be beyond the budgets of smaller laboratories, the advantages are great. The main advantage of using CAD/CAM in dentistry is that it allows the application of new and better materials that could not be used in the fabrication of prostheses based on the usual procedures used before the introduction of CAD /CAM system. Moreover, reductions in the labour and restoration costs can be achieved. The advantage with the most potential is the ability to control the quality of the prostheses (Miyazaki et al., 2009). After the successful use and observation of CAD/CAM in different dental applications such as inlays, onlays and FPDs (Williams et al., 2006), this system is expected to be used in producing removable partial dentures and dental implants.

Therefore, the application of CAD/CAM technology is promising in terms of the development of high quality devices in all dentistry fields (Mehl and Hickel, 1999, Miyazaki et al., 2009).

2.7.5 Development of CEREC machines

During the last few decades, the dream of producing chair-side all forms of ceramic crown has become a true option with the advent of the CAD/CAM system. There are different systems available on the dental market, such as: Celay, Mikrona, CEREC, Sirona Procera, and Nobel Biocare. All these systems are based on the use of digitally recorded preparation data to produce a machine based crown and crown core. The greatest success in using these systems for all-ceramic crown has been achieved by using CEREC 1(Mörmann et al., 1989, Mörmann, 2006). The positive results of long term studies on restorations such as inlays and onlays of feldspathic ceramic produced by using CEREC 1 have led to research being expanded to include tooth crowns (Reiss and Walther, 2000, Otto, 2004). CEREC 2 has allowed an all- ceramic crown to be produced for the first time, most often using traditional techniques such as reference impression or wax up (correlation technique) to support the design (Otto, 2004). When CEREC 3 was introduced to the dental market it became possible to fabricate all-ceramic crowns directly in routine clinical procedures at chair-side due to the possibility of not having to use any pre-impressions (see table 2-1) (Datzmann, 1996).

Table 2-1: Evolution of the CEREC system(Mörmann, 2006)

YEAR	HARDWARE	SOFTWARE CAPABILITY	RESTORATION TYPE	DEVELOPER
1980	Basic concept	Two-dimensional	Inlays	Mörmann (University of (Zurich) and Brandestini (Brandestini Instruments, Zurich)
1985	CEREC 1	Two-dimensional	First chairside inlay	Mörmann and Brandestini (Brains, Zurich)
1988	CEREC 1	Two-dimensional	Inlays (1), onlays (2), veneers (3)	Mörmann and Brandestini
1994	CEREC 2	Two-dimensional	1-3,partial (4) and full(5) crowns, copings (6)	Siemens (Munich, Germany)
2000	CEREC 3 & inLab	Two-dimensional	1-6 and three-unit bridge frames (inLab)	Sirona (Bensheim, Germany)
2003	CEREC 3 & inLab	Three-dimensional	1-6 and three- and four-unit bridge frames (inLab)	Sirona
2005	CEREC 3 & inLab	Three-dimensional	1-5 automatic virtual occlusal adjustment	Sirona

2.7.6 Single (monolithic) and Bi-layer (two-layer) All-ceramic crown

For a long time ceramic materials have been used as mono-phase (single) layer restorations (Kelly et al., 1989) . Single layer restoration was used more often for the anterior teeth because they are subjected to less biting force than the posterior teeth (McLaren and White, 2000). However, the new versions of the ceramic materials are crystalline in nature (McLaren, 1998). Single layer ceramic restorations have a great drawback in the form of relatively low strength (Liu and Chen, 1991, Sundh et al., 2005).

As a consequence of this disadvantage, attempts were made to enhance the low strength by reinforcing the glassy matrix of these materials. However, the result was an opaque ceramic that lacked some required properties, particularly when anterior teeth needed crowning, such as translucency, opalescence, and fluorescence, which normally give ceramics their attractive aesthetic uniqueness. Currently, the core and framework structure that is used for the construction of all ceramic crowns and fixed partial dentures using CAD⁄CAM is built up most often from zirconia, which is further veneered by feldspathic ceramic to obtain the required aesthetics. The new type of crown construction (core and veneering) combines both strength and aesthetics; for this reason it can be used for both the anterior and the posterior teeth (Shen and Kosmac, 2013) .

The structural integrity of the bi-layer ceramic system depends on several factors. The factors that must be considered during the fabrication of this system

include the framework design, veneering ceramic thickness, correct selection of the luting agent, insertion technique, and functional loads predict. Other important factors are layering technique, the difference in coefficient of thermal expansion of the materials being used, firing programme and cooling stresses (Isgrn et al., 2003, Fleming et al., 2005, Fleming et al., 2006). The appropriate bond strength at the core/veneer interface is considered an important factor that affects the structural integrity of bi-layer ceramic under applied force (Aboushelib et al., 2008 a).

Moreover, it has been found that the dual layer ceramic crown differs from the single layer ceramic crown in terms of stress distribution, which is related to the difference in elastic properties of the material used in bi-layer from homogenous single-phase material (Aboushelib et al., 2008 b). Stiffness disharmony can affect greatly the stress distribution between the first and second layers of the crown structure (core and the veneer interface). Normally, the elastic modulus of core ceramics material is high compared with the material of a veneering ceramic layer, whilst even if the stiffness disharmony is small, it can lead to lower peak stresses and smaller stress discontinuities in the core/veneer interface. Generally, the disturbances in stress distribution can cause shear stress concentration, and later, de-bonding in the core /veneer interface (Goetzen et al., 2003).

Most studies that have investigated the failure in all-ceramic crown have shown that the crack has mainly been initiated in the core/veneer interface

(Kelly et al., 1995, Zahran et al., 2008). Most marketable ceramic systems depend on the use of veneering ceramics of a slightly lower coefficient of thermal expansion compared with that of the framework material. The idea behind this slight coefficient of thermal expansion mismatch is to create compressive stresses in the weaker veneering ceramic and that will lead to enhancement of the general strength of the restoration (De Jager et al., 2005). This method is still used, with the porcelain being fused to metal restorations (PFM), and is also applied to metal free ceramic restorations (see table 2-2) (Twiggs et al., 2005).

Table 2-2: Suitable ceramic materials for use with CAD/CAM System

BLOCK NAME	System	Flexural strength	Clinical indication	company
Vitablocs mark II	Feldspathic ceramic (SiO_2-Al_2O_3-Na_2O-K2O)	154±15MPa	Onlay, 3 /4 crown, crown ,veneer	Vita Zahnfabrik
IPS ProCAD	Leucite glass ceramic (SiO_2-Al_2O_3-K_2O)	150 MPa	Onlay, onlay, 3 /4 crown, crown	Ivoclar Vivadent
IPS Empress CAD	Leucite glass ceramic (SiO_2-Al_2O_3-K_2O)	160MPa	Onlay, onlay, 3 /4 crown, crown, veneer	Ivoclar Vivadent
IPS e.max® CAD	Lithium- disilicate ceramic (SiO_2-Li_2O)	360-400 MPa	Veneers, inlays, onlays, crowns	Ivoclar Vivadent
Dicor MCG	Glass ceramic matrix with Tetra silicicfluoromica (K2MgDSisO20F4)	<100 MPa	Veneers, inlays, onlays, crowns	Dentsply
Paradigm c	Two face leucite glass ceramic	115-135MPa	Inlay, onlay, veneer, crown	3M ESPE
Paradigm MZ100	Hybrid composite with zirconia silica fillers	146	Inlay, onlay, crown, veneer	3M ESPE
In-Ceram Alumina	Aluminium-oxide (Al_2O_3)	350-500 MPa	Crown, FPD anterior	VITA Zahnfabrik
In-Ceram Spinell	(MgAl2 O4)	300-350MPa	Crown	VITA Zahnfabrik
Procera Alumina	Alumina	487-687 MPa	Veneer, crown, anterior FPDP	Nobel Biocare AB, Sweden
Lava	Zirconia (ZrO_2 stabilized by Y_2O_3)	1000-1200 MPa	Crown, FPDP	3M ESPE
Procera zirconia	densely sintered high-purity zirconium-oxide ceramic	1200 MPa	Crown, FPDP, Implant abutment	Nobel Biocare AB, Sweden
Cercon	ZrO_2	1200-1350 MPa	Crown , FPD for anterior and posterior	Dentsply DeguDent

2.8 Technical fabrication parameters

Several factors affect the longevity of the restoration. The fit or accuracy of the marginal and internal adaptation is valued as one of the most important requirements for achieving the best clinical quality and success of the fixed restorations(Qualtrough et al., 1993). There are various stages in the process of fabricating ceramic restoration such as 3D image capturing, model designing process and pressing or milling process. However, during each stage there are several factors that might affect the final fit of the restoration. Consequently, the longevity of a restored tooth with an ill-fitted crown could be compromised by restoration, tooth fracture, dental caries or periodontal problems (Felton et al., 1991, Qualtrough et al., 1993, Beschnidt and Strub, 2001, Beuer et al., 2009, Reich et al., 2011).

2.8.1 Capture of the preparation

2.8.2 Physical: (conventional impression)

Several factors have been identified which can affect the accuracy of dental impression, such as the correct manipulation of the materials, impression techniques, inappropriate management for the oral soft tissue, difficulties in accurate re-insertion of the impression to same position in wash technique, the wettability of the impression materials, the use of custom or stock impression trays and impression distortion before pouring(Thongthammachat et al., 2002, Cowie and Boksman, 2007, Christensen, 2008).

2.8.3 Optical: (the effect of the scanning powder)

There are ranges of intra-oral and lab-based optical data acquisition systems, such as Everest Scan II from KAVO, DENTSCAN from Delcam and inEos from Sirona. Some of these systems, like CEREC, use a contrast reflective powder for this process. There is an evidence to suggest that the thickness of the powder used could affect the accuracy(de Sousa Muianga, 2009).

2.8.4 Configuration of the spacer

2.8.4.1 CAD/CAM: (the pre-set up parameters value could not represent the true clinical value)

It has been found that when the luting space parameters are set to any value in microns, the internal and marginal gaps of the crowns are greater than the value that was set (Nakamura et al., 2003, Bindl and Mörmann, 2005).

The accuracy of the CEREC milling system is determined by the resolution of the CEREC capturing device (25 μm) and the reproducibility of the milling unit (± 30 μm). Excluding user-induced influences (e.g. preparation, powdering and exposure technique), the precision of CEREC 3D is in the range ± 55 μm. (The information was collected from some brochures of Sirona Dental Company).

After milling, the crown should be sintered and glazed. Sintering and glazing the crown result in a shrinkage of 0.3%(Reich et al., 2011) .

2.8.4.2 Pressed technique: (painting spacer layers)

The final film thickness of the interface lute depends on the skill and experience of the technician (how many spacer layers are required and how to apply them). The type and thickness of the spacer's powder could affect the internal and marginal fit of the restoration (Addi et al., 2002, Yeo et al., 2003, de Sousa Muianga, 2009).

2.8.4.3 Wax printer:

Wax printing can be considered as a new optimistic approach in producing an accurate restoration in dentistry. Some types of high precision 3D wax printers have been advertised to have a rate of error no greater than ±0.001 inch per inch(±0.0254mm) across the XYZ dimensions (The information was collected from brochures of Solidscape® and dentaCast® companies).

2.8.5 Fabrication of the crown

2.8.5.1 Milling in CAD/CAM:

Milling accuracy depends on;

- The CEREC software development (the accuracy of marginal and internal fit has improved with the development of the software from CEREC1 to the current version).
- The hardware has a great effect on the accuracy, such as the movement axis of the bur (2, 3, 4 or 5 axes of bur movement) as well as the shape of the milling bur. An introduction of the step bur with a tip diameter of 1 mm has represented a major improvement in the ability of the milling bur to cut a small area (The information was collected from brochures of Sirona Dental Company).

2.8.5.2 Pressing technique:

During the pressing technique of the ceramic ingot, several factors that might affect the accuracy of the crown; these include thermal shrinkage of the wax pattern and ceramic coping that occur upon cooling at room temperature and casting, respectively. On the other hand, the thermal expansion of the investing material could not compensate completely the aforementioned shrinkage. Thus, the significant shrinkage of the wax pattern could make an additional misfit (Schaefer et al., 2012) .

2.9 Performance of Ceramic systems

2.9.1 Failure of ceramics

A main problem with all-ceramic restorations is the existence of surface micro-porosities and microscopic cracks that develop during densification (Pröbster et al., 1997, Ohyama et al., 1999). As a stress-raising factor, ceramic defect areas or flaws have a strength-reducing effect on the whole structure, which can adversely affect the durability of the restoration (Tinschert et al., 2000).These defects are found in the material either intrinsic (for instance, a flaw that happens during densification) or extrinsic (such as flaws that might happen during fabrication, finishing and polishing) (Pallis et al., 2004). These flaws can decrease the fracture resistance of the all-ceramic restorations, prompting crack initiation and propagation, which can eventually lead to failure of the restoration (Morena et al., 1986, Kelly et al., 1995, Pallis et al., 2004).

Ceramic based restoration is naturally brittle and subjected to repetitive mastication forces during their clinical service. In the brittle materials, the flexural strength and fracture toughness could describe the response of these materials to the occlusal loads (Yilmaz et al., 2007).

Researches, during the past 30 years, have focused on improving the bulk strength of the ceramic materials by increasing the resistance of the materials to crack propagation. One of the most important measures to address this problem was achieved by incorporating leucite crystals into the ceramic structure and

generating barriers that would counteract the generated tensile stresses that cause the creation of microcracks and so prevent crack propagation (Dong et al., 1992, Ohyama et al., 1999). Thus the restoration does not suffer from catastrophic failure while functioning. Additionally, during the casting process the use of heat and pressure in combination has been shown to reduce the amount of ceramic shrinkage, resulting in higher flexural strength. The improvement of flexural strength and fracture resistance through adding leucite crystals is called dispersion strengthening (Dong et al., 1992, Brochu and El-Mowafy, 2002). Laboratory investigations have clearly proved that an increase in surface roughness of ceramic can significantly reduce its strength (De Jager et al., 2000, Pagniano Jr et al., 2005). It is well recognized that if the surface of glass is etched with hydrofluoric acid, this can increase the glass strength by several degrees of magnitude (Pagniano et al., 2005).

The mechanisms of impeding of the crack extension in the brittle materials such as the ceramic by microstructural, environmental and mechanical factors are called extrinsic toughening. The mechanism of the extrinsic toughing can be established by the formation of an inelastic zone that encloses the crack, which promote the resistance to crack propagating. The extrinsic mechanisms of toughening the brittle material have been categorized as (1) crack-tip deflection (2) crack-tip shielding (3) crack bridging (Ritchie, 1988, Ritchie, 1999, Pagniano et al., 2005, Launey and Ritchie, 2009).

Ceramic is inherently brittle materials and extremely sensitive to flaws. It has been recognized that cracking is one of the most important problems that glass ceramic suffers from. Generally, fatigue means the stress which needs to be applied might be lower than the stress required to cause an immediate fracture; this will produce failure of the material after a period of time (Adair, 1971, Launey and Ritchie, 2009).

Oral environment components such as the water in saliva and dentinal tubules as well as the effects of temperature can jeopardize a ceramic restoration's structure by increasing the effect of stress in the crack propagation process, which is called stress-corrosion (Morena et al., 1986, Kelly et al., 1995). In the stress-corrosion process, when glass ceramic is exposed to water, the glass will absorb a moisture film spontaneously, followed by degradation of the glass structure. The degradation of glass occurs due to the breakup of some of the silica bonding in the surface layers of the glass (Adair, 1971, Lohbauer et al., 2002).

It has been proved that the strength of the glass is affected by the surrounding medium. For example, the strength of the glass can be reduced by 20% or more if the newly cracked piece of glass ceramic is moistened by water (Adair, 1971). As a result, after long-term loading the crack propagation will occur at a stress level lower than expected (Raigrodski, 2004). Nevertheless, in the polycrystalline ceramics, where the glassy phase is missing, this phenomenon has not been seen (Raigrodski, 2004).

Stress corrosion of glass ceramic accompanied by residual stress, which is generated from both masticatory-related factors and mismatching of thermal expansion between the various components of the restoration, can predispose the ceramic to crack propagation in primary flaws (Morena et al., 1986). Hence, the ceramic restoration over time can become cracked under normal loads, even at near zero values, due to crack propagation. Even the small stresses which occur during fabrication or cementation can lead to the fracture of the whole restoration (Tinschert et al., 2000).

Generally, to estimate the longevity of all-ceramic restorations, fatigue testing and thermocycling have to be undertaken to simulate the natural oral conditions. It has been proved that there is a significant difference in the endurance limits of ceramic in terms of static and dynamic load application. It has been found that the endurance limit for fatigue cycling is approximately 50% less than the maximum fracture strength recorded by the static fracture strength test (Wolfart et al., 2007).

In general, there is a variation in the resistance of ceramics to tensile and compressive stress. Ceramic has less resistance against tensile stresses compared with compressive stresses.

Thus, the areas in ceramic structure that are subjected to higher tensile stresses are susceptible to fracture. Clinical failure of all-ceramic dental restorations is

frequently initiated as a fracture along internal surfaces and propagated through the material, leading to a fracture of all the restoration (Kelly et al., 1989).

Generally, the retrieval evaluation of clinical failure of all-ceramic restoration suggests that the majority (more than 85%) of these failures of ceramic restorations have a tendency to start from flaws and stresses initiated from the interface rather than from external surfaces(Thompson et al., 1994, Aboushelib et al., 2007). Hence, the interface is a location of high tensile stress; the internal surface characteristics of ceramic crowns are currently believed to be an important source of flaws (Kelly et al., 1995).

2.10 Structural integrity

The structural integrity is a term that indicates the ability of the body to survive the designed load without fracture. Patterns of failure or survival of the teeth are regarded as a key for understanding the structural integrity of the teeth (Lee et al., 2009). With the introduction or improvement of the dental materials and techniques, the preservation of tooth integrity has become the main trend of modern dentistry (St-Georges et al., 2003). Basically, there is a little knowledge regarding the fundamental nature of the enamel fracture process, especially in relation to tooth geometry and internal microstructure of the underlying structures. However, fracture properties of tooth crown has been thoroughly covered in the materials science literature (Lawn et al., 2007, Rekow and Thompson, 2007).

Evidences have revealed the fracture of the enamel most often start from the intrinsic defects, such as a hypocalcified fissures extending outward from the dentino-enamel junction. Basically, these flaws tend to lie within the organic sheet along the plane of weakness that delineates the enamel prism or structure. Nevertheless, it was proved that the external defects can be produced due to the force that exert in the mastication movement. These external defects yield by inter-prism slippage immediately below the occlusal contact (He and Swain, 2007). To date, few attempts have been made to quantify the fracture process in regarding to the bite force (Popowics et al., 2001).

Generally, a fracture or failure in any component of an adhesively cemented all-ceramic crown can be seen as a failure of the whole system as they work as a one unit. The failure rate may be worsened by exceeding the recommended tooth reduction during tooth preparation within the procedure of tooth restoration with an all-ceramic crown. Over preparation of a tooth weakens the remaining tooth structure and makes it fragile and prone to fracturing under low force (St-Georges et al., 2003).

The design of the ceramic crown can have a significant effect on the failure of the restored tooth. It has been proved that in a 1mm occlusal ceramic thickness the value of shear and tensile stress exerted on the tooth is much greater that the value of the force exerted if the thickness is 1.5mm (Cheng et al., 2003). Ceramic materials have a wide range of fracture resistance ability. Ceramics

with high fracture resistance, like zirconia or alumina, survive longer than those with low fracture resistance, such as feldspathic ceramic. A follow up study carried out on 86 restorations for 4 years revealed success rates of 100% and 98.3% in natural and implanted teeth respectively with procera all-ceramic crowns after 4 years (Zarone et al., 2005b).

Dental cement has two main functions: to establish or increase the retention of the prosthetic appliance to its abutments and to maintain prosthetic integrity (De La Macorra and Pradíes, 2002). Generally, the resin cement has a significant effect on enhancing the fracture strength of the all-ceramic crown and reducing the microleakage under it (Blatz et al., 2008). Resin cement is performing better than the ordinary cement when used with the crown restoration. It has been proved that the ceramic crown cemented with the resin cement results in a significantly higher fracture resistance value than cementing with the zinc phosphate and glass ionomer cements (AL-Makramani et al., 2008, Sorrentino et al., 2009).

Fatigue strength of the adhesively cemented tooth-ceramic crown complex can be affected significantly by the cement thickness, as restorations with a thick layer of cement exhibit a lower reliability under cyclic loading (Silva et al., 2008). Nevertheless, very thin cement layers should be avoided, as too thin the layer can adversely affect the longevity of the adhesively cemented all-ceramic crown (Mou et al., 2002).

All-ceramic crown manufacturing techniques can affect the success of the restoration and that in turn can affect the whole restored system. Reich et al. in their study have found that the cement under the machined crown is non-uniform and large gaps can be found occlusally compared with the marginal area (Reich et al., 2005). It has been confirmed that stress development under the uneven cement layer will vary and that might reduce the strength of the cement (Mou et al., 2002).

The uniformity and the width of the interface space between the restoration and the tooth wall might have a determining effect on the survival of the prosthesis (De Jager et al., 2005, Wang et al., 2007). The role of the uniformity of the cement on the structural integrity of a tooth restored with an adhesively cemented all-ceramic crown is still scarce and it would be very interesting to exploring that on the machined and pressed ceramic crowns.

2.10.1 Conventional full coverage crown restoration of the posterior teeth

The cast metal full coverage crown was for many years an excellent method for restoring the coronal part of carious or fractured teeth. The use of metal crown was considered for a long time as the mark of quality restorative care (Shillingburg et al., 2012). Gold was the most used metal for many years and

that was because of its noble properties. Nevertheless, lack of adhesion to the tooth tissue can be considered as the major disadvantage of gold.

Over many years, the cast metal crown has proved its worth through its excellent survival rates along with low rates of post-operative complications (Walton, 2002, Shillingburg et al., 2012). However, the increasing demand from patients for aesthetic tooth restoration, particularly in the anterior region, necessitated the search for other dental materials that would be more aesthetically pleasing.

As a result, porcelain jacket crowns have become more popular than cast metal crowns, as they possess excellent aesthetic properties.

Although the porcelain jacket crown is far more aesthetically pleasing than a cast metal crown and has been the material of choice since the early decades of the last century, its strength was initially not sufficient, especially when used in situations of heavy occlusion. Through the cooling of the porcelain from the furnace temperature, as the porcelain had low thermal conductivity, the outside would cool more rapidly than the inner side. As a consequence, the outer surface of the crown would contract more than the inner surface, resulting in compressive stress on the outer surface and residual tensile stress on the inner side, as the inner surface was protected from shrinkage by the outer surface. The tiny flaws in the inner surface of the crown acted as initiating sites for catastrophic failure. As a result, porcelain jacket crowns were restricted to use only in a very low stress-bearing anterior applications (Van Noort, 2007).

Due to a significant breakthrough in the early 1960s, when a patent was published, it has become possible to bond feldspathic glass to metal.

Major limitations of porcelain jacket crowns such as a low flexural strength (60- 70 MPa) and the inner surface flaws necessitated the use of a reinforcing metal substructure (Giordano et al., 1995). The main advantage of this type of crown is that it combines the strength of the metal coping with the aesthetic characteristics of the ceramic material. The crown consists of a cast metal coping with veneer ceramic fired over it. If the bond between the porcelain and the metal is created properly, internal cracking of the porcelain is eliminated by the strong metal barrier. Crack propagation within the veneer ceramic is prevented by the high fracture resistance capability of the metal coping substructure.

The major disadvantage of the metal ceramic crown is that destructive preparation is involved in applying the metal substructure, a thick layer of opaque ceramic, and the superstructure of translucent veneer ceramic. This limitation shows up more clearly in areas with increased aesthetic demand, such as the buccal or labial surface of the tooth, where extensive tooth preparation is required (Edelhoff and Sorensen, 2002, Tan and Dunne, 2004).

Even though the ceramic fused to the metal crown is far more aesthetically pleasing than a metal cast crown and has become the material of choice for the last few decades because of its adequate strength and predictable clinical results, it is still not as aesthetically pleasing as an all-ceramic crown (Tan and Dunne,

2004). The presence of the metal core does not allow the light to refract, making it more difficult to match the natural appearance of a tooth.

The recent progress in technology and research into new dental materials and the demand for high-quality cosmetic dentistry have resulted in the introduction and availability of a large number of materials for more aesthetically pleasing restorations. One of the most important new aesthetic approaches is the use of the all-ceramic crown (Haselton et al., 2000, Potiket et al., 2004). Although the conventional structure of all-ceramic restoration is crystalline filler dispersed in a glassy matrix, the structure of the new all-ceramic materials is crystalline (McLaren, 1998).

Recently, all-ceramic crowns have been considered the most aesthetic option for restoring the tooth. However, the use of the early all-ceramic crowns was restricted to the anterior teeth because of the relative weakness of the materials (Bergman, 1999). When the posterior teeth needed to be restored with all-ceramic crowns, with this area being subjected to deep biting force, their brittle nature and the possibility of fracture became a concern.

Recent developments in dental ceramics have included the introduction of ceramic core materials with high strength, such as the In-Ceram system (In-Ceram, Vita Zahnfabrik, Bad Säkigen, Germany), which allow the use of all-ceramic crowns even in a high stress area. The new all-ceramic materials exhibit no significant difference in terms of fracture strength compared with metal ceramic restorations (De Jager et al., 2006).

The core ceramic is fabricated by sintering high dense packed slurry (80 to 82 wt %) of pure Al2O3 followed by infiltration with molten glass. Later, it is veneered with feldspathic porcelain. As a result, ceramic materials can withstand micro crack propagation when placed in a high stress bearing area (Kelly et al., 1989).

As the glass and alumina form an interpenetrating network, crack propagation in the glass ceramic is limited effectively. As a result, overall, the crown materials will possess 3 to 4 times the flexural strength of the existing materials (Seghi et al., 1990, Giordano II et al., 1995, White et al., 2005). Burke et al.'s *in vitro* study reported that the fracture strength of the adhesively bonded all-ceramic crown is higher than that of restorations cemented with conventional cements such as zinc-phosphate or glass-ionomer cements (Burke, 1995, Casson et al., 2001, Burke et al., 2002).

2.11 Fracture mechanics of dental ceramic structure

Understanding the mechanism of ceramic failure is a key in developing stronger material and perfect design for an excellent clinical performance.

The clinical reports have indicated that the durability of all ceramic restoration is not as much that of its counterpart, which is ceramic fused to metal. From the materials standpoint, the brittle nature of ceramic structure is considered as the causative factor that makes the ceramic prone to fracture or failure (Sjögren et al., 1999, Malament and Socransky, 2001, Söderholm, 2012).

The important point to be considered that the strength of the ceramic tend to be a conditional property more than a merely inherent property. Thus, the performance evaluation should not depend on the strength data only; instead, the evaluation should consider the effect of microstructure of the material, processing history, methodology conditions, experimental environments and fracture mechanics characterization (Kelly, 1995, Söderholm, 2012).

Since the ceramic structure is inherently fragile in tension load with very little or no capacity to deform, the clinical durability of dental ceramic is controlled by the existence, severity, length and the homogenous distribution of structural flaws (voids and crack). The major local stress raiser areas in the brittle structure are the local extrusion and intrusion, inclusions, grain boundaries and the rapid change in the structure geometry.

Aforementioned structural flaws can be affected by the combination of the cyclic loading, temperature and the fluid in the oral cavity and the stress can be raised. The generated stress can adversely affect the durability of the ceramic by reducing the fracture strength and initiating of a crack. The crack, which is an inevitable in the structure of the ceramic that fabricated in a dental laboratory conditions, is considered as a potential site for dental ceramic failure (Tinschert et al., 2000).

When there is cyclic or fluctuating load even below the yielding strength, the brittle structure could manifest a fatigue failure. The fatigue failure is resulted from the development of a microscopic crack in the area of stress concentration,

which in turn these cracks could be merged to an ever-growing crack that lead to weakening of the restoration and ultimately lead to catastrophic failure (Wiskott et al., 1994, Crane et al., 1997).

Fracture toughness, which is the ability of the material to resist the propagation of the crack, is the most important parameter particularly to the brittle materials such as the ceramic. Fracture toughness is characterised by another factor, which is called stress intensity factor. The stress intensity factor can be simply described as a local stress that generated as a result of load application and when it became high enough it can initiate a crack and causes it to growth. Thus, when the stress intensity factor has reached its critical value, it simply means that it balanced the fracture toughness of the material.

Moreover, fracture toughness is determined by the cracks or flaws length that exist or initiated within the structure. Fracture toughness can be described in the formula of;

$$K_{Ic=} Y_{\sigma} \sqrt{\pi a}$$

Where $[K_{Ic}]$ is fracture toughness, $[Y]$ is a (dimensionless) constant factor related to the sample's geometry, $[\sigma]$ is the overall stress applied at failure, $[a]$ is a crack length (Wiskott et al., 1994).

It was reported that the bulk fracture is the most often feature of the clinical failure of the all ceramic restoration. The mechanism of the fracture of the all ceramic crown is manifested in three forms, (i) hertzian cone cracking at the

surface, (ii) sub-surface quasi-plasticity deformation zone at the area near the contact site and (iii) radial cracks at the bottom of crown surface (see figure 2-4). The radial crack is the most deleterious type of cracks and once it generated, it lead to a very fast degradation of the ceramic's strength (Thompson et al., 1994, Lawn et al., 2002, Lawn et al., 2004, Bindl et al., 2006, Aboushelib et al., 2007).

A rational design of any restoration has had, and often still has, an important requirement, which is how to reduce the stress concentration trigger area as far as possible. Since, it would be impossible to eliminate the generated stress completely; a great concern should be given how to decrease the effect of the inevitable remaining stress as far as possible.

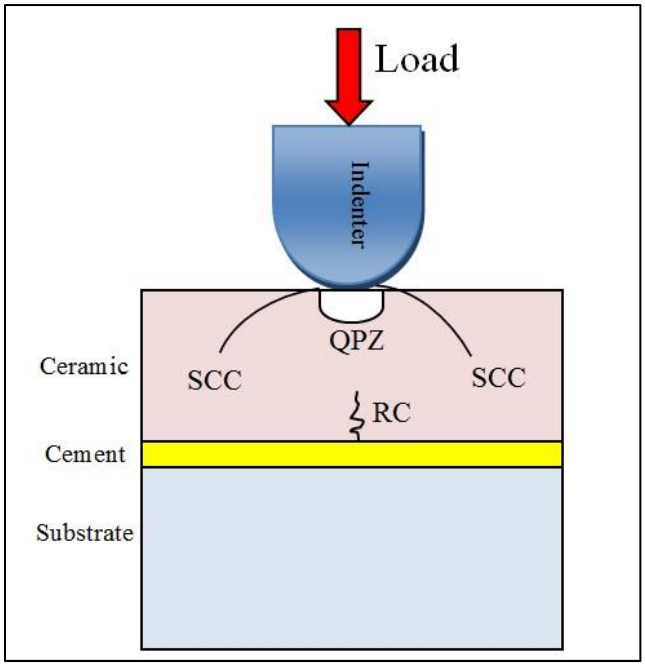

Figure 2-4: Ceramic crack types (SCC= surface cone crack, QPZ= quasiplasticity zone, RC= radial crack)

Fracture mechanics of the brittle ceramic structure can be expressed by Griffith's equation, which shows how the flaw size and surface energy affect the level of the generated stress and fracture strength:

$$\sigma f = \sqrt{2E\gamma_s / \pi c}$$

The symbols:

Ceramic fracture strength (σ f)

The modulus of elasticity (E)

The fracture-surface energy per unit length of the crack (γ_s)

The length of a pre-existing flaw or crack (c)

According to this equation, a concept would be applied that any processing step that could change the size, length, severity and distribution of the flaws, will adversely affect the material strength. Thus, regarding the stress intensity factor of Griffith's equation, the pre-existing ceramic flaws can show a growth in a brittle manner once the applied stress reaches a level equal to the fracture strength of the structure.

The water vapour factor at the crack tip may has a great effects on enhancing the stress generation and act as an effective contributor for the slow propagation of the crack. This effect occurs particularly in silicate-based glass ceramic, which result in bond rapture (Lohbauer et al., 2002).

Depending on the Griffith's law formula, the important approach for enhancing the fracture strength of the ceramic structure, since the E and γ are constant, can be achieved by reducing the flaw size (Crane et al., 1997, Lohbauer et al., 2002).

It has been reported, that the industrial fabricate ceramic, due to a perfect controlled manufacturing process of machined [CAD/CAM] block, shows a high Weibull modulus m 20 comparable with ceramic fabricated in dental laboratory which is m 5-15 (Tinschert et al., 2000, Jedynakiewicz and Martin, 2001).

Although, the machined ceramic, which is one of the industrial modified ceramic, it seems better than the laboratory fabricated ceramic. However, irretrievable failure of the machined [CAD/CAM] crowns by the crack was

recorded. Nevertheless, The effect of the machining action on the ceramic structure and how that induced crack is not well established and still need more studies (Hickel and Manhart, 2000, Bindl et al., 2006).

2.12 Fractography of the dental ceramic

The mechanism of the ceramic fracture has been a subject for investigation for some authors. It has been well noted that the ceramic's fracture initiation sites are affected primarily by the severity, location, size and distribution of the critical intrinsic and extrinsic flaws rather than by the structural thickness of the ceramic restoration (Thompson et al., 1994). The study of fractographic assesses the fracture mechanism of the microstructure by evaluating the interaction of the cracks with the applied stress and the resulted features on the fracture surface. Some of the fractographic studies have been conducted directly on the specimen fracture site using the SEM (Scanning electron microscopy), the Stereomicroscope and a combination of both techniques. A study by Scherrer et al has examined the fracture site by indirect means (Scherrer et al., 2007). By taking an impression of the remaining fracture site using a low viscosity impression material, a negative impression of the fracture site (a replica) could be obtained. Positive solid (cast) features of the fracture site could be obtained by pouring the replica with an epoxy resin and then gold coated for the later SEM analysis.

Understanding the causes of the fracture events of the dental ceramic could be considered as key importance in the restorative dentistry. In this way, the effect of some parameters on the fracture measures can be evaluated; such as ceramic material type, structure design and the effect of the laboratory induced flaws on the delivered final restoration (voids, crack, structural damages and residual stress)(Scherrer et al., 2007). However, there are several limitations to fractographic studies such as the fracture surface in the multiphase structure, coarse-grained, and porous structure does not have clear marking features make it difficult to interpret. Moreover, examining the fracture site directly could be impossible as one part of the fracture might be still strongly cemented onto the specimen and the other fractured part could be completely destroyed. Partial success was achieved in evaluating the fracture mechanism of the dental ceramic. There were very few studies in the literature that have been published considering the failure analysis of the fractured ceramic depending on the standardized approach of crack feature recognition. However, it becomes very clear that dental ceramic materials pose a special set of problems that could affect its performance (Thompson et al., 1994, Quinn et al., 2005, Scherrer et al., 2007, Scherrer et al., 2008).

2.13 Types of experiments for measuring stress distribution

A large number of researchers have focused on the study of stress distribution within the teeth and its effect on the mechanical behaviour of the restored tooth (Arola et al., 2001). Generally, any experiment in biomedical research should be done either on patients in the clinic (*in vivo*) or in the laboratory (*in vitro*). Although the data obtained *in vivo* experiments are quite valuable because of the possibility of simulation of the most variables that may affect the results, the time consuming nature, high cost and requirement for ethical approval of *in vivo* experiments make *in vitro* study more feasible (Sadighpour et al., 2006).

By means of *in vitro* studies, it is possible to estimate the *in vivo* usability for any material using very simple methods. *In vitro* studies are most popular because they are easy to set up compared to *in vivo* studies and less expensive. However, the reliability of *in vitro* tests is not as good that of *in vivo* tests because most of the relevant conditions that could affect the tests are difficult to replicate. Thus, it is not easy to draw clinical implications from *in vitro* test results (Kelly, 1999, Pospiech, 2002).

There are different approaches to performing *in vitro* testing and these can be classified as the mechanical destructive method and computational non-destructive method.

2.13.1 Mechanical destructive testing approach

In order to evaluate the load effects on restored tooth strength, different experimental methods can be used. Each of these methods has the ability to evaluate the testing process at a specific moment, starting with the generation of the stress and finishing with the failure or break of the tooth components (Soares et al., 2008).

In order to obtain the mechanical test with high reliability, it is essential that the result should be reproducible. Moreover, the criteria of survival (success) and failure should be based on an identified clinical performance requirements as much as possible. Kelly (1999) has standardized the ideal ceramic load to failure test by elucidating the most clinical relevant variables that might affect the survivability of fixed dental prosthesis. As the study claimed, the produced failure of ceramic restoration in any empirical test should be comparable to what often happen in the real clinical condition. Thus, to obtain result data reliably, essential test parameters should be applied such as the indenter contact area with the sample, the relevant restoration firmly cemented on the substrate, application of a dynamic load and finally the test should be under a wet environment.

However, due to the complex restoration geometry, some authors believe that there is no particular fixed standard method exists could apply for measuring the

strength of the all dental restoration (McCabe et al., 1990b, Kelly, 1999, Sadighpour et al., 2006).

2.13.1.1 Structural integrity test

Structural integrity is a term most often used in engineering any structure. It is points to the ability of the structure to withstand the designed service load by given maximum resistance to any aspect of failure such as; the deformation of the structure shape, fracture of the components and the fatigue failure. As well as, this term is used for indicating adequate functionality to the designed purpose. Thus, it is indicate the validity of the structures for the coveted service life.

Mechanical testing is a universal term used to describe a broad range of activities that are applied to determine the behaviour and properties of materials. Typically, this covers load application and measurement of the response. The load application may be either monotonic (static) or cyclic (dynamic) in nature and could be acting in a specific localized area or distributed at a single or multiple locations. Expanding on the aforementioned definition, mechanical testing is the process of applying force, pressure, heat and displacement and then measuring the response to the applied stimuli, to evaluate the new materials and a new design for a restoration and their possible effects on the final success and survivability of the dental restoration.

Strength is one of the main mechanical properties that can affect the clinical success rate of the dental restoration. Fracture strength testing has been reported as the most viable test among load-to-fracture tests to evaluate the strength of the dental restoration materials, both in static and dynamic modes (Sadighpour et al., 2006).

Generally, the static test is a test that is designed to examine the material to assess the integrity of the structure and whether it is affected by a change of materials or the final design. To assess the fracture strength of the dental restoration in a static mode, a static load is applied through the specific machine and then the maximum stress that is generated in the structure before a fracture is recorded.

Dynamic testing is intended to test a material under changeable rather than constant conditions. For dental material, the dynamic fatigue test is aimed at simulation of oral clinical conditions and examines the clinical performance of the restoration structure. Fatigue (reliability) test is used to determine survivability and a mode of failure whereby an object eventually fails after being repeatedly subject to a load. Fatigue failure today is explained in terms of the development of microcracks in a specific area called stress concentration area. if load application persist, these microscopic cracks could fuse to an ever-growing fissure which eventually lead to weakening the whole structure of the restoration (Wiskott et al., 1994). Catastrophic failure occurs as a consequence

of the final loading cycle that exceeding the ultimate mechanical capacity of the remaining intact parts of the tooth structures.

The fatigue mode test should attempt to simulate important clinical parameters such as the nature of the load, cycle frequency, stylus contact area with specimen, load contact angle and simulation of the natural conditions of the oral cavity, such as the moisture and the temperature(Morena et al., 1986, DeLong and Douglas, 1991, Kelly, 1999).

Fatigue limit and fatigue life can be used for characterizing fatigue behaviour of the materials. Fatigue limit is the maximum amount of stress that the structure can survive for the pre-set number of cycles. Fatigue life is a number of cycles that the structure can withstand between the known upper and lower limits. For quantifying the fatigue behaviour of the materials, fatigue limit has been adopted because it is quicker to administer than fatigue life, which can take months or years to test (Padipatvuthikul and Mair, 2008).

One of the most important factors to be taken into account during the dynamic mode of fatigue test of the restoration materials (for simulating the natural oral moisture conditions) is that the test must be performed under water. The idea behind performing the test under water is that during the cycles the water becomes trapped in small cracks and when the cracks relax, the water is compressed. Because the water, unlike other materials, cannot be compressed, it will act as a hydraulic piston and that will lead to an increase in the stress at the crack end. It has been found, the combination of constant cyclic stress under an

aqueous condition could result in a fatigue failure of the ceramic restoration up to 50% (Bindl et al., 2006, Padipatvuthikul and Mair, 2008).

Clinical trials are controlled by the final test results of any new dental restoration. The main disadvantage of clinical trials is the length of time involved. Typically, a good clinical trial should run for at least 5 years. The high expense of clinical trials also often restricts the researchers to acting only on small groups of the population, which can lead to inconclusive results due to population variability (DeLong and Douglas, 1991).

The advent of new dental materials coupled with the difficulty of conducting the clinical trials has increased the demand to develop a laboratory based test that imitates most of the natural oral environment conditions. Simulating the oral environment along with performing a fatigue testing is enabled by using a chewing simulator machine. It has been documented, the results drawn from the test performed at the chewing simulator machine show adequate correlation with the clinical performance data of the restoration. Generally, the data resulted from testing the restoration under a dynamic fatigue testing are more realistic than those derived from static fatigue testing as it restores most of the conditions that naturally exist in the mouth (DeLong and Douglas, 1991).

. .

2.13.1.2 Fatigue testing approaches

Understanding of ceramic mechanical properties has become extremely important. Define the factors that adversely interfere with mechanical properties of the ceramic structure has led the researchers to use and standardize several methodologies to achieve a full understanding of material behaviour under the load. Different ceramic mechanical properties were examined such as the wear and corrosion resistance, fracture strength, thermodynamic stability, and fatigue strength and life reliability.

In material science the performance of the structure is plotted in a curve called S-N curve or Wohler curve (see figure 2-5), which depicted the peak stress against the number of stress cycles to failure. (Lin et al., 2001b).

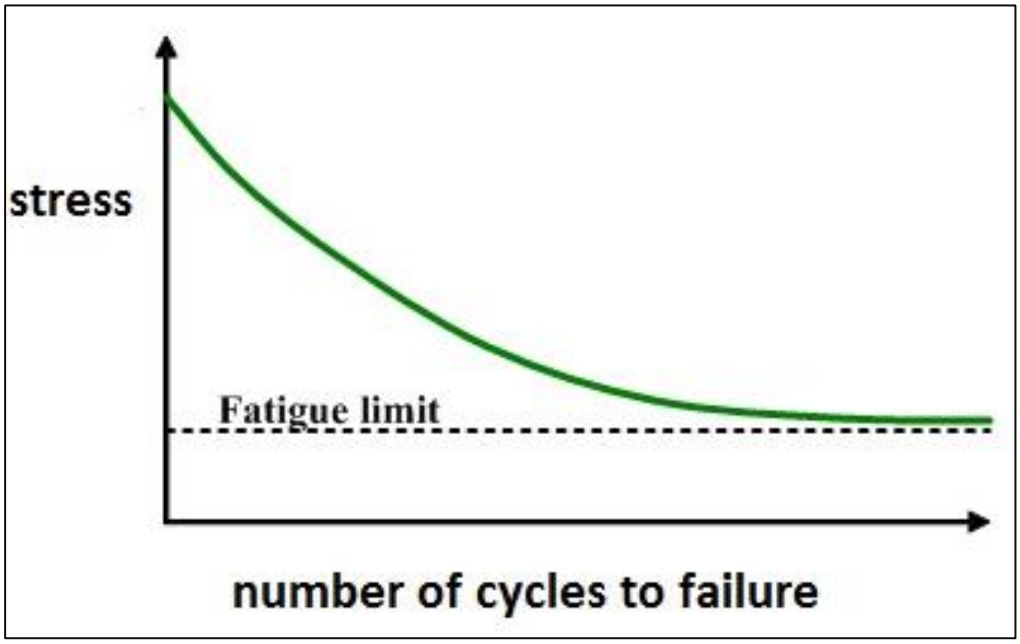

Figure 2-5: S-N curve [Wohler's curve]

Regarding fatigue property, there are several testing profiles and methods exist for estimating the fatigue strength and behaviour of the materials. Understanding of the Fatigue behaviour of any structure can be achieved through the two concepts; fatigue limit, which is the most magnitude of stress can the structure survived at a specific number of cycles and fatigue life, which is the maximum number of cycles that the body can withstand for the given amount of stress without failure. Since it is a quick test and does not take long time like fatigue life test which may take months or even years, Fatigue limit is used for determined fatigue behaviour of the structure (Padipatvuthikul and Mair, 2008).

The most appropriate method for evaluating fatigue limit is staircase method (or up and down method), which has been used in several studies(McCabe et al., 1990a, Wiskott et al., 1994, Drummond and Bapna, 2003, Lohbauer et al., 2003, Hayashi et al., 2008, Padipatvuthikul and Mair, 2008).

In this technique, the sample was subjected to a certain stress for a predetermined number of cycles. If the sample survived the cycled stress, the load would be increased for the next fresh sample by a fixed incremental load amount. The procedure would be repeated with the fixed incremented load until the sample showed failure. Thereafter, the load would be decreased for the next sample to the last load that was used before failure (endurance load).

Having quantifying the endurance load though the fatigue limit test, fatigue life test can be conducted at a load close to the fatigue limit load and the new samples to be cycled to fracture (Draughn, 1979, Padipatvuthikul and Mair, 2008).

According to the literature, a failure produced by 240000 cycles in a chewing simulator corresponds to one year of clinical performance of the restoration in real oral conditions (Sakaguchi et al., 1986). Thus 1,200,000 chewing cycles in the chewing simulator will copy five years of clinical service of the restoration in the oral environment (DeLong and Douglas, 1991, Wolfart et al., 2007).

Since, estimating the life stress or degradation of the structure taken a long time by aforementioned method. An accelerated life test was used as an alternative to staircase method. In this method, the sample subjected to a constant stress for a period (cycles) of time. Once the sample confirms a survival status, thereafter, the sample will be stepped to a higher stress for another period. The stepping will carry out repeatedly until the sample failed or survived in a predetermined time [figure 2-6].

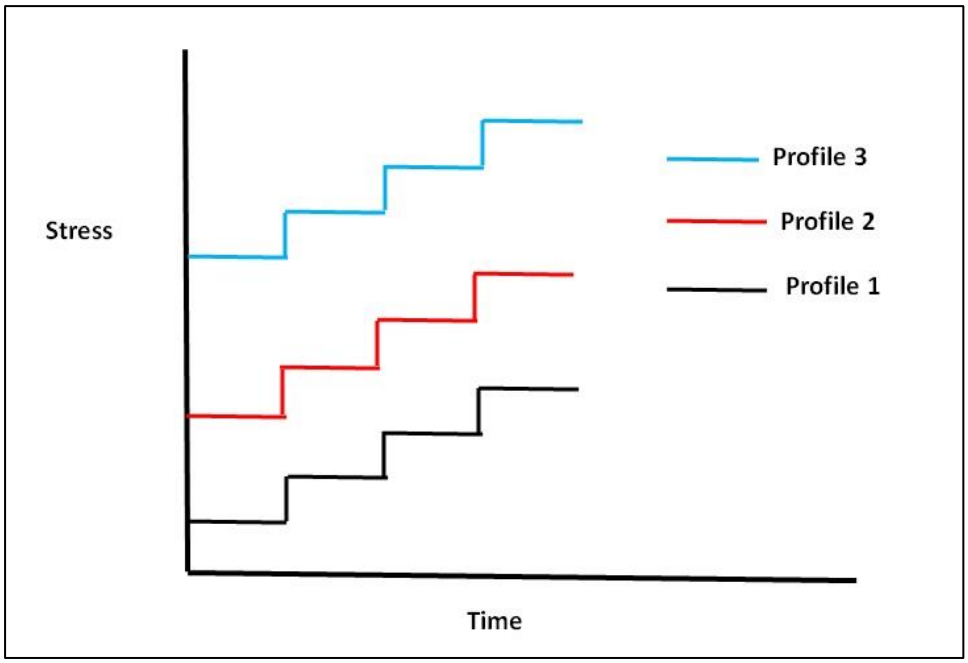

Figure 2-6: Step stress testing profiles

In order to promote the failure of the material in the accelerated life test in an extremely short time, several stress paths for utilizing the stress can be performed simultaneous in different stress profiles (Coelho et al., 2009, Baldassarri et al., 2011, Silva et al., 2011)**.**

Despite the accelerated life test or step stress testing yields life stress estimation in a very perceptible shorter time, however, still the staircase method is recommended by British, France, Japanese standard. Additionally, in step stress testing the accuracy of failure predication is less reliable as the test is performed in a short time. Thus, failure estimation cannot be guaranteed by the quick failure and the accumulative damage model is not considered.

Moreover, the researchers have faced difficulties in interpreting and analysing the step stress test data and most often they depend on an approximate evaluation for the result in order to achieve a more reliable test outcome. Also, the stress value is considered as one of the shortcoming of accelerated life test, where the failure of the tested subject occurs at a very high stress level, which does not replicate what normally happen in the real clinical situations. Generally, the constant stress testing by staircase method is more recommended over the accelerated life testing (Wiskott et al., 1994, Lin et al., 2001b, Nelson, 2005, Nelson, 2009).

2.14 Computational non-destructive test approach

The normal oral functions (biting and chewing) are acting as an external influence, whereas the stress is generated on the tooth structure as a normal response. The ways that the stress is transferred from the restoration throughout the tooth to the surrounding structure can be consider as a key for predicating the reliability of the restoration design. Because of the complex geometry and the access limitations to the oral cavity components, the oral environment is considered as a complex biomechanical system (Versluis and Versluis-Tantbirojn, 2011).

The majority of biomechanical studies of the intraoral environment have been done *in vitro* (Assunção et al., 2009). The destructive mechanical tests for determination of fracture resistance and the main mechanical properties of the materials are important means for assessing the behaviour of the tooth. However, the destructive test approaches have several limitations regarding the difficulties in describing the internal behaviour of the materials.

The limitations of the mechanical testing can be attributed to the wide variations in the anatomical form of the teeth, a wide mechanical and chemical interaction of the tooth tissues. Moreover, the time consumption, the risks of live experiment and the high cost could be considered as limitation factors of the *in vitro* stress evaluation test (Magne, 2007, Borcic and Braut, 2012).

Due to these limitations, the simulation approaches and the use of virtual models have become unavoidable (Magne, 2007, Soares et al., 2008).

The tooth body stress can be defined as a tooth response to the transferred masticatory force (Versluis and Versluis-Tantbirojn, 2011). However, this stress cannot be directly measured by the conventional mechanical testing. Moreover, based on an interpreting of the mechanical test data, it is unfeasible to understand the mode of failure in complex structures or when and where the failure process would start.

Computer-based study utilize the tooth restoration's components and the tooth surrounding tissue can act as the basis for the full understanding of the mechanical action that could carry out within this system. Understanding the mechanical behaviour of the structure under the load may help in introducing and optimising the ideal restoration design.

The success or failure of any dental prosthesis is based on its properties to resist and survive the applied occlusal load and effectively maintain the remaining structures. One of the major advantages of the non-destructive computer-based methods is the capability to optimise and evaluate the experimental design virtually. The trial beforehand for the design computationally, designing an applicable actual experiment can be confirmed (Magne, 2007, Borcic and Braut, 2012).

Therefore, simulating an object can reduce the need for an actual prototypes or conducting a real experiment. Additionally, the modelling and simulation could save time and money otherwise they would have to be spent on organizing a clinical trial or live experiment.

There are some conventional non-destructive methods for studying stress distribution within dental structures. Generally, the stress distribution has been analysed in several ways such as using two and three dimensional photoelasticity and the strain gauges (Yettram et al., 1976).

It has been noted, the material's shape and distribution of the stiffness of a complex structure are the main factors that affect the stress distribution within structure (Habelitz et al., 2001).

The two aforementioned classical methods for the stress analysis are inadequate to reliably predicting the failure and incapable to provide an accurate results for the stress distribution analysis within the tooth. These limitations are resulted from the complexity of the tooth structure as well as its structure is multiple layers with varying stiffness distribution. The strain gauge has a limitation that measures the strain at one point and in one direction. In addition, it cannot give information about the internal stress as it can only measure the external discontinuity of the surface. Even though, the visual information of the photoelasticity can give an initial picture for complete field stress distribution. The photoelasticity provides data of limited quality as the method cannot supply information of the state of each component in the tooth restoration complex, such as tooth structures, lute cement, restoration(Asundi and Kishen, 2000, Boschian Pest et al., 2006, Hasegawa et al., 2010).

A sophisticated innovation that implements the numerical analysis for the stress distribution called finite element analysis (FEA) has become available to use in dentistry. Using FEA, it has become possible to consider the stress distribution through the various components of the restoration simultaneously.

The numerical analysis method has been used successfully in many engineering and bioengineering fields since the 1950s and in dentistry since 1970s. Nowadays, FEA can be considered as the most comprehensive method currently available for measuring stress distribution in a complex dental system (Versluis and Tantbirojn, 2009).

By using FEA, it has become possible to calculate the stress distribution and deformations in a complex three-dimensional structure by dividing a large domains into a collection of much small simple-shape domains called elements, whose ends meet to form nodes (Boschian Pest et al., 2006). For individual elements, deformation (stress and strain) can be more easily and properly calculated than through calculations based on the whole undivided structure. Through the deformation assessment in each small element simultaneously then combines them properly, the deformation of the whole body structure can be assessed (Magne, 2007).

The analysis of stress distribution by FEA enables not only the understanding of the failure behaviour of the structure, optimising of the experiment through the mathematical simulation and choosing the perfect design of the tested structure for an ideal performance is achieved (Bona et al., 2013).

During the last decade, the use of FEA in dentistry has been substantially refined. Undoubtedly, nowadays the numerical approach to stress analysis has become a most comprehensive *in vitro* examination method, particularly in restorative dentistry (Versluis et al., 2004, Mohammed and Desai, 2014).

One of the main advantages of using FEA is that the time and the cost are reduced for bringing the simple concept or any new idea from the virtual status to make it applicable in the real clinical life. It allows the researcher to build more confidence in the final concept/project by testing the experimental subjects under all conceivable loading conditions. Moreover, the risk involved in the clinical experiment is reduced, the samples can be used several times and the test can be repeated with different strength measurement tests. Also, by using the FEA approach, different material properties can be assigned. Thus, the parameters of each component can be isolated, which enable for an assessment of the effect of each parameter precisely (Versluis et al., 2004, Magne, 2007, Sun et al., 2008, Magne, 2010).

2.14.1 Aspects of FEA

Modelling the components response to the mechanical action could be considered as a most challenged step in FEA simulating of the oral compartment. To validate the modelling and the numerical solution, several assumptions should be undertaken. FEA result's accuracy has been affected by these assumptions. The most important assumptions that substantially affect the FEA outcome can be categorised as: the geometrical details of the structures to be modelled, the properties of materials, the boundary condition and the interface between the structure components (Geng et al., 2001, Soares et al., 2012).

Similar to other physical structures, the analysis of the stress distribution for the tooth and its supporting tissues under any load conditions can be investigated by means of the finite element approaches. However, the structural modelling of the oral components can be modelled in either a 2D or 3D approach(Tajima et al., 2009) .

Using 2D or 3D modelling of the structure is dependent on some interrelated factors such as the purpose of the study, the difficulties in modelling the complex geometry, the analysis mode and the properties of the materials. For such a difficulty in modelling the complex geometry, the alveolar bone in some earlier 2D aspect of the FEA studies has been modelled as a regular rectangular shape. Whereas, the alveolar bone original shape is irregular.

Potentially, the 2-D Finite element analysis studies are more suitable for a qualitative analysis of the biomechanical behaviour, while in a quantitative stress analysis the overestimation of the stress analysis made the 2-D FEA worthless and incapable to show the actual model behaviours (Rieger et al., 1990, Van Oosterwyck et al., 1998, Romeed et al., 2006, Borcic and Braut, 2012).

Generally, the biological structure with a simple and regular form can be modelled adequately. However, modelling a biological structure of a complex and irregular shaped is difficult, especially when the structure includes thin

layers or interfaces. Therefore, in the case of complex structures the generation of an accurate finite element models can be challenging (Romeed et al., 2006).

Thus, the 2-dimensional analysis can give an immediate insight at low working cost and reduced time of the analysis steps. However, the 2D model results are limited in terms of complex biological structures. On the other hand, the 3D FE analysis could yield more realistic results even when the structure possesses complex geometry (Yang et al., 2001, Tajima et al., 2009).

Essentially, 3D modelling can provide much accurate and precise dependable data along with more realistic representation to the anisotropic properties and a non-linear behaviour of the material. In essence, the 3D modelling aspect of FEA studies started in a way of generating the model from the sectional images of the structure. Subsequently, the sectional image technique is no longer used as the development in the techniques of image digitalization has made the possibility of efficiently modelling of the complex anatomical structure is available (Geng et al., 2001, Borcic and Braut, 2012).

The interrelating nature of the FEA with the digital image acquisition technique; CT (computed tomography) and MRI (magnetic resonance imaging) has been proved in several studies. This combination can be simply described as an ability to transform a two or three dimensional object's geometry into a package of images data by some software from either CT or MRI to a FEA readable language called mesh. Obviously, the combination of these image digitizing

techniques with the FEA has enabled the biomedical studies to utilize an accurate model and stress analysis in the very complex living structures' geometry (Rieger et al., 1990, Van Oosterwyck et al., 1998, Geng et al., 2001, Romeed et al., 2006, Borcic and Braut, 2012).

Most previous studies for determining the stress distribution in dental structures have been based on geometrical modelling, which means that the accuracy of the data was compromised. The success of the modelling depends mainly on the precision in the simulation of the structure geometry, the structural characterization of the body material, the load and supporting conditions. Generally, the stress distribution in the biomechanical analysis, the accuracy of the modelled data has apparently affected the results of the analysis. Therefore, constructing a model using precise data is required(Hasegawa et al., 2010).

Modelling software can develop a 3-dimentioal model of an object depending on the data acquired from CT stack images, geometrical data acquired from 3D shape measuring devices and, in some cases, anatomic average dimensions. The traditional CT devices that were used in early studies on tooth examination were compromised by the limited capacity of the vertical resolution, which was 1-2 mm, and the X-rays were impaired via the interference of metallic substances. The low resolution of the traditional CT technology has rendered it incapable of adequate reconstruction of a small structure such as a tooth or dental restoration (Nielsen et al., 1995). The introduction of micro CT in dentistry has made the

acquisition of high precision and resolution data of the small objects such as a tooth possible (Jung et al., 2005, Magne and Oganesyan, 2009).

Micro CT scanning has a vertical resolution capacity of 100-200 µm. With the continuous progression of micro CT technology, at present, an axial scanning of < 10 µm is possible. Nowadays, with the innovations in the micro CT technology, FEA models have been transitioned from basic or simple 2D and imperfect 3D models to more sophisticated three-dimensional models. The method of image acquisition using micro scale CT has been widely used as a scanning tool for the three dimensional digitizing purposes in modelling dental structures. It provides a higher level of images precision, faster digitizing steps and finer geometrical descriptions (Jaecques et al., 2004, Tajima et al., 2009, Hasegawa et al., 2010).

More recently, the progression of the computer-aided techniques of geometry acquisition in parallel with the progression of three dimensional images processing and reverse engineering techniques has made the construction of a finite element models easier. Eventually, according to the impressive advance in the images digitize technique, the potential future dreams of FEA modelling of the whole human body by using the advance image digitalizing devices and techniques, could come true (Geng et al., 2001, Tajima et al., 2009).

Almost, developing a 3-dimensional finite element model compared with 2D model generation can be considered as a more labour-intensive process, more

cost, time consuming. Moreover, for generating the 3D model, an additional technology for acquisition of 3D geometrical data and 3D model developing may be required. However, the 3D model have outperformed the 2D model in determining the different mechanical behaviours of the most complex dental restoration structures (Yang et al., 2001, Tajima et al., 2009).

Assigning of materials properties in FE simulation has a substantial effect on the distribution of stress/strain in the modelled object. The isotropic and anisotropic behaviour of the structure are the most important properties that can be modelled in FEA.

In several studies the assumptions of the material properties were assigned as homogenous and linear with the elastic behaviour of the materials has been determined by the two constants which are the modulus of elasticity and the poisson's ratio. For example; in the earlier FEA studies, the trabecular bone has been ignored as the capability of modelling such a complex structure pattern was not available. Due to this limitation of the difficulty in modelling the trabecular bone, its properties were assigned as a homogenous, isotropic and liner elastic behaviour.

Afterwards, several researchers have found that the trabecular bone is not isotropic and not homogenous. Thus, the bone has different response and stress distribution when consider as non-homogenous anisotropic structure. thus, in FEA, the setup of material properties are very critical step to be considered,

otherwise the stress distribution will be altered and the result will lost it realistically in describing the actual behaviour of the materials (Lewis, 1993, Spears et al., 1993, Patra et al., 1998, Geng et al., 2001, Santiuste et al., 2014).

In FEA, the external effect (loading and constraint) on any modelled object can be defined by the boundary condition. Due to subjected load, the nodes of the FE model show a rotation and translation movements of an object in several directions. These movements are determined in six directions and defined as a degree of freedom. The degree of freedom is representing the most effective movement of these nodes. The degree of freedom is effectively associated with the boundary condition. Accordingly, the results of the FEA are significantly affected by the boundary condition. Hence, the boundary condition's selection and application can be considered as crucial step in FEA solution (Geng et al., 2001, Ko et al., 2012, Soares et al., 2012).

The interface between the modelled structures is considered as determinant factor that affects the stress distribution and the performance of the contacted structures. The interface between the structures in most of the FEA studies is defined as an intimate contact or ideal bond between these structures. However, some studies showed a mode of fracture that inconsistent with the experimental mode of fracture. It has been recorded that a non-linear simulation of the interface between the resin cement and the post and core can give a more realistic analysis (Wakabayashi et al., 2008).

Generally, each classical method for measuring stress analysis within dental structures has its limitations. For instance, the strain gauge can be used only for measuring the strain in the external surface and not internal stress. Regarding photoelasticity, it can only provide a quantitative value of stress distribution(Farah et al., 1973) .

Experimental research can be viewed as a more time-consuming process than the FE method as the FE method can minimize the requirements of the laboratory test. Moreover, finite element analysis can offer a faster solution in terms of testing some mechanical parameters, which can be changed more easily through the mathematical model than in a laboratory experiments. Nevertheless, in the mathematical approach the simulation of the all mechanical behaviour details of the testing object could be impossible. Therefore, the FE method should be viewed in combination with both experimental methods (*in vivo* and *in vitro*) not as an alternative(Soares et al., 2012).

Finite element analysis can give information that would be difficult or maybe impossible to obtain from an experimental observation. However, it is very difficult to perform a FEA without the experimental input and validation. For that reason, the use of data from the experimental work and computational mathematical analysis in combination seems to be a more reliable and more relevant approach (Soares et al., 2008).

2.14.2 Types of structural FE analysis (linear and nonlinear analysis)

There are different types of structural analysis, which is depending on the subject being modelled. Since the analysis depends on the model, either linear or nonlinear analysis could be used. These terms refer to the solution proportionality. If the outcome is independent of the loading history, it will be a linear solution. For instance, in a linear solution the outcome will be the same irrespective of the load conditions, such as whether the load is applied in one or multiple increments. Simply, the linear relation does not take into account the plastic deformation of the object. Elastic properties and plastic deformation are proposed as nonlinear material responses.

More often, in FEA studies the linear static model is extensively engaged. The linear analysis is applicable when the structure displays a linear stress/strain relationship up to a level called the proportional limit. The linear analysis validity could be doubtful when the study has to explore the realistic conditions that are regularly encountered in the intraoral environment. The realistic option is to consider the nonlinearities. For situations when conventional linear analysis cannot be performed, the nonlinear FEA has become a powerful tool for prediction of the stress / strain relationship within the subject structures.

The interface area in any structure is one of the most important areas affecting the performance of the material or the structure.

In some studies that utilizing the linear mode of static analysis, the perfect bond is a representative of an interface between the individual materials that shares the same node and they are with different elastic properties. Occasionally, the assumption of the interface surface as a perfect bond in studies utilizing the linear stress analysis approach leads to incorrect interpretation of the finite element analysis outcome. The erroneous explanation occurs, because even when there is a perfect bond, the possibility is still exist of microcracks that arise at the site where the stress generated exceed the strength of interfacial bonding.

It has been suggested that to predict the stress/strain status in a realistic situation across the interface between the tooth and dental restoration the analysis need to be regarded as a non-linear stress analysis. Nevertheless, the validity and reliability of such an approach have not been adequately established(Toms and Eberhardt, 2003, Wakabayashi et al., 2008).

2.14.3Types of FEA stress

Through using the finite element approach, it is possible to describe the mechanical behaviour of the examined materials by using a mathematical model. In this method, the characteristics of the investigated object are described mathematically and interrelated by formulae (Peters and Poort, 1983). The outcomes of the FEA are described as stress distributed in the examined body structure. This stress is represented either as a von-Mises stress, which is an equivalent combination of compression, tensile and shear stresses or as a maximum principal stress that can be considered as a tensile stress (Hamrock et al., 1999, Lin et al., 2001a, Pegoretti et al., 2002, Eraslan et al., 2009).

Dental enamel structures and most of the dental restorative materials, particularly the ceramics, are brittle materials in nature, and tensile stress can be considered as a factor that is responsible for the most failure of dental material(Spears et al., 1993, Hamrock et al., 1999, Eraslan et al., 2009). To assess the risk of failure of dental materials, it is more appropriate to consider the different types of stress (compressive, tensile, shear). As von-Mises stress includes all these types of stresses, it has been used in several studies of stress analysis in dentistry research (Eraslan et al., 2009). Additionally, von-Mises stress depends on the entire field of stress and it is used to a large extent as a possible damage occurrence indicator (Pegoretti et al., 2002, Pierrisnard et al., 2002).

Summary

The effect of the interface lute on the structural integrity of the tooth adhesively restored with an all-ceramic crown remains is an unknown parameter especially in relation to the interface geometry (thickness and uniformity).

Traditionally, the structural integrity of a restored tooth system (tooth-lute-crown) is tested by laboratory based mechanical testing. However, a more sophisticated FEA computer modelling seems to provide a non-destructive way of understanding the structural integrity of the system, which may complement mechanical testing.

Aims & Objectives

3 Aims& objectives

3.1 Aims of the study

1. To determine the effect that the interface geometry has on the fracture resistance of a tooth restored with a full-coverage adhesively cemented all-ceramic crown.

2. To explore the complementary relationship between two analytical techniques: in-vitro mechanical testing and FE analysis to determine the structural integrity of the restored crown-tooth complex.

3.2 Objectives

1. To develop and validate an alternative more accurate, reproducible and repeatable way of measuring the dimensions of the interface.
2. To explore the possibility of creating a uniform interface (width and uniformity) for pressed fabrication systems.
3. To compare the effect of different fabrication technologies (milling and pressed) on the geometry of the interface.
4. To assess the effect that fabrication technologies have on the development of flaws on the internal surface of the crown – An SEM investigation.

5. To determine the effect of the interface geometry [non-uniform (real) vs. uniform (virtual)] on the stress distribution of the restored crown-tooth complex – A FEA investigation
6. To determine the effect of the interface geometry on the structural integrity of the restored crown-tooth complex – A mechanical fatigue test investigation.
7. To determine the effect of the interface geometry on the stress distribution of the restored crown-tooth complex for pressed and machined ceramic crowns – A FEA investigation.
8. To investigate the relationship between the structural integrity data obtained from mechanical testing and the stress distribution data obtained from FEA.

3.3 Hypothesis

The nature of the interface (physical properties, dimensions and uniformity) affects the stress distribution and resistance to fracture of the restored ceramic crown-tooth complex.

Generation of a digital model of the restored tooth

4 Generation of a digital model of the restored tooth

4.1 Introduction

This chapter covers objectives 1, 5 & 7 of the thesis.

Digital 3D modelling and Finite element analysis (FEA) of the tooth-restoration complex are now well established important numerical approaches as effective *in vitro* experiment assays in a range of dental disciplines (Magne, 2007, Ko et al., 2012).

Early digital modelling techniques of dental structures used either scanned histological slices of a tooth, that were subsequently rebuilt digitally or the construction of a model from standard anatomical data from textbooks (Jaecques et al., 2004, Magne, 2007, Tajima et al., 2009). Both methods were labour intensive, time consuming and resulted in an over-simplified model of the complex tooth structure, which did not represent accurately the actual object's geometry.

More recently, micro CT scanners have been developed for the acquisition of digital radiographic data of small biological structures such as a tooth and related structures (Plotino et al., 2006, Magne and Oganesyan, 2009). Micro CT scan allows for higher accuracy acquisition of tooth morphology and density measurement combined with fine detail description and faster digitization. Improvements in CT technology and associated software have further

accelerated the application of this tool for effective 3D digital modelling of dental structures; with the ability of reducing the slice thickness from 1.5mm to less than 5µm. The ability to reconstruct accurate and high resolution 3D digital models permits the confident use of FEA for the analysis of the stress distribution based on reliable data values (Plotino et al., 2006, Magne and Tan, 2008, Magne and Oganesyan, 2009, Tajima et al., 2009, Hasegawa et al., 2010).

Modelling software is required to convert the stack of the CT data as stock image files to the 3D virtual model. Several software programmes have been used for the purpose of 3D generation of the scanned sample. Of these, Mimics® software (Version 14.1; Materialise Interactive Medical Image Control System) has proved to be very effective as it is compatible with the most common digitizing technologies [CT and MRI] output data (Fu et al., 2010, Ammar et al., 2011, Shahrbaf et al., 2013).

3D digital models created in this manner can be further modified to design custom features. FreeForm® technology (SensAble Technologies, Inc.) is a sophisticated CAD package software that uses a proprio-receptive feedback haptic arm; a tool that is analogous to a digital hand for the addition or subtraction of the structure in the manner of sculpting. The haptic arm enables not only visual insight for the user, but simulates the real sense of the external texture and the surface resistance of any object when manipulated by the

designer hand. Thus, the combined use of high resolution micro-CT scanning, sophisticated digital rendering of a 3D structure to create an accurate and high resolution model that can further be modified with the aid of Haptic technology provides us with unprecedented ability to create very effective models (Kusumoto et al., 2006, Williams et al., 2006, Ohtani et al., 2009, Shahrbaf et al., 2013).

4.2 Aim

To generate a digital 3D model of a typodont tooth restored with an adhesively cemented all-ceramic crown, using a combination of micro CT scan, Mimics® software and FreeForm® technology.

4.3 Objectives

To attain a viable combination between micro CT scan, Mimics® software and FreeForm® designing technology for generating an accurate 3D model, several steps should be implemented accordingly, which are:

1. To construct the physical model of the tooth-restoration-complex.
2. To obtain micro CT scan of the physical model
3. To construct the 3D model.
4. Modifying the 3D model by haptic arm and the FreeForm® technology.

4.4 Null Hypothesis

The combination of the micro CT images, Mimics® modelling software and FreeForm® technology cannot meet to generate an accurate and reliable 3D model.

4.5 Materials and method

4.5.1 Physical model creation

The protocols for tooth preparation, crown fabrication [milling] and subsequent crown cementation followed the related protocols that are fully described in chapter 5.

An upper right first premolar Frasaco® tooth (Frasaco, GmbH Oberhoferstrasse 1888069 Tettnang, Germany) was prepared in accordance with the guidelines for a standard all-ceramic crown by IPS e.max® (Ivoclar/Vivadent). The tooth preparation protocol is described in section [5.5.3.1]. A crown was milled from an IPS e.max® CAD block ceramic (e.max® CAD block, shade HT A3, Ivoclar Vivadent, Germany) via the CEREC® 3 inLab milling machine in accordance with the steps that fully described in section [5.5.6.6]. Thereafter, Variolink II resin cement [Variolink II, intro pack, Liechtenstein, Ivoclar/Vivadent] was used following a standard cementation technique that is described in section [5.5.6.8].

4.5.2 Digital scanning of the Physical model

Each sample was scanned by a micro CT scan (Skyscan® 1172 micro-CT; Aartselaar, Belgium). The micro CT scan parameters were set at 80Kv voltage, 124µA current, 10W power and 17.27µm image pixel size.

The output data set presented as a 4GB stack of TIFF file images. Volumetric reconstruction was carried out using Skyscan's NRecon® software that generates a set of cross section slices through the scanned sample from the acquired angular projections. NRecon® software can eliminate most of the extraneous data and errors by optimising the alignment, source beam-hardening improvement, correction of the ring artefact and images sharpness enhancement. The NRecon® can accept large format capacity of the angular projection images and reconstruct the images of object's cross section. Thereafter the redundant peripheral data was eliminated using the cropping tool of the CTAn® analyser (Skyscan, Aartselaar, Belgium). In this way the size of the file was reduced to less than 1GB [Figure 4-1].

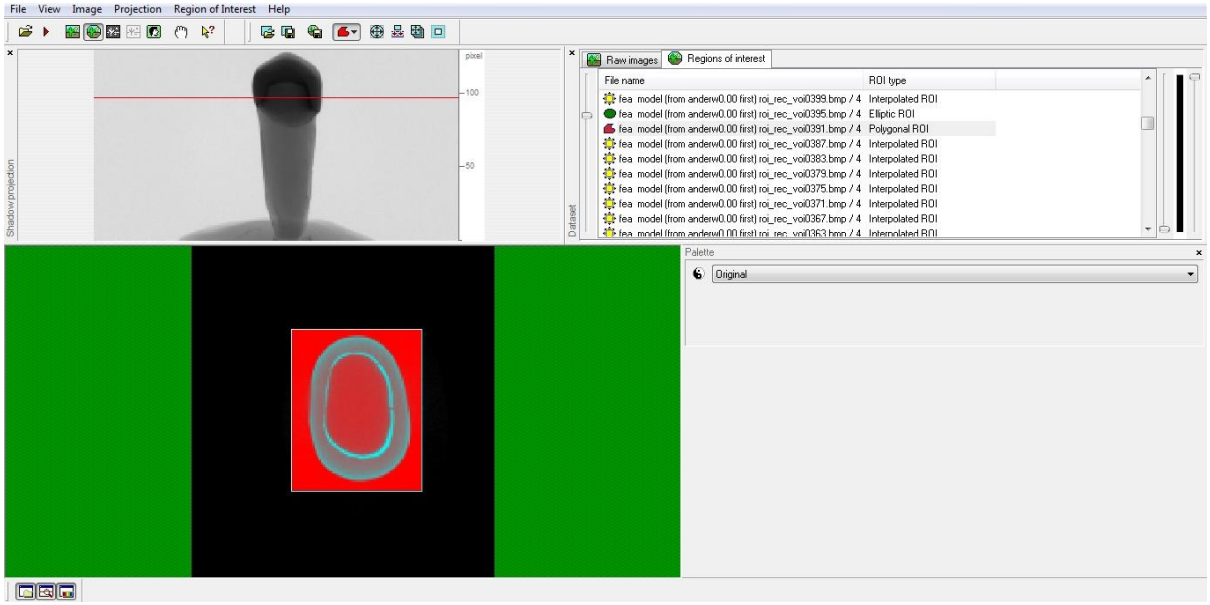

Figure 4-1: CTAn for pictures cropping (N Recon)

4.5.3 3D Modelling

The different densities of the tooth-restoration complex [dentine-cement-ceramic] enables for a perfect translation of these hard structures into distinct separate layers.

Generating a 3D model by Mimics® follows the sequential steps listed below and detailed thereafter:

a. Importing the raw images data from the micro CT scan and identifying the image details and orientations of the planes.
b. Segmentation (editing the mask) and thresholding (Boolean operation).
c. Creating the 3D object by the option of 3D calculation.

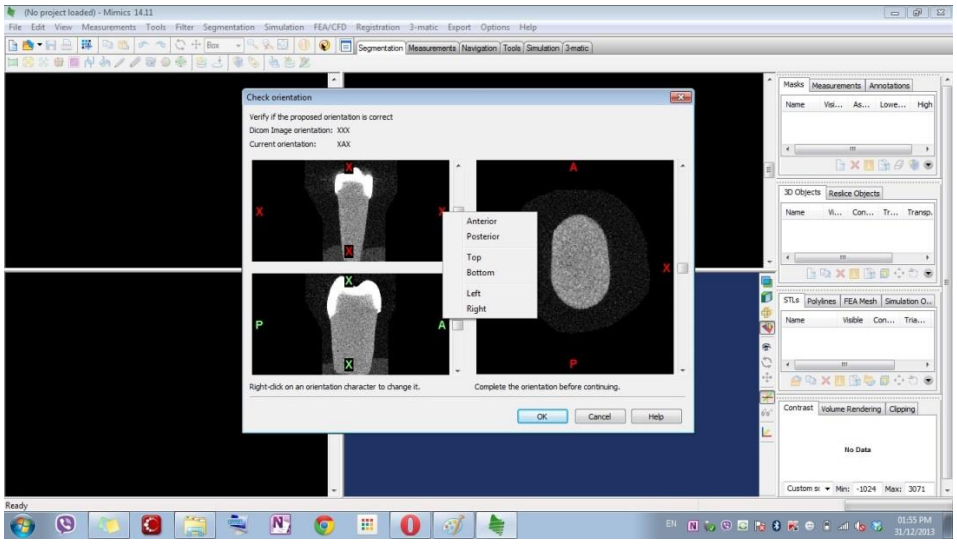

Figure 4-2: Identifying the image orientations of the planes

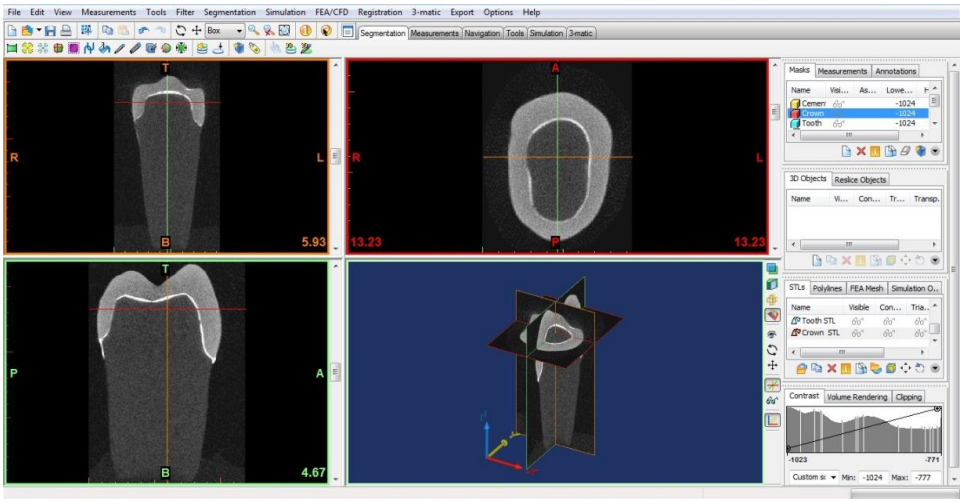

Figure 4-3: Mimics default view: 2D model in coronal, sagittal and axial views

4.5.3.1 Importing of the raw images data from the micro CT scan

In order to perform the modelling steps by Mimics® software, the stack of raw images data were exported from the micro CT scanner into Mimics® software. Subsequently, several parameters such as the image resolution and the orientations are defined in order to maximize the accuracy of the generated 3D

model for a perfect size matching with the original scanned samples [Figure 4-2] and [Figure 4-3].

4.5.3.2 Segmentation

The 2D object generated in Mimics® comes as a one part object without a distinct barrier between the individual components. Thus the segmentation option is required to separate the object into the various components (ceramic crown, cement interface and the tooth). The segmentation process is performed with the Mimics® software option of thresholding and mask creation. Depending on the different contrast scales of the tooth components, the thresholding option can differentiate the individual layer from the other by changing the thresholding scale as shown in [Figure 4-4].

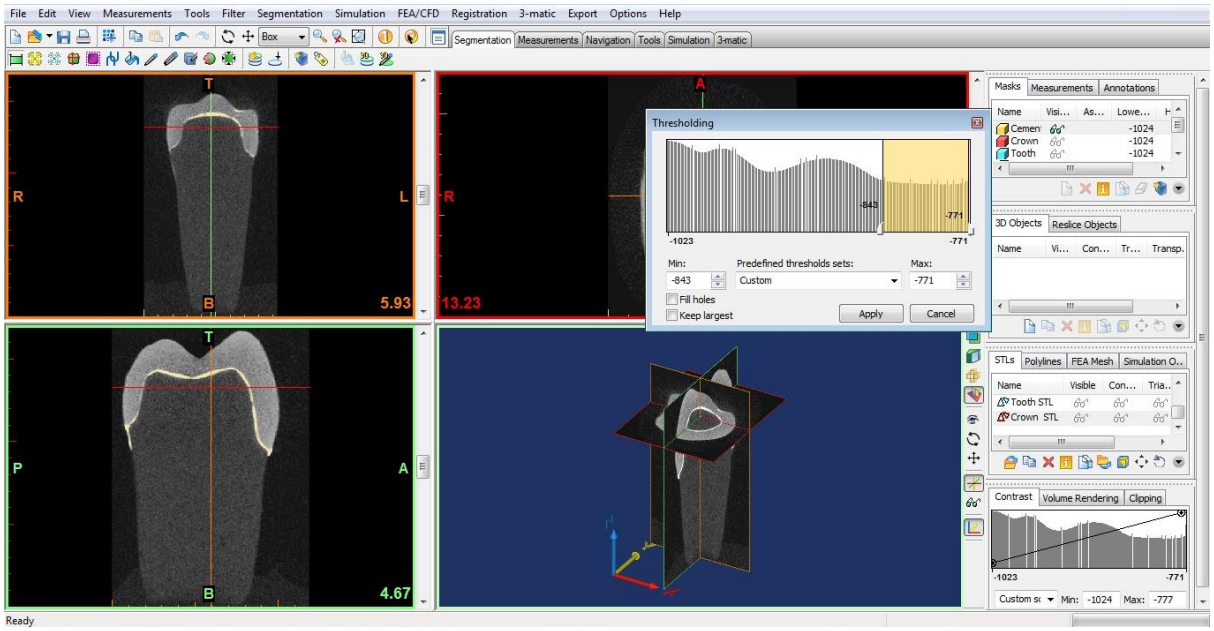

Figure 4-4: Thresholding option

A mask can be created by identifying the thresholding option to define the exact boundaries of one component such as the lute interface. The mask is a collection of pixels in a desired component in the 2D image where all the other functions (segmentation, editing, Boolean and 3D calculation) can be performed [Figure 4-4]. By creating a precise mask for the lute, the other components (the ceramic crown and the tooth) can be separated in masks sequentially [Figure 4-5].

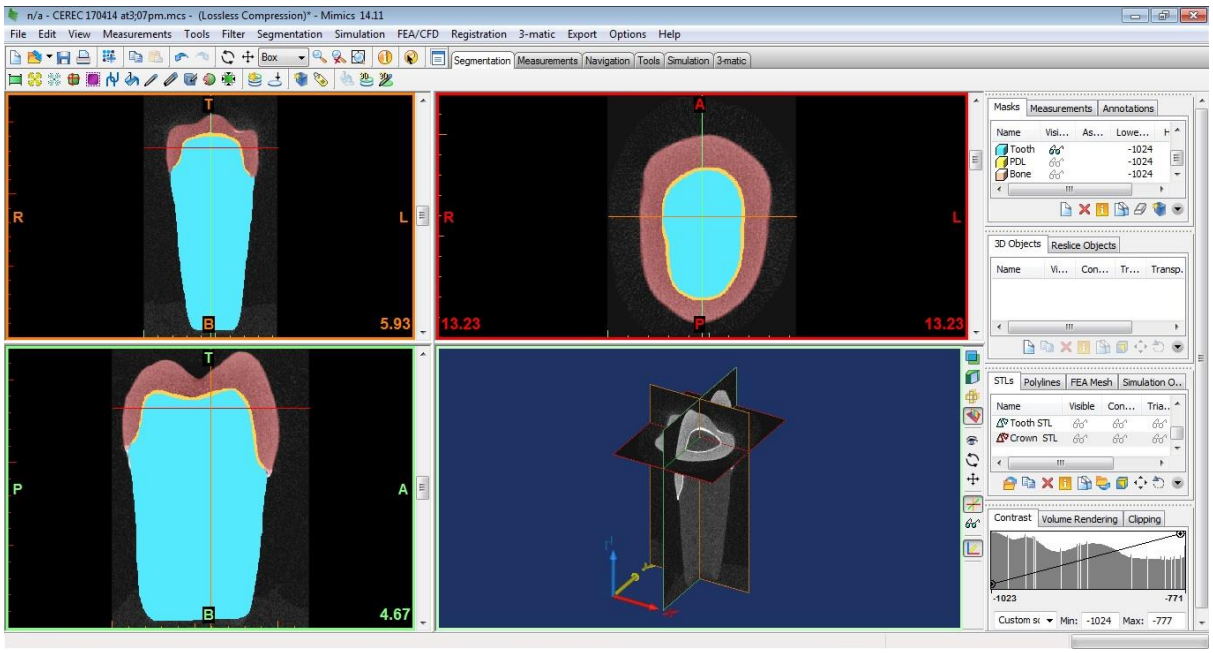

Figure 4-5: Masks generation

The segmentation function for the other components is performed with the 'Region growing' software tool. This tool enables the separation of the component that is not involved by the first default threshold to a new distinct mask. In this study, as the cement interface mask had a thickness below 200µm the 'multiple slices edit tool' was used to separate the crown mask from the cement interface mask. The 'multiple slices edit tool' removes noisy extraneous pixels in one slice and copies that for several slices using the interpolation option.

The creation of tooth masks followed the same steps. The Boolean tool was used to confirm the precise separation of these interrelated masks. The Boolean

tool offers a capacity to discriminate precisely between the boundaries and confirm an intimate interface [no dead space] between each mask with the other. In this way, the lute interface mask was ideally separated from the ceramic and tooth masks.

4.5.3.3 3D calculation

Following the perfect segmentation of all the components, a 3D model can be generated by using the option of 3D calculation. The 3D Calculation option is conducted separately for each mask that yielded an optimal 3D object as show in [Figure 4-6]and [Figure 4-7]. The generated 3D model of each component is exported in an STL [stereolithography] format to be used by FEA and CAD software.

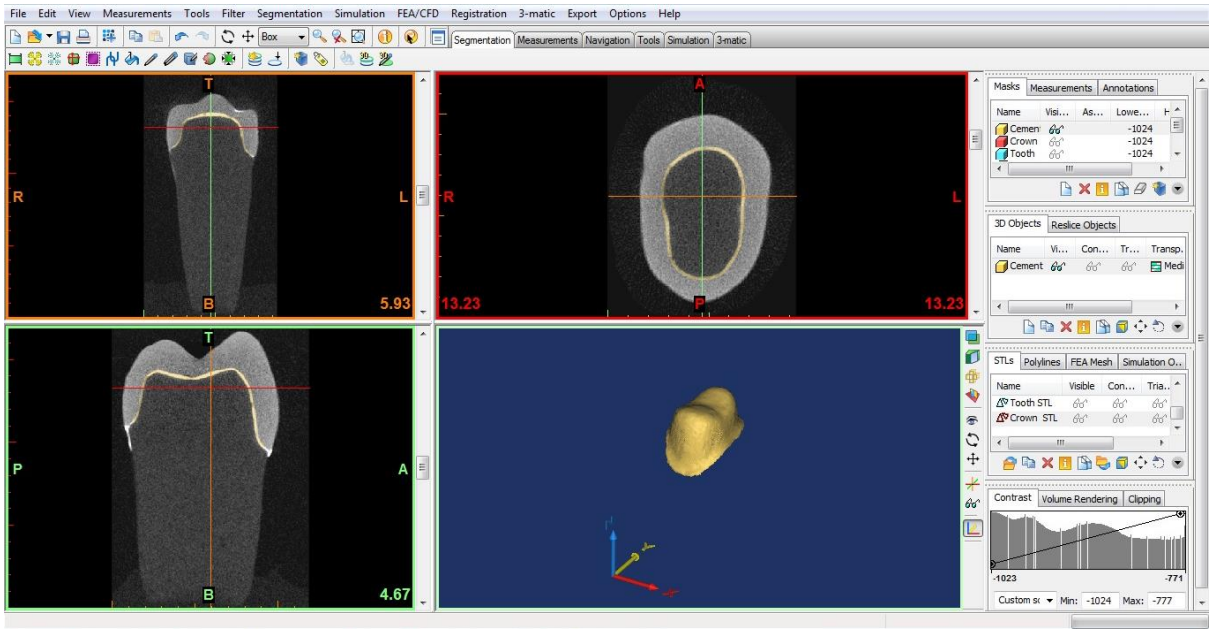

Figure 4-6: 3D calculation of the lute interface component

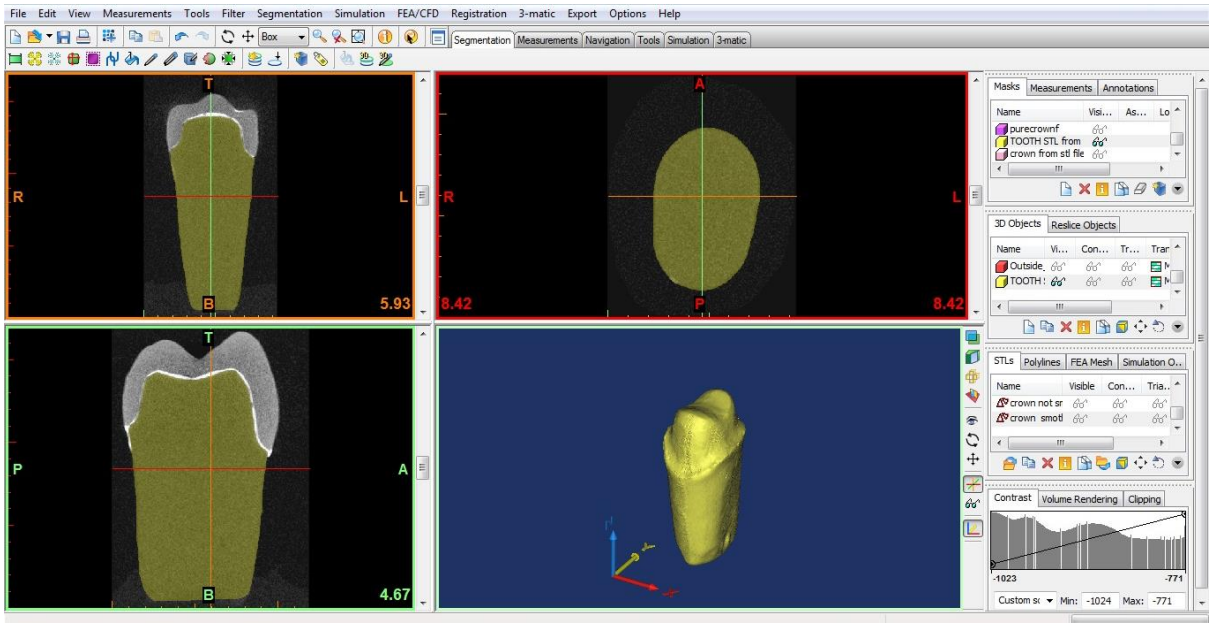

Figure 4-7: 3D calculation of the tooth component

4.5.4 Modelling PDL and Bone with FreeForm® haptic technology

As the digital 3D model was generated from an artificial tooth, the PDL and bone structures are missing.

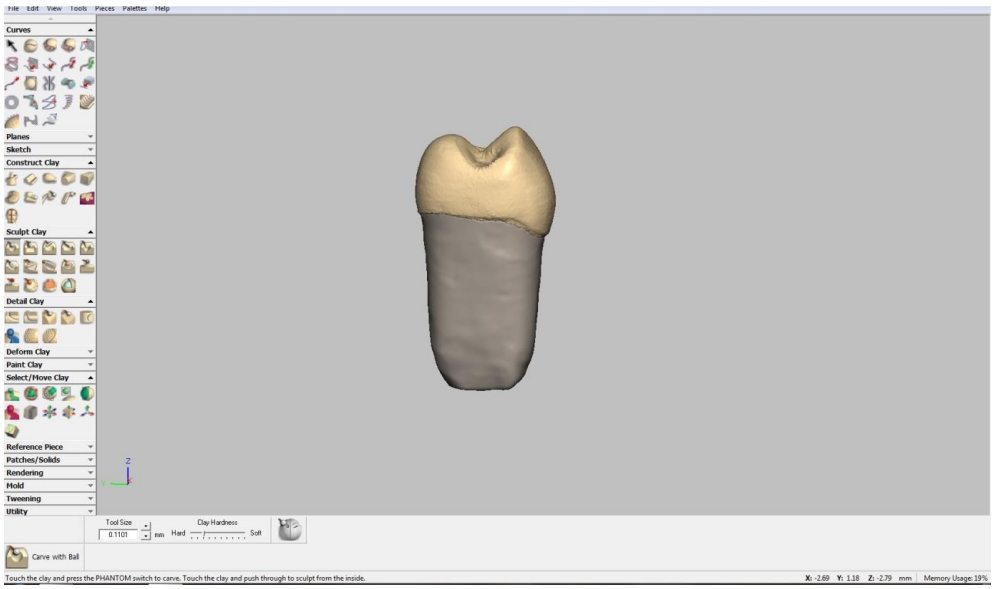

Figure 4-8: Import of STL files in FreeForm®

To create the PDL, the dentine (tooth clay object) was used as a guide. In order to obtain an ideal adaptation of the PDL around the root surface of the tooth clay, the tooth clay was duplicated. By the offset option, the tooth clay was offset externally by 0.222 mm in accordance with natural PDL dimensions [0.2-0.3mm] [Figure 4-9].

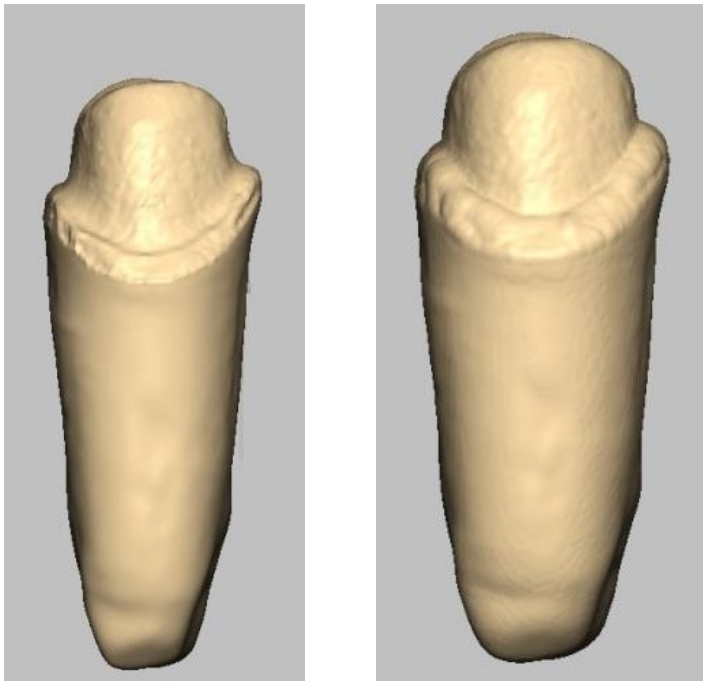

Figure 4-9: Offset step for generation of PDL-[A] original, [B] offset

When the offset is created in a new active clay, the duplicated tooth object is removed from the offset clay (using remove clay option) to leave an object with an inside empty space of an overall boundary thickness of 0.222mm. Haptic arm technology as a complementary tool of FreeForm® technology was adapted for the virtual modelling design of the PDL structure. A curve line was drawn by the 3D touch-enabled force-feedback system of the haptic arm (a tool that is analogous to a digital hand for the addition or subtraction of the structure in the manner of sculpting) on the active offset clay at a distance of 2mm below the coronal part of the tooth. The curved line can be adapted to the tooth surface by the option of fit curve. When the line fitted on the surface, an inside groove

corresponding to the curved line space was created by the Groove tool option. Subsequently, the inside grove was removed to leave a PDL part separated from the coronal part [Figure 4-10], [Figure 4-11] and [Figure 4-12].

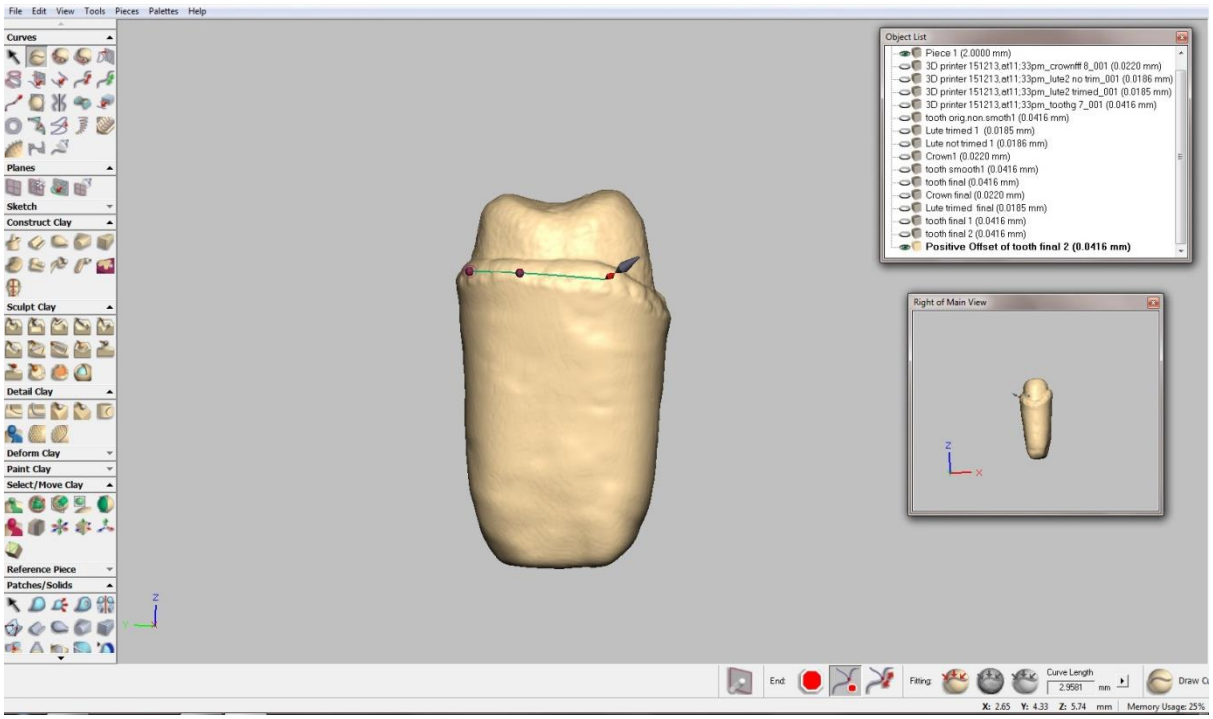

Figure 4-10: Drawing curved line to fit it on the surface

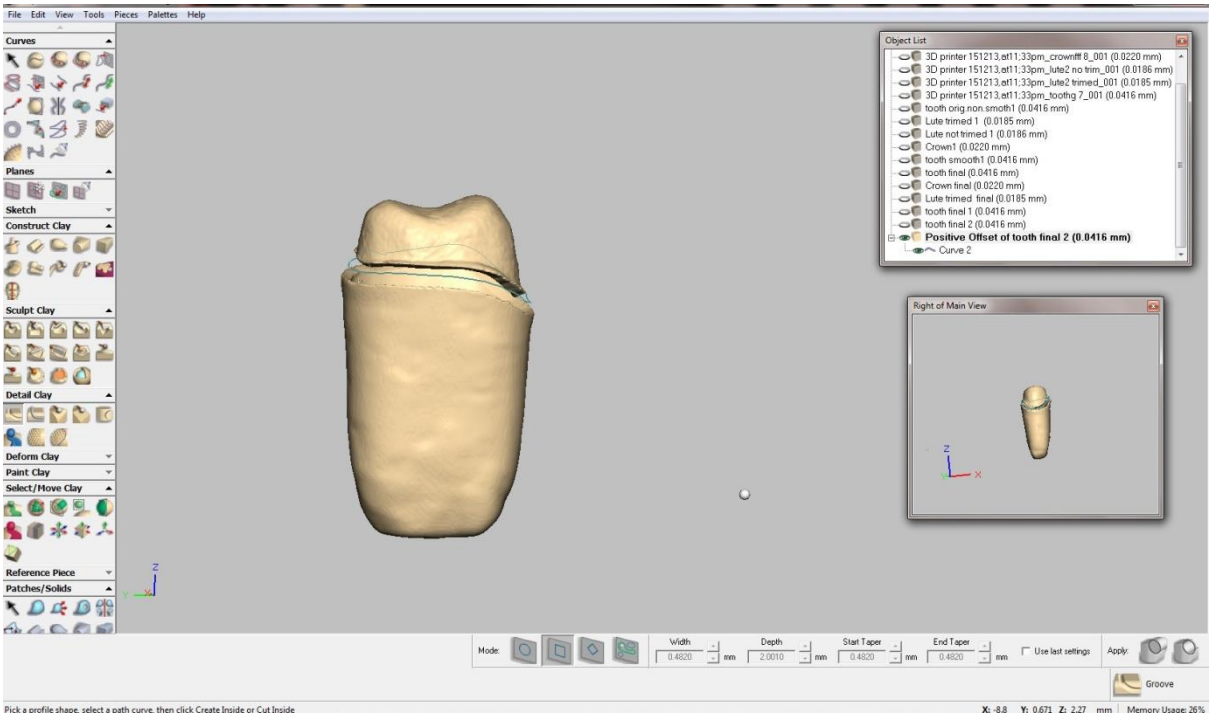

Figure 4-11: Generating the PDL by removing the coronal part of the offset

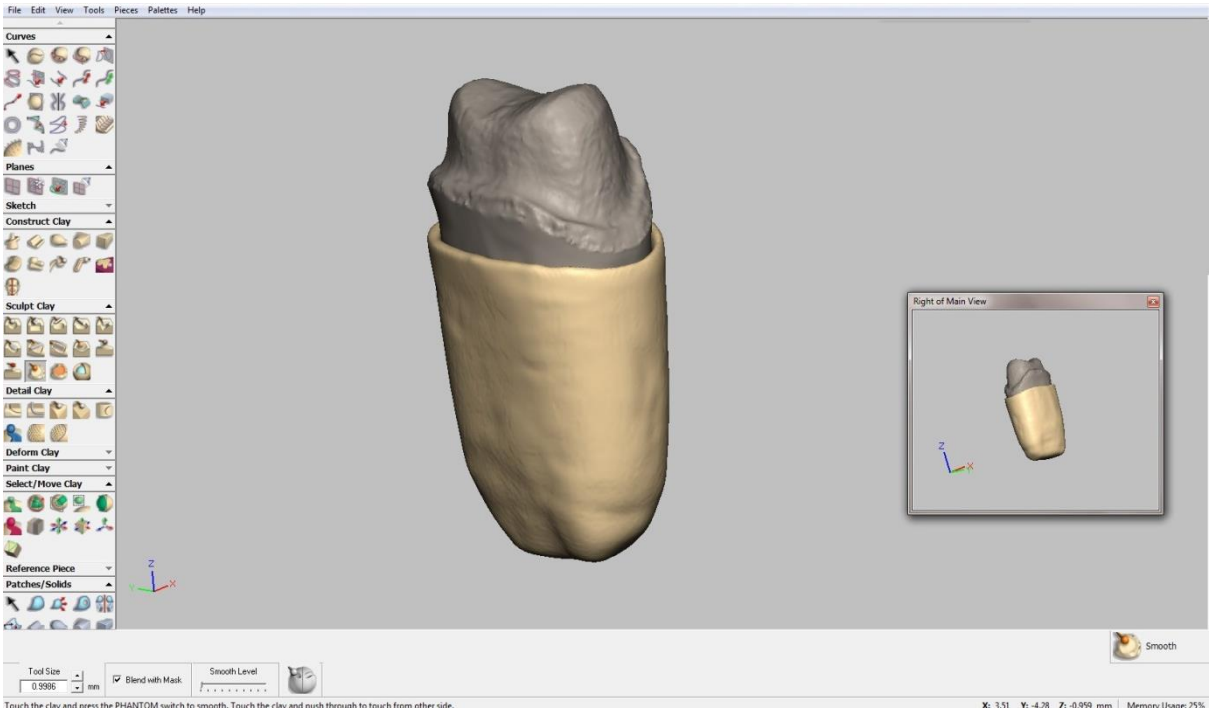

Figure 4-12: Perfect adaption of the PDL to the Tooth objects

The steps of construction the supporting bone were similar to that of the PDL. In order to achieve a perfect contact relation among these interrelated structures, bone-PDL-tooth, duplicated objects of the PDL and the tooth were requested. Through the software option of ‘combined clay’, the two duplicated clays [PDL and tooth clays] were combined in one clay object. Using an option of ‘construct clay’, an automatic cube object simulating the bone structure was introduced and applied to the activated PDL-tooth combined clay. Thereafter, the positive combined clay of PDL-tooth was subtracted from the created bone cubic clay by the option of remove clay to leave an exact space of the PDL and tooth objects inside the bone clay. Thus, each object was repositioned

accurately in its place and a perfect adaption of the interrelation objects [bone-PDL-tooth] was achieved [Figure 4-13] and [Figure 4-14].

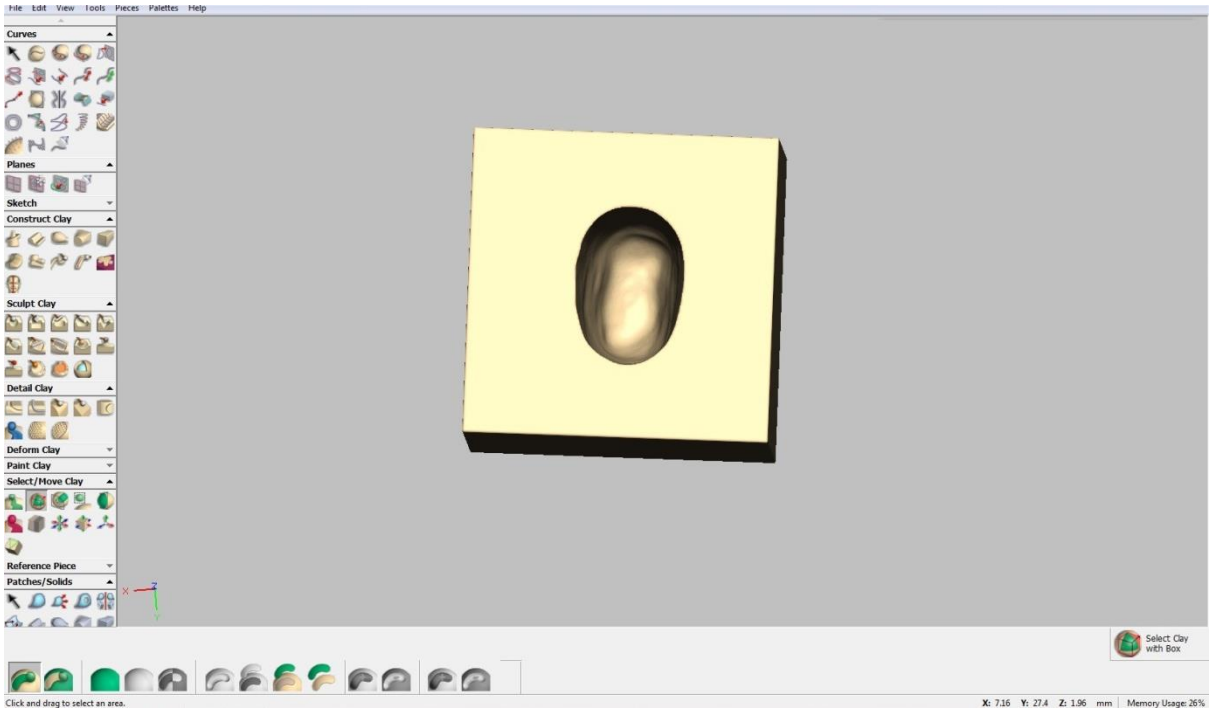

Figure 4-13: Automatic cube clay for bone simulation

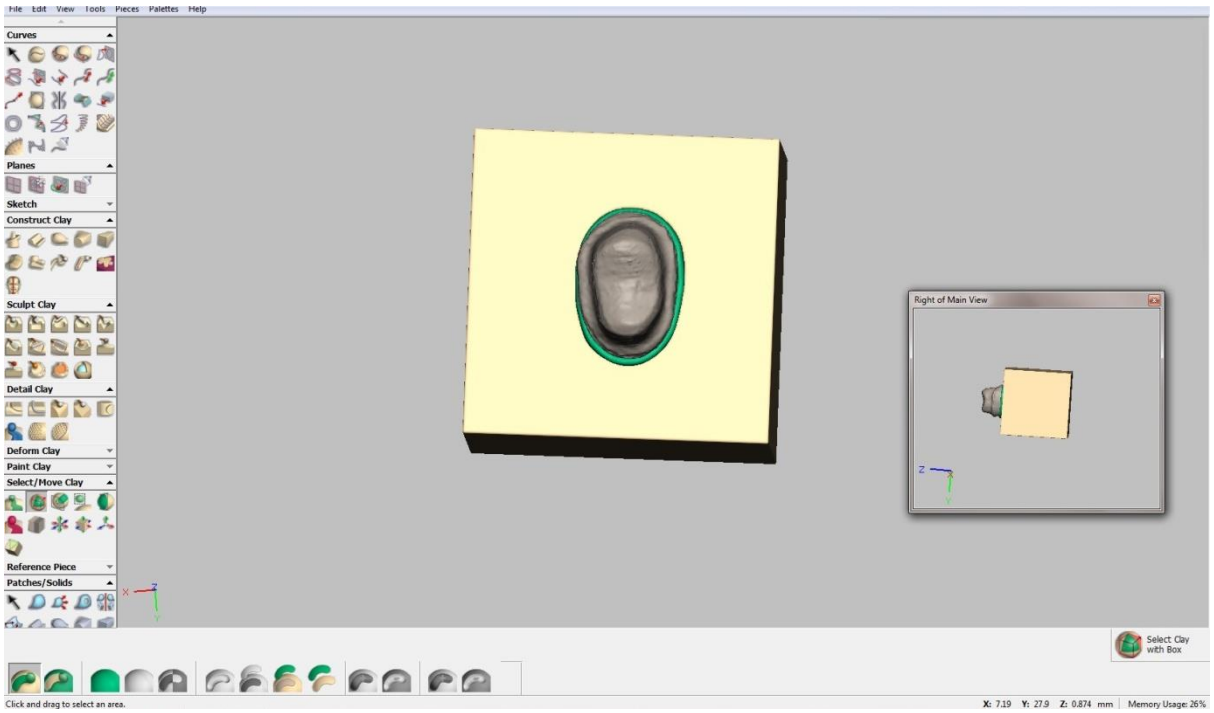

Figure 4-14: Optimum adaption between the Bone-PDL-Tooth

4.6 Discussion

In engineering, FEA is considered as a standard tool for assessing the stress/strain distribution in complex body geometry. However, the outcome reliability and accuracy can only be achieved when the precise life-like input data is given. Owing to the biological complex geometry of the body and dental structures, FEA has become a popular tool for assessing the stress distribution in most of biomechanical studies (Cattaneo et al., 2001, Geng et al., 2001, Tajima et al., 2009).

The use of image acquisition by means of the micro CT scan, as in the presented study, can produce a highly realistic model that is a true digital replica of the natural structure, within the limitations of the CT scanning technology. In this study, the combination of micro CT data and Mimics® modelling software was used. The 3D generated model had extracted from using the whole micro-CT slices compared with a study conducted at 2007 by Magine where he used just one out of 14 slices [81 slices total used] for the modelling purpose. Intuitively, a 3D model that depends on full acquisition data without any data exclusion could be considered as a more lifelike representative model (Magne, 2007).

For the present study, one of the major difficulties encountered with the 3D modelling steps was the inability to differentiate between the cement mask and adjacent mask during the thresholding steps. Since the thresholding tool

depends on the contrast scale between the layers, it was difficult to effectively separate the delicate thickness cement mask from the tooth mask and the ceramic mask. Although, it is time consuming and very labour intense, it was decided to identify the boundaries of the cement mask in each slice separately by using the edit tool. Thus, in contrast with other studies where the mask of the delicate interface might by created in other CAD software, the important masks of the present study [tooth-cement-ceramic] were entirely created within the Mimics® software. Since, the modelling steps have been mostly done manually which is more accurate than the automatically default operation, the model of the presented can be considered as an accurate reproducible model.

The optimum compatibility of Mimics® software with the CAD software was achieved with the use of an intermediate CAD programme [FreeForm® and haptic technology] in the modelling method. FreeForm® and haptic technology enable the designer of a 3D object relying on the tactile sensation and feeling-skill of the designer instead of the mathematical defined geometry in other CAD software. The sophisticated haptic handling tool and the enormous designing options of the FreeForm® software have allowed for a well-controlled modelling of the PDL and bone with retrieving a perfect interface among the components. Ultimately, the effective use of complementary software programmes has been used to great effect to develop a complex digital replica of a tooth restored with a ceramic crown that is supported in a block of alveolar bone with an

intermediate periodontal ligament of the correct dimensions and morphology. This model presents an ideal tool for FEA stress analysis.

4.7 Conclusion

1- The optimal complementary coordination between the 3D modelling tools of the Micro-CT, Mimics® software and FreeForm® with haptic technology has enabled the creation of an accurate and life-like 3D model. Thus, the Null Hypothesis that a valid and accurate 3D model cannot be generated by the combination of the micro-CT, Mimics® and FreeForm® technology can be rejected.

2- Since, the modelling steps depend mostly on manual work rather than an automatic operation, the 3D model can be considered as a valid and reproducible model with applications in FEA and other computational tests.

3- The presented methodology can be implemented for modelling accurately other dental or medical applications.

Development, validation and application of a novel technique for measuring the dimensions of the interface

Presented at:

- IADR/BSODR - British Society for Oral and Dental Research conference; Bath, UK, 2013.
    - *A Novel Technique for Characterising the Interface Geometry of Crowns* (Al-Marza et al., 2013)

- BSSPD - British Society of Prosthodontics Annual Conference; Dundee, UK, 2014.
    - *Validation of a novel technique for characterising the interface geometry of non-metallic crowns* (Al-Marza et al., 2014b)

5 Interface measurement

5.1 Introduction

This chapter covers objectives 1, 2 and 3 of the thesis.

The longevity of ceramic indirect restorations may be influenced by both the overall thickness of the luting agent and the quality of marginal adaptation (Qualtrough, 1993). A finding that is later confirmed by Wang et al, stating that the fit or accuracy of the marginal and internal adaptation is considered as a key requirement for clinical quality and success of fixed restorations (Wang et al, 2007). In addition to the actual thickness, it seems that the uniformity of the cement thickness affects the distribution of stresses within the cement and that a non-uniform cement thickness creates a less even stress distribution, that is likely to reduce the strength of adhesion of the adhesive cement (Mou et al., 2002). Reich et al. and Shu-Hui Mou et al. noted that in machined all-ceramic crowns, the cement thickness is not uniform (Mou et al., 2002, Reich et al., 2011); while Yeo et al. showed that pressed ceramic crowns have a more uniform interface, with less discrepancy and a good marginal and internal fit (Yeo et al., 2003). The effect of the interface geometry (dimensions and uniformity) on the fracture resistance of all-ceramic crowns has also been highlighted (Prakki et al., 2007, Giannetopoulos et al., 2010, Karatasli et al., 2011, Schaefer et al., 2012).

The internal adaptation of all-ceramic crowns is dependent on a number of factors: The accuracy and resolution of the master cast; the width of the spacer that is included in the design to allow a gap for the cement; the manufacturing technique, the physical properties of the lute and; the operator skill in achieving an effective cementation of the crown. This is further complicated as the master cast can be either a solid model (from an intra-oral physical impression) or a virtual digital model (from an intra-oral optical impression or optical scanned model). Thereafter, the crown can be fabricated by a range of techniques; manually hand-crafted either as an intermediate wax pattern or a definitive sintered porcelain device; digitally designed and subsequently cast, machined, sintered or pressed.

Given this range of variables, it is important to determine how they affect the internal dimensions. The human-operator variables (technician or clinician) are clearly impossible to quantify and an assumption has to be made that the skill mix of the individuals will be channelled to optimise this parameter. This leaves the nature of the ceramic, the fabrication technique and the role of the cement as variables that can be investigated and quantified.

In this respect, the role of the lute cement as a determinant of the interface dimensions has also been examined showing a relationship between the two (Schmalz et al., 1995, Addi et al., 2002).

Several methods have been used to characterize and measure the interface dimensions of the crown. The techniques used to date are by taking direct point

measurements of crown sections or of silicone replicas of the interface; both of which provide very limited data of questionable quality and use. The principal limitation is that these techniques are destructive and as such do not allow for repeated measurements (Shearer et al., 1996).

The replica technique was introduced by McLean and Fraunhofer in 1971 (McLean and Von Fraunhofer, 1971) and considered the gold standard technique for measuring the interface. Subsequently, it was used by other researchers for the purpose of measuring the internal adaptation of the restored teeth (Boening et al., 2000, Tinschert et al., 2000, Nakamura et al., 2003, Tsitrou et al., 2007, Reich et al., 2011).

The replica technique is considered as a reliable and non-invasive method. It is however, neither a reproducible nor repeatable technique. The concept that underpins the replica technique is the use a light body silicone impression material to replicate the space between the tooth and the restoration (Laurent et al., 2008).

A further disadvantage of this technique is that the measurements obtained from any section in any given plane may be different from those obtained on a different plane. It is a 2D system and can only be measured where it has been sectioned. Furthermore, it is not possible to standardize the position and the angulations of the measuring planes between samples, and that reduces the accuracy particularly when compared between different samples. The study conducted by Qualtrough et al, showed that it is just a measurement of the

silicone that occupies the interface gap, and does not replicate the behavior of the cement in the real clinical situation (Qualtrough et al., 1993).

Given the limitations of these techniques, there was a need to develop a new measuring technique that enable characterizing the internal dimensions and geometry of the interface in an accurate, reproducible and repeatable manner.

The introduction of micro CT scanning technology and the ability to acquire high resolution and data-rich geometry enables the creation of a very accurate 3D replica of the real object. Generally, the more accurate the data of the captured images and the created 3D model, the more accurate are the results obtained.

More recently, and because computer modeling software such as Mimics® software (Materialise Interactive Medical Image Control System, Materialise Co., Ltd) is compatible with micro CT scan based data, an effective alternative technique for measuring the interface has been developed, thus enabling the digital representation of radiopaque physical specimens in the form of an accurate 3D model. Within the software capabilities, the option of thresholding (separating a model into its component parts) has made further helped by producing 3D representation of the tooth, interface cement and the crown as independent structures that can be characterized.

In order to identify the boundaries of the interface on a micro-CT scan, it is necessary to have a clear contrast between the different substrates: Dentine-composite cement -ceramic. Composite cement was found to have insufficient

radiopacity and consequently it was not possible to separate this from the adjacent dentine and ceramic. To improve the radiopacity of the objects being examined, CT contrast agents (Iodine, barium, barium sulphate and gastrografin) are used to highlight specific areas. In the case of the crown-tooth model, it is necessary to ensure sufficient contrast difference between the interface cement and the adjacent ceramic and dentine structures on either side to enable their digital separation and manipulation.

Barium sulphate has been used for a long time in assessing dental failure (Webber et al., 1981, Fava and Saunders, 1999). Usually, to improve the radiopacity of the calcium hydroxide paste, barium sulphate has been used in a ratio of 1:4 (Dumsha and Gutmann, 1985) or 1:8 (Webber et al., 1981, Kleier et al., 1985).

There is a requirement to investigate how an interface geometry can be optimised and accurately characterised in a more accurate and reproducible manner.

5.2 Aims

1. To develop and validate an alternative accurate, reliable and reproducible measuring system of the interface.
2. To explore the possibility of creating a uniform thickness interface for ceramic crowns.

3. To apply the novel technique to characterise the interface geometry between ceramic crowns and tooth.

5.3 Objectives

1. To create an accurate 3D digital model of the cement interface of adhesively cemented all-ceramic crowns and measure the interface by the novel technique.

2. To validate the measuring system by compared the measurement of the virtual 3D model with the actual physical model using the laser micrometer.

3. To attempt the creation of a uniform film thickness of the interface by vacuum forming a polymer separator layer over the preparation die prior to manufacturing the crown.

4. To scan the cemented crown-tooth complex by micro CT and create an accurate 3D digital model of adhesively cemented all-ceramic crowns created by the two main fabrication techniques [Pressed and Machined techniques] on a restored tooth.

5. To compare the uniformity of the interface of five different fabrications processes: (i) Pressed with hand-painted separator; (ii) Pressed with heat-formed polymer sheet separator; (iii) Pressed with 3D printed wax pattern

and machined using (iv) Machined with CEREC 3 system and (v) Machined with Zirkonzahn® system.

5.4 The hypothesis

1- A digital measurement of the interface based on a micro-CT scan data will be more accurate and reproducible than the replica and sectioning technique.

2- The fabrication technique for the crown will affect the dimensions and geometry of the cement interface of ceramic crowns.

5.5 Materials and method

5.5.1 Developing the novel technique for interface measurement

5.5.2 Influence of Barium Sulphate on the viscosity of the cement

The addition of barium sulphate to the composite cement was considered in order to increase its radiopacity [Figure 5-1], but a concern remained that this may affect cement viscosity and in turn affect the ability to flow during the cementation preventing full seating of the crown.

The viscosity of the modified cement (resin cement + Barium Sulphate) was assessed with a rheometer [Anton paar, Physica MCR 301, Germany]. The following method parameters were used: 10 seconds mixing of the cement on a suitable pad; 5 seconds for placing the mixed cement in the rheometer plate; the rheometer cone oscillating at a strain rate (0.01% -1%) for an automatically

selected 30 measuring times; 0.5mm the gap between the cone and the plate during the measurement and; the test performed at room temperature. A recommended amount of Variolink II resin cement (0.180g) of base and catalyst in a 1:1 ratio [Variolink II, intro pack, Liechtenstein, Ivoclar/Vivadent, LOT R72873, and Exp. 2014-08] was mixed and directly placed in the measurement plate. The profile of cone movement enables a measurement for the flowability rate at 30 points by measuring the resistance of the resin cement against the vibratory motion. Similarly, the same protocol was used again for the cement that mixed with (0.004g) weighting [with Mettler AJ100 balance] of Barium Sulphate (SIGMA-ALDRICH, ReagentPlus99, Pcode 1001155483, Germany). The data was compiled and statistically analysed.

The bulk of gathered data of the cement thickness for all samples were analysed with a one-way ANOVA (Analysis of variance) and Tukey's HSD Post-hoc test at 95% confidence intervals by using the statistical package SPSS (IBM SPSS statistics version 20).

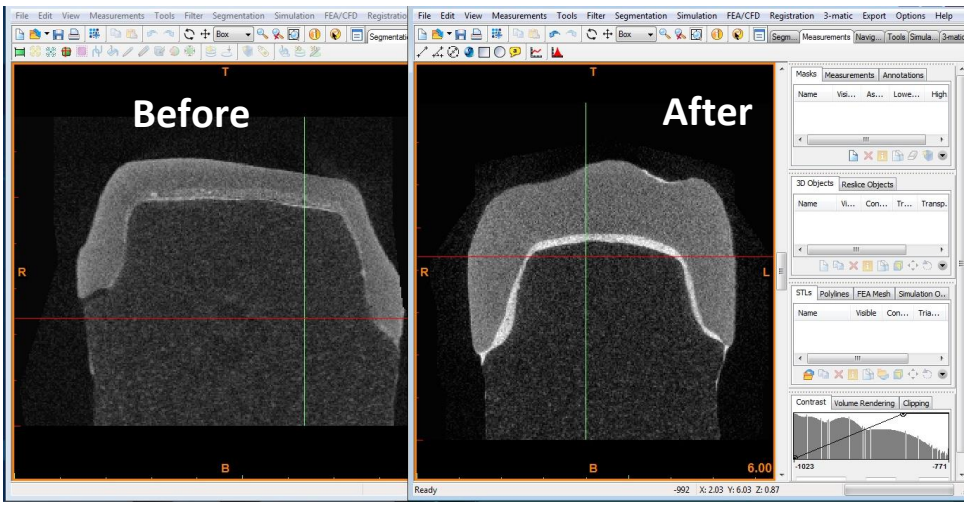

Figure 5-1: The cement interface before and after using Barium Sulphate

5.5.3 3D Model creation

5.5.3.1 Tooth preparation

An upper right first permanent premolar polymer tooth (Frasaco GmbH Oberhoferstrasse Tettnang, Germany**)** was selected to conduct the experiment. The tooth was embedded in its proper position in a Frasaco arch (Frasaco GmbH Oberhoferstrasse Tettnang, Germany). The preparation was based on the IPS e.max® system guidelines for standard all-ceramic crown preparation, according to Ivoclar/Vivadent guidelines [Figure 5-2] and [Table 5-1].

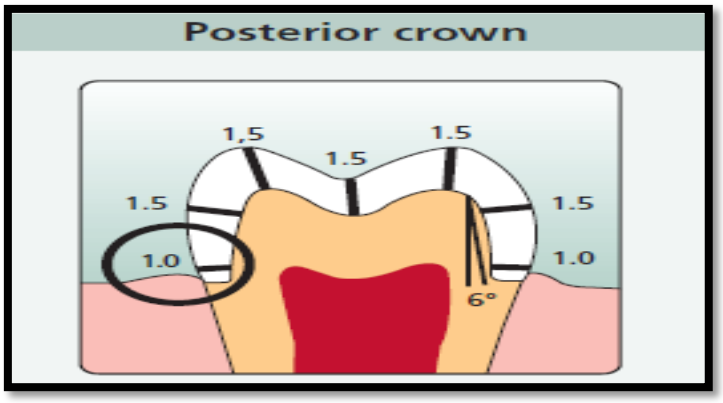

Figure 5-2: Illustration of maximum tooth preparation (From Ivoclar/Vivadent website)

Preparation guidelines

For e.max® Press:
http://www.ivoclarvivadent.us/zoolu-website/media/document/1269/IPS+e-max+Clinical+Guide

For e.max® CAD:
http://www.ivoclarvivadent.us/ivcadnews/september2012/files/ips-emax-ifu-chairside.pdf

Both web sites last accessed at 21/7/2011

Table 5-1: Preparation guidelines (adapted from Ivoclar/Vivadent website)

The occlusal reduction is	**1.5 mm**
The axial reduction is	**1.5mm**
The finishing line is (shoulder/deep chamfer all around)	**1.0 mm**
Taper degree	**6**

The preparation of the tooth was performed using diamond-coated burs in an air turbine with spray cooling.

5.5.3.2 Ceramic crown fabrication

In order to create a crown for developing the novel technique for the interface measurement, a CAD/CAM crown fabrication system was selected. The inEos (Sirona Dental Systems GmbH, Germany) system and CEREC inLab software version 3.60 were used for scanning and designing the crown. For milling of the restorations a CEREC 3 inLab (SIRONA Dental Systems, GmbH) was used. The IPS e.max® CAD (lithium disilicate) ceramic block for CEREC / inLab (shade HT A3, Ivoclar Vivadent, Germany) was used for milling of the crown.

In order to take an optical impression of the prepared tooth, the sample was sprayed with an optical scanning powder (CEREC powder VITA Zahnfabric, Germany). The crown restorations were designed using the CEREC inLab software version (3.6).

Due to the errors in the crown fabrication, the interface space is most often different from the desired. In this project to standardize the setup parameter of the cement thickness, a zero value of the thickness was designed within the CAD/CAM designing software. The thickness of the crowns was set up according to the recommendation from Ivoclar/Vivadent Company.

5.5.3.3 Cementation technique

According to the manufacturer's recommendation of cementing an e.max® restoration, Variolink II resin cement [Variolink II, intro pack, Liechtenstein, Ivoclar/Vivadent, LOT R72873, Exp. 2014-08] was selected to fill the interface gap. A suitable amount of base and catalyst in 1:1 ratio was mixed according to the manufacturer's recommendations. In order to ensure an effective contrast scale of the composite cement, the assigned amount of cement [0,180g] was mixed with a (0.004g) weighting [with mettler aj100 balance] of Barium Sulphate (SIGMA-ALDRICH, ReagentPlus99, Pcode 1001155483, Germany) as a contrast media as described previously. No acid etch was used neither on the abutment nor on the ceramic crown in this experiment to preserve the natural interface surfaces.

5.5.3.4 CT scanning

To replicate the interface geometry digitally, a high-resolution micro-CT scanner (Sky scan 1172 micro-CT, Aartselaar, Belgium) was used to scan the tooth that was cemented with the all-ceramic crown [Figure 5-3]. A resolution of 7.9 μm was selected with a distance between incremental slices that was the same as the resolution (7.9 μm).

[Table 5-2] shows the setup parameters of the CT machine for scanning the sample.

Table 5-2: Set up parameters of the micro CT scanner

The resolution	7.9 μm
The filter	Al Foil (1mm)
Camera	Medium (1000x2048)
Voltage	80kv
Rotation	360^{o}
Current	124μA
Power	10W

Figure 5-3: Sky scan micro-CT scanner

5.5.3.5 Mimics® modelling and measuring

The outcome of scanning the restored tooth sample was a stack of CT images. The CT images were then imported into Mimics®14.1 software (Materialise Interactive Medical Image Control System). Mimics® [image modelling software] allow transferring the images into a 3-dimensional object, which in turn allowed for more precise calculations in different directions. The measurement was done in three virtual planes; sagittal, coronal, and axial planes, which corresponded to the labio-lingual, mesio-distal, and horizontal planes respectively.

A novel method for measuring the interface dimensions with Mimics® software was developed. This method was performed by measuring the identical predefined nine points in the same cross sections for each sample. Since, the default view of Mimics® homepage centres each aspect view (sagittal, coronal, axial); the standardisation of the measuring technique is now possible.

In the axial cross-sectional of the default view, identifying the measurement planes achieved by drawing lines to set a measurement away by 0.5 mm and 1.0 mm from the (x, y) default axis lines (x and y are representing the horizontal and vertical 2D body directions respectively) in each direction (above and under to x-axis) and (anterior and posterior to y-axis) [Figure 5-4]. Ten cross-sections were selected for the purpose of setting a measurement for the sample. The measurement technique can be obtained in a very accurate scale. By scrolling the wheel of the computer's optical mouse above the requested aspect view that to be measured (sagittal or coronal), the main crosser line (x- or y-axis) can be moved over the axial aspect view until the required point is reached. Thus, a definite cross section became determinable in each sample by using this technique.

Similarly, the measurement points in each cross section were drawn according to their distance from the x-axis in the cross section to be measured. By drawing lines for set a measurement away by 0.5 mm above, and 1.0mm, 2.0 mm below the x-axis on the right and left side of y-axis, six points were drawn: marginal, mid-axial and axio-occlusal points (three points in the right side and three points in the left side) respectively. Due to the presence of two cusps in the upper first premolar, the other 3 points were the cusp tips and mid-occlusal points [Figure 5-5].

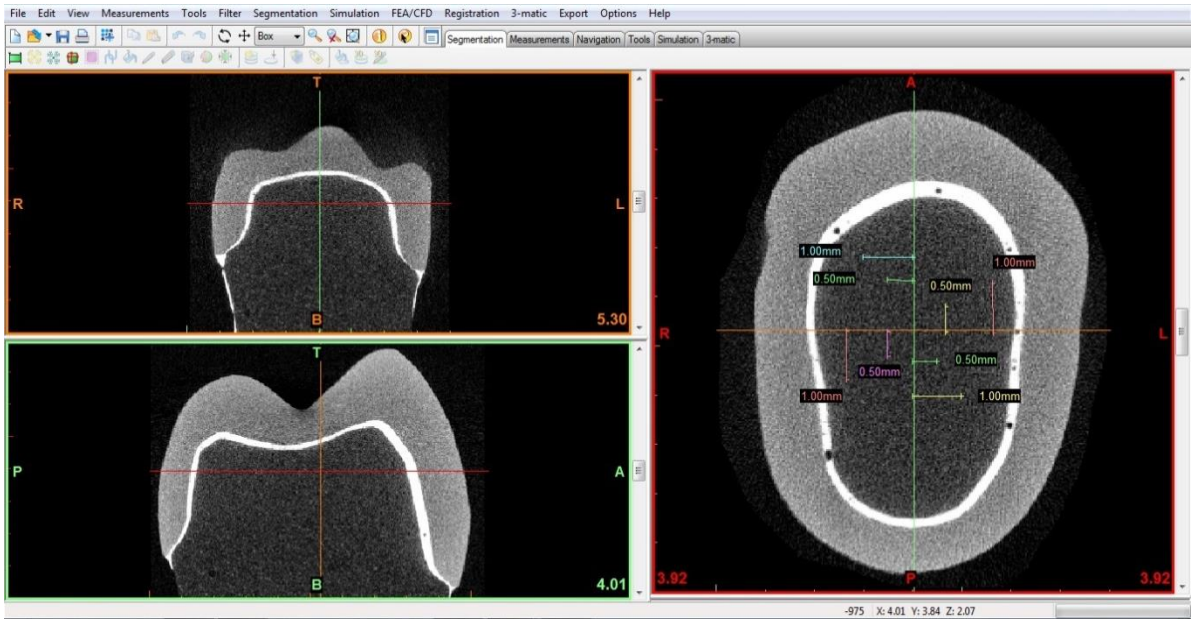

Figure 5-4: Mimics® default view and the standardise technique for cross-sections determination (novel technique)

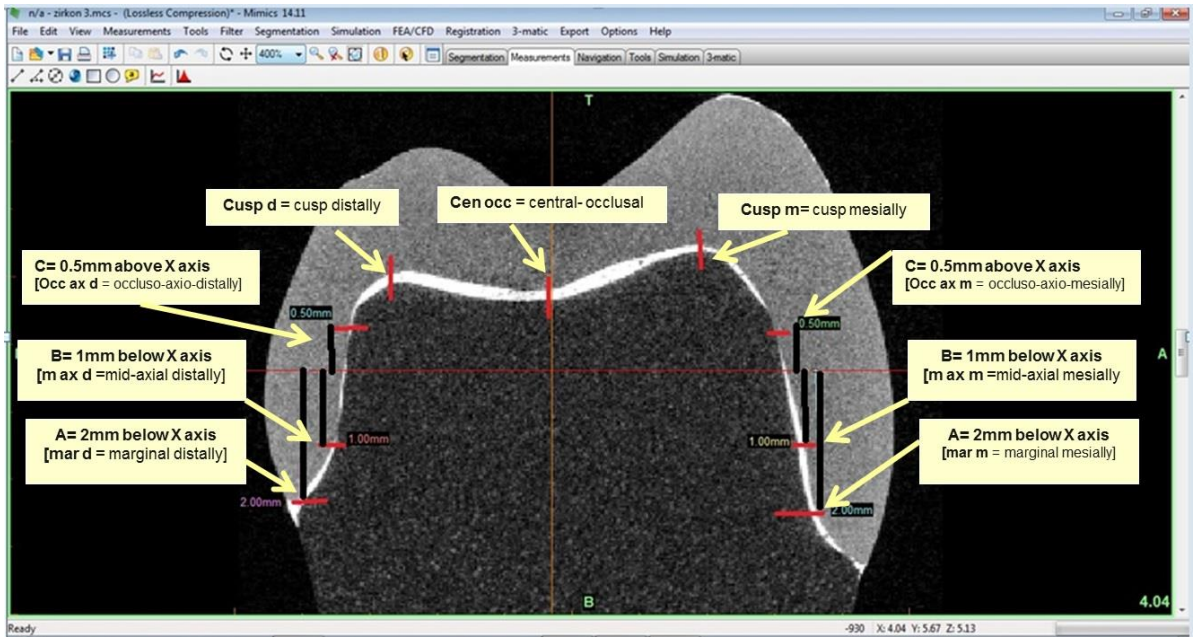

Figure 5-5: Determination of Measurement Points

Measurement points:

Table 5-3: Measurement point abbreviation

Abbreviation	Name
mar m	**marginal mesially**
max m	**mid-axial mesially**
occ ax m	**occluso-axio-mesially**
cusp m	**cusp mesially**
cen occ	**central- occlusal point**
cusp d	**cusp distally**
occ ax d	**occluso-axio-distally**
max d	**mid-axial distally**
mar d	**marginal distally**

Using the *measuring tool* option in Mimics® software console, each point was precisely measured. The measurement was performed considering the width of the highly contrasting cement from the external tooth surface to the inner surface of the restoration. Ultimately, 9 points were taken per a plane, making a total of 90 measurement points per sample collectively.

In order to check the reliability of measuring the interface in any aspect (coronal, sagittal and axial), a measurement in a 3D aspect was conducted for some randomly selected points [Figure 5-6].

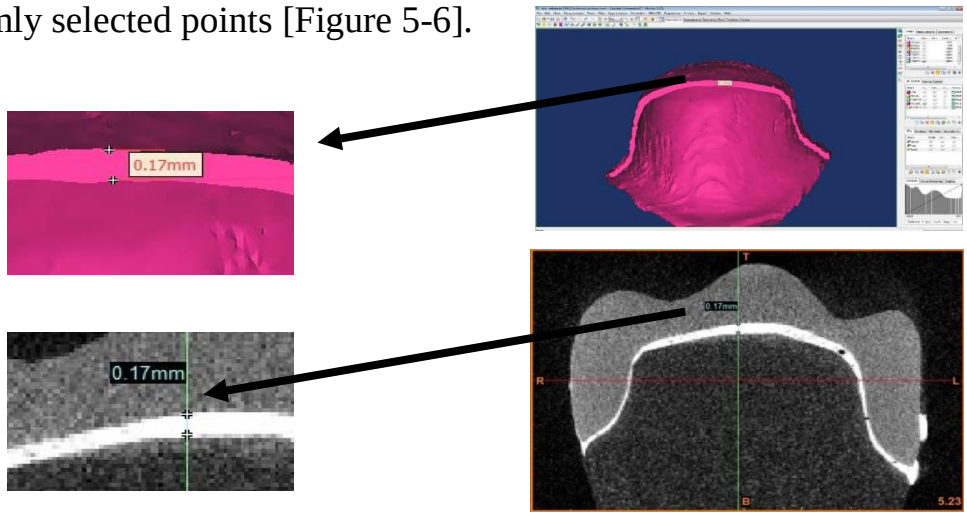

Figure 5-6: Measuring same point in 2D and 3D

Each point was measured twice to decrease the level of error. The data were sorted into tables according to the points of measurement for each cross-section at each direction.

5.5.4 Validation of the measurement technique

To validate the introduced technique, a comparison of regular physical and virtual model measurements was requested. A cylindrical ceramic object was used for conducting the experiment [Figure 5-7]. The specimen was scanned by the same micro CT scanner that has been used in the former experiment and the images data were exported. Thereafter, the images were imported in Mimics® software and used for constructing the 3D model of the ceramic disc. The measurement tool of Mimics® was used for measuring the diameter of the 3D object [Figure 5-8].

Figure 5-7: The ceramic disk specimen

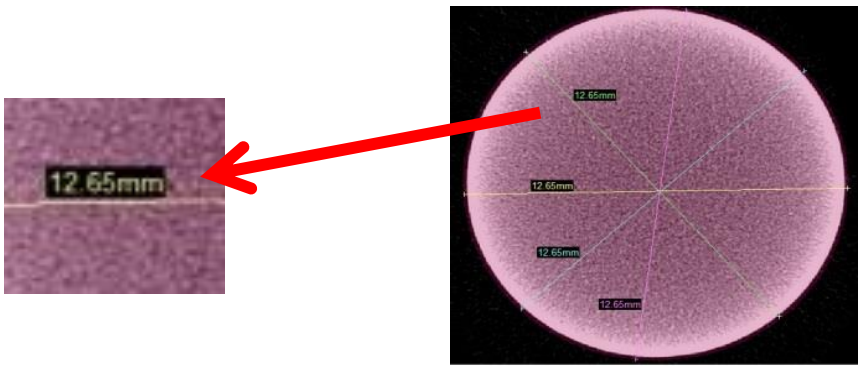

Figure 5-8: Mimics measurement

The same ceramic disk was used again for the actual measurement purpose.

A custom build laser micrometer measuring device that has been validated in former studies was used for the actual measurement of the ceramic disc (Martin and Jedynakiewicz, 1998, Martin et al., 2003). This device has designed to allow for 360° stepwise rotation of the specimen holder where the laser beam scans the work-piece [Figure 5-9]. The scanning array of the laser beam is emitted from the laser source and aimed directly at the ceramic disc specimen edge on, so that it is measuring the diameter of the disc [Figure 5-10]. The segment of the beam that is obstructed by the specimen will be interpreted as the diameter of the disc. A measurement was performed for each 1.8° of the ceramic disc specimen in a total of 200 steps. At each step, 256 repeated measurements were made and, thus 51200 measurements were obtained per cycle. Thereafter, the generated electrical current will be sent back to the computer as a measurement data and the mean of the 200 steps of the diametral measurement will be displayed directly [Figure 5-11].

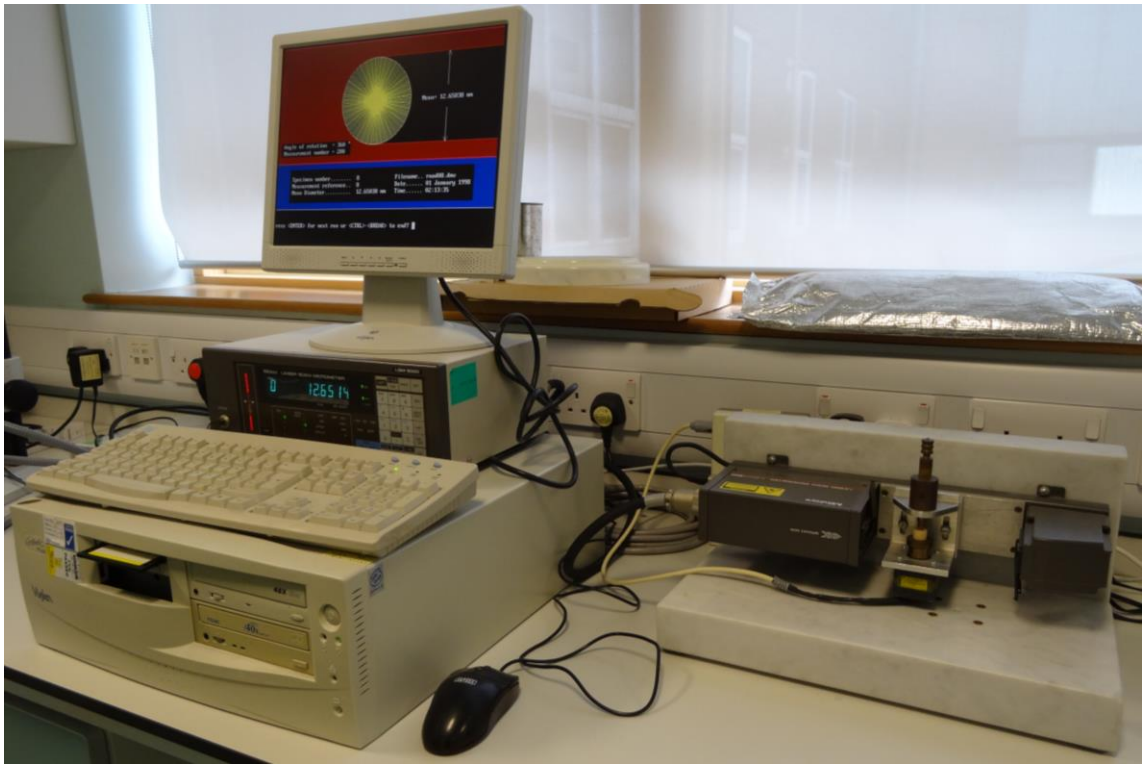

Figure 5-9: Laser micrometer assembly

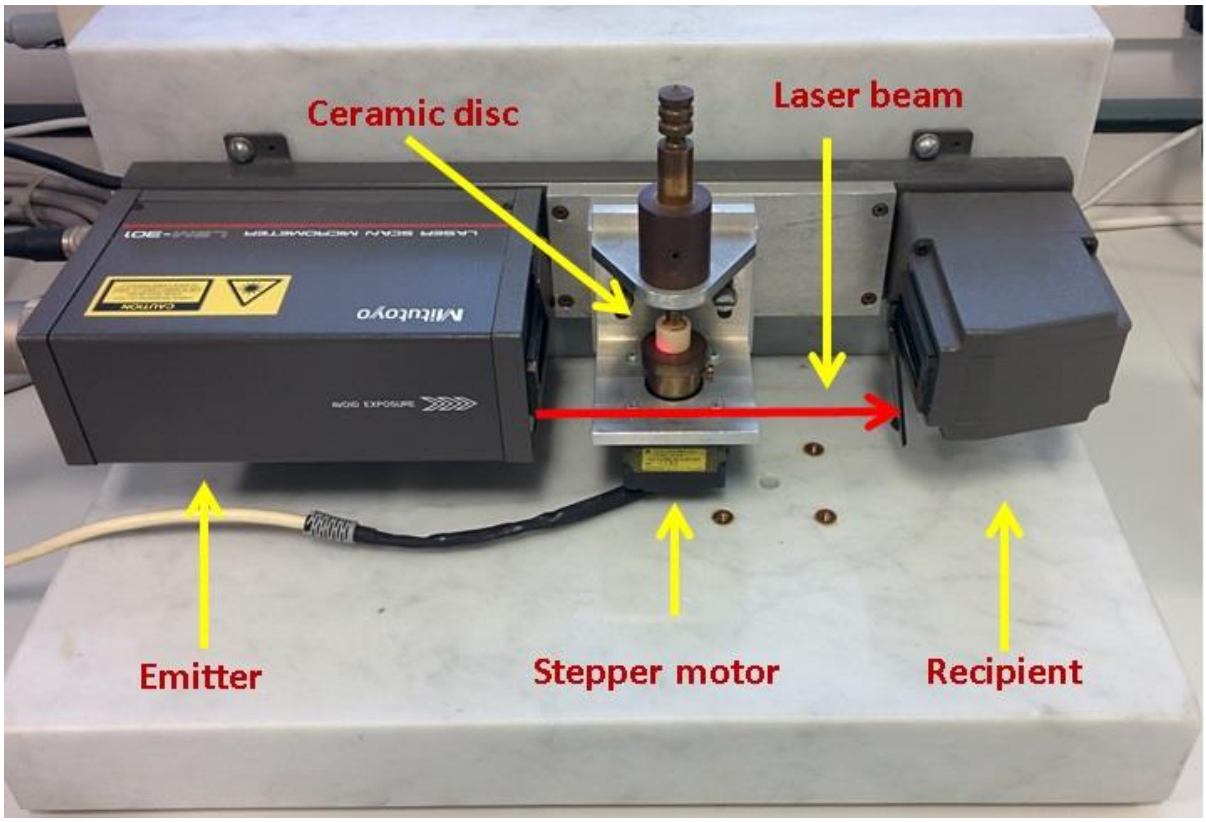

Figure 5-10: Laser beams scanning the ceramic disc

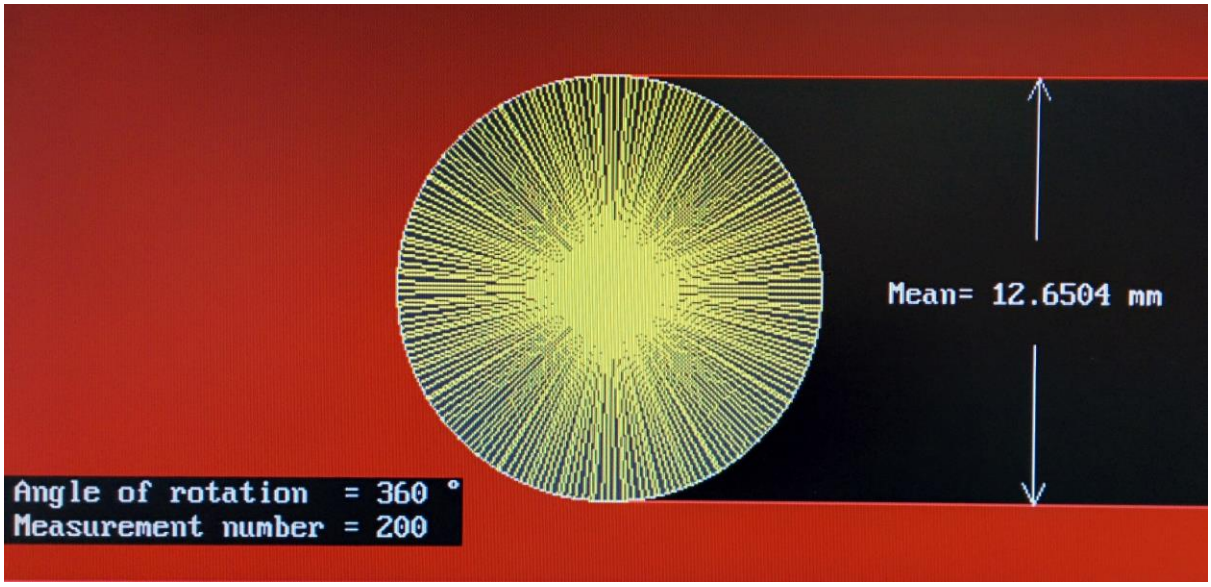

Figure 5-11: Laser micrometer measurement

5.5.5 Development of a new technique for creating a uniform thickness interface for pressed ceramic crowns [the vacuum-formed spacer technique (Isofolan®) samples]

For the purpose of creating a hypothetically uniform interface space between the crown and the tooth, a vacuum-formed polymer sheet of 100 µm thickness (Isofolan® SCHEU DENTAL, GmbH, Germany) was moulded onto the preparation dye with the aid of a Biostar machine. The prepared tooth sample was positioned in the central base of the Biostar. Through the action of heat and pressure, which were pre-set according to the manufacturer's guidance (220◦C and 2.6 bar pressure), the Isofolan® elastic foil sheet (Polyethylene low density PE-LD; thickness 100 µm, SCHEU DENTAL, GmbH, Germany) was adapted to the external surface of the sample. In this way, the thin Isofolan layer created a space corresponding to the space that would be created by the technician using the die spacer [Figure 5-12]. Subsequent steps of wax build up, wax lost technique and pressing the ceramic into the mould were followed the same route as in normal creation of a manual pressed ceramic crown.

A

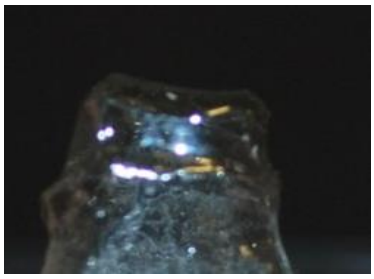

B

C

Figure 5-12: Vacuum formed Isofolan® on die (A) and following removal from die (B). Biostar vacuum forming machine (C)

5.5.6 Measurement of the crown-tooth interface width.

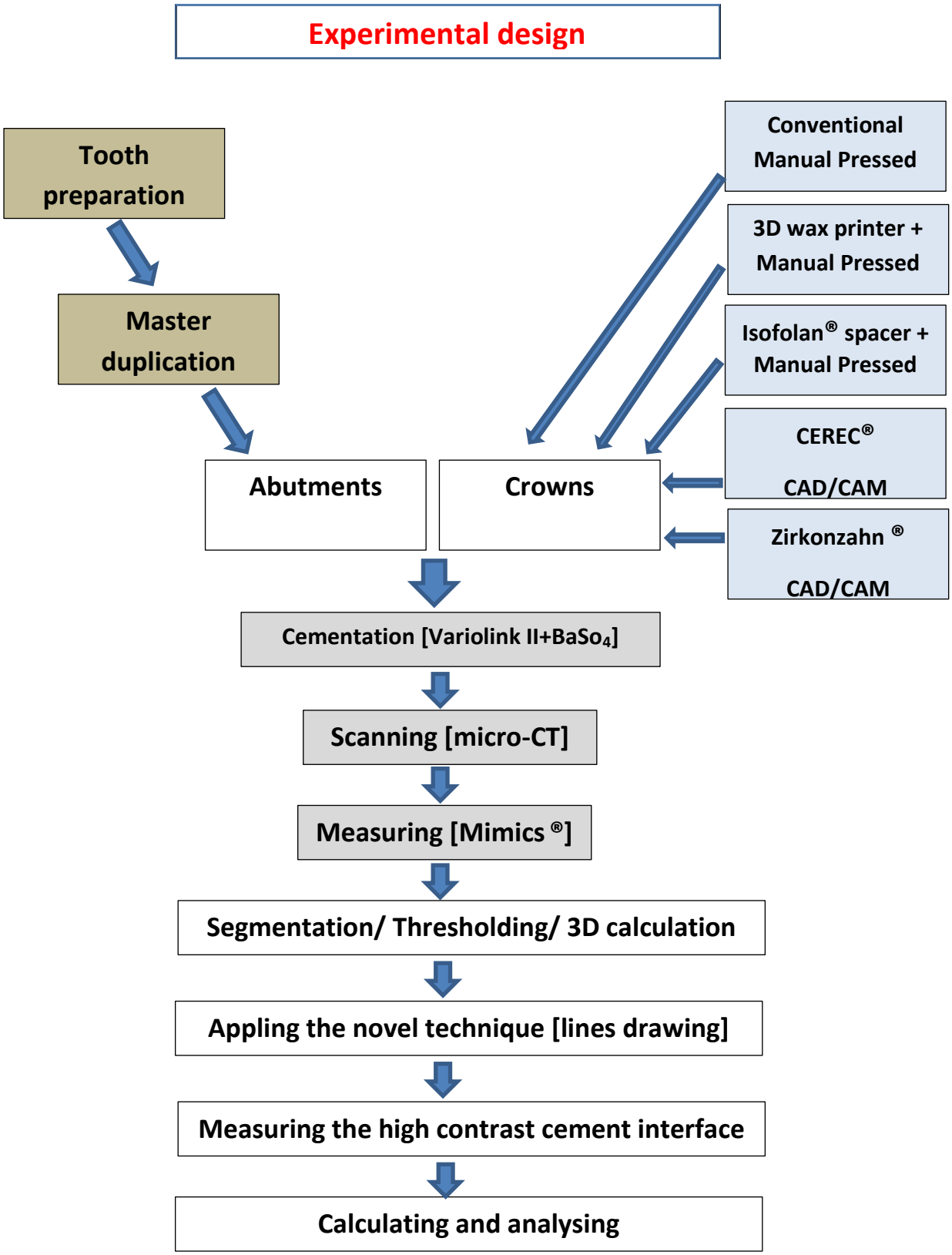

Figure 5-13: Experimental method steps for measuring the interface

Table 5-4: Dependent and independent variables tested in this experiment

Dependent variables	Independent variables
Cement interface thickness	Tooth preparation
Cement interface uniformity	Cement type
	Cement elastic modulus
	Ceramic fabrication techniques

5.5.6.1 Tooth preparation and sample creation

In order to exclude natural teeth variables (tooth size, dimensions and dentine structure), a plastic typodont permanent upper right first premolar tooth was used (Frasaco GmbH Oberhoferstrasse 1888069 Tettnang Germany**)**. The tooth was embedded in its correct anatomical position in a Frasaco arch (Frasaco GmbH Oberhoferstrasse 1888069 Tettnang Germany). The preparation protocol was the same to the earlier protocol in this experiment [fully described at section 5.5.3.1], following the guidelines from the manufacturer (Ivoclar/Vivadent) for the preparation of anterior and posterior crowns (IPS e.max® Press | IPS e.max® CAD)

The prepared typodont tooth was used as a master die and duplicated to fabricate 15 tooth replicas from the dentine-like polyurethane-based resin material (AlphaDie® MF, Schütz Dental GmbH, Rosbach, Germany) that has

an elastic modulus (14800 MPa) closely matched to dentine(Kohorst et al., 2007, Sarafidou et al., 2012).

Dublisil 15 (Addition-vulcanising vinyl-polysiloxane, Dreve Dentamid GmbH, Germany) was employed for the fabrication of the master die mould. Fifteen samples were duplicated from the master prepared tooth and were divided into five equal groups according to the following crown fabrication techniques:

a. Conventional pressed technique:
    i. Hand-painted separator on a solid model
    ii. Wax printed (3D wax printer) crown from a digital model obtained by digitally scanning the preparation die.
    iii. Heat-formed polymer separator on a solid model (Isofolan®)
b. Machining technique (CAD-CAM): CEREC® and Zirkonzahn®. Two different milling systems were tried to ensure that there would not be a milling-system variable that would affect the outcome.

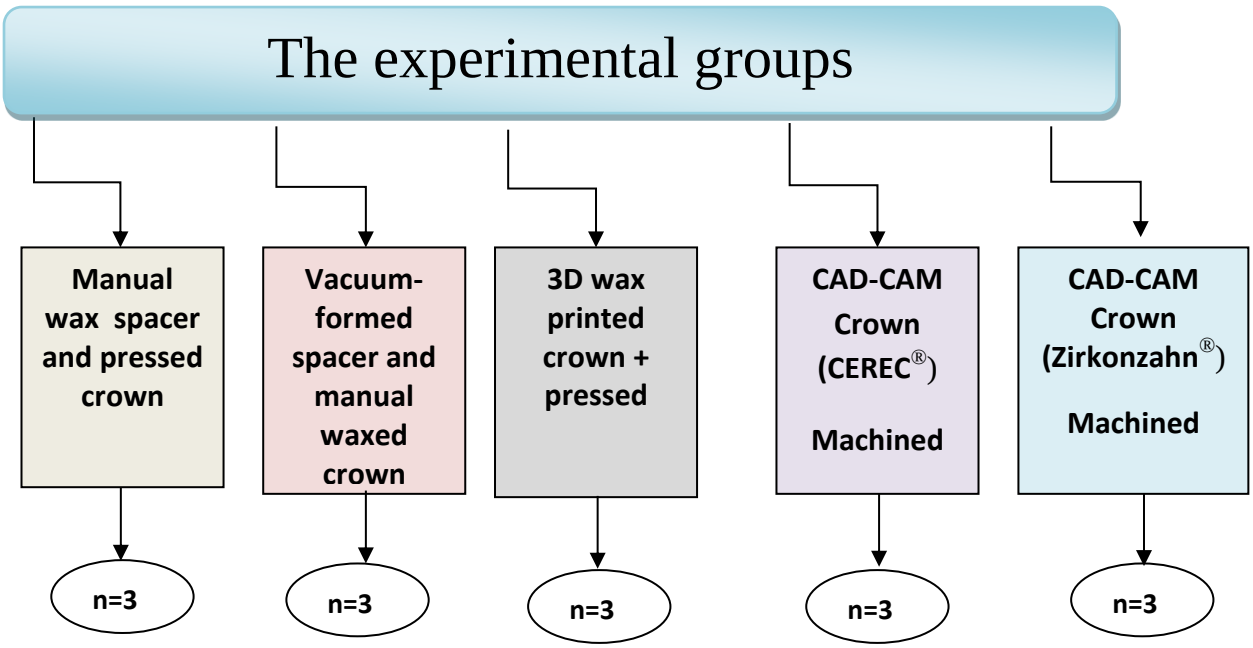

Figure 5-14: The experimental groups [n=3 crowns per group]

5.5.6.2 Nomenclature for the experiment

For this experiment, several techniques will be used and for ease of description I will simplify this by refereeing to each technique as follows [Table 5-5].

Table 5-5: Nomenclature of the experiment

Terms used in the Thesis	Description			
	Working model	**Spacer**	**Crown design**	**Crown fabrication**
Manual Pressed	**Solid stone cast from a silicone impression**	**Manually generated using (Surefit™ gold Die Spacers, Harvest Dental)**	**Manually designed and generated by wax**	**Conventional Pressed using e.max® Press ceramic ingot**
Vacuum Spacer (Isofolan®)	**Solid stone cast from a silicone impression**	**Vacuum formed using (Isofolan® SCHEU DENTAL, GmbH, Germany)**	**Manually designed and generated by wax**	**Conventional Pressed using e.max® Press ceramic ingot**
3D Printer	**Digitally scanned from a solid stone cast from a silicone impression**	**Digitally generated by software design programme (3M ESPE Lava™ Scan ST scanner)** **(Set at 0 microns)**	**Two stages:** **(i)Digitally generated by software design programme (Zirkonzahn® software)** **(ii) Physically printed in wax by a 3D wax printer (Solidscape® 3Z lab)**	**Conventional Pressed using e.max® Press ceramic ingot**
Machined Zirkonzahn®	**Digitally scanned from a solid stone cast from a silicone impression**	**Digitally generated by software design programme (3M ESPE Lava™ Scan ST scanner)** **(Set at 0 microns)**	**Digitally generated by software design programme (Zirkonzahn® software)**	**Machined using a Zirkonzahn® 5-axis wet milling machine using e.max® CAD**
Machined CEREC®	**Digitally scanned from a solid stone cast from a silicone impression**	**Digitally generated by software design programme (inEos®(Sirona Dental Systems GmbH, Germany))** **(Set at 0 microns)**	**Digitally generated by software design programme (CEREC inLab software® Version 3.60)**	**Machined using in-Lab CEREC 3 wet milling machine using e.max® CAD**

5.5.6.3 Manual Pressed samples

An expert senior technician constructed the 3 pressed crowns by following the manufacturer's guidelines for constructing lithium-disilicate glass ceramic crowns. A new brush was used to apply an even layer of the die spacer (Surefit™ gold Die Spacers, Harvest Dental) on the coronal part of the master die. Two coat layers were applied; each coat created 6µm of space (according to product's leaflet information). Thus, the total space was 12µm ±2µm.

Construction of the crown followed a very precise technique including three layering steps. The technician painted the die with a very thin layer of a copy separator (Pi-Ku-Plast trennlak®, Bredent medical GmbH & Co.KG /Senden/ Germany), which helps to separate the wax pattern easily from the die later. Subsequently, coat of spacer (Pi-Ku-Plast HP 36®, Bredent medical GmbH & Co.KG /Senden/ Germany), which comes in a form of monomer and polymer, was applied carefully and uniformly on the first created layer. This material is reported to have polymerization shrinkage of less than 0.036% with an advantage of setting very hard even in the very thin margin. Upon a complete setting of this layer, a very hard and stable shell was created.

The last layer was involved adding a wax on the created shell for shaping an anatomical crown according to the requested dimensions. This step was conducted by using dipping wax (Belle wax™, belle de st Claire, kerrlap, Kerr) to create a suitable contour of the tooth with 1.5mm thickness occlusally and axially, and 1.0mm at the margins. The crown was invested in a phosphate

bonded investment material (SHERA FINE-RAPID®, Sherkstoff technology, Germany). A suitable amount of powder was mixed with a recommended amount of liquid (SHERALIQUID®, Sherkstoff technology, Germany). Vigorous mixing by hand for 15 seconds was followed by mixing under vacuum for 60 seconds (mixing speed is 250 rev/min). Before the investment step, a thin layer of the surface tension release agent (SHERAMASTER®, Sherkstoff technology, Germany) was sprayed on the waxed-up sample to eliminate the chance of air bubbles being trapped during the investment step and to increase the wettability.

According to the lost-wax technique, the investment ring was put in a conventional pre-heating furnace for burning out the wax at 850 ◦C for 1 hour. Later, the investment container was positioned accurately in the Ivoclar press furnace (Programat EP 5000®) and the IPS e.max® Press ceramic (e.max® press ingot LT A3, Ivoclar Vivadent, Germany) was pressed into the mould in accordance with the recommended instructions.

5.5.6.4 3D wax Printer samples

A 3D printer (Solidscape® 3Z lab) was used to produce a wax pattern for a full coverage crown [Figure 5-15]. The same digital STL file used with the Zirkonzahn® CAD/CAM machine was also used with the 3D wax printer. Three wax patterns of full anatomical crown were printed using the same parameters

of the milled crowns. The subsequent steps for pressing the ceramic were the same to the manual pressed technique.

Figure 5-15: 3D wax printer

5.5.6.5 Vacuum-formed interface space generated samples

The vacuum-formed Isofolan® elastic foil sheet (Polyethylene low density PE-LD; thickness 100 µm, SCHEU DENTAL, GmbH, Germany) interface-space generated crown fabrication technique is used to create an interface space. The actual crown fabrication technique is the pressing technique as described previously. Three crowns were created in this manner.

5.5.6.6 CAD-CAM machined samples – CEREC®

The inEos® (Sirona Dental Systems GmbH, Germany) system and CEREC inLab software® (Version 3.60) were used for scanning and designing the crown. For milling of the restorations a CEREC 3 inLab®, (SIRONA Dental Systems, GmbH) machine was used [Figure 5-16]. The milling unit was calibrated in accordance with the manufacturer's recommendations.

In order to take an optical impression of the given tooth, the sample and its adjacent teeth were sprayed with an optical scanning powder (CEREC powder VITA Zahnfabric, Germany) before and after the preparation. The crown restorations were designed using the correlation mode option to create a crown with the same morphology as the original tooth (Frasaco® upper first premolar tooth).

The thickness of the crowns (an overall thickness of 1.5mm and the finishing line of 1.0mm) was set as per the manufacturer's recommendations (Ivoclar/Vivadent, Germany) and the interface was set to zero spacer.

For the milling process, "Endo mode" was selected and the cylindrical bur (REF 58 55 734) and the step bur (REF 60 52 265) according to the manufacturer's instructions were used. The IPS e.max® CAD (lithium disilicate) ceramic blocks for CEREC / inLab (shade HT A3, Ivoclar Vivadent, Germany) were used for milling the crowns. Also, in accordance with the Ivoclar /Vivadent recommendation, a Programat P300 furnace was used for final crystallization of the milled crowns.

By means of visual examination, several milled crowns were excluded. The selection criteria for each crown were: Perfect fit of the crown, single path of insertion, intact marginal integrity, and effective crown morphology. Any crown that did not meet these criteria was replaced by a new one.

Figure 5-16: CEREC InLab CAD/CAM machine

5.5.6.7 CAD- CAM machined samples –Zirkonzahn ®

An alternative milling system (Zirkonzahn®system (CAD/CAM system 5-TEC, Zirkonzahn, Italy) was tested to check for variation between the output between different techniques. Zirkonzahn® CAD/CAM system is a wet, water-cooled milling system (analogous to CEREC®) that can mill several types of materials

such as zirconia, resin, wax, sinter metal, wood, titanium, chrome cobalt and glass ceramic. This system has milling units that can operate to mill the object in 5 axes.

A physical silicone impression was taken from a Frasaco® full arch with a complete set of unprepared teeth sited in their correct position in the arch for the upper and lower jaws. The heavy body impression material [Express™ 2 Penta™ H, 3M ESPE, LOT507417 and Exp. 2015-01] and light body impression materials [Express ™ 2 light body standard, LOT505184 and Exp. 2015-01] with aid of 3M ESPE Pentamix 3 delivery unit. A further impression of the same Frasaco arch after replacing the prepared upper first premolar (master tooth) with the unprepared one was taken. The casts were scanned by 3M ESPE Lava™ Scan ST scanner. Similar to the CEREC inEos scanner, the correlation mode option was used. The parameters were set up analogous to the CEREC parameters. The final design was exported in a format of STL file and sent to Zirkonzahn® CAD/CAM system in Italy. The STL file was imported in the open system Zirkonzahn® milling machine. Using the IPS e.max® CAD blocks (shade HT A3, Ivoclar Vivadent, Germany) and by the action of five axes milling bar, 3 crowns were fabricated. Programat P300 furnace was used for final crystallization of the e.mac crowns according to the recommendation of Ivoclar/Vivadent Company.

5.5.6.8 Cementation technique

In order to standardise the cementation procedure, the tensometer (Lloyds Instrument Model LRX, Lloyds Instruments, USA) was used to apply a constant pressure and time throughout the cementation of the crowns. A special jig was created that attached to the tensometer, which was filled with a heavy-bodied impression material (Aquasil Putty, blue colour, Dentsply Detrey) and an impression of the coronal 1/3 of the ceramic crown was obtained. Thus, an even and uniform occlusal cementation pressure analogous to that of finger pressure of the dentist was applied during the cementation. The device applied a 40N pressure in a compression mode for 3 minutes for cementing each crown [Figure 5-17]. Then the crown margins were exposed to the blue LED light of a light cure device (coltolux75) for 20 seconds as recommended; then any excess material was removed.

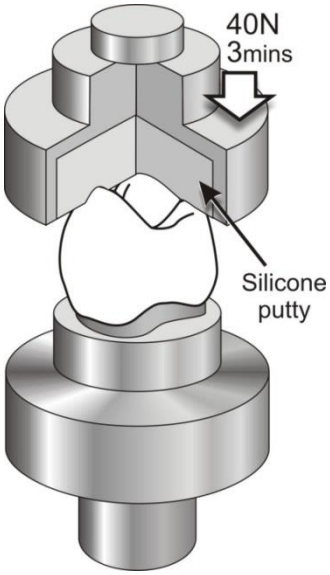

Figure 5-17: Cementation technique by universal testing machine

5.5.6.9 Post-cementation CT scanning

All teeth with the cemented crowns were scanned as per the protocol described in section [5.5.3.4]. However, during the scanning interval, the alignment of the samples in the same position was required. In order to achieve that, a replica mounting base for the root of the master die was fabricated from a silicone putty impression material. A straight vertical line was drawn as an indicator on the mounting base and the base holder of the micro CT in order to keep a constant alignment for each sample during each scanning interval. Thus, eliminating the variable of the samples position during the scan can be achieved [Figure 5-18 and 5-19].

Figure 5-18: Alignment of the sample in the Micro CT scanner

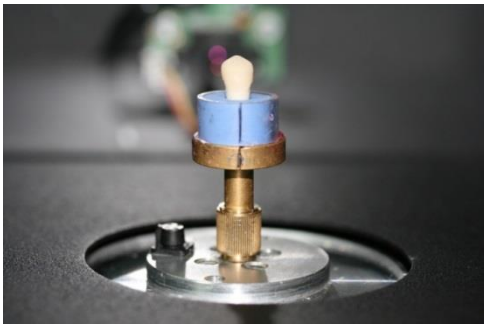

Figure 5-19: Replacing the sample in the mounting base

5.5.6.10 Interface measurement

The interface was measured using the novel technique described in section [5.5.3.5].

The average widths of the cement at different points and standard deviation were calculated. The statistical package [IPM SPSS statistic 20] at an alpha level of 0.05 was used and ANOVA (one-way analysis of variance) and Post-Hoc Tukey tests were performed to compare the differences between the five techniques regarding the dimension of the interface cement in different areas of interest.

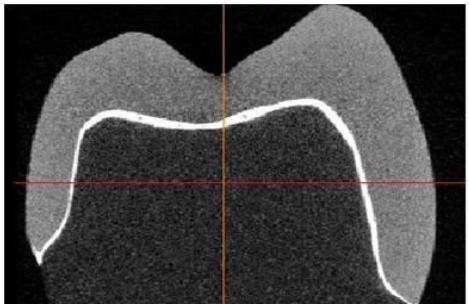

Manual waxed

+ Pressed

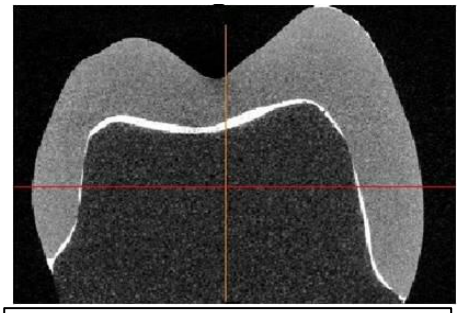

Wax 3D Printer +

Pressed

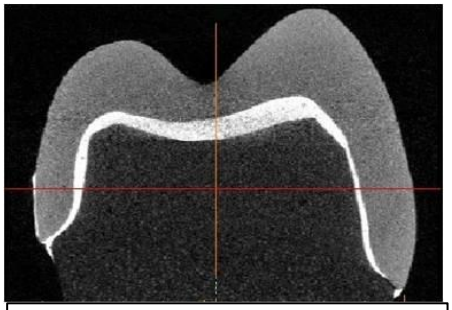

Isofolan ® spacer, manual waxed

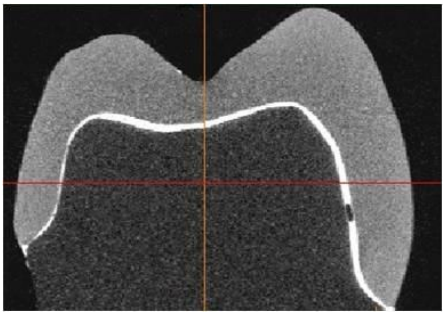

Zirkonzahn®

(CAD-CAM)

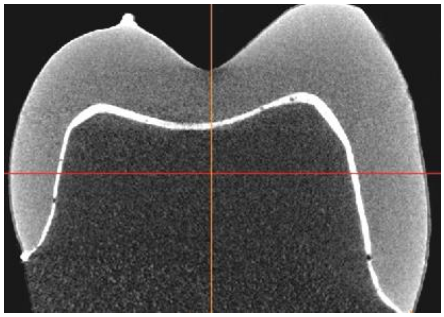

CEREC®

(CAD-CAM)

Figure 5-20: Representative Mimics view for each group

5.6 Results

5.6.1 Viscosity of cement with the addition of Barium Sulphate (BaSO4)

The behaviour for the Variolink II resin cement with and without Barium Sulphate ($BaSO_4$) is shown in [Figure 5-21]

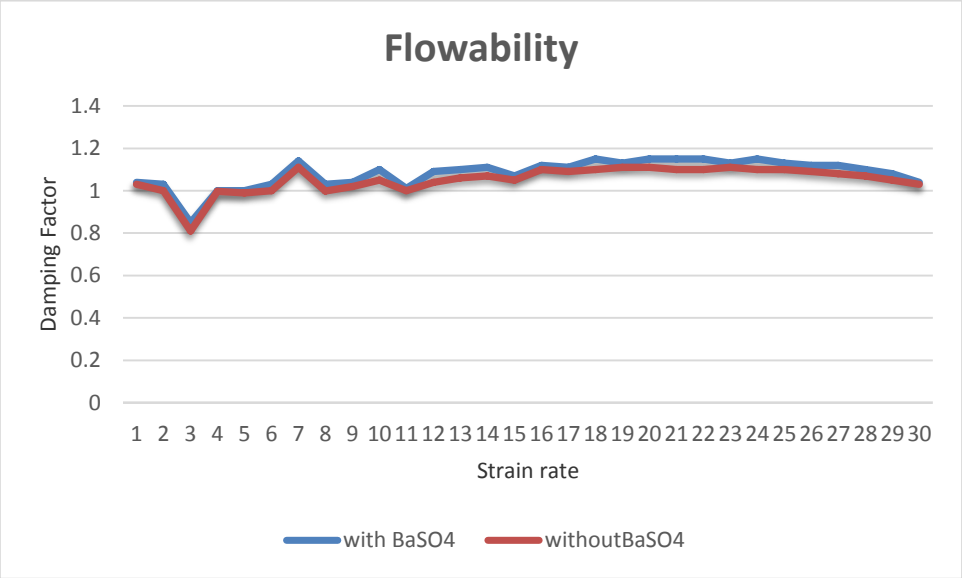

Figure 5-21: Flowability of Variolink II resin cement with and without $BaSO_4$

Table 5-6: Flowability of Variolink II with and without BaSO4 (Paired Samples Test)

Paired Samples Test

		Paired Differences					t	df	Sig. (2-tailed)
		Mean	Std. Deviation	Std. Error Mean	95% Confidence Interval of the Difference Lower	Upper			
Pair 1	noBaSO4 - withBaSO4	-1.15000	5.26525	.67974	-2.51016	.21016	-1.692	59	.096

The paired t test for comparing the behaviour of the cement with and without barium sulphate is shown in [Table 5-6]. The result indicated that the addition of barium sulphate to the cement at a ratio of 0.004g of Barium Sulphate to 0.180g of cement increased the radiopacity of the cement to an appropriate level but did not affect its viscosity.

5.6.2 Validation of the measuring technique

The digital measurement technique recorded a diameter of 12.65µm [Figure 5-8]. The actual physical disk diameter measured with a laser micrometer was 12.650µm [Figure 5-11]. A comparison of the 3D virtual and the laser actual measurement for the disk's diameter demonstrated a perfect correlation between the two to an accuracy of 1µm.

5.6.3 Evaluation of the cement interface geometry: I - Mesio-distal

Table 5-7: Mean values of cement thickness at each measured point cross the all the planes measured in mesio-distal direction [the measurement in µm].

	mar m	m ax m	occ ax m	cusp m	cen occ	cusp d	occ ax d	m ax d	mar d
CEREC1	**213**	**174**	**96**	**154**	**144**	**114**	**156**	**162**	**92**
CEREC2	**154**	**160**	**106**	**198**	**207**	**208**	**142**	**160**	**94**
CEREC3	**162**	**210**	**136**	**186**	**192**	**174**	**150**	**178**	**122**
zirkonzahn1	**88**	**112**	**102**	**128**	**194**	**192**	**168**	**108**	**112**
zirkonzahn2	**72**	**130**	**132**	**148**	**180**	**156**	**108**	**106**	**78**
zirkonzahn3	**112**	**86**	**98**	**152**	**184**	**150**	**126**	**96**	**90**
Manual pressed 1	**108**	**114**	**124**	**147**	**140**	**150**	**128**	**102**	**100**
Manual pressed2	**94**	**92**	**96**	**108**	**122**	**96**	**94**	**88**	**96**
Manual pressed3	**120**	**110**	**106**	**142**	**142**	**154**	**106**	**110**	**112**
Isofolan1	**108**	**274**	**140**	**236**	**244**	**308**	**190**	**292**	**86**
Isofolan2	**108**	**110**	**98**	**282**	**256**	**230**	**232**	**302**	**208**
Isofolan3	**154**	**232**	**188**	**296**	**296**	**158**	**142**	**226**	**108**
3D print 1	44	92	92	98	98	100	90	92	50
3D print 2	**48**	**64**	**86**	**122**	**112**	**114**	**68**	**66**	**46**
3D print 3	**48**	**58**	**78**	**122**	**116**	**116**	**68**	**64**	**48**

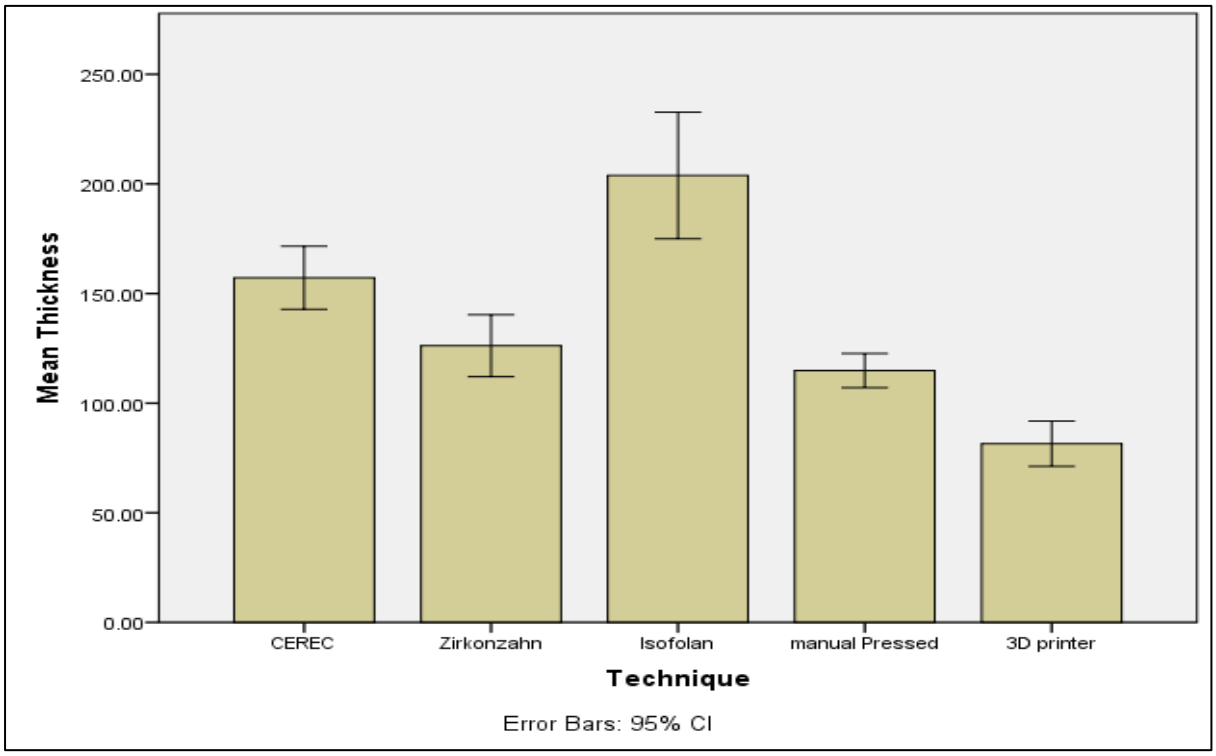

Figure 5-22: Mean values of cement thickness for the samples' groups at all planes measured in mesio-distal direction [the measurement in µm].

Table 5-8: The Minimum, Maximum and SD of the cement thickness for all samples in mesio-distal direction [in µm]

	MINIMUM	MAXIMUM	Range	SD
CEREC1	**92**	**213**	**121**	**12.97861**
CEREC2	**94**	**208**	**114**	**13.73133**
CEREC3	**122**	**210**	**88**	**9.35381**
zirkonzahn1	**88**	**194**	**106**	**13.40582**
zirkonzahn2	**72**	**180**	**108**	**11.92104**
zirkonzahn3	**86**	**184**	**98**	**11.31262**
Manual pressed1	**100**	**150**	**50**	**6.33772**
Manual pressed2	**88**	**122**	**34**	**3.44444**
Manual pressed3	**106**	**154**	**48**	**6.15339**
Isofolan1	**86**	**308**	**222**	**27.21315**
Isofolan2	**98**	**302**	**204**	**26.12600**
Isofolan3	**108**	**296**	**188**	**22.35571**
3D printer 1	**44**	**100**	**56**	**7.10243**
3D printer 2	**46**	**122**	**76**	**9.68389**
3D printer 3	**48**	**122**	**74**	**10.06338**

Table 5-9: ANOVA test to compare the thickness of the cement for all the groups in a mesio-distal direction

ANOVA

Thickness

	Sum of Squares	df	Mean Square	F	Sig.
Between Groups	231261.007	4	57815.252	32.089	.000
Within Groups	234220.296	130	1801.695		
Total	465481.304	134			

Table 5-10: POST HOC test for comparing a pair of means between groups in mesio-distal direction

	CEREC	Zirkonzahn	Manual Pressed	Isofolan	3D print
CEREC			*	*	*
Zirkonzahn				*	*
Manual Pressed	*		*	*	*
Isofolan	*	*	*	*	*
3D print	*	*	*	*	*

*The mean difference between each pair is significant at the 0.05 level.

5.6.4 Evaluation of the cement interface geometry: II – Bucco-lingual

Table 5-11: Mean values of cement thickness at each measured point cross the all planes measured in bucco-lingual direction [the measurement in µm]

	mar b	m ax b	occ ax b	cusp b	cen occ	cusp l	occ ax l	m ax l	mar l
CEREC1	116	108	258	86	190	126	146	236	118
CEREC2	106	110	166	76	232	196	122	146	106
CEREC3	164	116	172	106	206	144	174	242	132
zirkonzahn1	120	162	220	202	172	158	122	118	122
zirkonzahn2	112	220	210	130	174	146	124	98	82
zirkonzahn3	78	124	80	116	174	162	108	58	86
Manual pressed1	106	106	108	110	146	130	114	114	116
Manual pressed2	128	126	124	154	136	132	128	124	130
Manual pressed3	98	108	118	114	168	126	116	110	106
Isofolan1	278	218	208	162	270	212	108	132	160
Isofolan 2	284	282	266	278	268	236	98	98	94
Isofolan3	182	222	190	242	258	330	140	130	120
3D print 1	76	136	78	94	100	178	110	90	74
3D print 2	64	118	134	156	130	168	82	78	54
3D printer 3	62	112	138	162	124	158	80	80	54

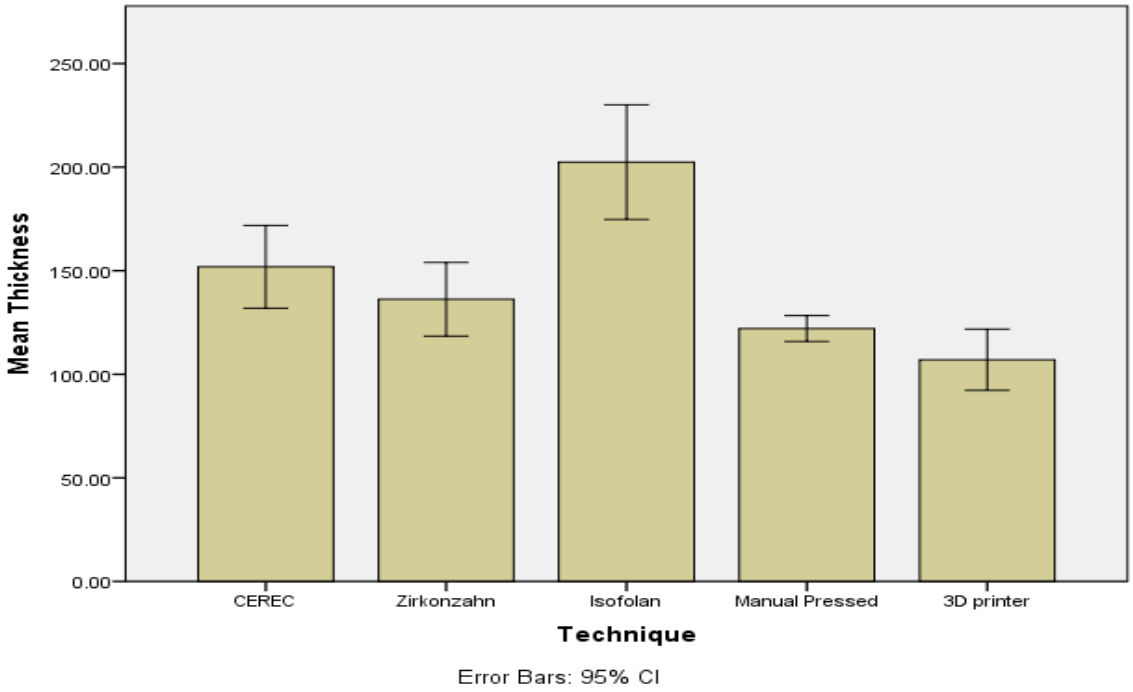

Figure 5-23: Mean values of cement thickness for the samples' groups at all planes measured in bucco-lingual-direction [the measurement in µm].

Table 5-12: The Minimum, Maximum and SD of the cement thickness for all samples in a bucco-lingual direction [in µm]

	MINIMUM	MAXIMUM	Range	SD
CEREC1	**86**	**258**	**172**	**60.37752**
CEREC2	**76**	**232**	**156**	**49.92995**
CEREC3	**106**	**242**	**136**	**43.38715**
zirkonzahn1	**118**	**220**	**102**	**38.00146**
zirkonzahn2	**82**	**220**	**138**	**48.23899**
zirkonzahn3	**58**	**174**	**116**	**39.11237**
Manual pressed1	**106**	**146**	**40**	**13.22876**
Manual pressed2	**124**	**154**	**30**	**9.327379**
Manual pressed3	**98**	**168**	**70**	**20.28409**
Isofolan1	**108**	**278**	**170**	**58.46746**
Isofolan2	**94**	**284**	**190**	**87.30852**
Isofolan3	**120**	**330**	**210**	**68.75157**
3D printer 1	**74**	**111**	**37**	**14.75635**
3D printer 2	**54**	**136**	**82**	**31.73326**
3D printer 3	**54**	**138**	**84**	**31.59905**

Table 5-13: ANOVA test to compare the thickness of the cement for all the groups in a bucco-lingual direction

ANOVA

Thickness

	Sum of Squares	df	Mean Square	F	Sig.
Between Groups	145391.704	4	36347.926	16.346	.000
Within Groups	289083.556	130	2223.720		
Total	434475.259	134			

Table 5-14: POST HOC test for comparing a pair of means between groups in bucco-lingual direction

	CEREC	**Zirkonzahn**	**Manual Pressed**	**Isofolan**	**3D print**
CEREC				*	*
Zirkonzahn				*	
Manual Pressed				*	
Isofolan	*	*	*	*	*
3D print	*			*	

***The mean difference between each pair is significant at the 0.05 level.**

5.7 Discussion

The replica technique has, to date, been considered as an effective way for measuring the cement interface. Its principal advantages are that it is easy and fast to perform; economical with few materials and has little need of sophisticated equipment, other than a low magnification optical microscope with its image analysis software. Conversely, it also has a number of disadvantages that limit its applicability. It is a 2D system with measurements only taken in the plane of section; the sample is destroyed and can be used for one time only; it is impossible to replicate the exact position of the cut planes, hence of limited value for comparison between samples and finally, it should be noted that this technique relies on the measurement of the silicone that occupies the interface gap, and does not replicate the behaviour of the cement in the real clinical situation. Thus, an alternative technique that would overcome these limitations to improve predictability and reliability; thus addressing the need for a standardised technique (Groten et al., 2000, Naert I et al., 2005 , Moldovan et al., 2011)

Computer-aided methods for measuring the interface dimensions are reproducible, non-destructive and accurate and thus can provide valuable additional information about the measured specimen (Moldovan et al., 2011).

In this study, the assessment was performed by combining micro CT scan images and digital analysis software (Mimics®14.1 software, Materialise

Interactive Medical Image Control System). Measuring the cement interface using this methodology (radiopaque cement, micro-CT and 3D image modelling and analysis software) enabled a high accuracy and intra- (within the specimen) and inter- (within the various specimens) reproducible measurements to be taken.

To enable visualisation of the cement, there is a requirement for a high contrast. This was achieved by adding barium sulphate to the recommended cement (Variolink II, intro pack, Liechtenstein, Ivoclar/Vivadent, LOT R72873, and Exp. 2014-08). The addition of a new constituent to the cement requires that we ensure that its rheological properties remain unaffected so that the seating of the crown is not impeded by a potentially greater viscosity or flow rate.

In Rheology, damping factor is considered as a measurable parameter, which is quote 'the restraining of the tested material to the vibratory motion by energy dissipation' (Romberg and Popp, 1998, Hassan et al., 2011, Noroozi et al., 2012). Through comparing the damping factor for both samples, a flowability rate can be assessed. It has been found that the flowability rate of Variolink II without barium sulphate was not significantly different than the flowability of the Variolink II mixed with barium sulphate. [Table 5-6] shows the comparison between Variolink II with/ without adding barium sulphate by using paired t test, which revealed no significant difference between them.

The measurements that were carried out in the mesio-distal and bucco-lingual direction of the cement thickness have been compared in the five tested groups by using a one-way analysis of variance [ANOVA] with Tukey's Post Hoc test. The data showed that the difference in cement thickness between these five fabricating techniques was significant in both directions (mesio-distally and bucco-lingually). The post hoc test for multiple comparisons was carried out to compare each pair of groups' means. The post hoc test data for the mesio-distal measurements [Table 5-10] illustrated a high significant difference ($p<0.05$) between most of the groups. However, there was no significant difference between machined groups [CEREC® and Zirkonzahn®]. On the contrary, the post hoc test data of bucco-lingual measurements revealed a non-significant difference between most of the groups except for the vacuum-formed spacer (Isofolan®) group [table 5-14]. An important finding of this study was the possibility of each ceramic fabrication technique creating a unique interface geometry.

In this study, we also evaluated the maximum and minimum cement thickness and compared these that with the accepted standard (50-100 μm) for the cement thickness for all five crown systems. The maximum and the minimum means of cement thickness at the mesio-distal plane have been shown in [Table 5-8]. It is of particular note that the vacuum-formed spacer technique created the maximum interface width (308μm in MD direction and 330 μm in BL direction)

when compared to that created by the 3-D wax printer (44 μm in MD direction and 54 μm in BL direction). It was also noted that the 3D printer technique is able to produce the thinnest thickness over the entire cement length (most uniform) among the compared groups.

Both of Table 5-8 and Table 5-12 show that the two groups [manual pressed and the 3D printer] have the lowest standard deviation (SD) values compared with the other three groups in both directions (mesio-distal and bucco-lingual). Statistically, the low SD means the gathered data is distributed very close to the mean. Therefore, the thickness of the cement interface of the manual pressed and the 3D printer groups could be described as a most homogenous thickness compared with the other groups.

The opposite can be seen with a high SD in the [CEREC® and Zirkonzahn®] machined groups followed by the vacuum-formed spacer technique (Isofolan®) group in both directions (mesio-distal and bucco-lingual). Thus, these groups show a high discrepancy of the cement thickness over all measured points and indicate a high cement width compared to the 3D printer and manual pressed groups.

According to our findings, the greatest consistency in width measurements, and thus the most uniform width was noted for the manual pressed and 3D printed samples. The manual pressed crowns show the smallest range of variation

between the maximum and the minimum means of the measured points of the three samples.

The lower range values for the manual pressed and the 3D printer samples give another indication of the homogeneity of the interface in these two groups. However, both machined groups show close range values to each other but a slightly higher range difference than the first two groups. The negative impacts of the technical steps of the ceramic fabrication technique on the regularity of the interface were confirmed by the vacuum-formed spacer technique (Isofolan® group) as they showed the highest range values were [222, 204, 188µm] and [170, 190, 210µm] mesio-distally and bucco-lingually respectively.

The adaptation of the internal occlusal surface in both pressed groups' samples [manual and 3D printer] was significantly better than the machined and vacuum-formed spacer [Isofolan®] groups. The technique with best occlusal adaptation was the manual pressed with a minimum value of 96µm and 110µm and the maximum value of 154µm and 186 µm respectively. However, the machined groups recorded a higher minimum and maximum in mesio-distal and bucco-lingual direction. The paradoxical result which is completely opposite to the hypothesis regarding the thickness of the cement was demonstrated by vacuum-formed spacer [Isofolan®] group where the minimum were 158µm and 130µm and the maximum were 308µm and 330µm respectively.

The discrepancy in the occlusal thickness values for the machined crowns (CEREC® and Zirkonzahn®**)** is attributed to the inability of the standard milling burs to accurate machine the intricate internal occlusal morphology surface of the crowns. The required area to be cut under the cusps is often smaller than the diameter of the milling machine bur. Thus, the bur created more space than is normally required. The use of a bur with a smaller diameter-cutting tip is not cost-effective as this would wear very fast, thus rendering the bur useless.

The rational explanation for the large range value of the vacuum-formed spacer technique (Isofolan®) cement thickness could be attributed to the non-uniform application of heat and pressure during the fabrication process that causes dragging of the polymer from the uppermost surface (occlusal) towards the lowest surface (cervical margin); thus resulting in a thin occlusal and thick cervical margin width.

All the groups share the same trend of less discrepancy in the marginal adaptation compared with occlusal adaptation. The 3D printer samples show the minimum mean thickness in the measured marginal points in all directions (bucco-lingually and mesio-distally) followed by manual pressed samples.

Notwithstanding, the cement thickness for both the pressed technique groups was within the clinically acceptable value of 120µm. For the machined (CEREC® and Zirkonzahn®) and vacuum-formed spacer technique (Isofolan®) groups, the cement thickness was within the maximum clinically acceptable

values. The logical explanation is that the interface space could be better controlled by applying the layers of the die spacer either manually or by software compared with the creation of the interface by the action of burs or pressing a vacuum-formed polymer sheet of Isofolan® onto the tooth.(Boening et al., 2000, Wolfart et al., 2003, Yeo et al., 2003) .

An interesting finding was the marginal cement thickness was mostly smaller in the mesio-distal plane than the bucco-lingual plane, regardless of the technique. A possible explanation to this finding is that the mesial and distal walls in the upper first premolar are normally wider than the buccal and lingual walls. Thus, the wide surface of the wall allows for more homogenous adaptation of the overlay materials than the small wall.

Moreover, it has been found in the present study that the occlusal segment shows a large interface thickness compared with the interface thickness at the marginal area, regardless of the technique and the direction of the measurement. A finding that is in accordance with the finding of other studies (Reich et al., 2005, Reich et al., 2011, Spohr et al., 2013)

Ultimately, this study has shown that the thickness of the cement across all measured points in all cross-sections was more uniform for the pressed crowns (manual and 3D wax printed, but not vacuum-formed spacer technique (Isofolan®)) compared with the machined crowns (CEREC® and Zirkonzahn®);

a finding that is in accordance with Yeo et al. and Aboushelib et al (Yeo et al., 2003, Aboushelib et al., 2012).

5.8 Conclusions

1. High accuracy and intra- (within the specimen) and inter- (within the various specimens) reproducible measurements can be achieved by means of digital image analysis of micro-CT scanned specimens. The proposed 3D measuring technique is valid for the proposed measurement. Accordingly, the hypothesis regarding the accuracy of the data of measuring the interface by the computational method can be accepted.

2. The interface uniformity and pressure/heat spacer technique are negatively correlated. The hypothesis that the interface of the pressed ceramic might be more homogenous with the aid of heat-formed polymer sheet (Isofolan®) compared to hand-painted pressed or machined is rejected.

3. The interface cement of pressed crowns with a 3D printed or hand-painted spacer was significantly thinner and of a more uniform thickness than the crowns with vacuum-formed spacer (Isofolan®) or machined CAD/CAM techniques (CEREC® and Zirkonzahn®).

4. The pressed (manual and 3D wax printed) crowns have shown the least variation between marginal, axial and occlusal thickness of the interface compared with vacuum-formed spacer (Isofolan®) or machined CAD/CAM (CEREC® and Zirkonzahn®) crowns.

5. The variations of the cement thickness across all points in vacuum-formed spacer (Isofolan®) crowns were significantly greater than in the

pressed (manual and 3D wax printed) and machined CAD/CAM (CEREC® and Zirkonzahn®) crowns. The internal interface geometry for the former was less homogenous.

6. There is no significant difference in the dimensions and geometry of the interface achieved by either of the CAD-CAM machinable techniques (CEREC® and Zirkonzahn®); a point of importance for subsequent experiments requiring CAD-CAM prepared crowns.

An SEM characterisation of the internal surface of machined and pressed ceramic crowns

6 SEM evaluation

This chapter covers objective 4 of the thesis.

6.1 Introduction

The composition and microstructure of the dental ceramic could be considered as determinants of the quality, longevity and long term clinical performance of the ceramic crown-tooth complex. It is known that the fracture initiation site for the ceramic under the load is predominantly controlled by the density, severity and location of the critical flaws within the ceramic structure rather than its thickness (Thompson et al., 1994, Chinn, 2002, Guazzato et al., 2004b).

The term microstructure indicates a structure level of approximately 0.1-100µm between the visible light's wavelength and the naked eye's resolution limit. Microstructure is a broad name for some other structures and features included such as grains, grain boundaries, micro crack and pores. Most of the physical and chemical properties such as the thermal, visual, electrical and mechanical features are considerably affected by the body microstructure. Several studies have tried to correlate the actual mechanical behaviour of the tested material with the characteristic feature of its microstructure (Martínez Fernández et al., 2003, Mandal et al., 2004, Meyers and Chawla, 2009).

In particular, within ceramic systems, the generation of flaws is of importance. Step-induce flaws are considered to occur in most of the ceramic fabrication techniques, which vary in shape, distribution and size; in accordance with the manufacturing technique.

Lithium disilicate glass ceramic is produced by Vivadent/Ivoclar Company as an IPS e.max® lithium disilicate ceramic®. The main components of IPS e.max® are lithium dioxide, quartz, phosphor oxide, alumina, potassium oxide and some other minor components. The manufacturers have designed this ceramic system (IPS e.max®) to be utilized by either pressing a molten ingot in a furnace using the lost-wax process or machined by CAD/CAM technology. The IPS e.max® needle-like crystal microstructure offers an excellent durability and strength with outstanding optical properties. These properties have made the IPS e.max® an ideal ceramic for use in many dental applications; anterior/posterior crowns, inlays/onlays, anterior three-unit bridge, labial veneers and implant restoration (Vivadent. and Ivoclar., 2009).

During the manufacturing process, the ceramic is subjected to a sequence of varying melting and cooling stages to give the final product of 70% crystal volume incorporated a glass matrix in forms of either ingot (IPS e.max® press, Ivoclar Vivadent, Germany) or block ceramic (IPS e.max® CAD, Ivoclar Vivadent, Germany). The composition and most of the physical properties such as coefficient of thermal expansion, chemical solubility and modulus of elasticity of the e.max® Press and e.max® CAD are reported to be the same.

However, the size and the length of the ceramic crystals show different rates. The e.max® Press shows crystals measurement of approximately 3 μm to 6 μm in length, while the e.max® CAD show a crystal length of 1.5 μm (Vivadent. and Ivoclar., 2009).

During the laboratory fabrication techniques, the processing heat required for pressing the ceramic is likely to induce pores within the ceramic structure particularly when the temperature exceeds the manufacture recommendation for the temperature degree. It is well noted, that lithium disilicate has 3% porosity after the heat-pressing step. Moreover, high pressing temperature could introduce a contamination of the pressed ceramic structure by the reaction with the phosphate-bonded investing materials (Kelly et al., 1989, Kelly, 1995, Harvey and Kelly, 1996, Chen et al., 1999, Denry, 2013) .

A concern exists that the actual machining action can induce flaws in machined ceramic (Rice, 2002, Guazzato et al., 2004a). Although, the thermal processing step for the final crystallization of 'blue stage' ceramic is important to reduce the residual stress that arises from the machining action, it is now known that machining damage is not healed by the heat treatment (Denry, 2013). Moreover, the size of the machining flaws as evaluated by some in depth fractographic studies has revealed a considerable dependency of the flaws size variation as a function of machining force rather than the ceramic grain size (Kelly, 1995, Harvey and Kelly, 1996, Chen et al., 1999).

Any flaws and residual stress induced within the fabrication process could detrimentally affect the strength and the performance of the ceramic restoration. The majority of the quantitative fractographic studies that rest on the clinical failure data of the ceramic crowns showed that the cracks-induced failure are often concentrated in the inner surface of the occlusal part where the tensile stress is accumulated (Kelly et al., 1989, Piddock and Qualtrough, 1990, Harvey and Kelly, 1996, Chen et al., 1999) .

A microstructural comparative evaluation of the internal surface of lithium disilicate (e.max®) crowns fabricated by these two processes (Pressed vs. Machined) is warranted to aid our understanding of their performance.

6.2 Aims

To characterise the micro-structural features of the inner surface of lithium disilicate ceramic crowns fabricated by either pressed or machined techniques.

6.3 Objectives

1- To fabricate crowns by the two regimes: CEREC®CAD/CAM and manual conventional pressed techniques using lithium disilicate blocks and ingots [e.max® CAD and e.max® Press respectively].

2- To characterise by the SEM the microstructural features of the internal fitting surface of the crowns with and without acid conditioning.

6.4 The hypothesis

There is a similarity in the microstructure of the machined and pressed lithium disilicate glass ceramic and both are free of technique-induced flaws.

6.5 Materials and method

6.5.1 Specimen creation

The protocols of the tooth preparation and crowns fabrication [machined and pressed] followed the corresponding protocols for the samples creation that have been fully described in sections [5.5.3.1], [5.5.6.3] and [5.5.6.6] respectively. Using the CEREC® inLab 3.6 CAD/CAM machine, four crowns were milled using IPS e.max® CAD ceramic (e.max® CAD block, shade HT A3, Ivoclar

Vivadent, Germany) as shown in [Figure 6-1]. For the pressed group, four crowns were pressed manually using IPS e.max® Press ceramic (e.max® press ingot, shade LT A3, Ivoclar Vivadent, Germany) as shown in [Figure 6-2].

Figure 6-1: IPS e.max® CAD block

Figure 6-2: IPS e.max® Press ingot

The pressed crown samples were sandblasted during the removal of the investing materials. After the thermal processing and final crystallization for both samples in both groups, half of each group [n=2] were etched with IPS Ceramic Etching Gel (5% HF [hydrofluoric acid]) for 20 seconds according to Ivoclar/Vivadent protocols.

6.5.2 Samples scan by Scanning Electron Microscope [SEM]

All samples were gold coated and 8 magnification powers were selected [300X, 600X, 1200X, 2400X, 5000X, 1000X, 20000X and 40000X]. The inner side [fitting surface] in each sample [crown] was imaged.

6.6 Results

6.6.1 Non-etched Pressed and Machined lithium disilicate crowns

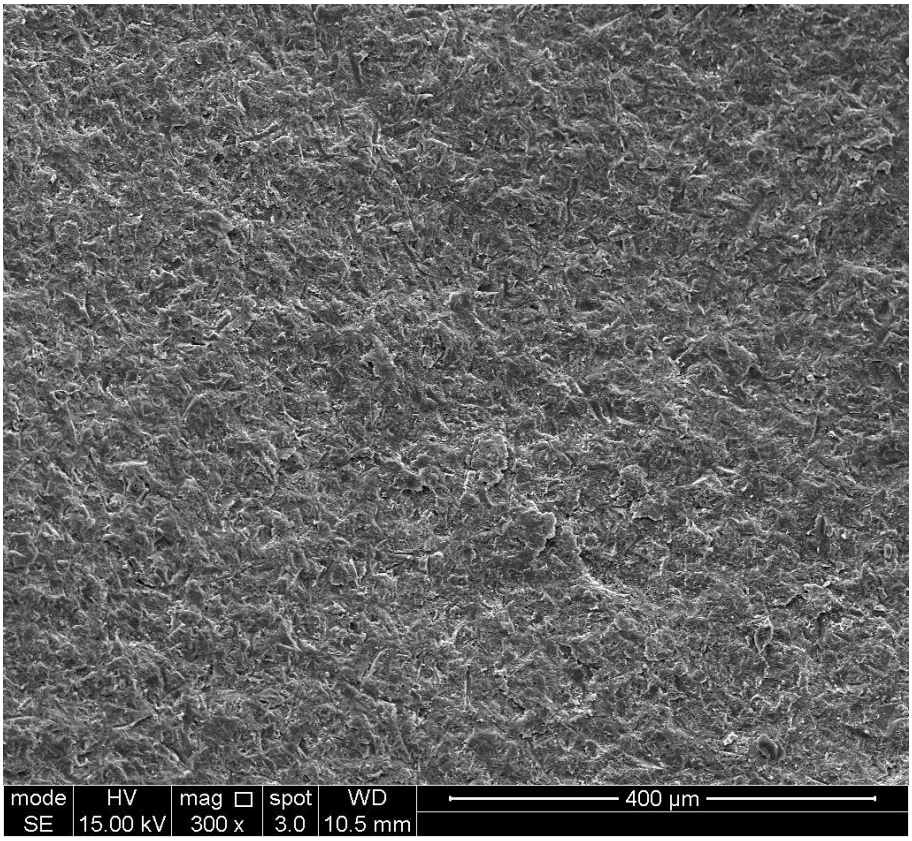

Figure 6-3: SEM of e.max® pressed non-etched at 300x

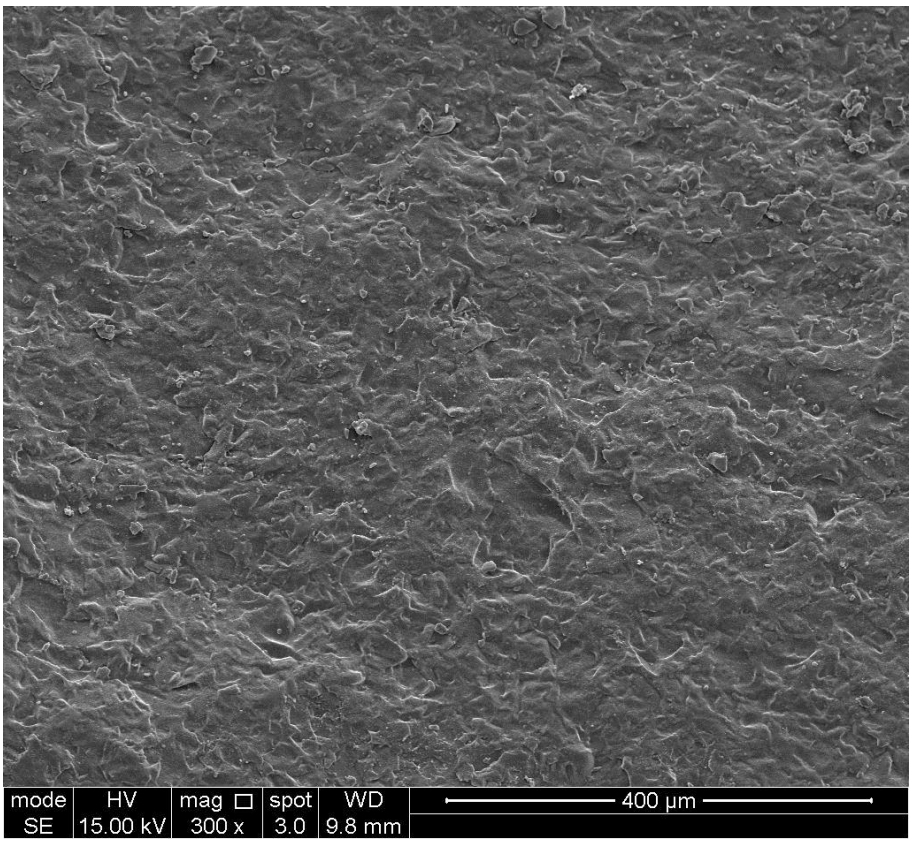

Figure 6-4: SEM of e.max® machined non-etched at 300x

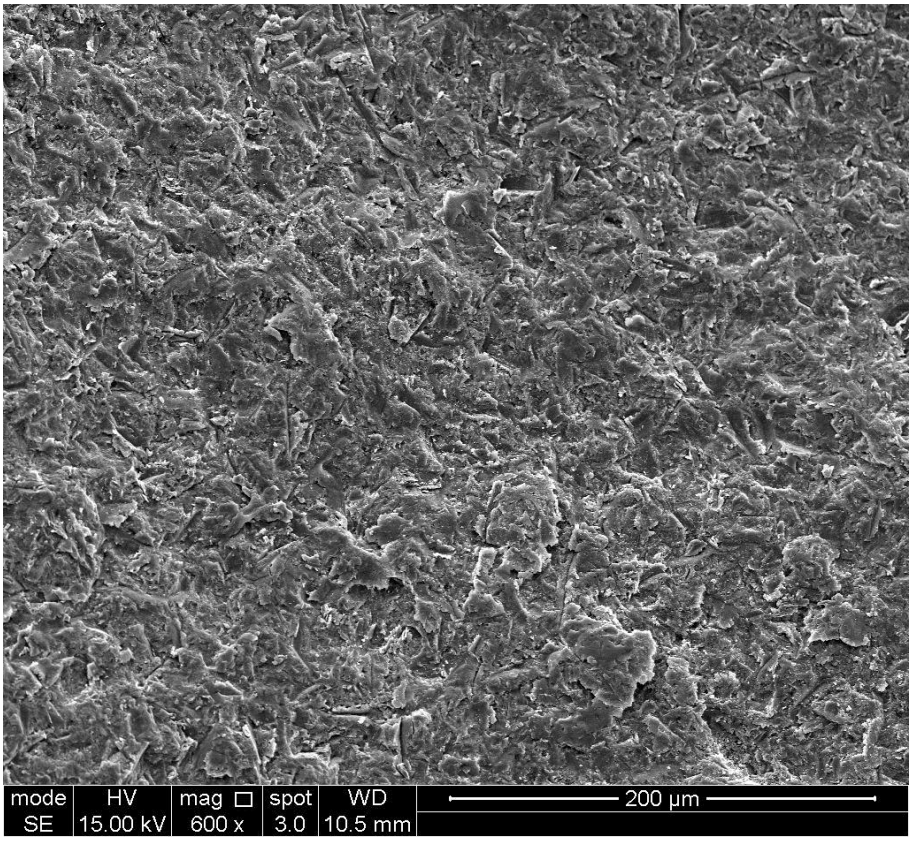

Figure 6-5: SEM of e.max® pressed non-etched at 600x

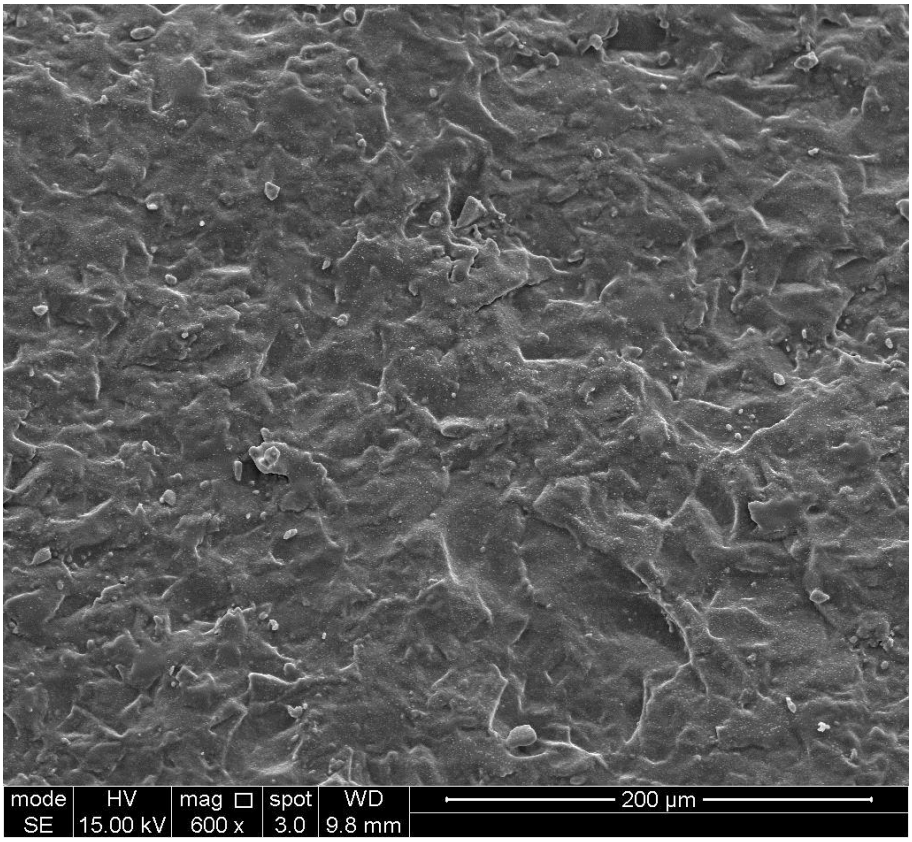

Figure 6-6: SEM of e.max® machined non-etched at 600x

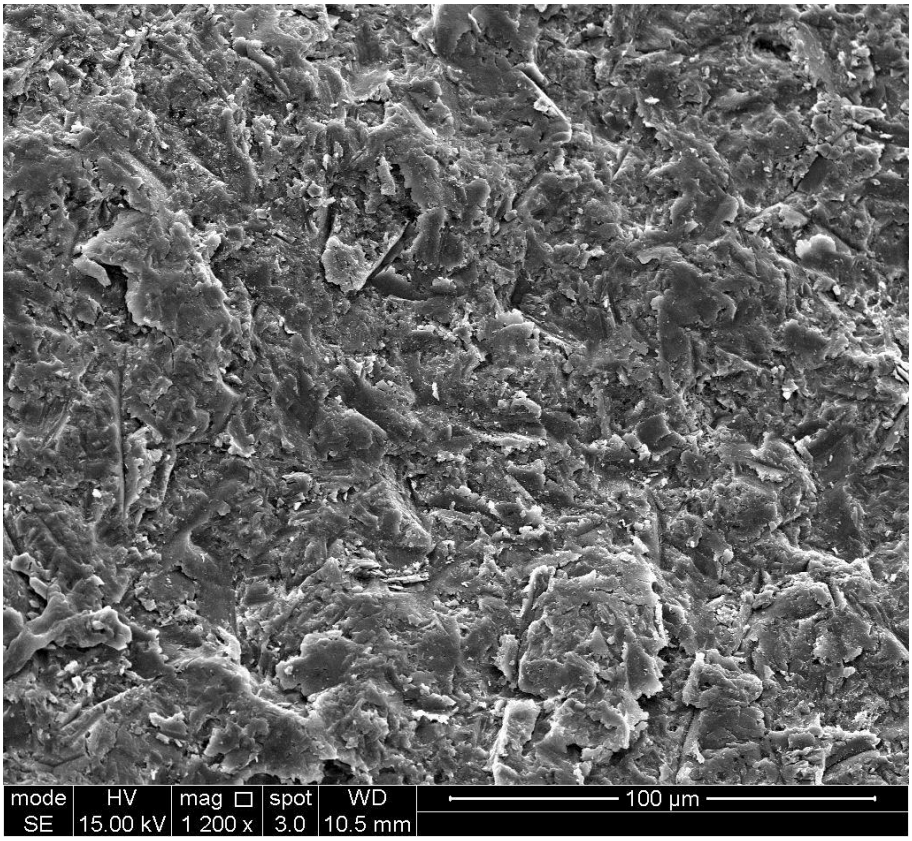

Figure 6-7: SEM of e.max® pressed non-etched at 1200x

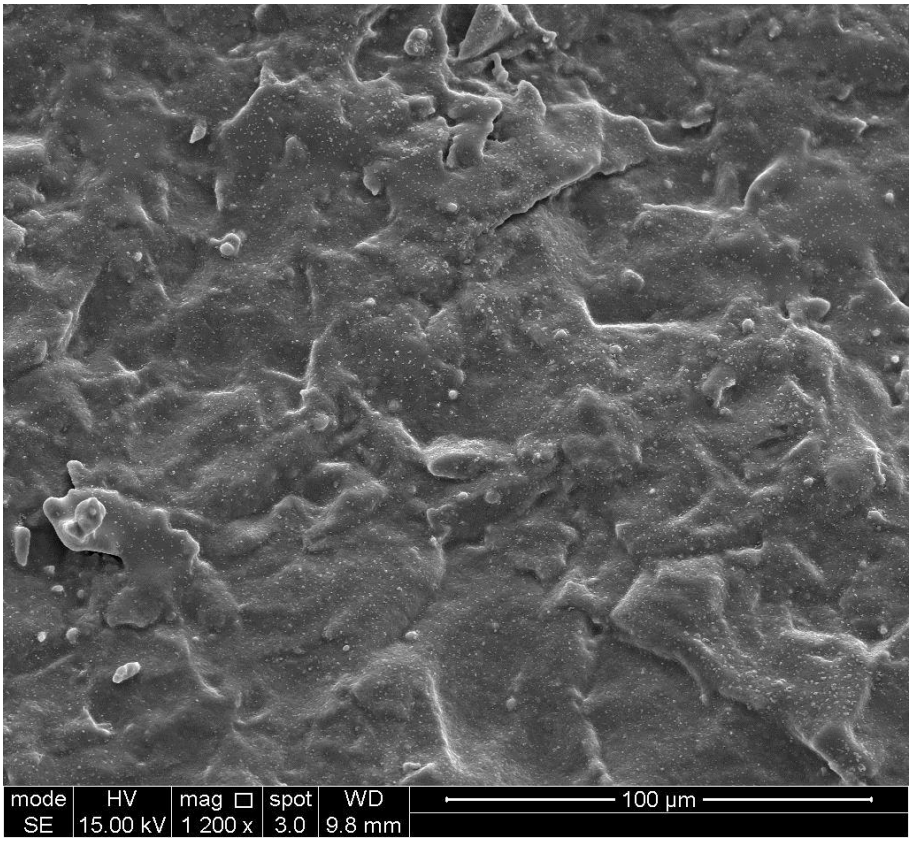

Figure 6-8: SEM of e.max® machined non-etched at 1200x

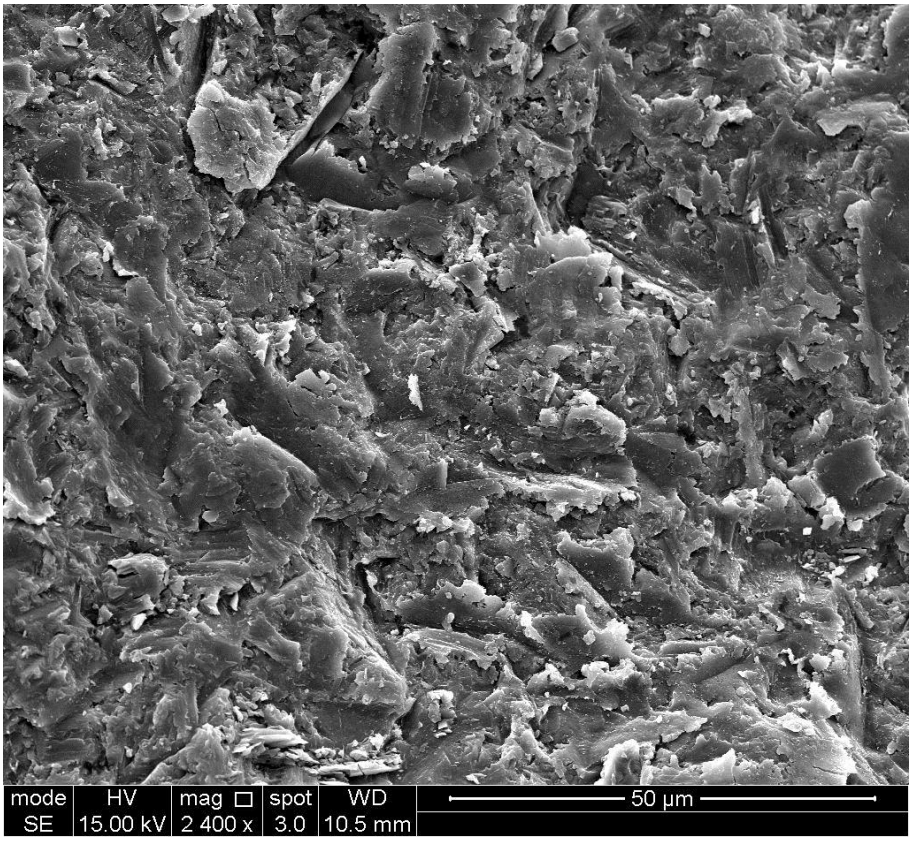

Figure 6-9: SEM of e.max® pressed non-etched at 2400x

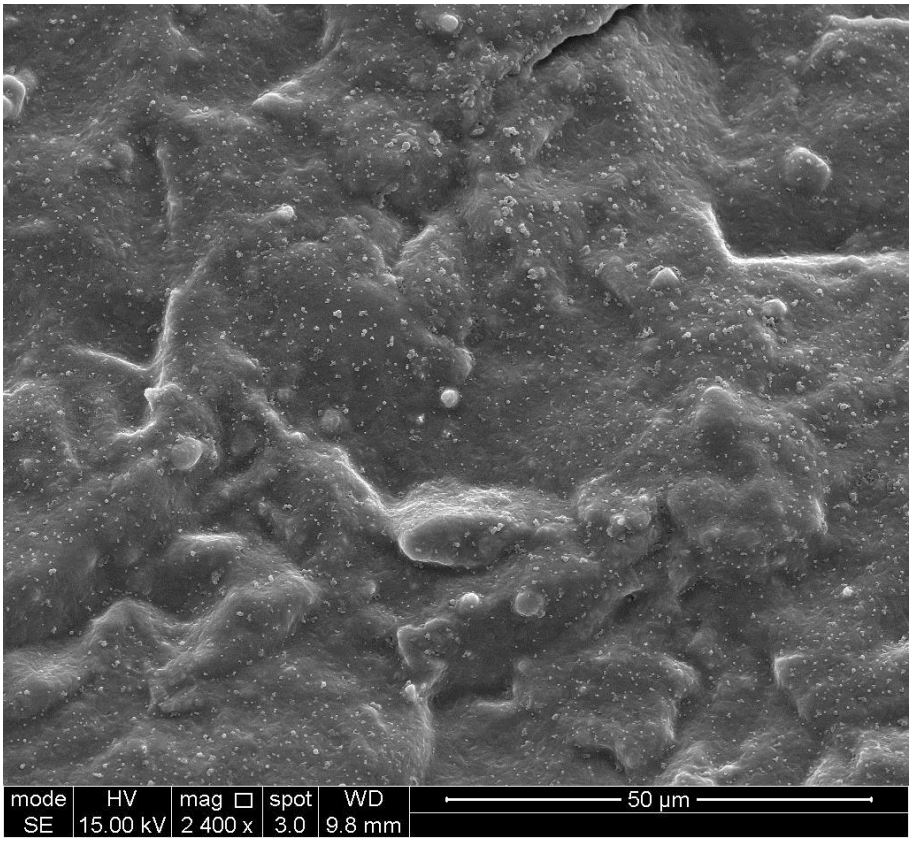

Figure 6-10: SEM of e.max® machined non-etched at 2400x

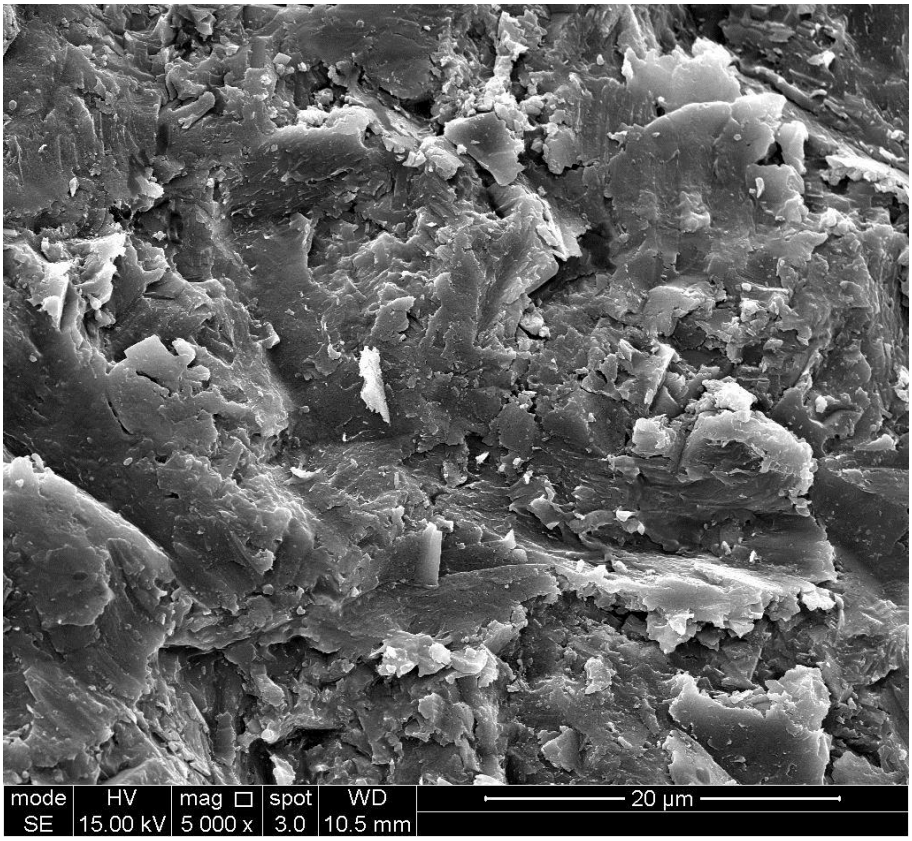

Figure 6-11: SEM of e.max® pressed non-etched at 5000x

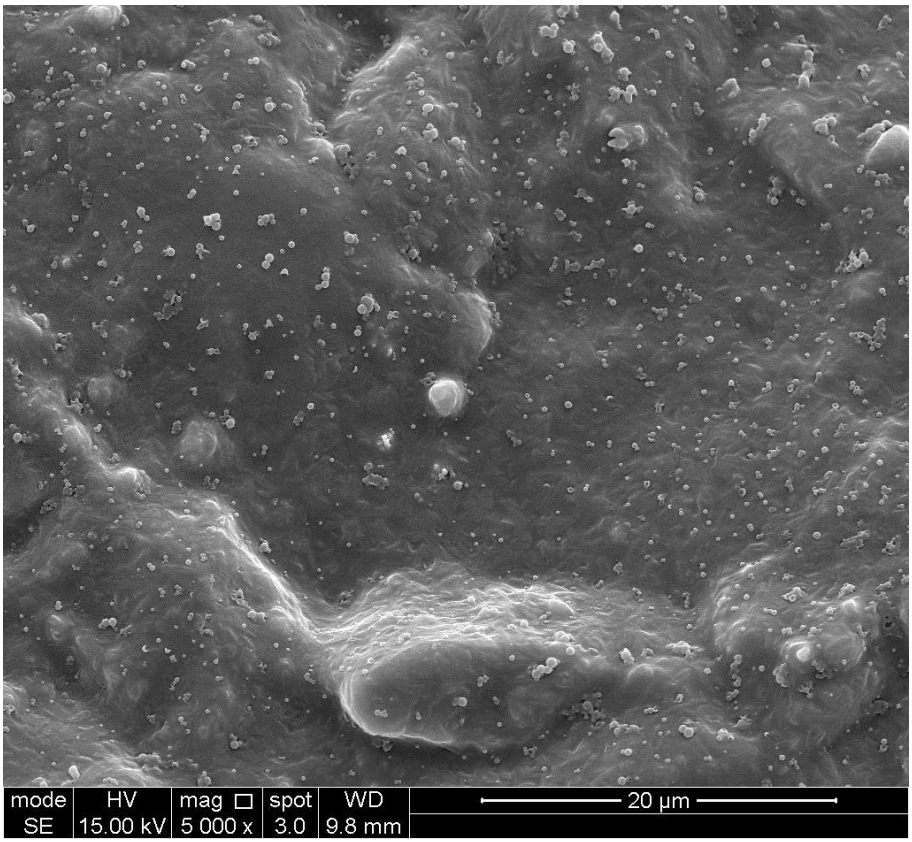

Figure 6-12: SEM of e.max® machined non-etched at 5000x

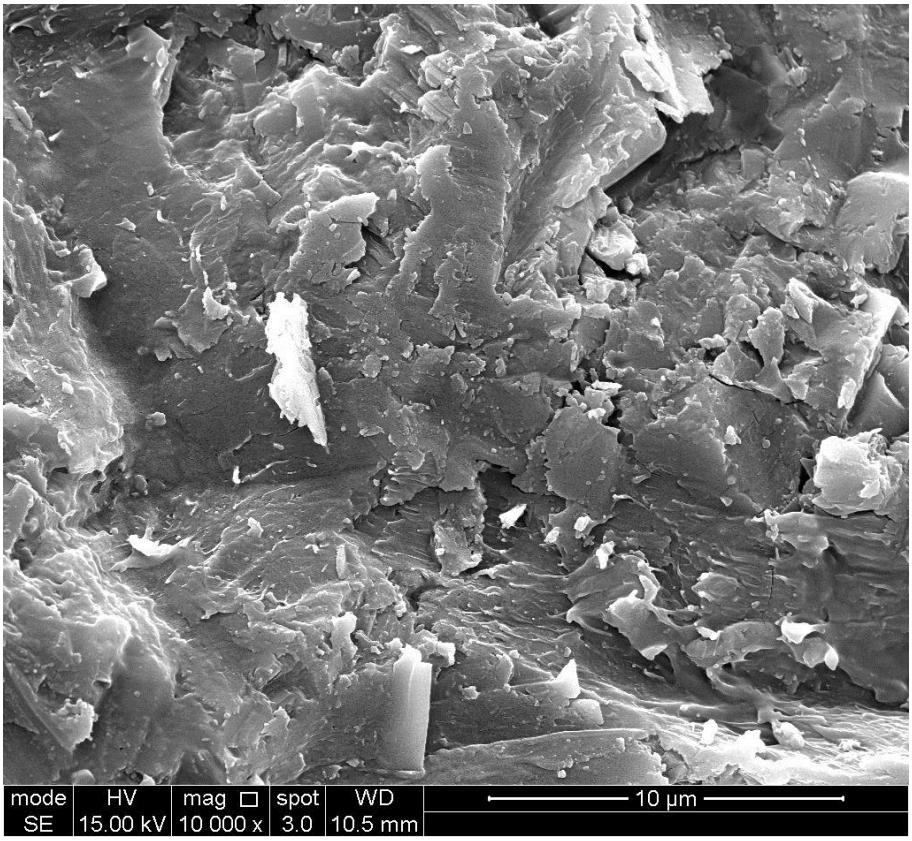

Figure 6-13: SEM of e.max® pressed non-etched at 10000x

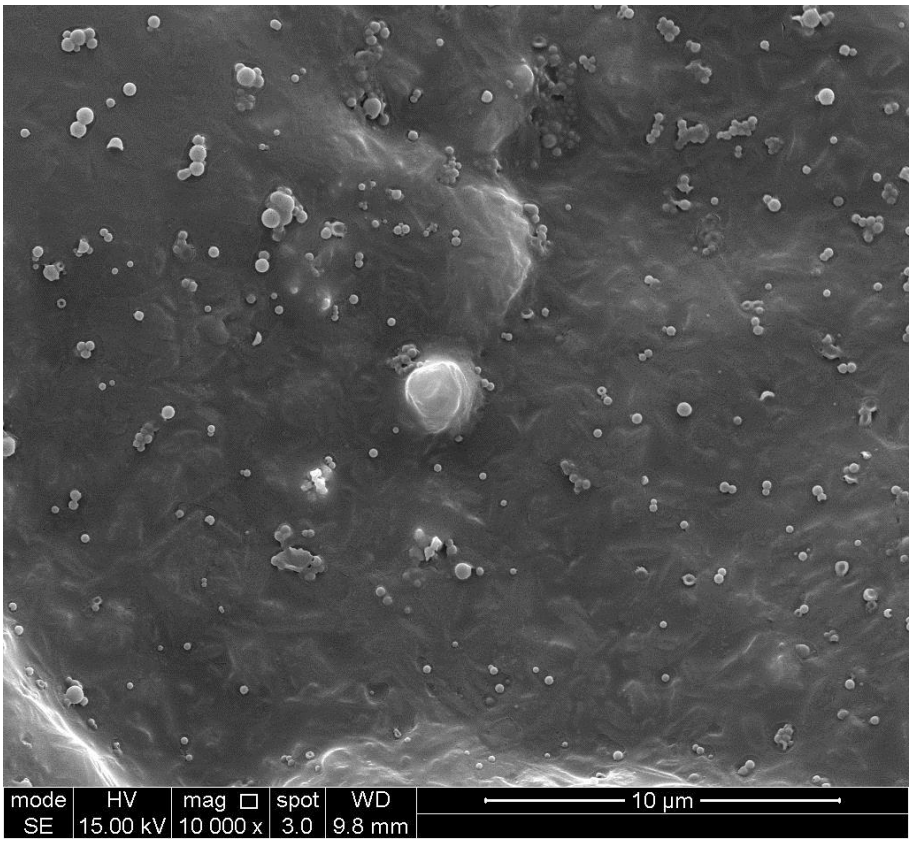

Figure 6-14: SEM of e.max® machined non-etched at10000x

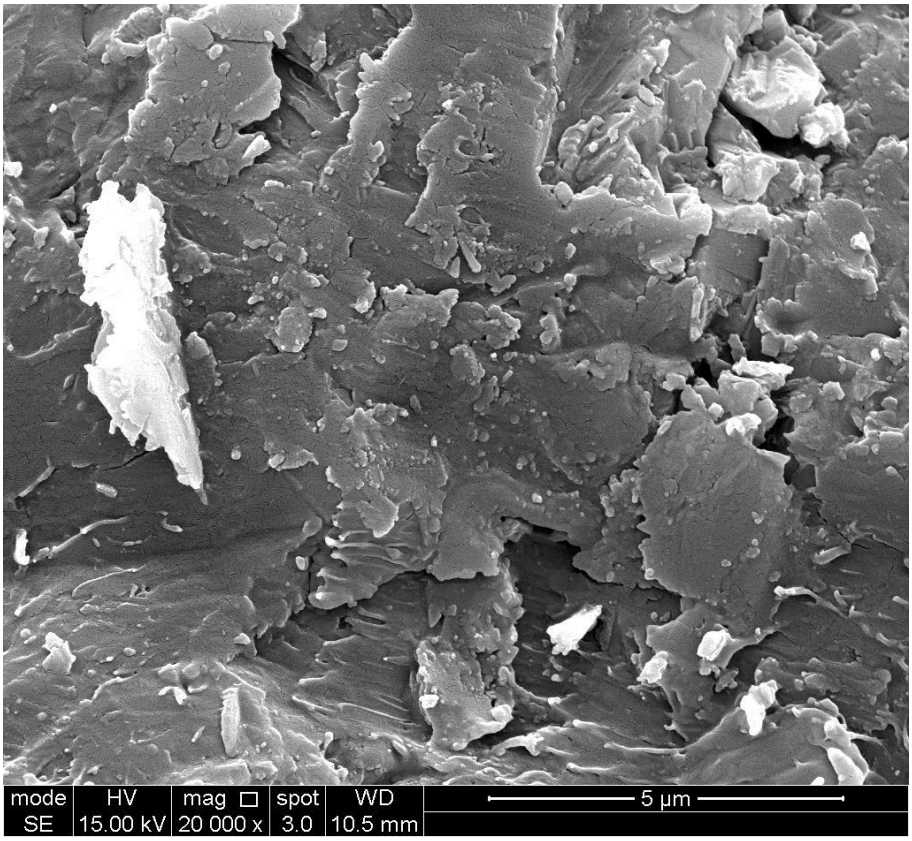

Figure 6-15: SEM of e.max® pressed non-etched at 20000x

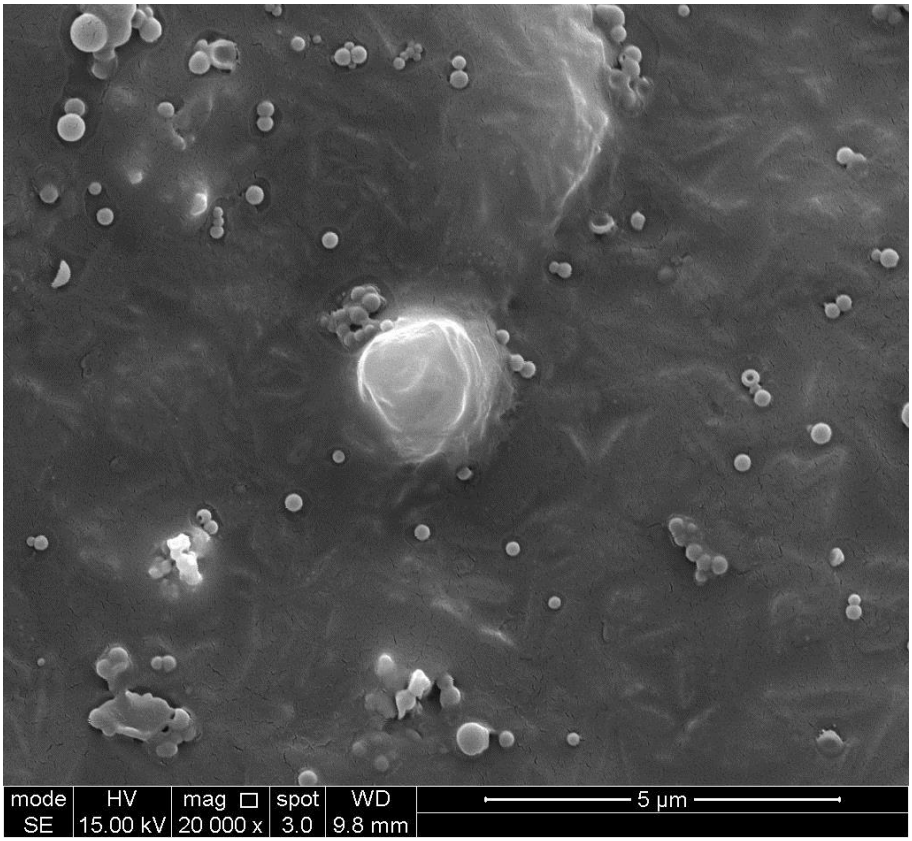

Figure 6-16: SEM of e.max® machined non-etched at 20000x

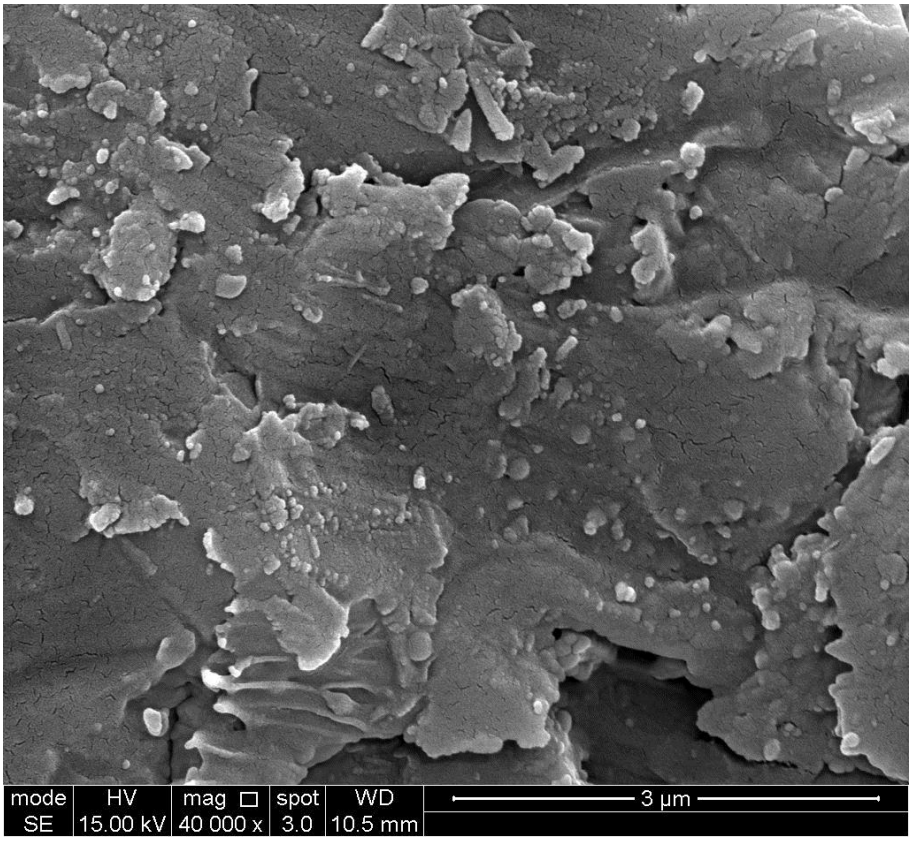

Figure 6-17: SEM of e.max® pressed non-etched at 40000x

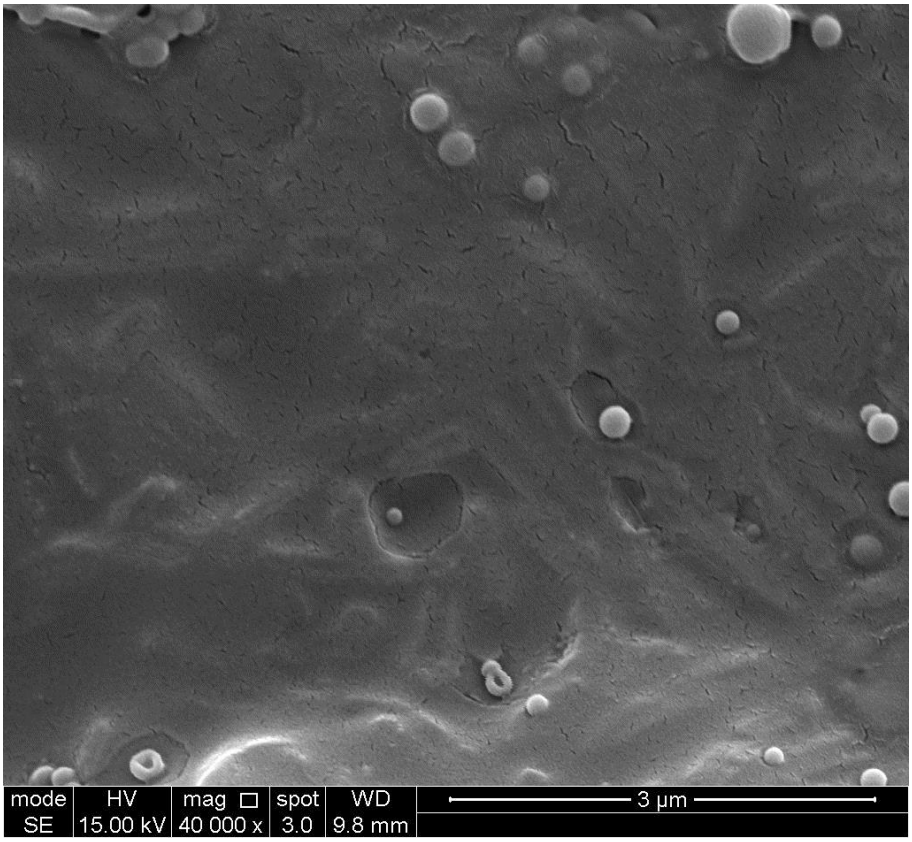

Figure 6-18: SEM of e.max® machined non-etched at 40000x

6.6.2 Etched Pressed and Machined lithium disilicate crowns

The same methodology that used for scanning the non-etched Pressed and Machined lithium disilicate crowns was followed.

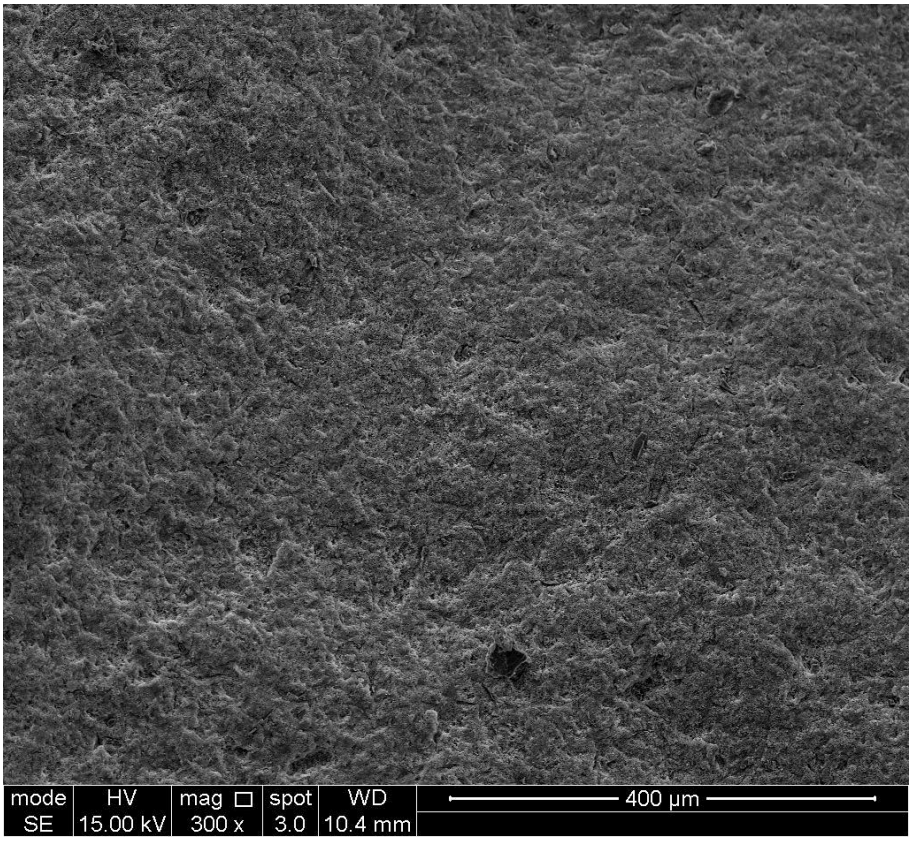

Figure 6-19: SEM of the etched e.max® pressed at 300x

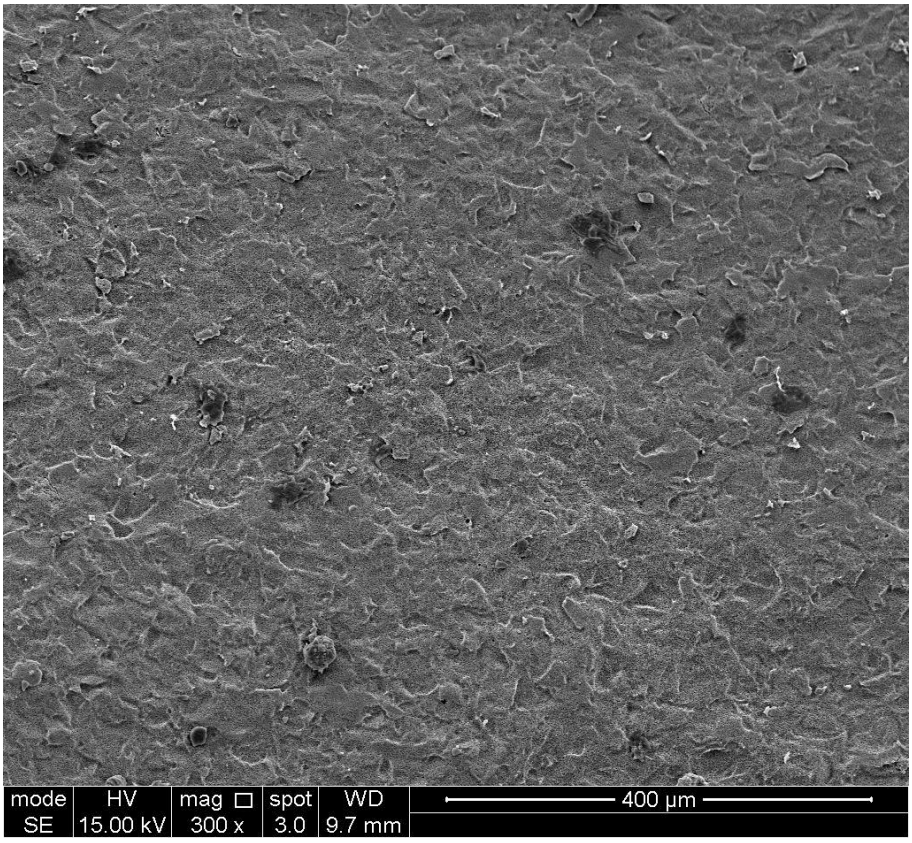

Figure 6-20: SEM of the etched e.max® machined at 300x

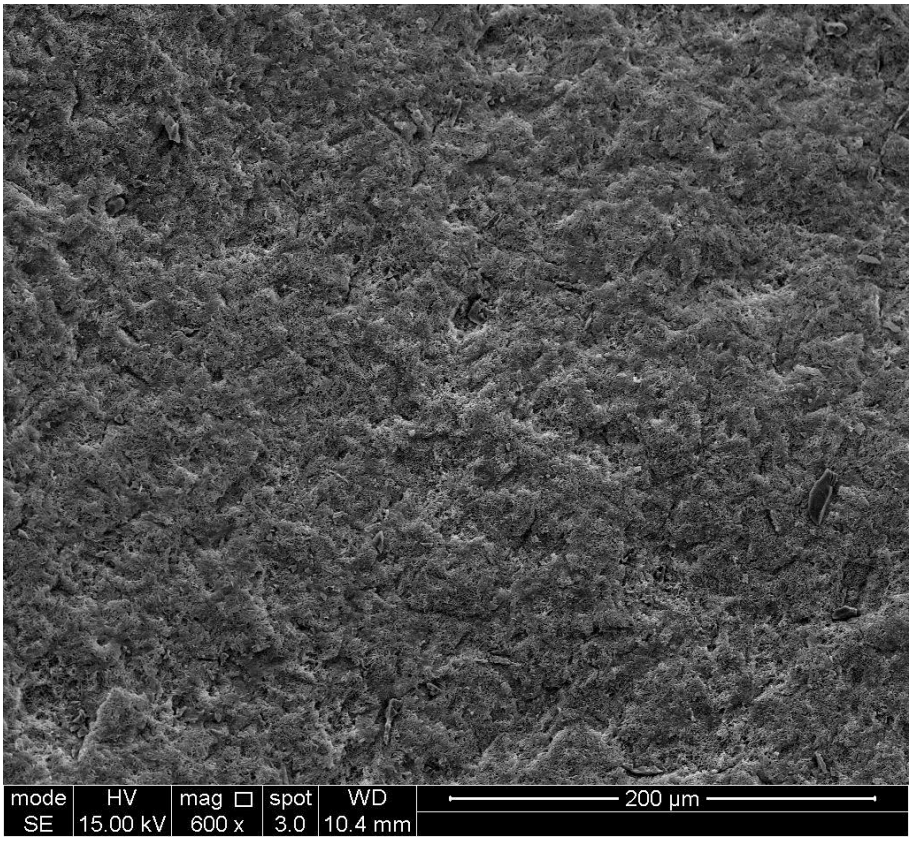

Figure 6-21: SEM of etched e.max® pressed at 600x

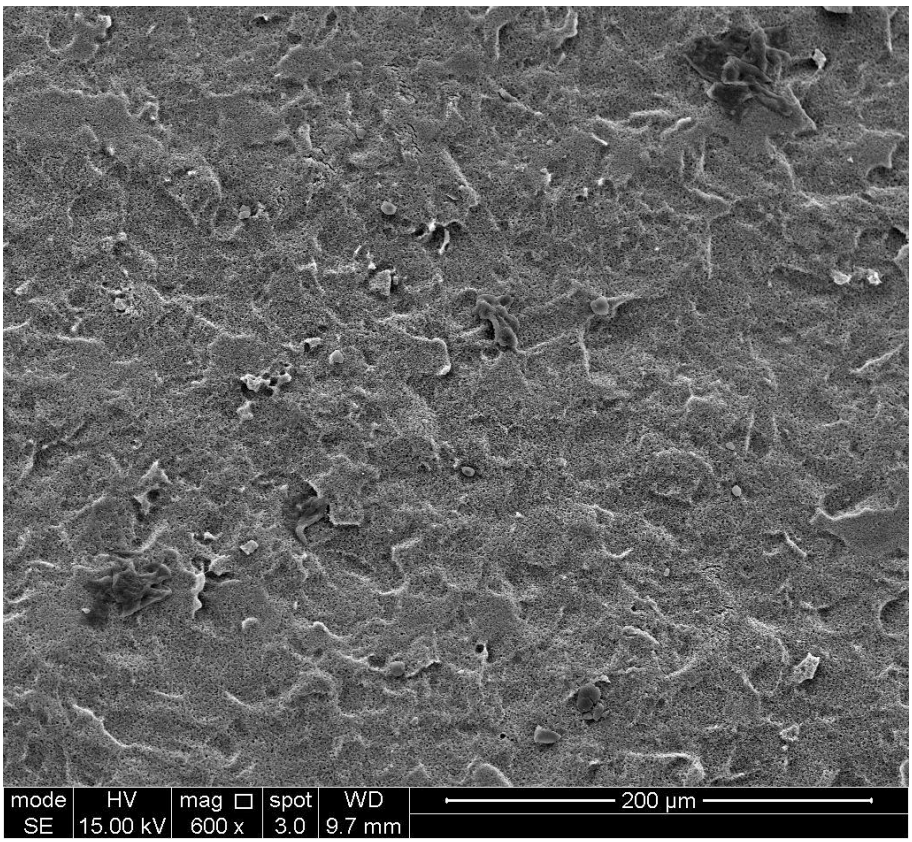

Figure 6-22: SEM of etched e.max® machined at 600x

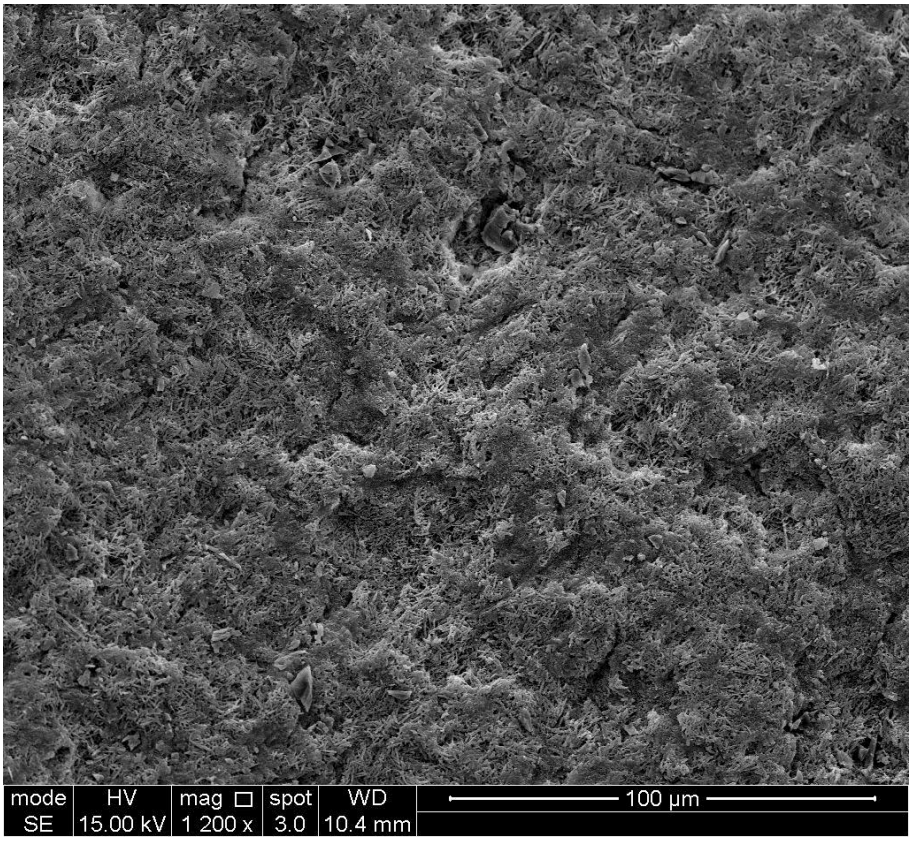

Figure 6-23: SEM of etched e.max® pressed at 1200x

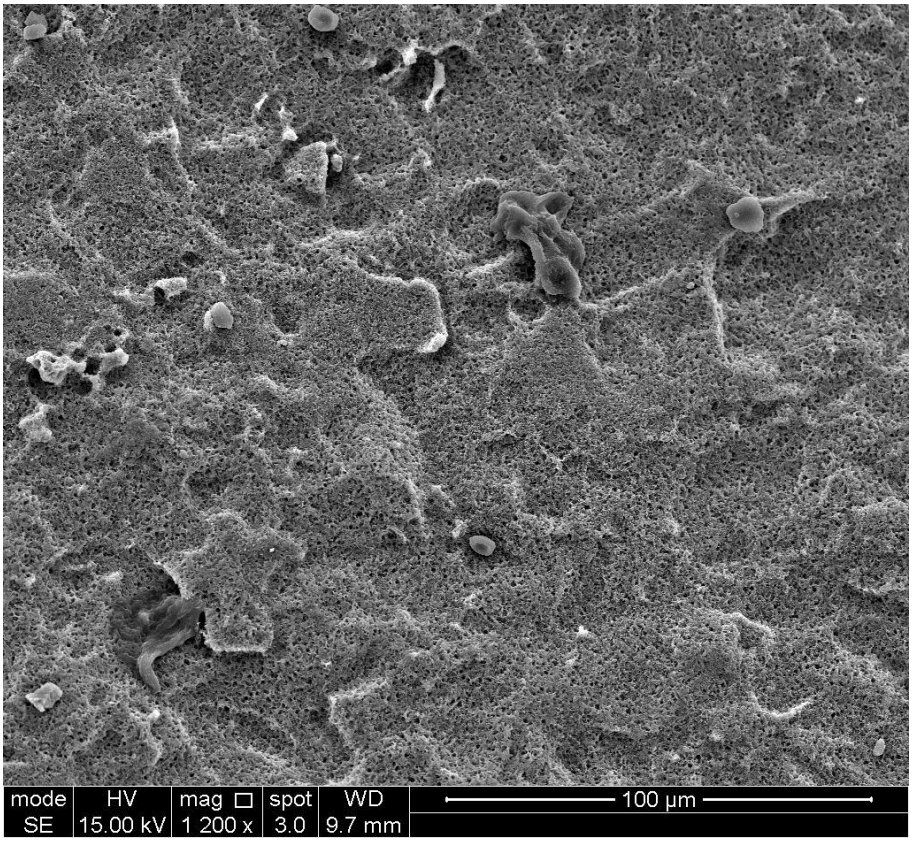

Figure 6-24: SEM of etched e.max® machined at 1200x

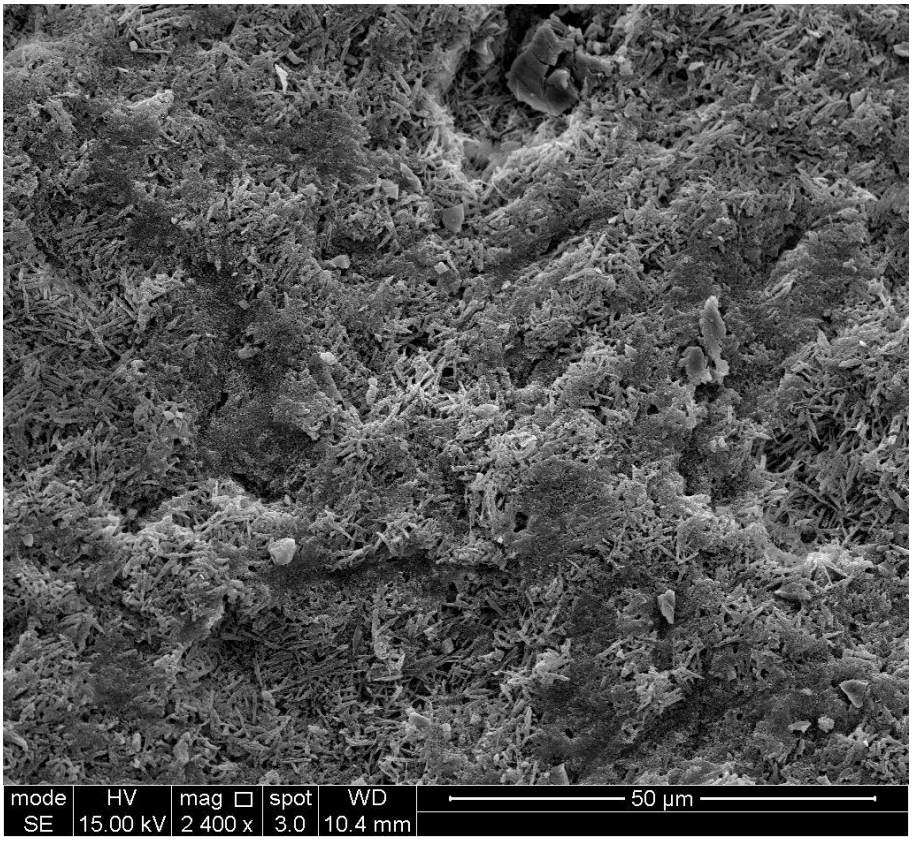

Figure 6-25: SEM of etched e.max® pressed at 2400x

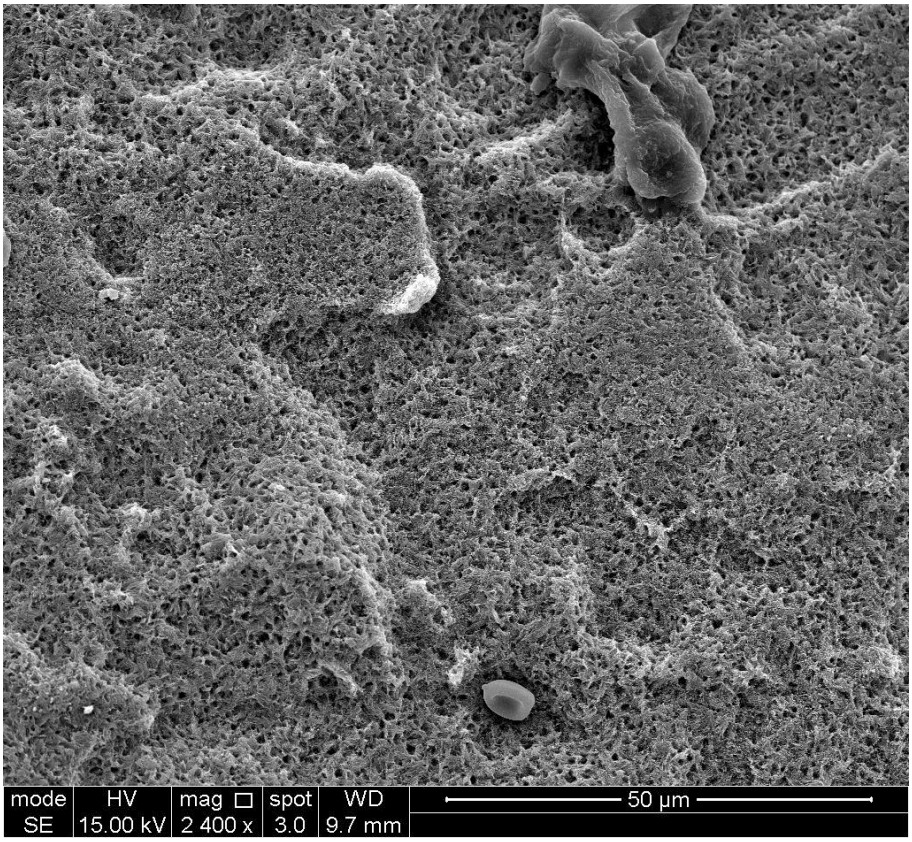

Figure 6-26: SEM of etched e.max® machined at 2400x

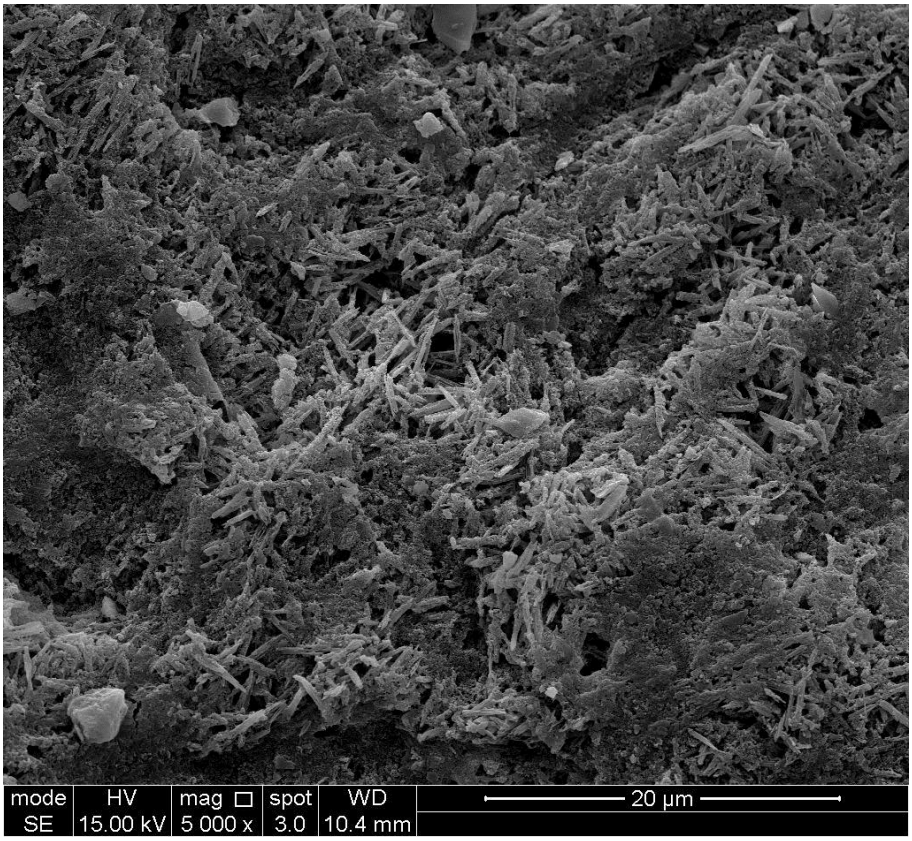

Figure 6-27: SEM of etched e.max® pressed at 5000x

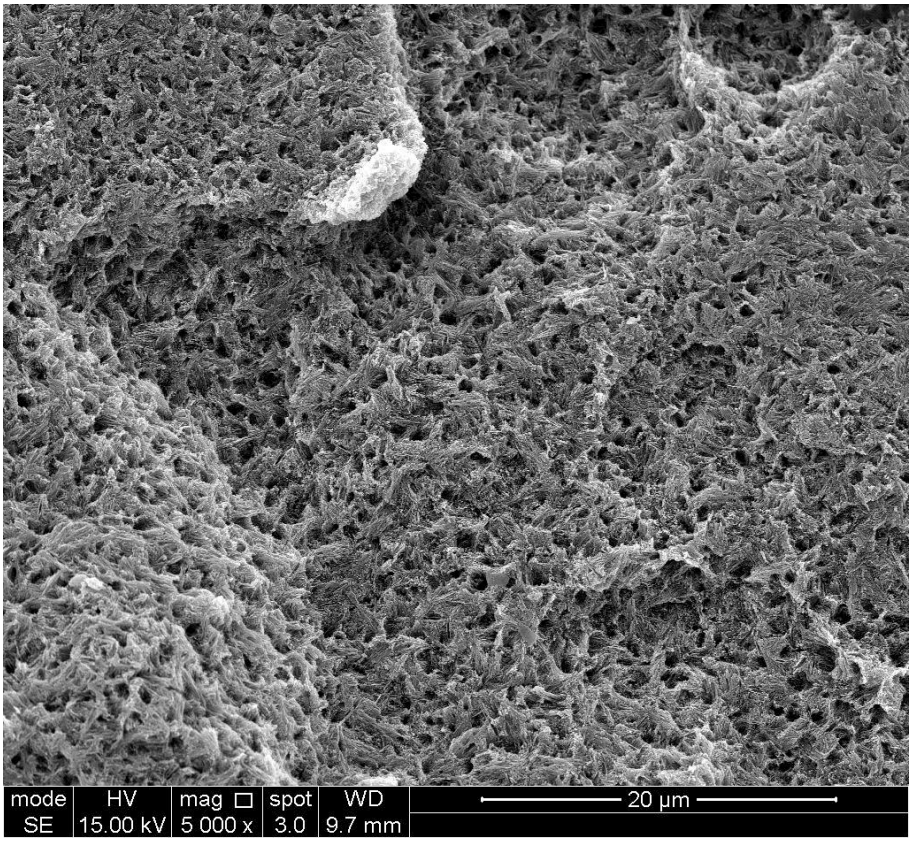

Figure 6-28: SEM of etched e.max® machined at 5000x

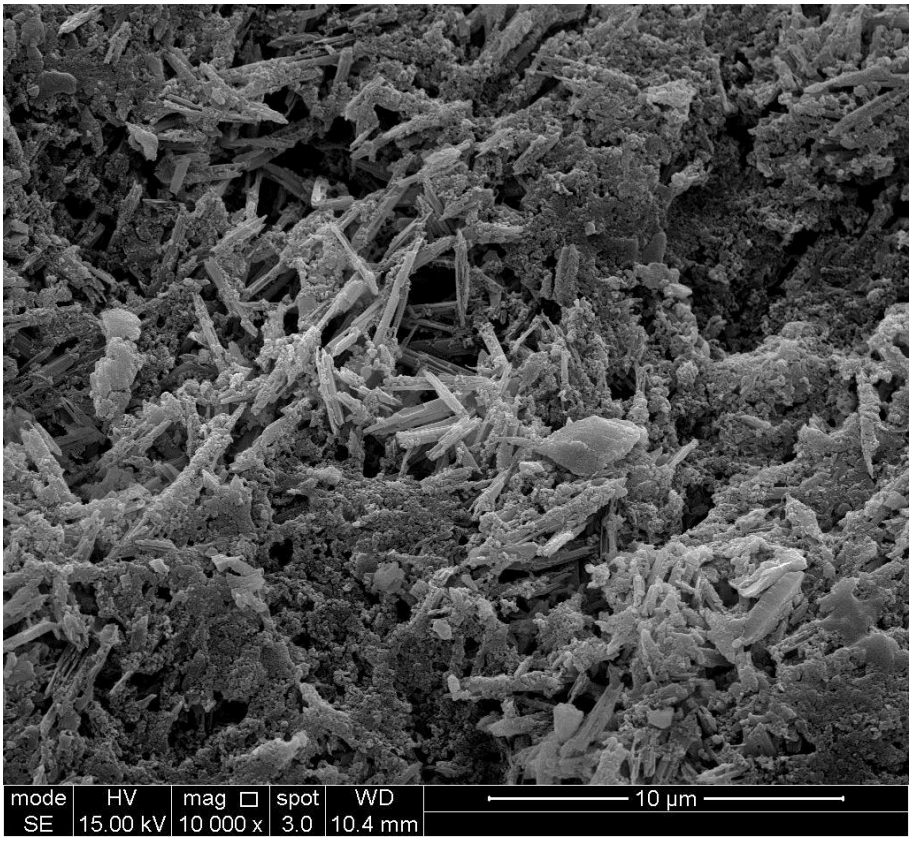

Figure 6-29: SEM of etched e.max® pressed at 10000x

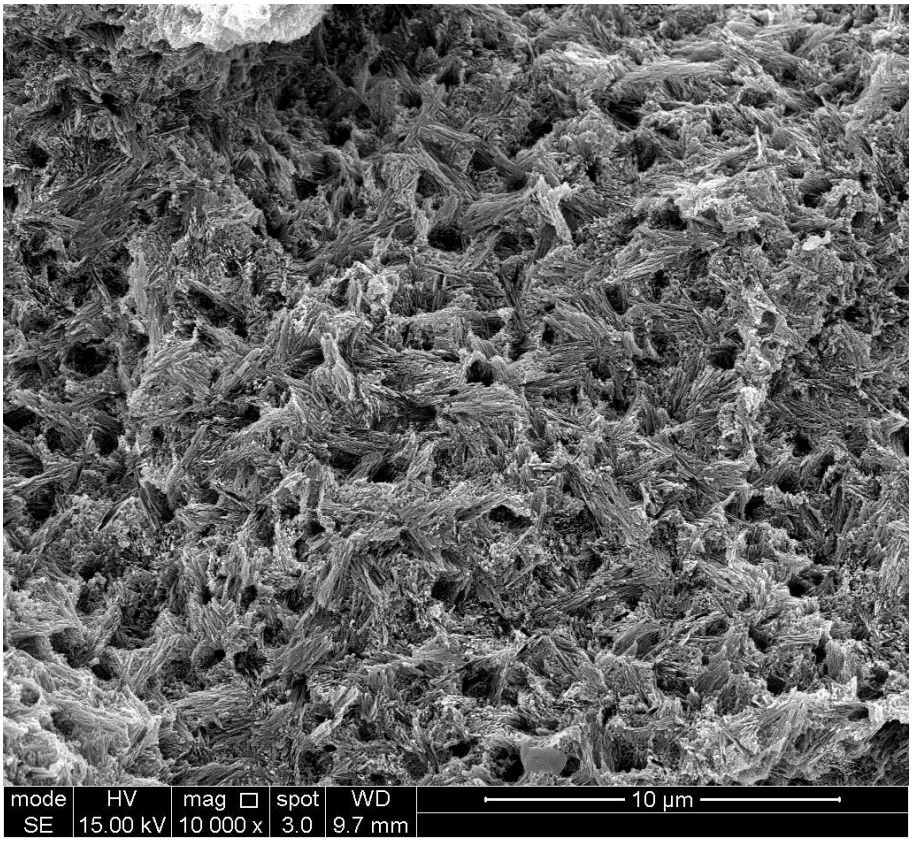

Figure 6-30: SEM of etched e.max® machined at 10000x

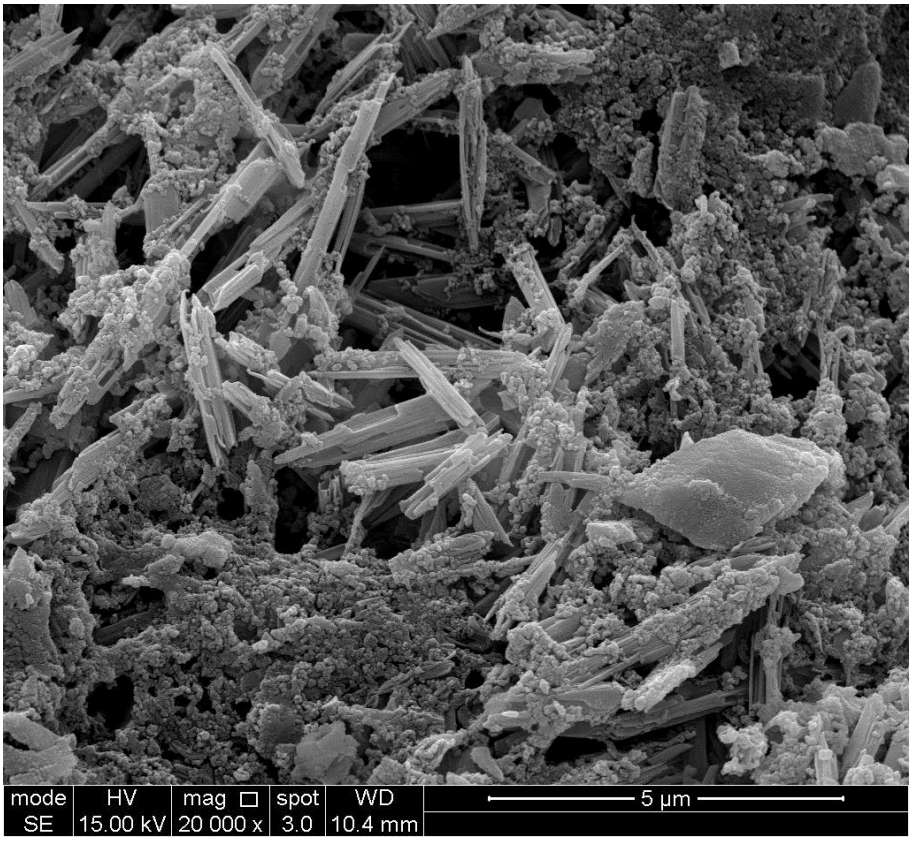

Figure 6-31: SEM of etched e.max® pressed at 20000x

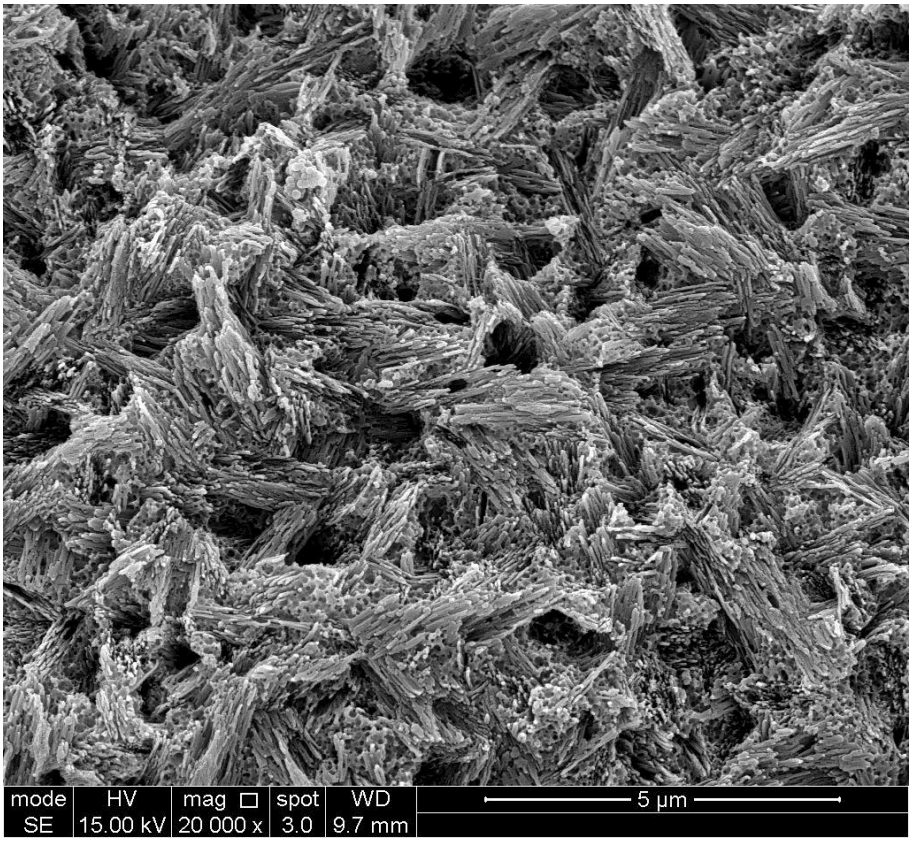

Figure 6-32: SEM of etched e.max® machined at 20000x

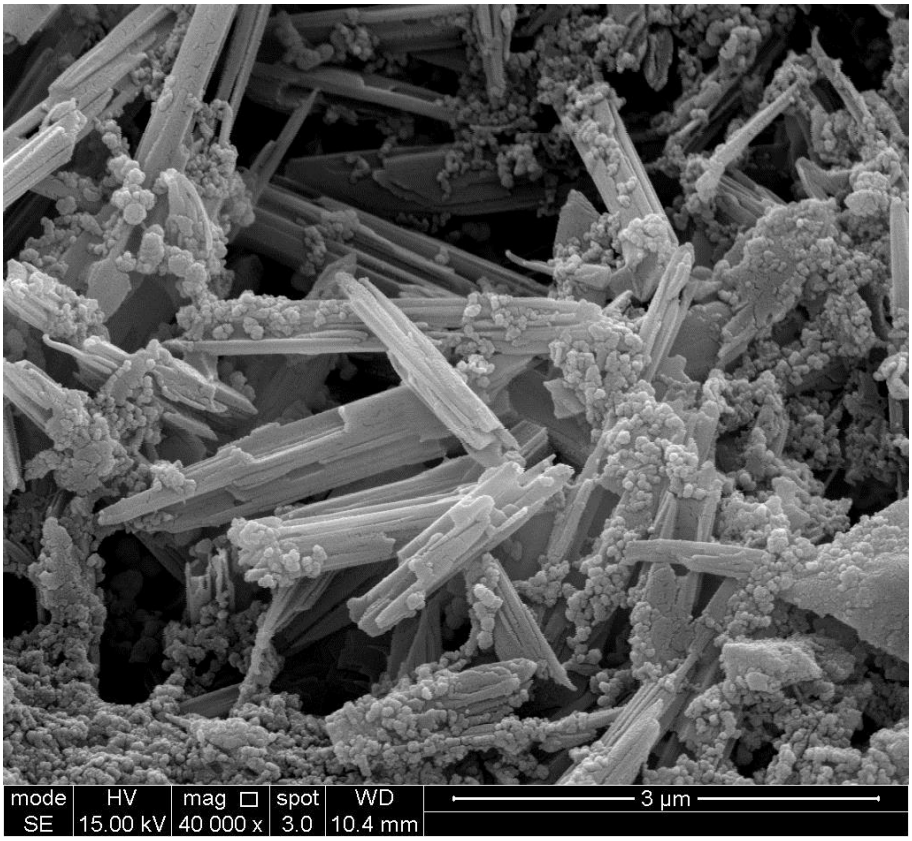

Figure 6-33: SEM of etched e.max® pressed at 40000x

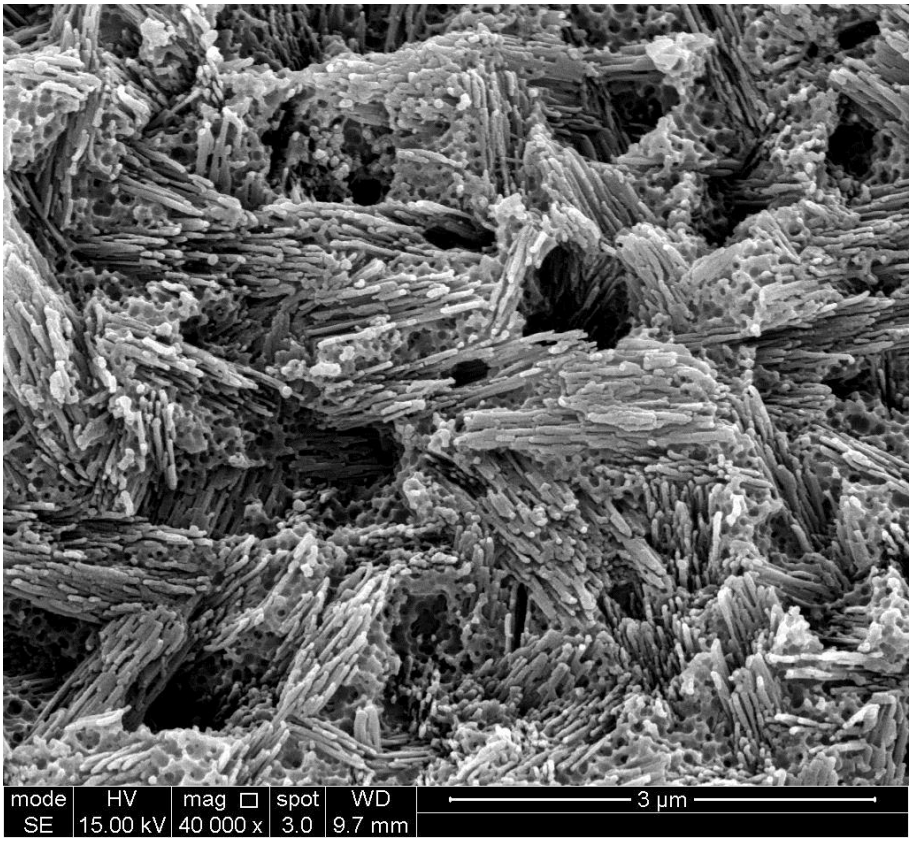

Figure 6-34: SEM of etched e.max® machined at 40000x

6.7 Discussion

Ceramography is a branch of the science concerned with the geometrical characteristics of the ceramic by preparing, examining and evaluating ceramic microstructures. This study was a ceramography study that investigated objectively the microstructural features of the two aspects of the lithium disilicate ceramic [e.max® Press and e.max® CAD].

According to the scientific reports by the manufacturer, the features of lithium disilicate ceramic [pressed and machined] are the same, except for the crystal's size and shape (Vivadent. and Ivoclar., 2009). The differences in the shape and the size have an impact on the strength and toughness of the ceramic. The pressed lithium disilicate crystal shows a crystal length of 3 μm to 6 μm, compared to just 1.5 μm for the machined lithium disilicate ceramic. Thus, the flexural strength differences of the e.max® Press [400MPa] to [360MPA] for the e.max® CAD; and the fracture toughness of [2.75MPa] for the e.max® Press and [2.25MPa] for the e.max® CAD could be attributed to the larger size and the length of the pressed microstructure crystals [data collected from some brochures and websites].

- Manufacturer's brochure (Ivoclar/Vivadent and products, 2014)
- Manufacturer's materials brochure (e.max, 2014)

The SEM microstructural investigation for the non-etched pressed and machined ceramic crowns have shown very close features at low magnification

powers of 300X, 600X and 1200X. Both groups show a homogenous structure without any significant difference [Figures 6-3, 6-4, 6-5, 6-6, 6-7, 6-8]. Whereas, at higher magnification, different geometric textures and crystal shapes become obvious. The inner surface of the pressed crown show crystals with a sea-wave form, which are of a larger size and with sharper edges [Figures 6-11, 6-13, 6-15, 6-17] compared to the jelly-like appearance of the machined crown [Figures 6-12, 6-14, 6-16, 6-18]. In this latter group the inconsistency in the shape of the pressed crystals is likely to be related to the sandblasting of the pressed crown during the removal of the investing materials.

The second scenario was to compare a specific area in both groups of the etched samples. The similarities at the microstructure features that are seen at a low magnification power of 300X are clearly visible all the way up to the magnification power of 2400X. Both groups of crowns showed a sponge-like inner surface texture [Figures 6-19, 6-20, 6-21, 6-22, 6-23, 6-24, 6-25, and 6-26]. However, with the higher magnification powers, the large needle-like crystals of the e.max® pressed crown compared with the e.max® machined crown crystals can be discerned [Figures 6-27, 6-28]. Moreover, in both groups' samples there were hole-like spaces that most likely caused by the dissolution of the glass matrix by the effect of the etching agent [Figures 6-27, 6-28, 6-29, 6-30, 6-31, 6-32].

It has been found, that the pressing heat would enhance the growth of the microstructure crystals of the lithium disilicate ceramic. The higher magnification images [Figures 6-33, 6-34] show that in both groups of the etched samples the needle-like shape of the pressed crystals is significantly larger than the machined crystals and that came in accordance to Albakry et al findings (Albakry et al., 2004a).

At a magnification power of 40,000X, the images of the etched machined samples show a larger pores size than the pressed group sample and that is in agreement with Albakry et al. (Albakry et al., 2004a).

The effect of the porosity on the structural strength has been thoroughly investigated by some authors. It has been shown that the porosity could act as a stress concentrator that reduces the ceramic structural strength. Moreover, the porosity could reduce the cross-sectional area under the applied load that has a detrimental effect on the structural strength. Thus, the pressed lithium disilicate ceramic possesses higher strength than the machined lithium disilicate ceramic in respect to the size and distribution of the pores within the structures (Wagh et al., 1993, Rice, 1996, Albakry et al., 2004a).

From a mechanical point of view, the degree of crystallinity, crystals' length and size are directly proportion to the fracture toughness of the glass ceramic(Becher, 1991, Quinn et al., 2003, Guazzato et al., 2004b). The crystals of the lithium disilicate ceramic after pressing show a homogenous crystals

distribution with the crystals size increase double of those before pressing (Albakry et al., 2004b). The favourable properties of the pressed microstructure crystals would enhance the structure crack bridging that could contribute in the toughening mechanism by increasing the energy that required for the crack to propagate (Baran et al., 2001, Albakry et al., 2004a).

No evidence of fabrication-induced flaws in either sample was seen. Therefore, based on the difficulty in investigating the internal flaws by the SEM, it was not possible to consider which group could have higher fracture toughness than the other.

6.8 CONCLUSION

Within the limitations of this study the following conclusions were drawn:

1- The etched machined lithium disilicate ceramic crowns show significantly more pores compared to the etched pressed lithium disilicate ceramic. Therefore, the hypothesis of 'There is a similarity in the microstructure of the machined and pressed lithium disilicate glass ceramic and both are free technique-induced flaws' is rejected.

2- A uniform dispersion of the needle-like crystal can be seen with the pressed lithium disilicate ceramic.

3- The toughening mechanism by crack bridging could be confirmed by the long needle-like crystals in the pressed ceramics.

4- No evidence can be taken from this study regarding the process-induced flaws in either group.

5- No micro-cracks could be detected in either group.

An FEA investigation of the effect of the interface geometry on the stress distribution of the restored crown-tooth complex

Part of this study has used published data (Shahrbaf et al., 2013)

7 FEA of real VS virtual

This chapter covers objective 5 of the thesis

7.1 Introduction

The nature of the interface cement has long been considered to be critical in the overall structural integrity of the crown-tooth complex (Rekow et al., 2006). Significantly, the elastic modulus and the adhesion to the substrates have been extensively studied. However, the effect of the interface space geometry (width and uniformity) is less well understood. In particular, whether the space is of uniform or non-uniform dimensions and the effect of this on the stress distribution and the structural integrity of the restored tooth complex. Different investigations have revealed that the clinical success of cemented all ceramic restoration can be enhanced by the thin and uniform cement thickness (Mou et al., 2002, Piemjai et al., 2002, De Jager et al., 2005, Giannetopoulos et al., 2010).

De Jager et al, (2005) have found that the stress distribution is considerably higher in a non-uniform cement thickness compared with a uniform thickness. Conversely, a study by Mou et al, (2002) has addressed the negative impact of the uneven cement thickness on the cement adhesion strength and this in turn would affect the longevity of the restoration; a finding that has been supported by other groups(Mou et al., 2002, Piemjai et al., 2002, De Jager et al., 2005, Vargas et al., 2011)

Notwithstanding, the majority of the published studies that investigate the influence of the geometry of the dental cement on the stress state of restored tooth are inconclusive. This study seeks to clarify, by the use of 3D-FEA, the effect of the uniformity of the interface thickness on the stress distribution through adhesively bonded full-coverage all-ceramic to the uniting cement and the underlying tooth. This is a hypothetical scenario as the ability to create an interface of a perfectly uniform interface width is currently not possible with the existing manufacturing technologies. The use of computer simulation to create a virtual interface of even thickness dimensions can be utilised with the combined use of digital modelling software and haptic technology.

7.2 Aim

To verify, using 3D FEA, the role of the interface cement geometry on the stress state in a tooth adhesively cemented with all ceramic crown.

7.3 Objectives

1- To digitally generate, by using the FreeForm® haptic technology (SensAble Technologies, Inc.), an ideal uniform cement interface on a 3D model of a tooth restored with an adhesively-united all ceramic full-coverage crown. This study is based on the modification of a previously created 3D model from our research team [the 3D FE model is quoted from a published study (Shahrbaf et al., 2013).

2- To generate an accurate 3D mesh for the uniform cement object that has been created.

3- To evaluate by FEA the stress distribution pattern in a restored tooth with [artificially-created] uniform cement interface and compare it with the identical model [naturally-created] non-uniform cement interface geometry of the published study model.

7.4 Null Hypothesis

The uniform geometry of the cement interface negatively affects the stress state in the tooth restored with all-ceramic crown.

7.5 Materials & Methods

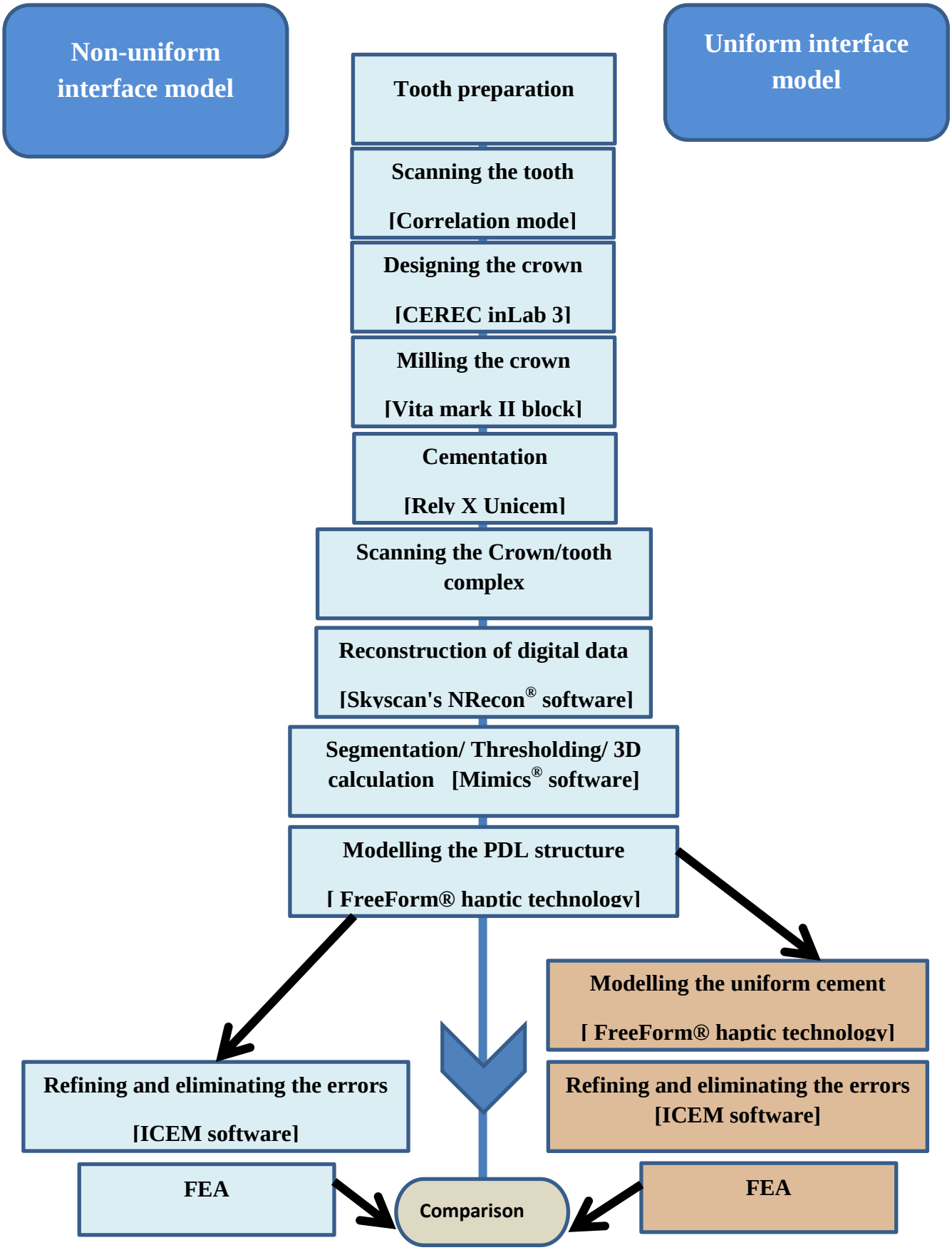

Figure 7-1: Flaw chart of the experiment steps

7.5.1 3D model generation of the tooth-restoration complex

An existing peer-reviewed 3D digital model of a tooth-crown complex has been digitally modified to create a uniform cement space (Shahrbaf et al., 2013). A new cement interface object with a cement interface of a uniform width was recombined with the already present 3D FE model. This has been done in accordance with the method described below.

7.5.2 Sample selection and model preparation

A sound caries-free maxillary first premolar was selected and the debris and calculus were carefully removed manually with a conventional hand scaler. The tooth root was fixed in a cylindrical base filled with acrylic resin. A conventional preparation for an all-ceramic crown was carried out according to the following parameters: occlusal reduction [2mm], axial reduction [1.2-1.5mm], shoulder finishing line [1mm] and a taper degree of 12^0.

An indirect restoration of full-coverage all-ceramic crown was milled from a ceramic block [Vita mark II block (2M2C I12, shade A 2) Vita Zahnfabrik, Bad Sackingen, Germany] using the CEREC inLab 3 in ‘correlation’ mode, that copies the shape and dimensions of the original tooth crown, as described in chapter 5.

The crown cementation protocol was followed as described in chapters 5 and 8); with the variation that the cement material used was Rely X Unicem® Clicker (3M ESPE, Seefeld, Germany).

7.5.3 3D model and FEA model generation

The sample (crown-tooth complex) was digitised using the sky scan micro CT scanner [Skyscan® 1072] as per the protocol detailed chapter 4. The scanning parameters were: image resolution of 12.5µm, medium camera (1000×2048), rotation (359), Al foils filter (1mm) and voltage (50Kv).

According to the Sky® scan manufacturer's recommendation, the images were reconstructed by Skyscan NRecon® software and exported as bitmap (bmp) files.

Thereafter, the acquired data images were processed by Mimics® software [Mimics® 13.1, (Materialise interactive medical image control system) Materialise Co., Ltd. Belgium]. This sophisticated modelling software enables to import the micro CT images stack and showing the scanned object in 2D views (axial, coronal and sagittal). Using the image's density threshold, segmentation functions in Mimics® were carried out to separate the structure into different layers (ceramic, resin cement and dentine). Subsequently, all the segmented layers were calculated in 3D and the tooth structures were presented in a form of 3D object.

Modelling the PDL structure and repositioning the whole structures in their correct position in the bone were carried out by FreeForm® haptic technology following the same steps that have been fully described in chapter 4.

For configuring the FE model, the 3D model was exported as a stereolithography (STL) file. The STL is an object of a shell format in a form of small triangles [mesh]. Because of the complex geometry of the given 3D model, some missing triangles and elements of voids and errors existed in the model. The model created in STL file format was repaired with the aid of a different software programme; ICEM software [version 11, ANSYS, Inc] and all the unwanted errors were defined and eliminated. The quality of the STL file was confirmed by the ICEM software for each individual component and STL files with high quality mesh were exported.

For carrying out the finite element analysis for the tooth model, the stress state should be evaluated through the whole tooth body and its supporting structures. Hence, the mesh in the shell format should be transformed to a volume mesh.

Volume mesh enables the analysis of the stress stats in the body structures as a whole unit structure rather than just for the external surface such as the shell mesh does. According to quality mesh index, a high quality volume mesh of the tooth and its supporting structures was generated using Hypermesh® software (Version 10.0, Altair Engineering, Inc.). Moreover, within each layer, the

quality of different elements was assessed and all the free edges were removed and the general quality index of all the elements was recovered.

Based on the defining and refining of the errors, the accuracy of the volume mesh of the presented 3D model was confirmed by the Shahrbaf study (Shahrbaf et al., 2013).

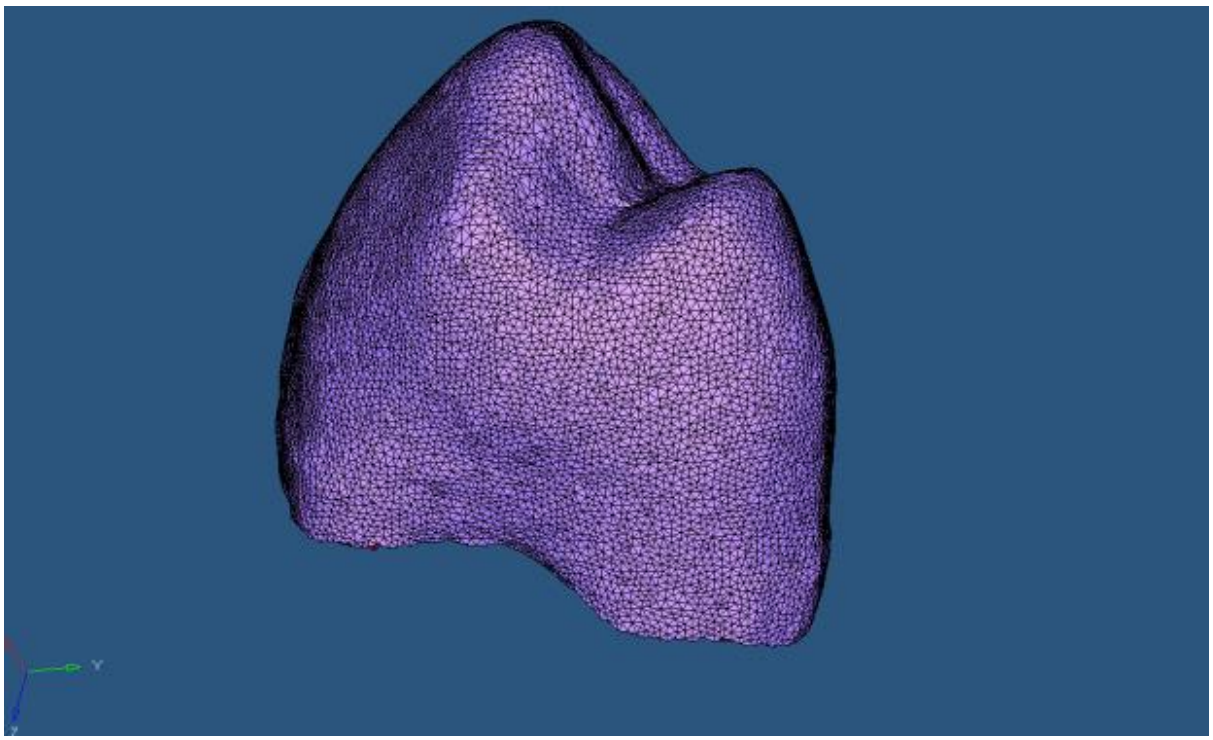

Figure 7-2: 3D volume mesh of the ceramic crown component

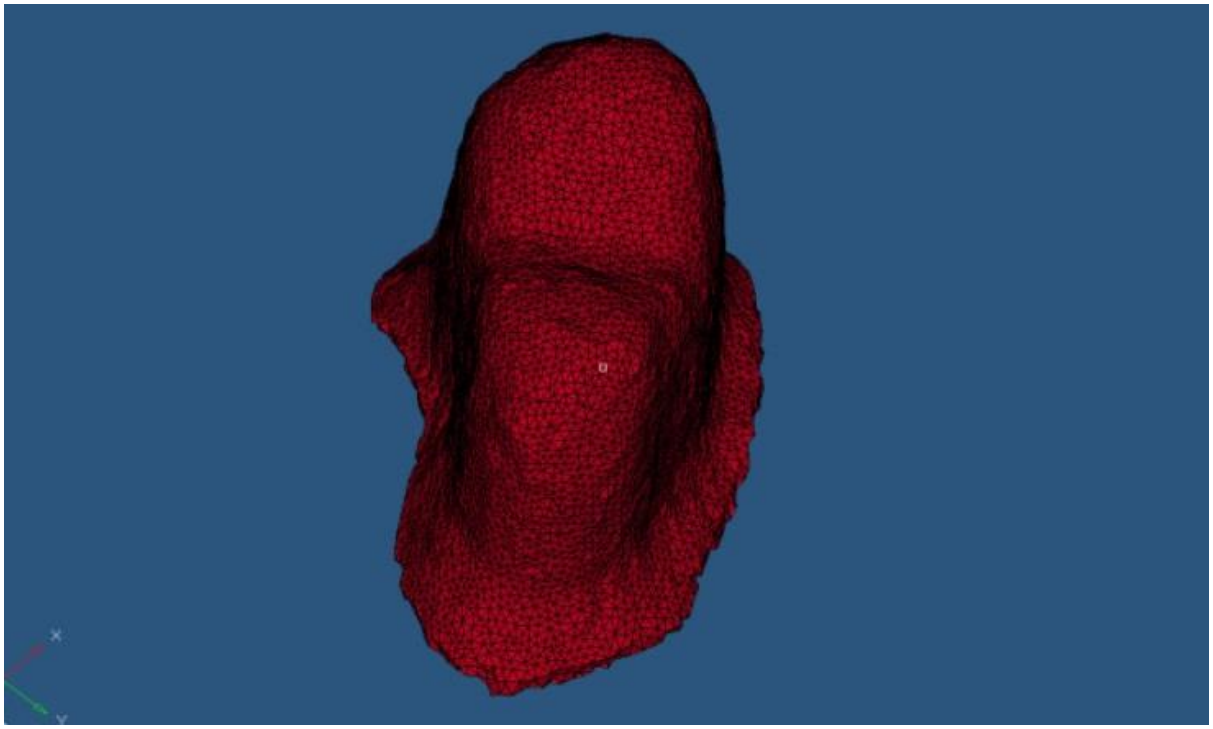

Figure 7-3: 3D volume mesh of the cement interface component

Figure 7-4: 3D volume mesh of tooth component

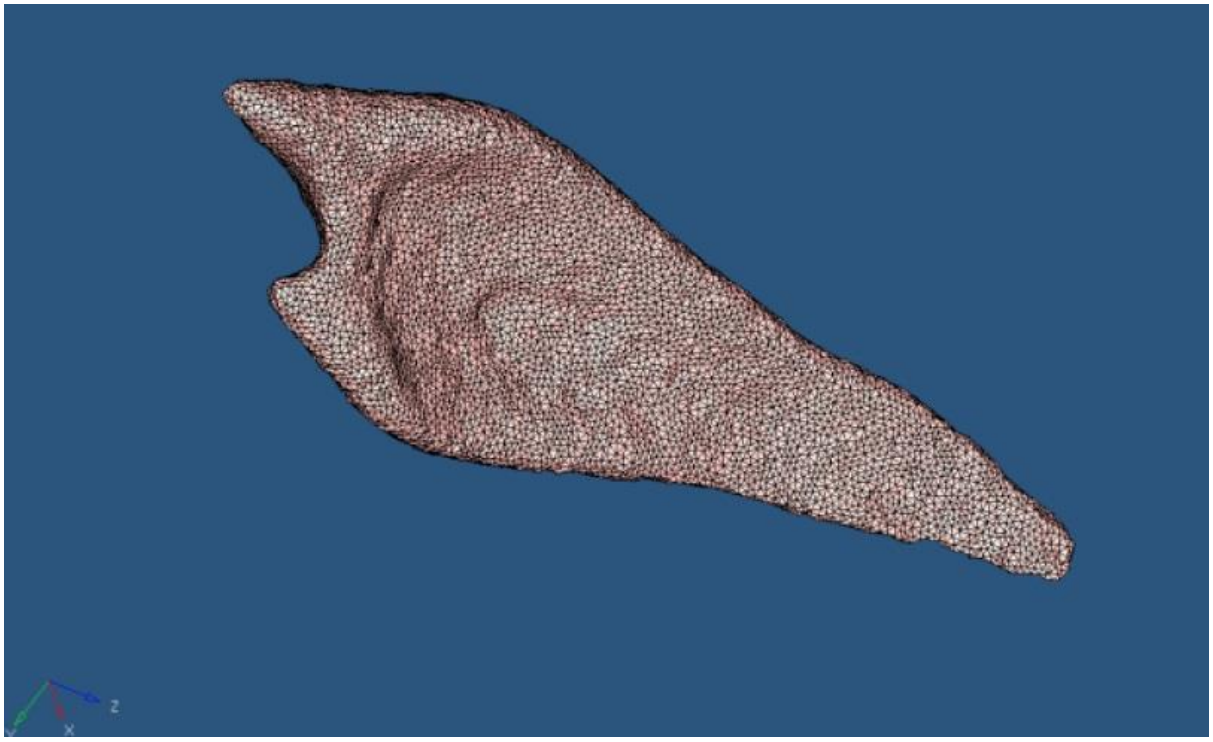

Figure 7-5: 3D volume mesh of pulp component

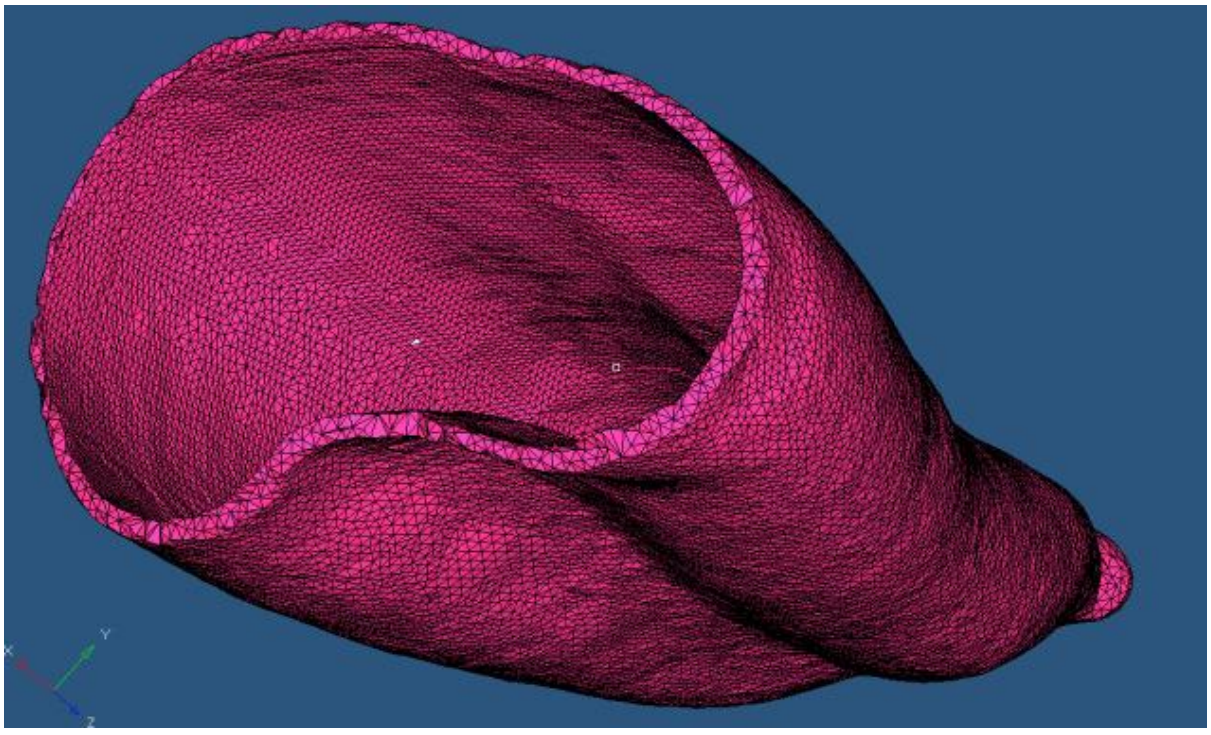

Figure 7-6: 3D volume mesh of PDL component

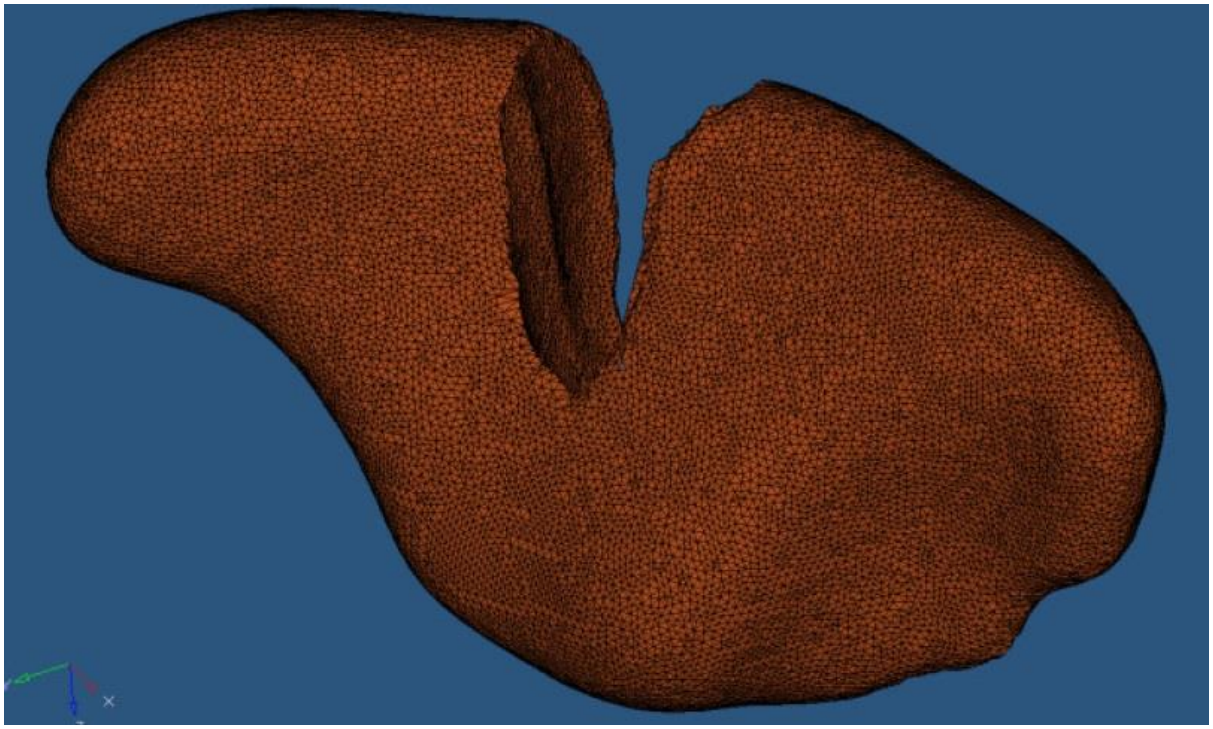

Figure 7-7: 3D volume mesh of cancellous bone component

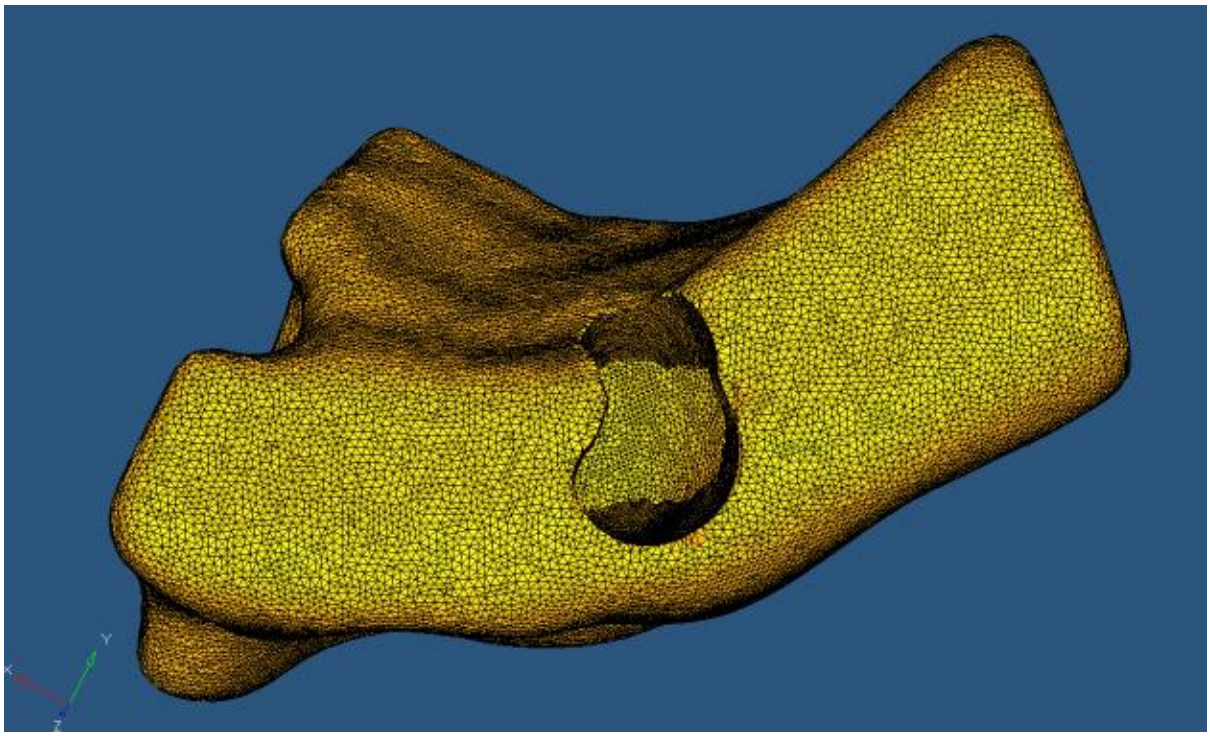

Figure 7-8: 3D volume mesh of cortical bone component

7.5.4 Generation of a 3D component of a uniform cement interface

For generating an ideal uniform interface with an optimum adaptation on the tooth and crown components of the original 3D FE model, the original tooth was used. The tooth STL has been imported in the FreeForm® software (SensAble Technologies, Inc.) and presented as a 'clay object'. The tooth clay model was duplicated to support the new layer of the interface. By an option of layer and the haptic technology, a uniform layer that analogue to a cement interface was laid evenly over the coronal part of the tooth.

Thereafter, the uniform interface generated layer was combined with the tooth clay by the option of company into clay to be as clay of one object. By the option of remove clay from, the uniform interface cement-like object was separated from the original tooth clay. The generated uniform interface object was repositioned in the presented 3D FE model with an optimum adaptation to replace the original non-uniform cement interface object [Figure7-9].

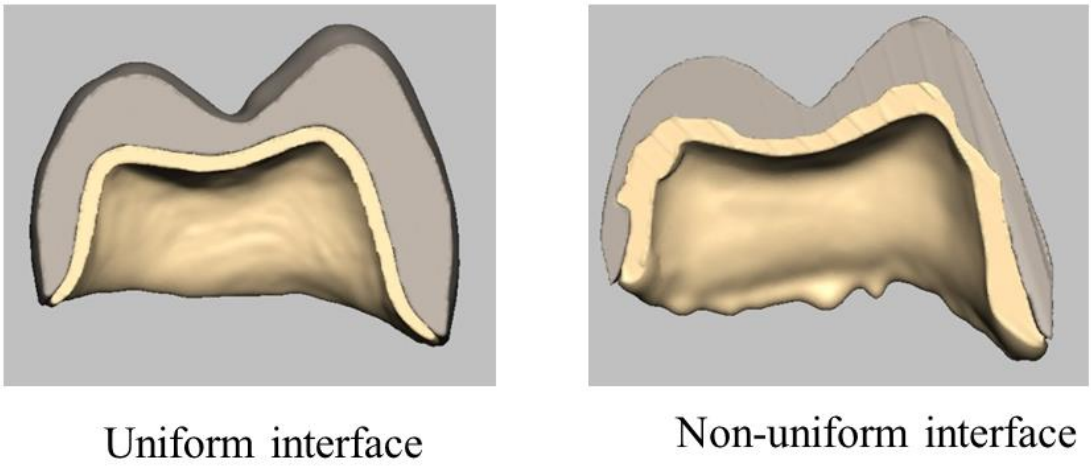

Figure 7-9: Uniform VS non-uniform cement interface

In order to achieve an optimum bond between the generated uniform cement layer and the exist crown, the same procedure of 'combine and subtract clay' were followed with crown as well.

Keeping the file format consistency of the generated uniform interface with the other components of the 3D FE model is required. In order to eliminate the errors and transferring the shell mesh to volume mesh, the same steps are used for the all components were followed.

7.5.5 Material properties

Since this experiment intended to compare the results with the results of the original published study (Shahrbaf et al., 2013), the materials properties must to be identical. Thus, to carry out the FEA using Hypermesh® software (Version 10.0, Altair Engineering, Inc.) on the modified model, the same assumptions have been considered. The layers' structure was assumed to be as homogenous, isotropic properties and have linear elastic behaviour. The bond interface between the compartments was assumed rigid. Thus, no slip interface condition was assumed between the layers. According to Spears et al and Meyer et al, the enamel and the bone are known to be anisotropic structures. However, an assumption were made for both as a homogenous isotropic structures (Spears et al., 1993, Meyer et al., 2001). These assumptions for the brittle materials in non-failure condition were verified to be reasonable by Ausiello study (Ausiello

et al., 2004). The other parameters such as modulus of elasticity and Poisson's ratio were selected form the literature (see table 7-1).

Table 7-1: Materials properties according to the original study (Shahrbaf et al., 2013)

Material type	**Elastic modulus (MPa)**	**Poisson's ratio**
Crown	69000	0.25
Cement	8000	0.33
Dentine	18600	0.31
Pulp	2	0.45
Periodontal ligament	50	0.45
Trabecular bone	13700	0.30
Spongy bone	1370	0.30

7.5.6 Boundary condition and load application

To achieve a fair comparison between the original (non-uniform cement interface) and the modified (uniform cement interface) models, the FEA must to perform under identical boundary and load application conditions. The boundary condition [zero displacement] has to be identified to apply the FE analysis. It is a simulation of the actual relationship between the tooth and its supporter structures such as the PDL and the bone. In order to achieve results with high accuracy, the boundary condition was identified at the most outer surface nodes of the cortical bone that were constrained in all direction (X, Y, and Z).

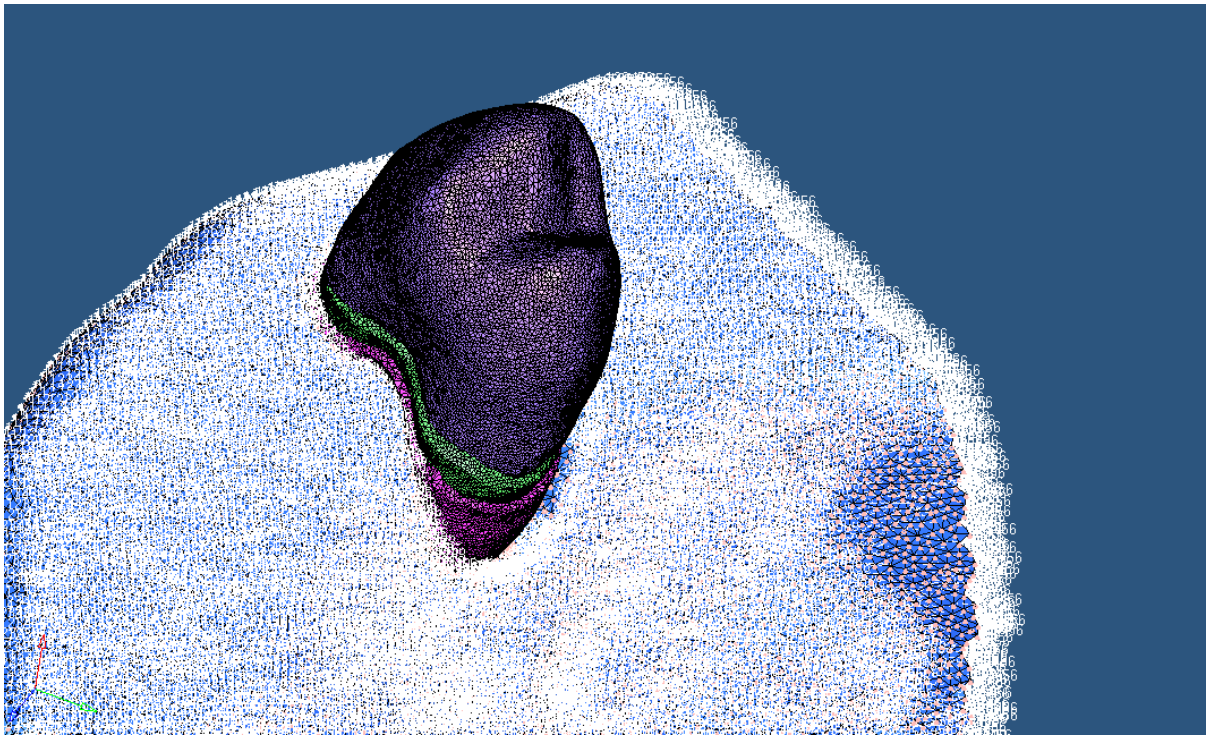

Figure 7-10: Boundary condition

To investigate the stress state in any structure, a load has to be applied. Two points were selected for the load application on the outer surface of the crown. These points are a collection of nodes located on the occlusal surface on the buccal inclination of the palatal cusp and the palatal inclination of the buccal cusp. In order to simulate the average occlusal load [300N] subjected on the premolar, the nodes of each selected point were subjected to 150N load that collectively would simulate the average mastication load of 300N [Figures 7-11 and 7-12].

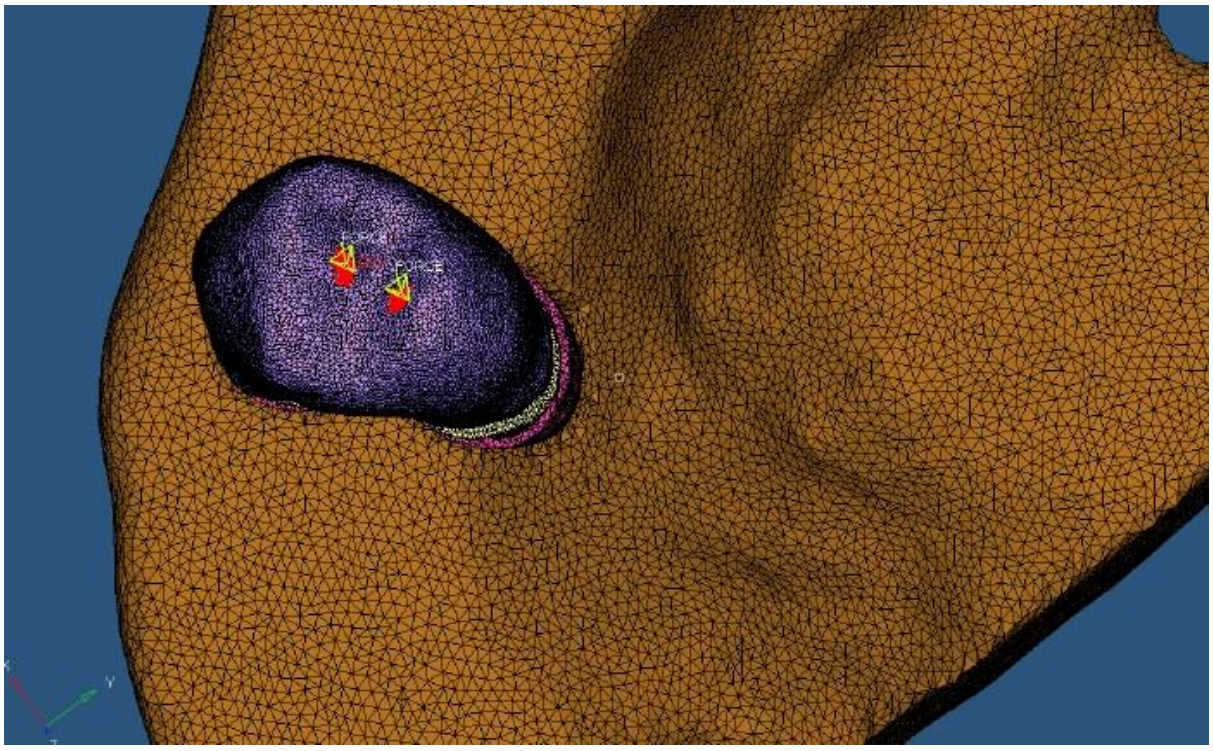

Figure 7-11: Load application on the two points of the crown

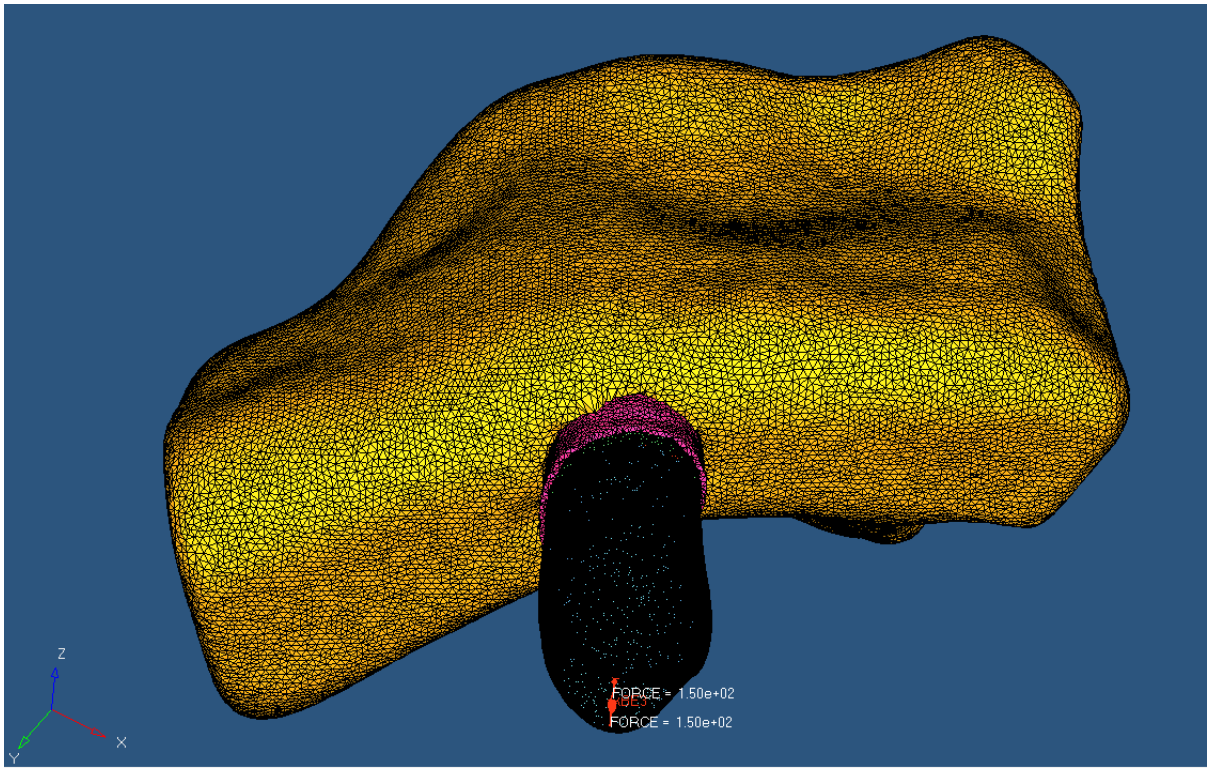

Figure 7-12: load of 150N in each point to be 300N in total

7.5.7 Convergence test analysis

It is well documented that some factors such as the elements number, meshing quality and the boundary condition have a critical effect on the reliability and the validity of the FEA (Bowley et al., 2013, Ha et al., 2013). To minimize these factors effect, the model's accuracy was verified by the convergence test. By this test, the accuracy and the reliability of the FEA result with computational means could be assured. The original (non-uniform cement interface) model was subjected to this test by increasing the number of the elements by 10%. The convergence test was conducted by changing successively the element numbers, which change the mesh size. The refining of

the mesh was performed till the analysis indicate a constant stress value on each compartment with the further mesh refining, thus, no further refinement was required.

Since, the convergence test was carried out for each of the layers of the presented model; performing the convergence test on the modified uniform interface cement layer was required. The convergence test was conducted and the optimum meshing nature for the analysis is assured.

7.6 Results

Since, the intention was to compare the FEA of the original (non-uniform cement interface) model to that of the modified (uniform cement interface) identical model. Thus, the distributed cloud of von-Mises stress and the maximum principal stress were calculated for the modified model in each object separately.

The peak values of von-Mises stress for each component of the modified (uniform cement interface) model are shown in [Tables 7-2] and [Figures 7-13].

Each component of the modified (uniform cement interface) model showed slightly higher values of stress compared with the analogous components of the original (non-uniform cement interface) model respectively. However, the differences in the stress values weren't too high and did not rise to the level of

significance. Moreover, the stress values in both models look the same in most of the components except the crowns.

Table 7-2: The peak values of von-Mises stress (MPa) for each component for the modified (uniform cement interface) and original (non-uniform cement interface) models.

component	Modified model (Uniform cement interface)	Original model (Non-Uniform cement interface)
Cement	33.05	24.69
Crown	691.31	590.5
Dentine	46.91	24.79
PDL	6.8	3.23
Spongy Bone	8.3	8.46
Trabecular Bone	34.91	18.65

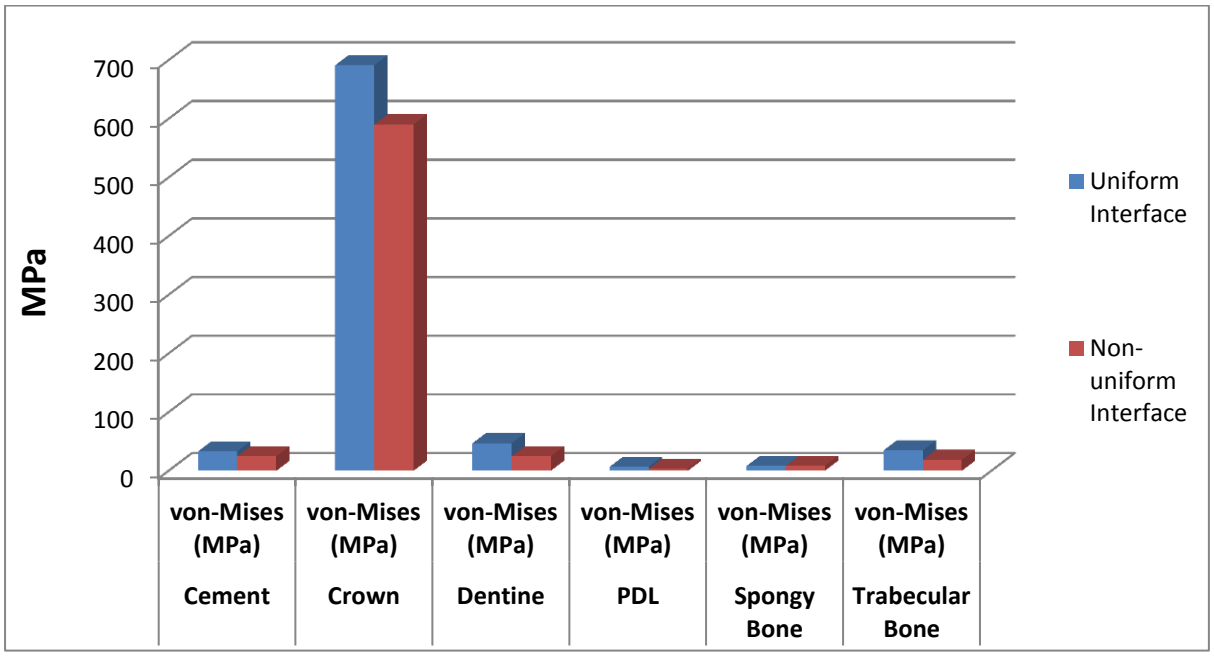

Figure 7-13: The peak values of von-Mises stress in each component for the non-uniform VS. Uniform interface models.

von-Mises stress state in the tooth component of the modified model

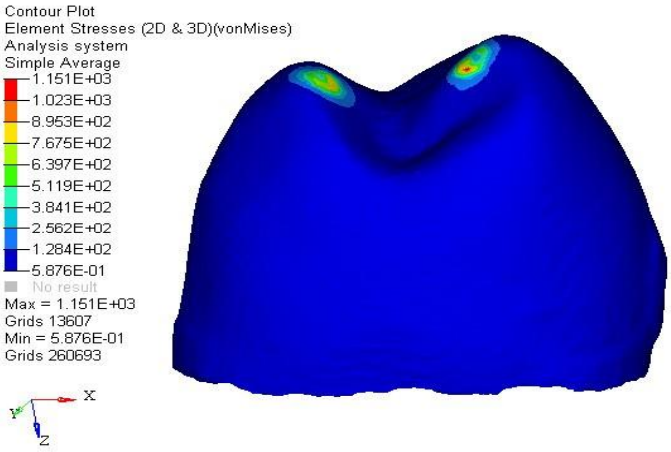

Figure 7-14: von-Mises stress pattern in the crown of the modified model

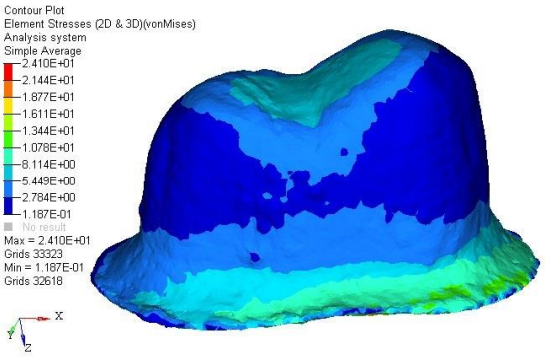

Figure 7-15: von-Mises stress pattern in the cement of the modified model

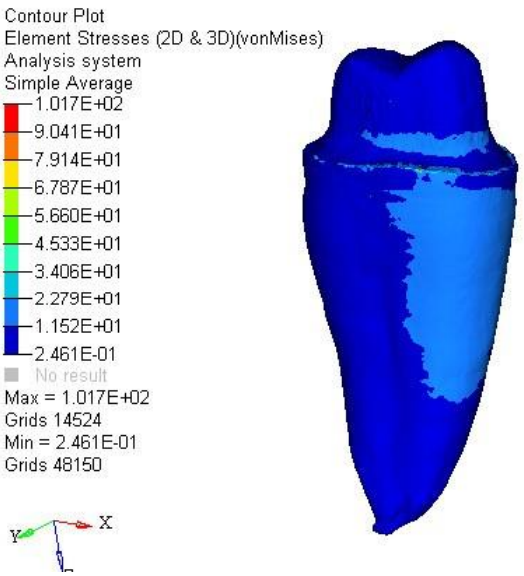

Figure 7-16: von-Mises stress pattern in the dentine of the modified model

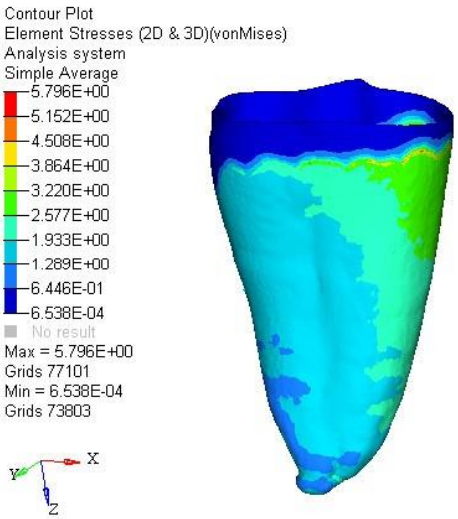

Figure 7-17: von-Mises stress pattern in the PDL of the modified model

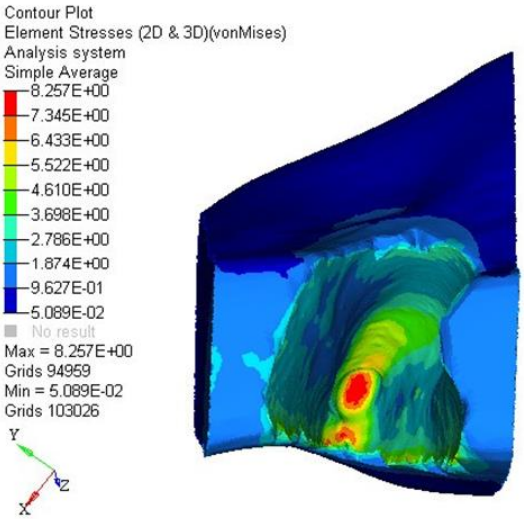

Figure 7-18: von-Mises stress pattern in the Spongy bone of the modified model

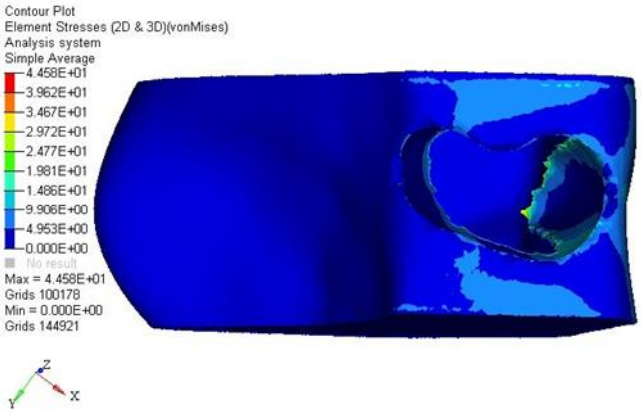

Figure 7-19: von-Mises stress pattern in the Trabecular Bone of the modified model

von-Mises stress state in the tooth component of the original model

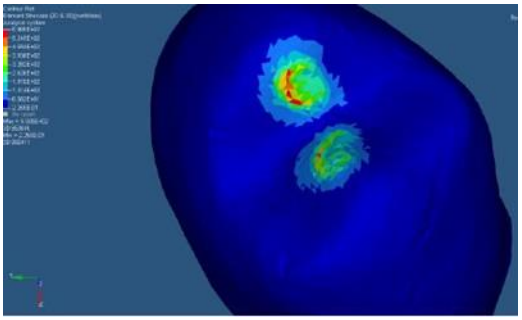

Figure 7-21: von-Mises stress pattern in the crown of the original model

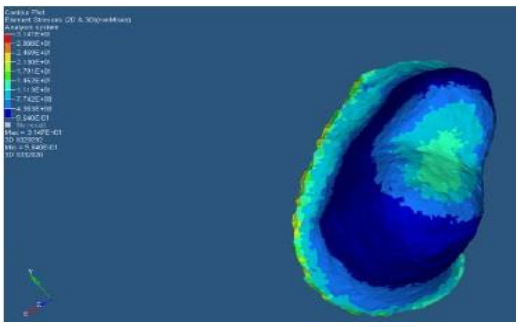

Figure 7-20: von-Mises stress pattern in the cement of the original model

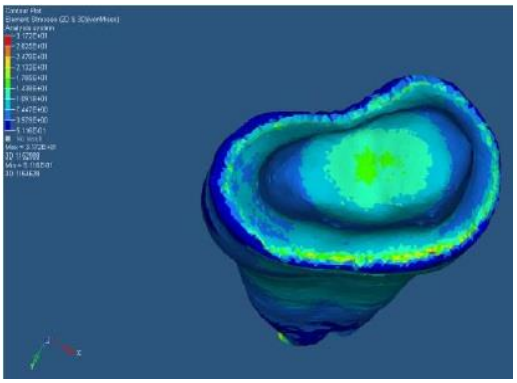

Figure 7-23: von-Mises stress pattern in the dentine of the original model

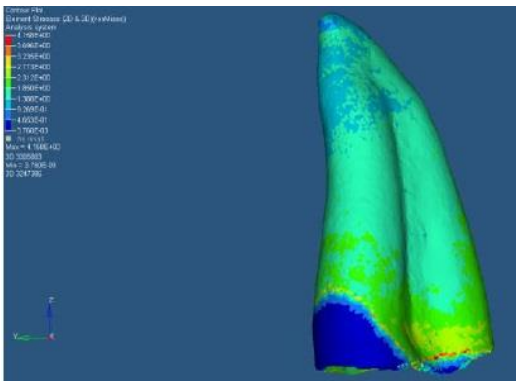

Figure 7-22: von-Mises stress pattern in the PDL of the original model

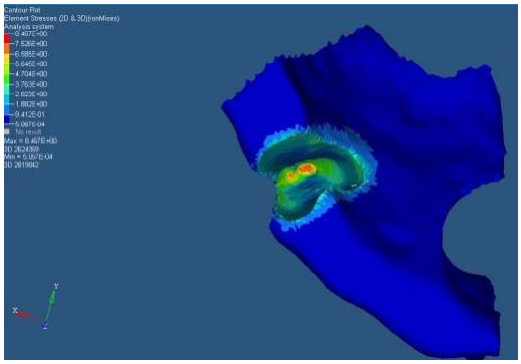

Figure 7-25: von-Mises stress pattern in the Spongy bone of the original model

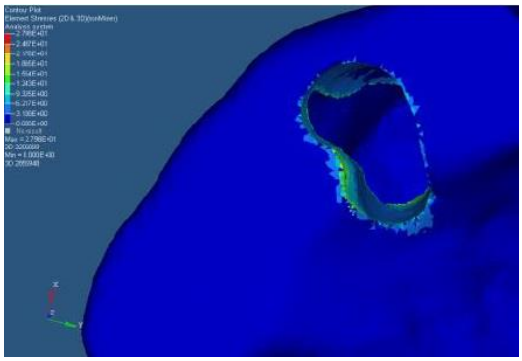

Figure 7-24: von-Mises stress pattern in the Trabecular Bone of the original model

The peak values of maximum principal stress for each component of both model are shown in [Tables 7-3] and [figures 7-26].

In contrast to the von-Mises stress, [Tables 7-3] shows that the maximum principal stress was higher in most components of the original (non-uniform cement interface) model compared with the analogue components of the modified (uniform cement interface) model. However, these slightly higher stress values seen can be considered as a not important. Moreover, the stress distribution pattern was displayed in the same pattern in both models regarding the von-Mises stress and maximum principal stress [Figure 7-26 and 7-13].

Table 7-3: The peak values of maximum principal stress (MPa) for each component for the modified(uniform cement interface) and original (non-uniform cement interface) models

component	Uniform Interface models	Non-uniform Interface models
Cement	8.61	9.3
Crown	386.31	388.5
Dentine	7	10.99
PDL	4.11	2.99
Spongy Bone	7.37	6.3
Trabecular Bone	31.61	22.68

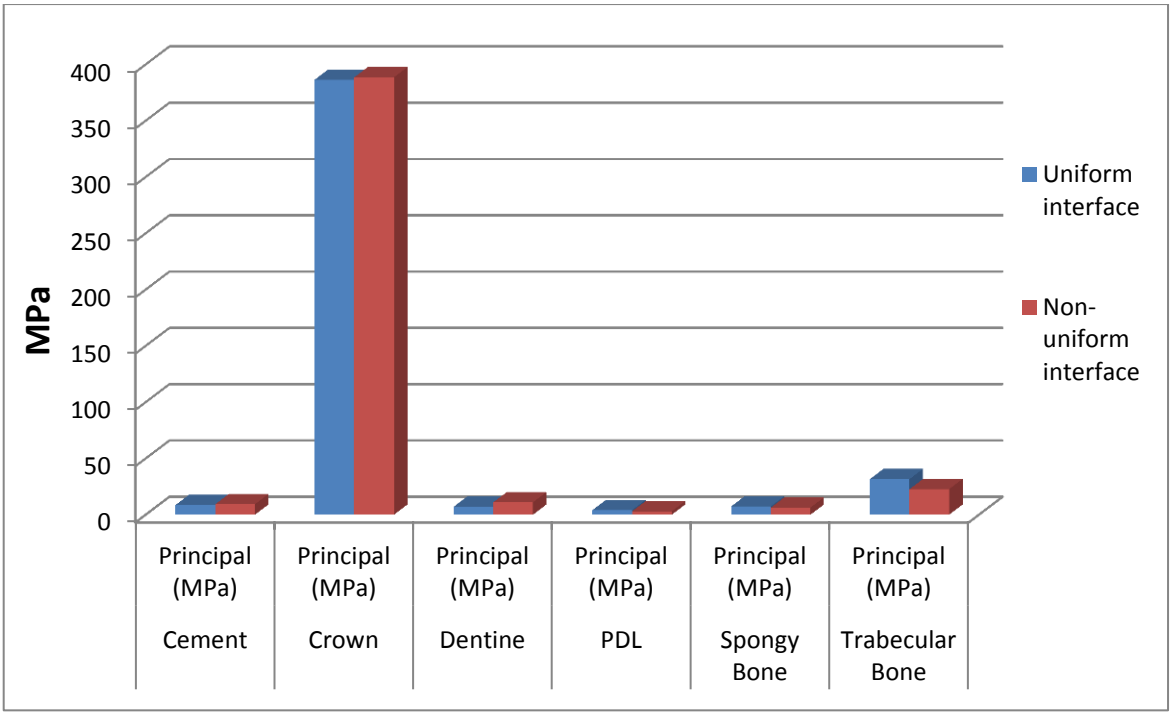

Figure 7-26: The peak values of maximum principal stress in each component for the non-uniform VS. uniform interface models.

7.7 Discussion

In this investigation, the finite element analysis data from the previously published study (Shahrbaf et al., 2013) were compared with the finite element analysis data of the present study. This comparison can be considered as an attempt to establish a theoretical estimate of the effect of a uniform interface on the stress state of the restored tooth complex.

Farah et al. had introduced the FEA to dentistry to investigate the stress distribution within the teeth (Farah et al., 1973). Since then, many researchers have investigated the stress distribution in several restoration designs and dental materials. The occlusal load has been a subject of 3D FEA investigation by Hojjatie and Anusavice and Palamara et al. (Hojjatie and Anusavice, 1990, Palamara et al., 2000). Additionally, the influence of cement parameters such as cement microstructure, cement type, layer design, and margin design on the stress distribution have been defined by many authors (Shinohara et al., 1989, Kamposiora et al., 1994, Proos et al., 2002, Proos et al., 2003, De Jager et al., 2005).

Based on the ability of stress analysis and failure prediction by computational modelling, FEA has been considered as an effective tool for evaluation of all ceramic restoration failure (De Jager et al., 2005, Kayabaşı et al., 2006).

The core analysis of this study has been done on the seven solid volume components of the 3D FE model [crown, cement, dentine, pulp, PDL, spongy bone and trabecular bone]. Six of these components except the cement layer had

identical layering arrangements as the physical sample of the previously published study (Shahrbaf et al., 2013). The remaining layer [cement component] was virtually modified by FreeForm® technology in order to provide a layer of uniform thickness and offer a new arrangement of model compartments that have not been evaluated in the earlier study.

The generation of the uniform interface with FreeForm® software was hampered by some software related limitations. The first challenge was the limitation of adding the minimum thickness of the cement interface layer. The FreeForm® technology was incapable of generating less than a 180µm hole-free uniform layer. The second problem was that the entire cement interface thickness is 180µm without considering the ideal marginal thickness; that is, it was not reduced to a thinner thickness at the margins. Moreover, the steps of generating the optimum contact between the modified cement layer and the adjusting structures [crown - cement - dentine] led to a third problem. In this step, in order to establish the ideal contact between these layers [crown-cement], the cement layer should be added to the crown to be, by one unit and subsequently should be subtracted to eliminate any free spaces. This step should be confirmed to the [dentine- cement] layers as well. This process inevitably generates internal point and line angles on the internal surface that may act as a stress trigger area and compromise the crown structure.

It should be noted, this study focus at the components where the fracture is likely take place such as the crown and cement components.

Evaluating the stress state in the crown component according to the data obtained in [Table 7-2]; there is no significant change in the von-Mises stress state for the two models. There was a slight rise in the stress level in the occlusal surface of the modified crown (uniform cement interface) model in the loading points, but in the bulk of the crown there is no real change in terms of the stress state in both the models(Figure 7-14 and 7-21). The peak values of von-Mises stress within the crown of the (uniform cement interface) model was 691.31 MPa compared with the original (non- uniform cement interface) model's crown 590.5 MPa. The crown of the modified (uniform cement interface) model show slightly higher von-Mises stress values. The generated sharp internal line angles and the 180µm cement layer thickness at the margin could be considered as contributing factors of the high stress in the modified crown.

The internal and marginal thicknesses of the cement interface have been considered as contributory factors in the clinical durability of all ceramic crown. It has been well documented that the large cement marginal thickness could compromise the strength of the all-ceramic crowns. However, marginal adaptation range up to 100µm has been considered as clinically accepted (Qualtrough et al., 1993, Beschnidt and Strub, 1999, Mou et al., 2002, Reich et al., 2005).

The uniform cement interface layer of the modified model, the results of the peak values of von-Mises stress as shown in [Table 7-2] and [Figure 7-15 and 7-

20] indicated that there was no important difference in the stress state between the modified (33.05 MPa) and the original (non-uniform cement interface) model (24.69 MPa) under the distributed load. The slight difference of the calculated von-Mises stress values between the cement components of the modified and the original models could be attributed to the variability in thickness of cement at the margin. The original model has recorded the marginal adaption of 17.1µm buccally and 141.3µm lingually compared with the marginal high thickness of 180 µm for the modified model. The reason why it is higher thickness because, in FreeForm® CAD software the minimum thickness that could be generated with hole-free layer is 180µm.

Moreover, it is true that the original (non-uniform cement interface) model has larger discrepancy compared to the modified (uniform cement interface) model along the entire cement thickness, but the marginal adaption of the original (non-uniform cement interface) model is still clinically within the accepted range. While, the generated uniform cement thickness was 180µm for the whole length of the interface, which can be considered as ideal interface geometry, however, it is not the case in reality.

Considering the similarity in the stress states in the crown and cement components of both the models, the application of the concept of the uniform cement interface seemed promising. Since, the uniform interface cement doesn't appear to negatively affect the stress state in the crown and cement components in the modified model comparing with the original model.

The results data in [Table 7-2] have demonstrated a non-significant difference for the von-Mises stress state between the dentine of the original (non-uniform cement interface) and the modified (uniform cement interface) models. However, result predict that the slightly higher stress values demonstrated at the dentine of the modified model [46.91MPa] compared with [24.79MPa] for the original model could be ascribed to the straightening of the dentine-cement interface to be an analogue of the uniform cement layer. The straight walls of the dentine surface could possess sharp corners at the surface line angles which act as stress concentration and that is why the dentine of the modified model has shown high stress level.

Comparing the stress state in both models, the dentine seems to have effectively absorbed and redistributed the generated high stress and created a situation where the stress was distributed throughout the support structures in a benign manner (the PDL and the bone) [Figure 7-16 and 7-23].

For the other components such as [PDL, Spongy Bone, Trabecular Bone] the peak values of von-Mises stress were slightly higher in the modified model comparing with the correspondent components of the original model. However, this stress is not high enough to cause a distortion in the [PDL, Spongy Bone, Trabecular Bone] structures. Thus, the stress state analysis depending on evaluating the stress concentration area revealed that there is no significant influence of the modified cement design on the stress state of the PDL, the spongy bone and the trabecular bone components compared with the

corresponding components of the original model [Figure 7-17, 7-18, 7-19, 7-22, 7-24 and 7-25].

Intuitively, the support structures for the restored tooth complex such as the PDL and the bone are not expected to be a failure initiating sites. However, the stress in the support structures is more benignly distributed in the original model comparing to the modified model.

It can be seen, that the peak values of maximum principal stress of each component in the modified (uniform cement interface) model showed a very close trend to the analogue component of original (non-uniform cement interface) model [Table 7-3] and [Figure 7-26]. The peak values of maximum principal stress contradict the peak values of von-Mises stress in the cement, crown and dentine components. These components in the original model (non-uniform cement interface) components show slight higher maximum principal stress values in each component with its corresponding component of the modified (uniform cement interface) model. However, the stress state of maximum principal stress of the modified model indicated no significant difference in any component with its correspondent of the original component.

Based on the slight variation for both models in terms of the peak values of von-Mises stress and the peak values of maximum principal stress, it can be suggested that the modified (uniform cement interface) model would not be compromised by the modified uniform cement interface. Thus, the performance

of these two models (uniform/non-uniform) is not affected as the failure is likely to take place either in the crown or the cement.

The slight difference in the peak values of von-Mises stress and the peak values of maximum principal stress between the components of the two models could be attributed to the software limitation. The high cement thickness of the modified model has affected the reliability of the FEA result. Although, the high marginal thickness [180µm] of the modified model has affected the stress distribution, but a close stress values to the original (non- uniform cement interface) model can be still claimed.

Although limitations still exist, which can potentially have a slight effect on the resulted stress values; this study highlighted a more favourable distribution of the generated stress within the restored tooth when the cement interface is uniform compared with the non-uniform interface. Searching the literature revealed that there is no similar study has been conducted regarding the cement uniformity except a study by De Jager et al. where a stress analysis on the restored tooth with uniform cement was investigated (De Jager et al., 2006). However, in their study, they have used a FE model of a restored tooth with a uniform cement thickness of 140µm for the entire cement thickness and 25µm for the margin.

It can be speculated, that if the uniform cement interface with internal thickness of 100μm and marginal thickness of a minimum accepted thickness (50 μm) can be digitally achieved, the restored tooth components could show a more benign distribution of the generated stress.

As there is no similarity, thus, it is difficult to compare the presented study result with any other study. However, in this study the preliminary results obtained for this thickness of the cement interface may be used as a basic data starting point for a more detailed stress analysis at later stage.

7.8 Conclusions

With the limitations of the presented study, the following conclusions can be drawn:

1. With regard to the crown and cement components, the stress state in both the models is unaffected whether the cement layer is uniform or non-uniform.
2. With the limitation of the thickness of the uniform cement, the uniform cement demonstrated a benign stress distribution in all the model's components compared with the non-uniform interface model. Therefore, the null hypothesis that "The uniform geometry of the cement interface negatively affects the stress state in the tooth restored with all-ceramic crown" can be rejected.
3. The effective dissipation of the stress in the support structures of both the models indicates the functionality of the dentine structure in absorbing and conveying the generated stress effectively whether the cement layer is uniform or non-uniform.
4. The resultant data of the presented study could be considered as a promising starting point for further detailed investigation on the proposed correlation between the cement geometry [thickness and uniformity] and the stress distribution.

Effect of the interface geometry on the structural integrity of the restored crown-tooth complex

[A mechanical fatigue test investigation]

Presented at:

- The 7th International Association for Dental Research/Pan European Regional Congress (IADR/PER) in Dubrovnik, Croatia
    - *Effect of Interface Geometry On The Integrity Of Ceramic Crowns* (Al-Marza et al., 2014a)

8 Mechanical fatigue testing

This chapter covers objective 6 of the thesis.

8.1 Introduction

Dental ceramic restorations are structurally brittle, are susceptibility to tensile stress and as such are a category of materials that fail under time-dependent stress. Microscopic cracks act as a local stress concentration sites that cause the ceramic to manifest fracture at a stress significantly lower than its theoretical strength under a repeated load (Piddock and Qualtrough, 1990, Sadighpour et al., 2006). However, the ceramic crown should not be considered as a stand-alone entity but as part of a crown-tooth complex that is a multi-faceted compound structure, where a larger number of factors; both intrinsic and extrinsic to the restored tooth, all play a role in determining the overall structural integrity. It should be noted that some aspects of the compound system would act synergistically to improve the structural integrity, whilst others, if not carefully designed and matched may actually precipitate failure. Intrinsic features of the crown-tooth complex would include: The nature of the ceramic microstructure; the actual thickness of the ceramic; the interface dimensions and internal geometry; the elastic modulus of the cement and the supporting substrate (dentine or restorative material); the quality of the adhesion of the cement to the ceramic and supporting tooth substrate. Extrinsic factors to consider are mechanical, environmental and biological features of the mouth,

such as: The magnitude and direction of the applied loads, the level of periodontal and alveolar support for the tooth, the wetness of the oral environment, caries and biological biofilms.

Considering the role of the cement, there is evidence showing the influence of the cement film thickness on the fracture resistance of the all-ceramic crown (Prakki et al., 2007, Fleming and Addison, 2009). However, the full effect of the cement resin geometry in terms of overall thickness and dimension on the fracture resistance of the all-ceramic restoration has not been well established.

Thus, there is a distinct need for specific tests, prior to clinical trialling, to help better understand the mechanical behaviour and interaction of these factors (Kelly et al., 1996, Sadighpour et al., 2006, Rekow et al., 2011).

In-vitro testing of the strength of the crown-tooth complex can be undertaken as a static, progressive loading, test that will determine the ultimate fracture strength of the system or as a dynamic, fatigue, test that will reveal its behaviour under repeated loading. Strictly speaking, fatigue can be conducted in different load rate profiles such as static or dynamic fatigue profile. However, it is well documented that the behaviour of brittle structure under the cyclic loading is important and outperforms the static profiles (Yoshida et al., 2004).

It should be noted that neither of these tests, static or dynamic, are in any way analogous to real-life clinical performance, nor can the data be used to extrapolate real predicted survival of the restorations, but they will indicate the

probability of early failure and assist with the optimisation of the intrinsic factors as detailed above. Notwithstanding, we know that in order to approximate the laboratory mechanical model to the clinical situation, we need to carefully consider and match as many of the extrinsic variables as possible, such as the stylus contact to the specimen, the perfect cementation of the restoration to the substrate, the load application in a dynamic profile, the presence of a periodontal ligament and that the test should be conducted under a wet environment (Kelly, 1999, Anusavice et al., 2007, Zhang et al., 2013).

The polymer material AlphaDie® MF [Schütz Dental GmbH, Rosbach, Germany] was chosen as a substitute for dentine. The AlphaDie® MF material has an elastic modulus closely matched to that of dentine and has the ability to bond to the composite luting cement. It is widely used in the literature as dentine-like material (Kohorst et al., 2007, Sarafidou et al., 2012). However, it should be noted that AlphaDie® has a different structural design than dentine. Dentine is anisotropic by virtue of tubular form, while AlphaDie® MF is isotropic by virtue that it is a composite with evenly dispersed particles, which may lead to different mechanical behaviour under loading conditions.

Fatigue is a general term refers to strength degradation in an aqueous environment whereby ultimately the structure could fail under a repeated load, even it below the critical stress limit, as a result of progression of subcritical crack growth. The structural strength is negatively correlated with the

subcritical cracks when the stress level increases, resulting in an acceleration of the cracks progress, which leads ultimately to the failure. In line with the stated, the clinical evidence shows that the failure of dental prosthesis is not coming as a result of the acute incidence of overload rather than the repetitive stress that yield fatigue-related failure (McCabe et al., 1990a, Wiskott et al., 1994, Zhang et al., 2013).

Fatigue testing can be conducted in several ways; a direct method, which is called 'fracture mechanics method' by testing an induced crack object for investigation of crack growth and; an indirect method 'strength measurement techniques' that is dependent on measuring the strength of the object within the given time interval to evaluate the fatigue properties of the materials.

In order to obtain the most valuable data from fatigue testing, it is critical that we calibrate the test to the actual samples being tested. In this way, we need to know the maximum failure load for a fixed number of cycles (Fatigue limit) for the system and then the number of cycles that it will survive at that particular load (Fatigue life). Key to these, is also the frequency of load impact, the immersion in water at a particular temperature. The staircase methodology [fully described in section 2.12.1.2] is considered as the most appropriate technique used for evaluating the fatigue behaviour of the ceramic structure.

This study aimed to evaluate by the stair case methodology the fracture resistance of the pressed and machined all ceramic crowns as a function of the nature of the cement interface geometry.

8.2 Aims

To evaluate, by means of mechanical fatigue testing, the effect of the cement interface geometry on the structural integrity of the restored tooth-crown complex.

8.3 Objectives:

1. To create different crown-tooth models, that will yield different interface geometries (as shown in Chapter 5), using 3 different ceramic fabrication techniques as the following:
    a. Machined CEREC crowns: *Machined CAD-CAM group*.
    b. 3D wax-pattern printed and subsequently pressed crowns: *Digital Pressed group*.
    c. Manual waxed patterns and subsequently pressed crowns: *Manual Pressed group.*
2. To determine the Fatigue Limit of the adhesively cemented ceramic-crown tooth complex.
3. To determine the Fatigue Life of the adhesively cemented crowns under fatigue dynamic loading in the chewing simulator.

8.4 Null hypothesis

1. The Machined and Pressed (digital and manual) all-ceramic crowns will manifest the same fracture resistance and fracture mode under the effect of cyclic fatigue loading.
2. The nature of the cement interface geometry of the machined and pressed (digital and manual) ceramic fabrication techniques will not have any effect on the fracture resistance of the restoration under fatigue loading.

8.5 Materials and method

8.5.1 Sample preparation

The protocol steps of sample preparation [tooth preparation, master die duplication, crown fabrication techniques and cementation technique] were the same as those described in chapter 5.

The ceramic crowns were etched with IPS ceramic etching gel [hydrofluoric acid] for 20 seconds and subsequently rinsed with water, in accordance with the manufacturer's guidance. Although the tooth is polymer-based, it was treated with phosphoric acid [37%] for 20 seconds and subsequently rinsed with water, to remove any biofilm and grease residue from the surface. The crowns were subsequently cemented with Variolink II [Variolink II, intro pack, Liechtenstein, Ivoclar/Vivadent, LOT R72873, Exp. 2014-08].

In order to test ceramic crowns with different thickness and geometries of the cement interface and according to our findings based on cement interface thickness presented in chapter 5, three out of the five ceramic fabrication techniques were used: (i) CEREC as machined group, (ii) 3D printer as a digital-designed and pressed groups and (iii) manual pressed as an entirely manual process with hand waxing and pressing [Figure 8-1]. The interface features of these crowns were: (i) Thick and non-uniform interface created by a machined crown (CEREC®) (mean 157µm ±36); (ii) thin thickness and most uniform interface created by a conventional pressed crown (mean 114µm ±19)

and; (iii) thinnest and uniform interface created by the 3D printer-pressed crown (mean 81µm ±26) [Figure 8-2]. The lithium disilicate glass ceramic IPS e.max® CAD (block shade HT A3, Ivoclar Vivadent, Germany) and IPS e.max® Press (ingot shade LT A3, Ivoclar Vivadent, Germany) were selected for fabricating the crowns. [Table 8-1] shows the basic physical properties of IPS e.max® Press and IPS e.max® CAD glass ceramic.

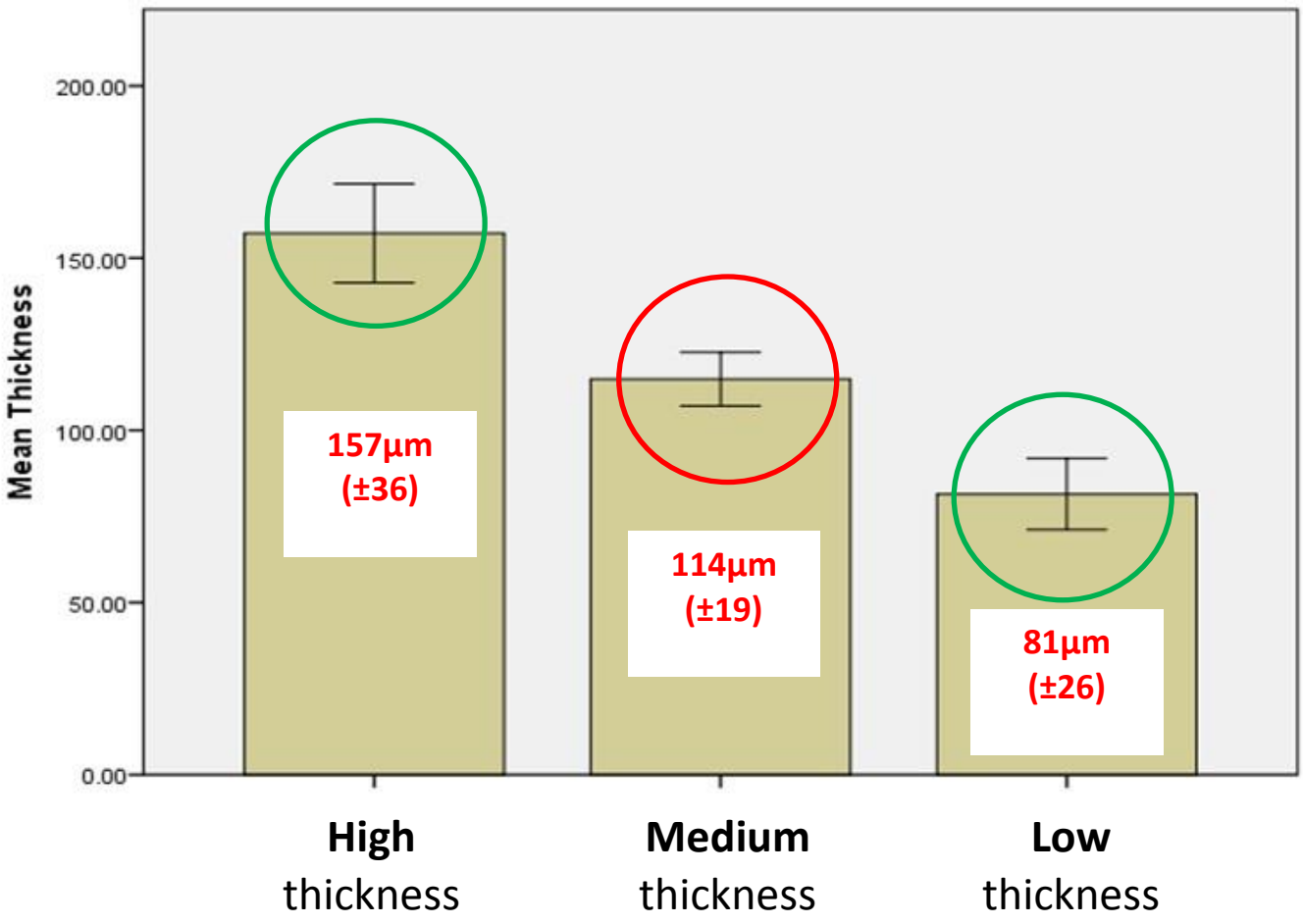

Figure 8-1: Mean (3D) and SD cement thickness of the test groups

Table 8-1: Physical properties of IPS e.max® Press and CAD ceramic [the data collected from Ivoclar/Vivadent websites]

physical properties	IPS e.max® Press	IPS e.max® CAD
Flexural strength (biaxial) [MPa]	360	400
Fracture toughness [MPa $m^{0.5}$]	2.25	2.75
Modulus of elasticity [GPa]	95	95
Vickers Hardness [MPa]	5800	5800
Chemical solubility [µg/cm^2]	40	40

8.5.2 Periodontal Ligament (PDL) simulation and samples mounting

The alignment of the sample was achieved by placing the tooth in an inverted vertical direction (upside down) according to the long axis of the tooth by using the dental surveyor [Figure 8-3]. The prepared typodont tooth was painted evenly with a thin layer of die separator and embedded upside down till 2 mm above the CEJ in a square container filled with Dublisil® 15 A and B (Addition-vulcanising vinyl-polysiloxane, Dreve Dentamid GmbH, Germany) [Figure 8-4]. Thereafter, a cylindrical copper specimen holder was used for the root of the tooth located in the centre of the cylinder base [Figure 8-5]. The two bases were

surrounded by a large square base container and then filled with Dublisil® 15 A and B [Figure 8-6].

Accordingly, each sample was put in the first mould and inserted in the second mould with the cylinder base to be filled with polyurethane-based resin material (AlphaDie® MF, Schütz Dental GmbH, Rosbach/Germany). After the recommended setting time of AlphaDie® MF, the tooth was gently removed from the cylindrical base in order to leave a space to be occupied later by PDL simulator impression material [Figure 8-7].

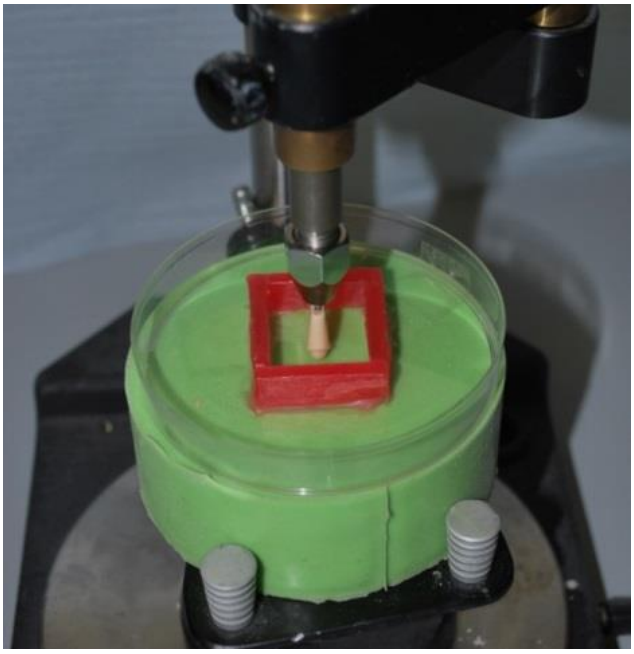

Figure 8-2: Alignment of the tooth in the dental surveyor

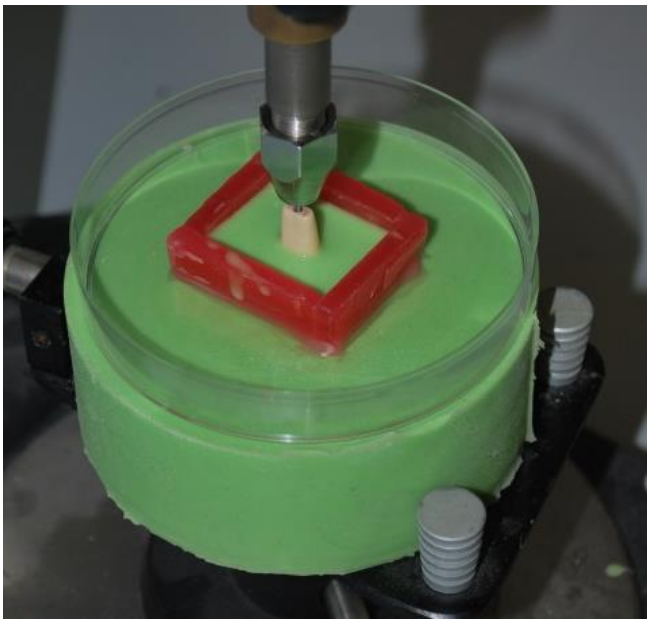

Figure 8-3: Covering the coronal part of the sample by the Dublisil 15 A and B material

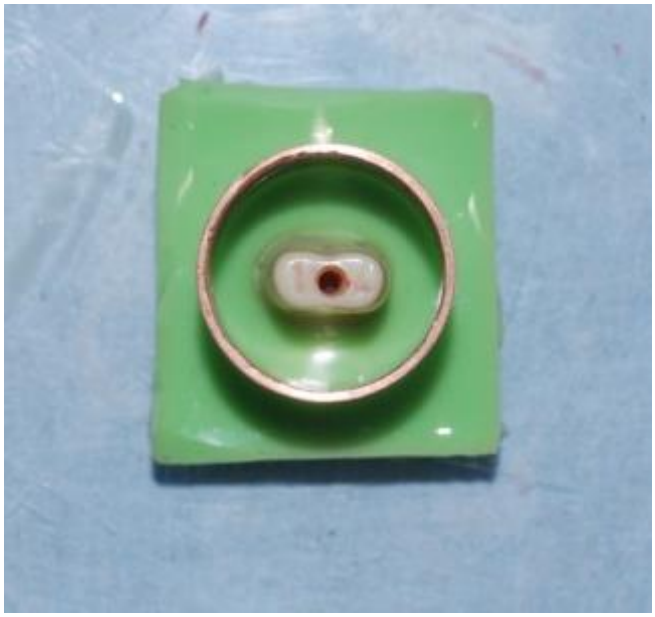

Figure 8-4: the metal base cylinder covered the root of the sample

Figure 8-5: the mould of the ideal alignment of the samples

Figure 8-6: Actual sample in the base

According to the study by Brosh et al., the light body silicone impression material, President Plus® ® light body [Coltène, Altstätten, Switzerland] proved as the most effective PDL simulation material due to its matched resilience to natural PDL. The pre-created socket was injected with President Plus ® light body and the tooth was immediately re-inserted into the socket. In this experiment, a space of 200µm thickness of the light body impression material was replicated to allow for 50µm movement in order to approximate the normal physiological tooth movement of Grade Zero tooth mobility [figure 8-8]. Subsequently, after the recommended setting time, the excess light body material over the socket was cut off with a surgical scalpel blade (Wolfart et al., 2007, Brosh et al., 2011).

Figure 8-7: PDL simulation
(tooth crown embedded in acrylic for this specimen to facilitate sectioning that enables visualisation of the tooth and PDL in cross-section)

8.5.3 Mounting the specimen in the fatigue testing machine

The fatigue machine tester has been constructed and used in another published studies (Padipatvuthikul and Mair, 2008, Mair et al., 2011). This machine simply works by applying an axially aligned load onto the crown of the tooth specimen. The load is generated from the weighted metal discs from one side and transferred through a leverage arm to the indenter at the opposite end of the arm. The following parameters can be adjusted on the machine: The magnitude of the load (between 4Kg to 80Kg), the size and point of application of the load, the directional vector of the load, the frequency of the load and can be undertaken in a dry or temperature controlled wet environment. The machine has an automatic cut-off so that it will cease to apply the load upon fracture of the specimen, thus enabling observation of the fracture specimens relating to the moment of fracture

The fatigue machine tester has five separated stations that enable testing five specimens independently and simultaneously. The design of the mounting base was modified to allow for the movement of the specimen in the all directions in order to adjust the contact point of the indenter to the occlusal surface. A customised stainless-steel indenter with a spherical tip-profile of 4.25mm diameter was used as this creates two equidistant occlusal contacts on the cuspal inclines of the occlusal surface (Tsitrou et al., 2010). This creates an axial compressive load on the occlusal surface of the tooth. A disc cushion of light-body silicone was placed between the indenter point and the load transfer arm in order to dampen the impact of the load on the specimen, in a manner analogous to the PDL of the antagonist tooth in the mouth [Figure 8-9].

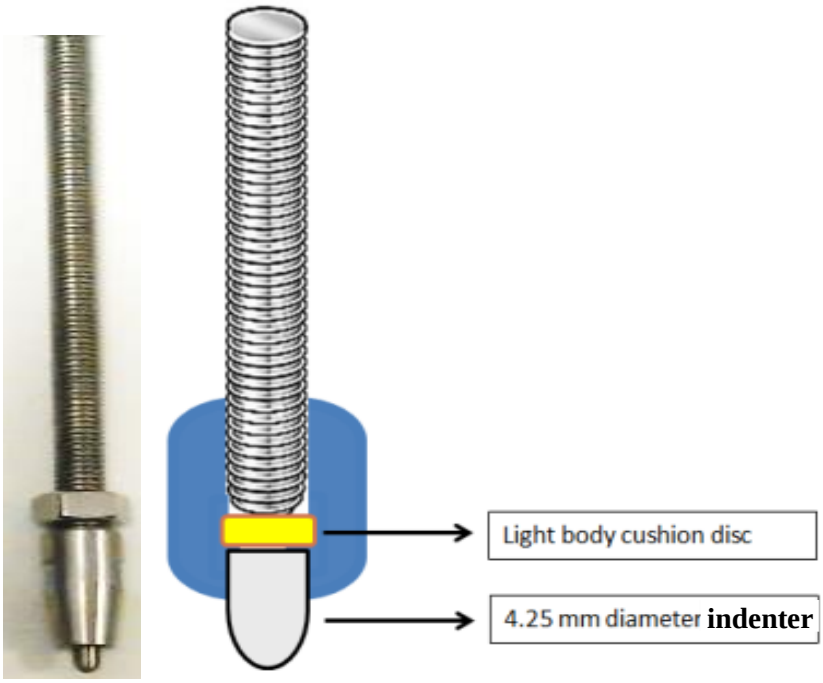

Figure 8-8: Indenter design

Each station's arm is connected to an independent cycle counter that can stop counting automatically when the sample fractures. The cycle frequency was set at 60 cycles/minute. Throughout the experiment, the specimens were permanently immersed in recirculating heated water at 37C˚ [Figure 8-10].

Figure 8-9: Fatigue machine tester

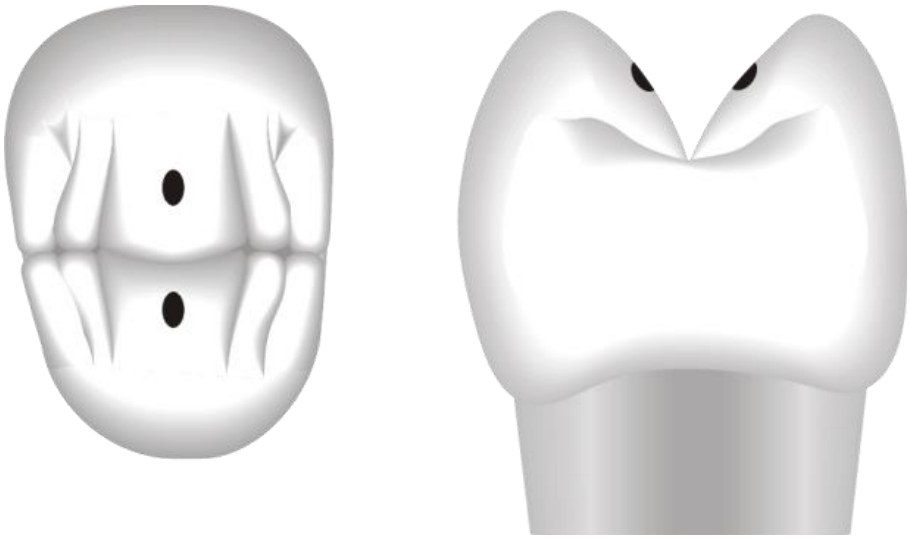

Figure 8-10: Diagrammatic representation of the occlusal contact points of the indenter on the tooth surface.

The contact points of the indenter on the tooth were confirmed with occlusal indicator paper for all specimens as per the diagrammatic representation shown [Figure 8-11]. The indenter contacted the occlusal surface of the tooth in the lingual inclination of the buccal cusp and buccal inclination of the lingual cusp.

8.5.4 Load cell calibration

A highly sensitive force sensor device was used to calibrate the load [LOAD CELL model TR150, version V1.10, UK]. The load cell was centred in the mounting base of one station in the exact potion where the actual specimen should to be placed [Figure 8-13]. To calibrate the load, discs of 0.5Kg were placed in a sequential and incremental manner and the force in Newton was

recorded [Table 8-2]. The load/force calibration was taken over two measurements for each load.

Figure 8-11: Load weight disc of 0.5 Kg

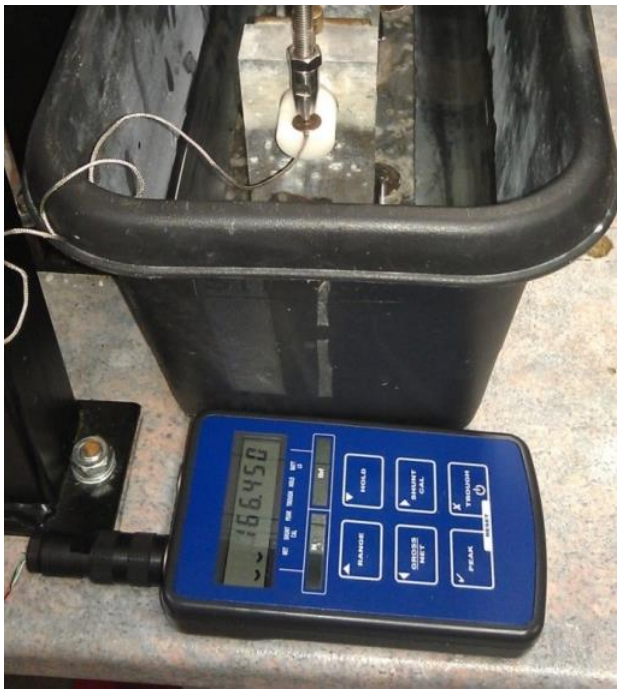

Figure 8-12: Force sensor device

Table 8-2: Load calibration

Load	Net (Newton)
zero load (just the load of the arm)	180
0.5 Kg	215
1 Kg	250
1.5 Kg	284
2 Kg	320
2.5 Kg	355
3 Kg	390
3.5 Kg	420
4 Kg	453
4.5 Kg	487
5 Kg	522
5.5 Kg	553
6 Kg	589
6.5 Kg	621

8.5.5 Fatigue limit experiment

Evaluation of the fatigue limit by the staircase method (as described by Draughn in 1979) has been fully described in [section 2.13.1.2]. 21 teeth were restored with full-coverage [CEREC] machined crowns that were adhesively cemented, as previously described. However, a hypothesis has been considered that the crowns fabricated by the two processing methods of lithium disilicate ceramic [machined and pressed] would be quite similar regarding the endurance limit if they cycled for short period.

According to the currently accepted testing variables of the staircase methodology, the samples were cycled with an assigned load for 5000 cycles in a water bath at 37C˚ at a rate of 60cycles/minute. The experiment conducted by cycling the first sample with 3 kg and then incrementally adding 0.5 Kg loads for a fresh specimen every time. The fatigue behaviour of the samples during the fatigue limit test is shown by [Figure 8-14].

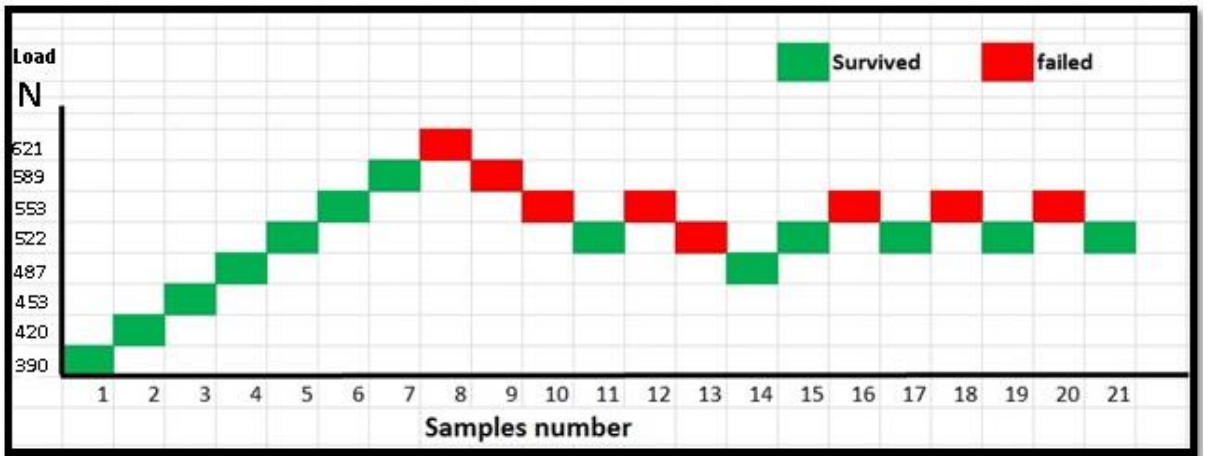

Figure 8-13: Staircase for fatigue limit of CAD/CAM specimens

8.5.6 Fatigue life experiment

When the fatigue limit has been evaluated, a load value for fatigue life can be defined. Generally, the load for testing the fatigue life would be close to the fatigue limit load. In the fatigue limit experiment the maximum load that the sample had survived for 5000 cycles was 5Kg, therefore, the load of the fatigue life would be reduced by 1Kg. Thus, the samples would be cycled to failure at a load value of 4Kg that computes to 453N according to the load calibration test [Table 8-2] at a frequency of one Hertz (one impact/second).

20 samples per group were assigned. Simultaneously, five samples of the same group were placed in the five stations of the machine and cycle to failure under the assigned load. Following the fracture failure of a specimen the counter would stop and the number of cycles was recorded. At this point, the fractured components were retrieved and carefully bagged for later fractographic analysis. A fresh specimen would be placed, the counter reset to zero and the experiment re-commenced.

8.5.7 Fracture mode

In order to investigate the differences in the fracture mode of the specimens under the fatigue load, the code of the fracture was recorded for each fractured samples (Burke, 1999). The fractured sample was dried and the fracture parts were visually inspected and recorded. The assessment of the fracture extension was followed Burke's classification for the code of fracture [Table 8-3].

Table 8-3: Burke's classification of codes of fracture

The code	Characterization
Code 1	Minimal fracture or crack in crown
Code 2	Less than half of crown lost
Code 3	Crown fracture through midline: half of crown displaced or lost
Code 4	More than half of crown lost
Code 5	Severe fracture of tooth and or crown

8.6 Results

8.6.1 Fatigue strength

8.6.1.1 Fatigue limit

Through the application of the staircase methodology, the fatigue limit load value was defined when the samples showed a constant rate of survivability under a specific load. The samples in the fatigue limit experiment have shown a failure at a level of 5.5Kg. While, at a level of 5Kg the samples survived the load for the 5000 cycle [Figure 8-14]. Thus, a 5Kg load could be defined as a fatigue limit load as several samples have showed a constant success rate at that level. Accordingly, the samples would be expected to survive more cycles if they are subjected to a load close or slightly lower to the fatigue limit load

value. Thus, the fatigue life experiment was setup at load of 4kg [453N] and to be run for 1,250,000 cycles.

8.6.1.2 Use of Weibull statistics for probability distribution

Prediction of the ceramic strength could be achieved by adopting the probability distribution, which can be considered as the best way for effectively describing the variation in the life expectancy. Although several ways have been adopted for the probability distributions, Weibull analysis has been shown by the literature as the overwhelming choice for predicting the fracture strength of the ceramic and composite materials (Baran et al., 2001, Thomason, 2013).

8.6.1.3 Fatigue life

The fatigue life experiment translates the survivability of the sample based on the number of cycles to failure. In order to apply Weibull analysis, special analysis software [Reliability and Maintenance Analyst, version 4.5.9, Novell, USA] was used. Using this software, the two Weibull parameters [α, β] could be obtained. The mean number of the survived cycles would be indicated by the α parameter. While, the failure interval in relation to the mean could be indicated by the β parameter [scale parameter] or some time called Weibull modulus, as following:

β <1 indicates an early failure in relation to the mean

β =1 indicates a regular intervals of failure throughout the experiment time

$\beta > 1$ indicates a late failure interval

Basically, the higher β value means the more reliable the sample as it indicated the higher ratio of late to early failure.

To simplify the Weibull statistics concept, if the [α, β] data were plotted, the β would determine the slope of the line and the α indicates how far the line is located to the right [further to the right = greater number of the survived cycles]. The more reliable sample means high β value with a very upright line. Conversely, the sample with low β value shows slop line and that mean less reliable. The relationship between these two parameters is shown in [figure 8-15].

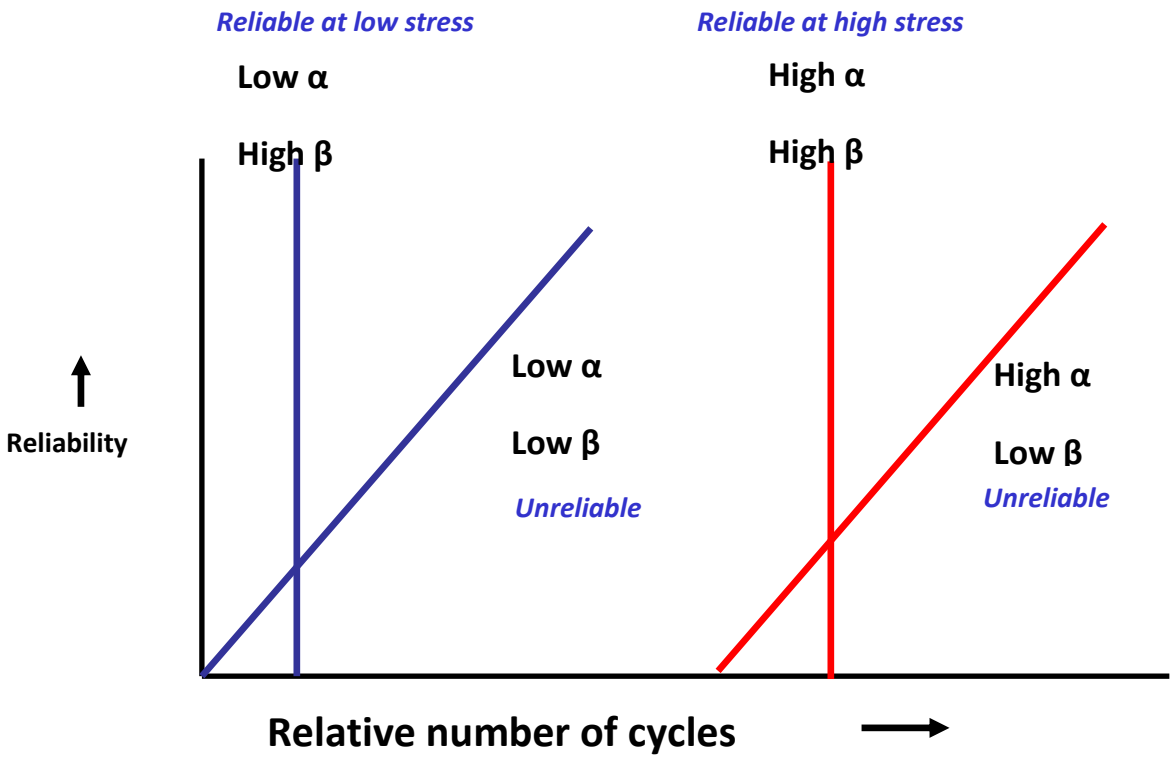

Figure 8-14: The relation of β to α parameter in Weibull analysis

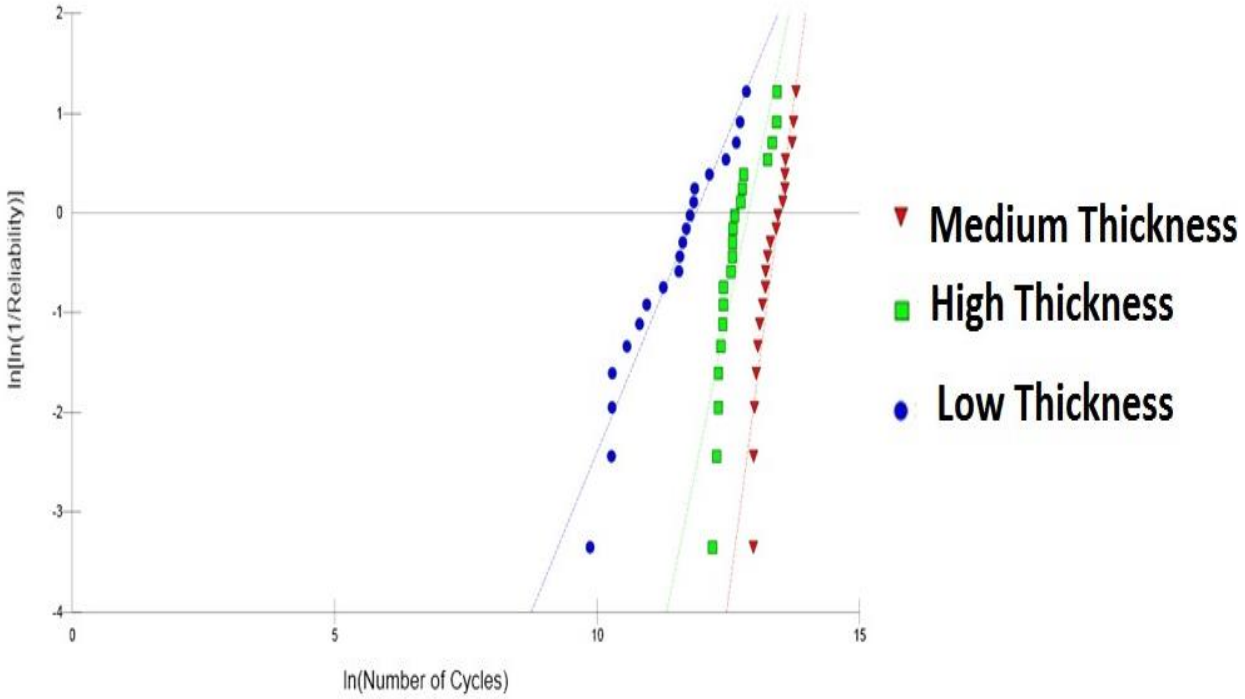

Figure 8-15: Weibull probability plot of the all the groups at 453N load

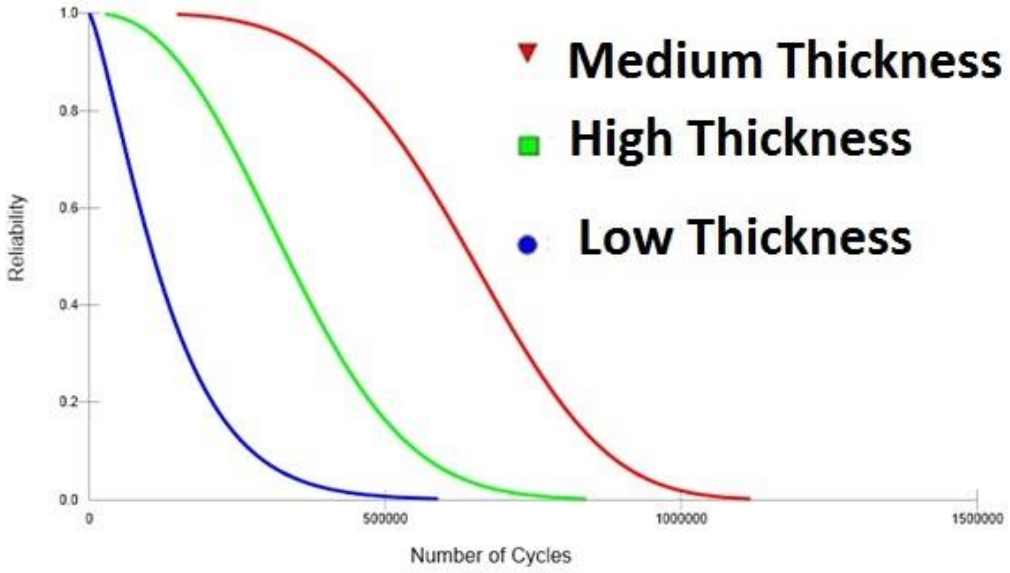

Figure 8-16: Weibull maximum likelihood comparison of the all the groups

In order to investigate the level of the significance between the mean values of the survived cycles between the three groups, at an alpha level of 0.05, a one-way ANOVA (Analysis of variance) test was carried out using (IBM SPSS statistics version 20).

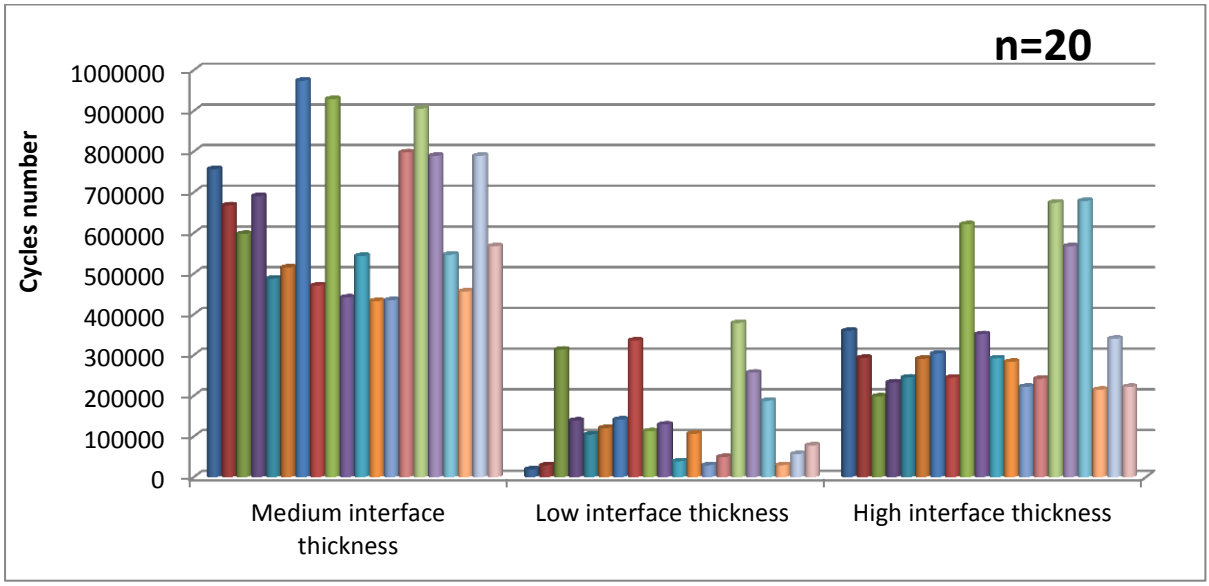

Figure 8-17: Number of cycles at failure (columns refer to different specimen)

Table 8-4: The maximum and average of the survived cycles for all the groups

Groups	**Maximum**	**Average**
Medium interface thickness	974286	639857
Low interface thickness	378945	132882
High interface thickness	678660	343864

Table 8-5: ANOVA test for all the groups comparing the survival cycles

ANOVA					
Cycles					
	Sum of Squares	**df**	**Mean Square**	**F**	**Sig.**
Between Groups	2.594E+12	2	1.297E+12	56.898	0.000
Within Groups	1 .299E+1 2	57	22797978312		
Total	3.894E+1 2	59			

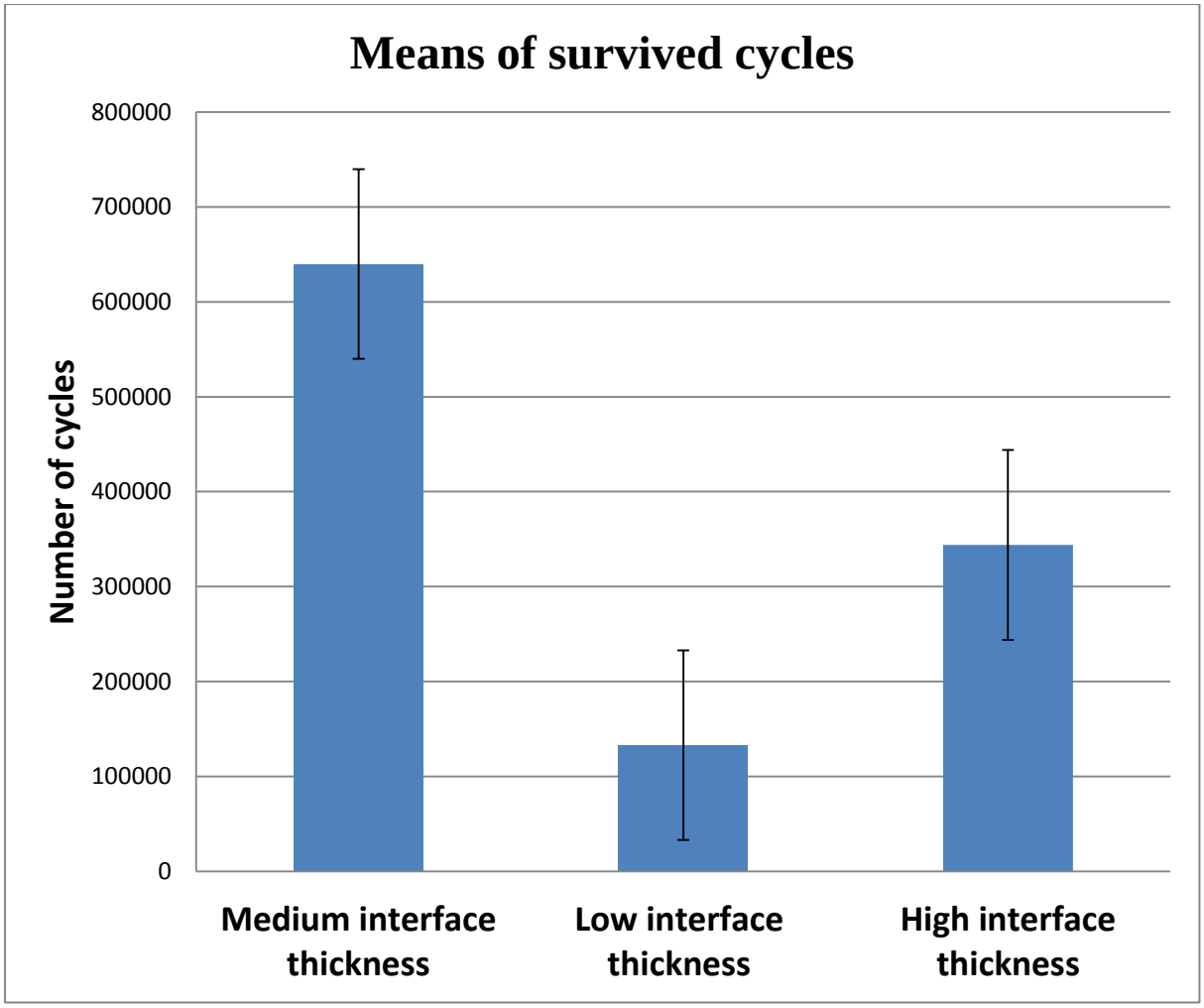

Figure 8-18: The mean values and SD of the survived cycles for all the groups

8.6.2 Fracture mode analysis

Each fractured sample has been examined and the code of the fracture is recorded according to the Burke's classification for codes of fracture [Table 8-6].

Table 8-6: Mode of fracture in the group samples

The code	Medium interface thickness	Low interface thickness	High interface thickness
Code 1	0	1	0
Code 2	9	3	2
Code 3	7	2	5
Code 4	4	10	8
Code 5	0	4	5

Figure 8-19: Fracture code 2

Figure 8-20: Fracture code 3

Figure 8-21: Fracture code 4

‘’One-way ANOVA on ranks’’ for non-parametric data analysis ‘’Kruskal-Wallis’’ was applied to determine if there are statistically significant differences among groups’ samples regarding the fracture mode recorded [Table 8-8]. The statistical analysis of the code data has demonstrated a significant difference between the three groups [$p<0.05$].

Table 8-7: Kruskal-Wallis Test showing the mean rank of fracture mode for each group

Ranks		
technique	N	Mean Rank
Medium interface thickness model	20	19.80
Low interface thickness model	20	35.03
High interface thickness model	20	36.68
Total	60	

Table 8-8: Kruskal Wallis test for the fracture mode for each group of samples

Test Statistics	
	code
Chi-Square	12.309
df	2
Asymp. Sig. [*P-value*]	0.002

The mean difference between groups is significant at the 0.05 level. ($p<0.05$)

8.7 Discussion

This investigation evaluated and compared the fracture strength of 3 types of all ceramic crowns (the crowns divided according to their cement interface geometry) under the fatigue loading. Fracture and fatigue behaviour of all ceramic crown-tooth complex could be affected by several variables. Thus, to obtain a high reliability of predicting the long term success of dental restoration, simulation of the oral environment was designed by utilizing the chewing simulator (Rosentritt et al., 2006, Heintze et al., 2011, Yildiz et al., 2013).

In order to minimise the variables of using natural tooth it was designed to construct the abutment from the polyurethane-based resin (AlphaDie® MF, Schütz Dental GmbH, Rosbach, Germany).

The all-ceramic crown fabrication techniques involved in this study were based on the different cement interface that would be generated by each fabrication technique, as detailed in chapter 5.

It is well documented from the retrieved clinical data that the initiation and propagation of the crack due to the fatigue effect of the masticatory force is supposed to be the common case for the clinical failure of the all-ceramic restoration (Zahran et al., 2008). In this study, the cyclic fatigue loading with the most of the oral environment factors has been considered in order to compare the fatigue strength of the samples.

Since, the literature is inconclusive regarding the stress generated from biting forces, the stress or the load values for simulating the natural biting force on the

dental restoration were used in different values according to the ways of the measurement. 300N is a commonly used load value for the average mastication force subjected to maxillary premolar in some studies (DeLong and Douglas, 1991, Kelly, 1999, Craig R, 2006, Kassem et al., 2012, Kawai et al., 2012).

The calculated load for fatigue life experiment was based on the load value of the fatigue limit experiment. The estimated fatigue life load was 453N, which is higher than the average load on the premolar area that has been recorded in other studies.

The statistical analysis by ANOVA one-way test of the result [table 8-5] showed a significantly higher difference between the three groups. Since, the test and the sample parameters were fixed for all the groups, the possible explanation of this clear difference between groups could be related to the differences in the cement geometry.

Considering the **α** and **β** parameters of the Weibull analysis, samples of the medium interface thickness were found to be more reliable than the other two groups [Figure 8-16]. The scale [β] parameter of the medium interface thickness group shows more upright line slope and further to the right side than the others [figure 8-16]. Although, the group of the high interface thickness shows less reliability than the medium interface thickness group, but still more reliable than the low interface thickness group [figure 8-16].

The low reliability of the low interface thickness group in surviving the load could be related to the very thin thickness of the interface. In our finding in chapter 5, the average interface thickness of the 3D printer crown (low interface thickness group) was (mean 81µm ±26) especially at the mesio distal measuring direction. Although the low interface thickness group samples show more uniform interface film thickness compared with the high interface thickness group samples (mean 157µm ±36), the low film thickness of the low interface thickness group samples may contributed in decreasing the fracture strength under the repetitive load.

The study conducted by Prakki et al. has suggested that the higher film thickness of the uniform cement interface could increase the fracture resistance of ceramic disc when the ceramic thickness below 2mm (Prakki et al., 2007). The maximum thickness of the ceramic crowns used in this experiment was fixed to be 1.5mm. Therefore, the thin film thickness of the low interface thickness group samples has correlated negatively with the fracture strength. Thus, our finding regarding the correlation between the interface thickness and the fracture strength of the ceramic restoration is in accordance with Prakki study.

Moreover, the low fracture strength of the low interface thickness group could be related to the resin cement physical properties. The high polymerizing shrinkage stress even over a very small area of the cement interface could contribute in a cement crack generation that is liable to create stress

concentration leading to failure of the restoration under occlusal force. A reasonable standard film thickness (50-100µm) may have favoured greater absorption of the stress produced by the resin cement polymerization shrinkage that contributes to a substantial stress relief at the resin cement interface (Choi et al., 2000, Braga et al., 2002, Spohr et al., 2013).

The medium interface thickness (mean 114µm ±19) group samples have manifested a higher fatigue resistance by surviving a maximum of 974,286 cycles with an average was 639,857 cycles. The high interface thickness (mean 157µm ±36) group samples showed less reliability compared to the medium interface thickness group samples by surviving a maximum of 678,660 cycles with an average of 343,864 cycles.

A possible explanation for the difference in the survival between the medium interface thickness group samples and the high interface thickness group samples could be related to the uneven stress distribution within the ceramic structure due to the uneven cement thickness and geometry. According to our finding in chapter 5, regarding the cement interface thickness, the machined sample (the high interface thickness group) shows higher discrepancy and thickness above the accepted standard compared with the pressed sample (the medium and uniform interface thickness). It has been suggested that the stress distribution in a non-uniform cement interface will vary and the adhesive cement strength might be reduced. The stress distribution could be affected by the uneven cement film thickness and that liable to affect the structural integrity

of the restored tooth. The stress distribution in the non-uniform interface could affect the bonding surface by increasing the maximum shear stress to values exceeding the bond strength of the cement layer to the restoration and tooth walls (Mou et al., 2002, De Jager et al., 2005). Thus any defect in the cement interface due to the stress generation could impair the integrity of the system.

It is well established through the examination of the clinically failed all-ceramic crowns that the failure is initiated from the interface surface where the micro flaws exists and stress generated as an opposed to the occlusal surface damage (Chen et al., 1999, Kelly, 1999). It has been shown that the CAD/CAM fabrication technique could induce subsurface defects. Process dependent micro-defects that could be induced by the bur's grinding action of the CAD/CAM machine might be contributed in weakening the ceramic structure. (Sindel et al., 1998).

Moreover, the higher life time achieved by the manual pressed (the medium interface thickness) samples could be related to the cement interface nature. According to our finding in Chapter 5, the manual pressed samples showed an ideal standard uniform cement interface thickness (mean 114µm ±19). The uniform interface geometry could be an explanation of the benign or an even stress distribution within the restored tooth. Since, all the parameters were fixed for both (manual pressed [medium interface thickness] and machined [high interface thickness]) groups, the non-uniform interface thickness is the most

likely cause for uneven distribution and undesirable stress concentration that led to a short life time of the machined samples.

Another possible explanation of the high fracture resistance of the manual pressed crowns could be related to the technical lab steps involved. The single professional technician with an expert technical skill who fabricated the crown could contribute effectively in reducing the process-dependent defects in the ceramic structure during the pressed technique. The spacer that has been used for generating the interface space (Pi-Ku-Plast HP 36, Bredent medical GmbH & Co.KG /Senden/ Germany) has reported to have a low [less than 0.036%] polymerising shrinkage. The low polymerising shrinkage of the spacer could contribute effectively in keeping the generated interface space as a uniform and that in turn increase the performance of the ceramic crown.

There is no study in the literature that compares directly the fracture strength of the pressed against machined lithium disilicate all ceramic crowns. Yildiz et al have reported that the Onlays fabricated by pressed technique showed higher fracture resistance than Onlays fabricated by CAD CAM technology (Yildiz et al., 2013). Considering the ceramic fabrication technique, the finding of this study is in accordance to the present study.

The Maximum Likelihood Estimation [MLE], which depends on the given data of the Weibull parameters has indicated that the samples with the medium interface and uniform thickness could survive even more cycles compared with the other [Figure 8-17].

Taking the result of the survived cycles one step further, [Figure 8-18] showed a considerable variation in the survived cycles between samples over each group and cross the groups. The most likely cause of this observed variation could be related to the variability of the flaws distribution within the ceramic structure.

It has to be considered that no sample has survived the proposed cycles' number [1,250,000 cycles]. The reasonable explanation is the adopting load of 453N is higher than the clinically recorded bite load [300N in premolar segment] has made the test as an aggressive load cycling test [heavily stressing the entire crown], which could be considered as the limitation factor in this study.

This test was an aggressive approach for evaluating the fracture strength of the samples. Accepting this limitation, the results of this study could be accepted for these 3 groups since all the other testing conditions and parameters were fixed for the all samples.

It has been noted by Yildirim et al that the selection of the abutment or the supporting materials has a substantial effect on the fracture strength of the ceramic restoration(Yildirim et al., 2003). The statistical analysis of the code data of the fracture mode has shown a significant difference between the groups. The variation of the mode of the fracture could be related to the mechanical properties of the AlphaDie®. Although Alpha die is used in many other studies and has properties closely match to dentine, it lacks the structural integrity of dentine. Alpha die is a composite material that is isotropic, while dentine is an anisotropic in its behaviour. While, we can match the properties in

terms of elastic modulus of the two materials, but not match the structural behaviour of the materials, because there is a fundamental differences in the internal structure of the materials that contribute to the different mechanical behaviour under the load. Hypothetically, the perfect replacement will be using materials closely match to dentine properties but in the same structure of dentine.

8.8 Conclusions

Within the limitations of this study the following conclusions were drawn:

1. There is a relationship between interface thickness and structural integrity.
2. Uniformity of the interface geometry is an important determinant of the structural integrity.
3. The crowns with the medium cement interface thickness and most uniform cement interface exhibited large Weibull modulus compared with low and high cement interface thickness of the other tested groups and that implies greater clinical reliability for the crown with this cement interface features. Thus, the hypothesis of ‘’The Machined crown with thick/high discrepancy interface and the Pressed crown with thin/uniform interface all-ceramic crowns manifest the same fracture resistance and fracture mode under the effect of cyclic fatigue loading’’ could be rejected.

4. The non-uniform interface dimension and the proposed production of strength-limiting surface flaws of the CAD/CAM fabrication technique increased the failure rate of the crowns under the cyclic loading.
5. The lowest Weibull modulus and high failure rate were recorded with the thinnest and uniform cement interface crowns [the 3D wax printed and pressed crown group]. Therefore, to optimize structural reliability of this type of cement interface profile, more attention should be paid to setup the thickness of the interface within the reasonable standard (50-100µm).

Therefore, the null hypothesis that 'The nature of the cement interface geometry of the two ceramic fabrication techniques will not have any effect on the stress distribution and fracture resistance of the restoration under fatigue loading' can be rejected.

Effect of the interface geometry on the stress distribution of the restored ceramic crown-tooth complex
An FEA investigation

The work of this chapter has been submitted for the ConsEuro 2015 Conference at King's College London Dental Institute, London 14 – 16 May 2015.

9 FEA of Pressed VS Machined crown

This chapter covers objectives 7& 8 of the thesis.

9.1 Introduction

In the 1970s, Farah et al pioneered the numerical evaluation of the stress distribution in dentistry. This has continued to evolve into sophisticated Finite Element Analysis (FEA), leading to greater accuracy and resolution in stress modelling through dental biomechanical structures (Farah et al., 1973, Shetty et al., 2010, Chen et al., 2014).

The underlying principle of FEA is to simplify a complex structure into discreet defined elements that can be attributed with specific physical and mechanical properties, known as finite elements. The elements are interconnected via linking nodes to form a mesh of polygon shapes. In principle, the smaller the elements, the greater the accuracy of the individual simulated behaviour of each individual element as it is simulating a smaller component of the real structure. However, this increase in accuracy and resolution at a local 'element' level is potentially negated by the complexity of mapping and computing the behaviour of a larger mesh model made up of smaller and more complex polygon shapes with many thousands of elements. Thus a simple mesh model of simple polygon shapes (e.g.: triangle, tetrahedral) with large elements is easy to design and compute, but will provide low resolution data; whilst a complex FEA mesh model made up of small elements in multi-sided polygon shapes (e.g.:

decagons, dodecagons) has the potential for greater accuracy and resolution but is significantly more complicated to map and compute with increased levels of error. The challenge for the FEA scientist is finding the correct balance between the two, which is towards the most complex and potentially most accurate. Establishing this balance, between mesh complexity and computational capability, is referred to as convergence analysis; which is further described in the methodology of this section.

Once a mesh has been created, the elements can be programmed with the properties of the structure it is modelling, such as compressive strength, tensile strength, yield strength, elastic modulus and Poisson's ratio. In this way, the reaction of the structure to the application of certain loads can be determined. Thus, by calculating the deformation of each element [stress and strain], the deformation of the whole elements of the structure can be evaluated. When there is load application, an internal stress or strain will be generated in the loaded body. The shape of the body and the stiffness distribution would effectively influence the stress distribution within that body (Goetzen et al., 2003).

Potentially, a realistic picture of the biomechanical stress/strain behaviour details of the structure subjected to the load could be full acquisition by FEA result. Therefore, the FEA results can be effectively interpreted under a basis of

stress concentration points. These points are important as they work as a predictor for the most likely failure imitation site in the loaded structure.

FEA can describe the stress state as a form of stress clouds distributed in the examined body structure. The stress clouds are represented either as a von-Mises stress, which is an equivalent combination of compression, tensile and shear stresses or as a maximum principal stress that can be considered as only a tensile stress (Hamrock et al., 1999, Lin et al., 2001a, Pegoretti et al., 2002, Eraslan et al., 2009).

The analysis of the stress distribution enables the prediction and understanding of the mechanical failure behaviour of the complex dental biomechanical system and also helps to revise and optimise structures for mechanical experimentation prior to in-vivo testing (Della Bona et al., 2013).

In the complex compound dental biomechanical structure of the tooth + cement + ceramic-crown, the interface dimensions [thickness and uniformity] and physical properties are considered as a key determinate of its mechanical behaviour (IWerner, 1998, Malament et al., 2002, Ausiello et al., 2004).

The influence of different cement interface thicknesses [25 and 100μm] on the stress state of the ceramic crown-tooth complex has been examined by Kamposiora et al using the FEA. This study was accomplished by using a simple 2D FEA model [300 elements and 500 nodes] of the lower premolar and

employing 4 different elastic modulus of different types of cement agents [Zinc phosphate, Zinc polycarboxylate, glass ionomer and composite resin cements]. The result showed a higher stress generation at the thinnest cement thickness. On the other hand, Wimmer et al. have evaluated by a sophisticated 3D FE model of 3 unit FPD [with (105,527) tetrahedral elements and (191,041) nodes] a stress state in the zirconia framework with the cement interfaces thickness of [50 and 150μm]. The pulp and the periodontal ligament were not modelled. The effect of two Young's modulus of the cement material was evaluated [self-adhesive resin (RelyX Unicem) with low elastic modulus of 4.9 GPa and glass ionomer cement with higher elastic modulus of 20.1 GPa]. They have found that increasing the cement thickness from 50 to 150μm led to increase the stress generation in the restoration structure components (Kamposiora et al., 1994, Wimmer et al., 2014).

In addition to the effect of the thickness, the evenness (uniformity of thickness) of this appears to also have an effect on stress distribution. In one study, De Jager et al. found that an uneven cement thickness could increase the shear stress at the cement interface and that would put the integrity of the compound system at risk; stating that it is advisable to make the cement interface of a uniform thickness to increase the durability of the ceramic restoration (De Jager et al., 2005). However this is only one study and provides limited data. It is of significant interest to elucidate this further and examine further the interrelation

of the cement thickness and uniformity on the stress state of the restored tooth, leading to the research question of ‘is the stress distribution and fracture resistance of the all ceramic crown-tooth complex affected by the internal interface cement geometry.

9.2 Aim

To evaluate, by means of FEA, the relative contribution that the cement interface geometry has on the stress state in a ceramic crown-tooth complex.

9.3 Objective

To compare the stress pattern of the tooth-crown complex with two different ceramic fabrication techniques [pressed and machined]; that are representative of two different internal interface geometries (as described in Chapter 5).

9.4 Null hypothesis

The different cement interface geometries would not affect the stress state of the adhesively cemented tooth crown complex.

9.5 Materials and methods

9.5.1 Physical model creation

In order to eliminate the variable of the natural tooth preparation, a reinforced dentine-like polyurethane-based resin material [AlphaDie® MF, Schütz Dental GmbH, Rosbach, Germany] which has stiffness close to dentine was used for creating the master abutment for both ceramic fabrication techniques (Kohorst et al., 2007, Sarafidou et al., 2012).

Moreover, it has been found that the amount of the developing stress is determined by the elastic modulus and the thickness of the cement. Thus, it was decided to use one type of cement [Variolink II, intro pack, Liechtenstein, Ivoclar/Vivadent] in order to eliminate the variable of the elastic modulus if different cements material implemented in the study (Ausiello et al., 2004, Liu et al., 2011).

Two different fabrication technologies, manual pressed crown (known from here on as ‘pressed model’) and the CAD-CAM machined crown (known from here on as ‘machined model’), have been chosen as representative of different interface geometries (Chapter 5). The pressed model has shown to have the thinnest (mean 114μm ±19) and most uniform cement interface thickness compared with the thickest (mean 157μm ±36) and non-uniform cement interface thickness of the machined crown.

The same protocols described in chapter 5 were followed for the tooth preparation, fabrication of crowns and cementation regime.

9.5.2 Digitizing the Physical Model

9.5.2.1 Micro CT scan

The scanning steps have been done in accordance with the scanning protocol described in chapter 4.

9.5.3 3D FEA model creation

Following the same protocols for establishing the supporting structures and generating the 3D model and that have been fully described in chapters 4 and 5 respectively, 3D FEA models for the teeth restored with the two types of crowns (pressed and machined) were generated.

Following the similar steps described in chapter 7, the 3D FEA STL model (generated by the combined use of Mimics® and FreeForm® software), the shell mesh was refined by using 'error defining and refining algorithms' from ICEM software [version 11, ANSYS, Inc.]. Subsequently, the model shell mesh was transferred to the 3D volume mesh using Hypermesh® software (Version 10.0, Altair Engineering, Inc.) that rendered a model suitable for FEA and the accurate evaluation of the stress distribution in the entire biomechanical structure.

9.5.4 Materials properties

The following modelling assumptions were made:

- The elastic modulus and poisson's ratio attributed to the mesh elements were based in accordance with the existing literature [Table 9-1].
- A static linear stress analysis was performed.
- The interface between the components (crown and tooth) was assumed as a perfectly adhesive union. Accordingly, no slip interface condition between the layers was assumed.
- The materials of the components were assumed to be as a homogenous, isotropic and displaying a linear elastic behaviour. Although, the enamel and the bone are known as anisotropic structures, the physical behaviour of the components materials is assumed to behave isotropically. This assumption is considered as a reasonable assumption for the brittle materials in non-failure conditions (Ausiello et al., 2004, Soares et al., 2012).

Table 9-1: Modulus of elasticity and Poisson's ratio of the materials

Material type	Modulus of elasticity (GPa)	Poisson's ratio	Reference
e.max® Press crown	95	0.23	(Ma et al., 2013)
e.max® CAD crown	95	0. 23	(Ereifej et al., 2011)
Variolink II cement	8.3	0.35	(Dejak and Mlotkowski, 2008)
Alpha Die® MF	14.8	0.30	(Schutz Labortechnik, Rosbach, Germany)
PDL	0.05	0.45	(Dejak and Młotkowski, 2013)
Spongy bone	1.37	0.30	(Eraslan et al., 2009)
Trabecular bone	13.7	0.30	(Eraslan et al., 2009)

9.5.5 Boundary condition and load application

The external influences such as the load and the constraints on the modelled structure are defined by the concept of boundary condition. In this way, the natural relationship between the tooth and its supporting structures (PDL and the bone) is simulated in FEA by applying a boundary condition or zero displacement. In this 3D FEA model, the boundary conditions were defined at the most outer surface nodes of the cortical bone that were constrained in all direction (X, Y, and Z) where a high accuracy result can be obtained.

Using Hypermesh® software (Version 10.0, Altair Engineering, Inc.) and following the same load application design detailed in chapter 7, two points on the outer occlusal surface, on the buccal inclination of the palatal cusp and the

palatal inclination of the buccal cusp, were selected for the load application. In order to apply an average load on the natural premolar tooth, each of the two occlusal points was subjected to a load of 150N, that would equate to 300N collectively, that simulates the average load of the mastication on the premolar [Figure 9 1].

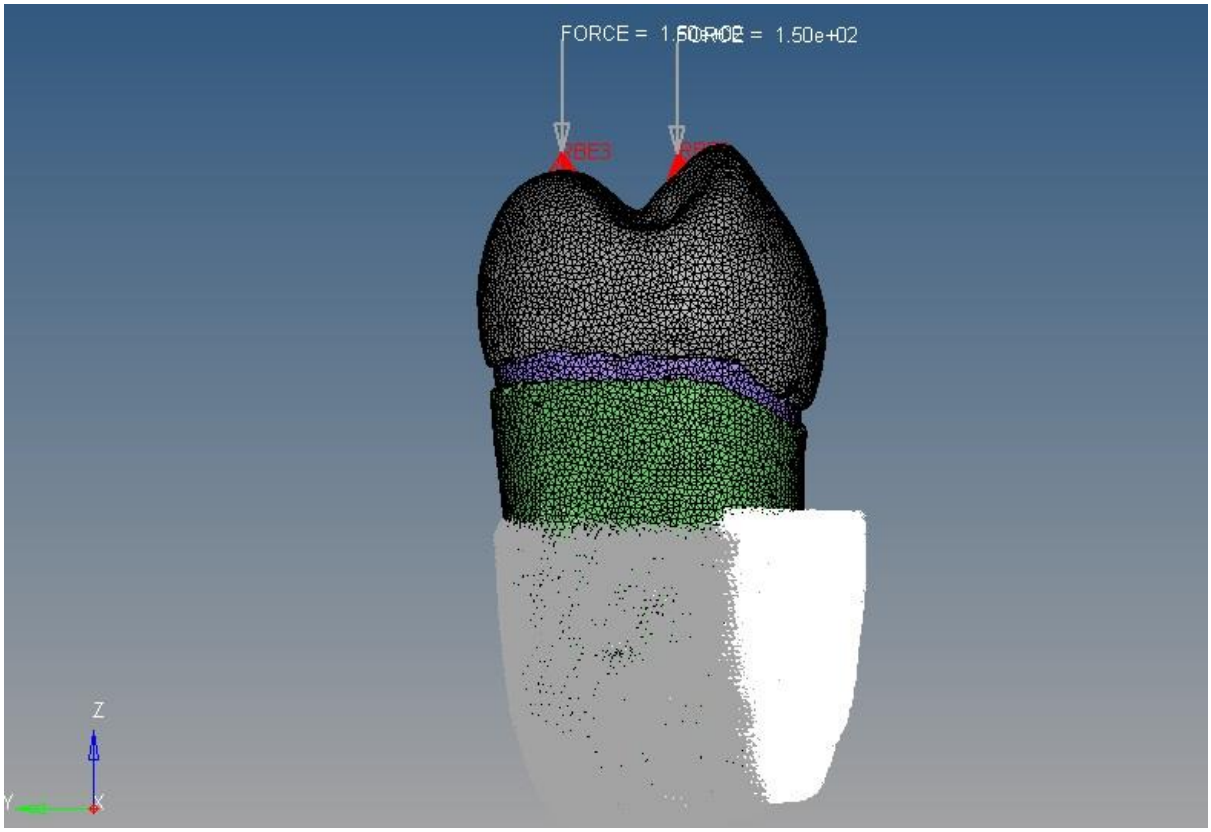

Figure 9-1: Load application to the occlusal surface of the crown-tooth complex

9.5.6 Convergence analysis

In finite element analysis, a convergence analysis is used to render a mesh that balances the accuracy and the computational resources. This step runs an

analysis for different mesh distributions by increasing the number of elements. Thus, the convergence analysis test can verify if the obtained rendered mesh is an accurate and true model or if it contains errors of noise or artifacts associated with a resolution beyond its capabilities.

The 3D FE model was subjected to this test by sequentially increasing the number of the elements by 10% that would also affect the shape and size of the mesh distribution creating more complex polygon mesh. The stress would be calculated for each iteration of the model. This process would continue until the observed stress indicated a constant stress value for each component; at which point it would be concluded that a further refinement of the mesh would not yield a matched increase in accuracy or resolution. After conducting this test, the obtained mesh was confirmed being an accurate representation of the modelled tooth-crown complex. Table 9-2 illustrate the total number of the elements and nodes for the pressed and machined model.

Table 9-2: Final number of elements and nodes in both models

Total number	**(thick/ non-uniform interface)**	**(thin/ uniform interface)**
Nodes	65088	44622
Elements	336280	226244

9.6 Results

The results of the computational analysis were calculated for each type of stress [von-Mises stress and the maximum principal stress] and presented for each model separately.

9.6.1 The stress values in the (thin and uniform interface) model

The von Mises stress distributions were computed for the tooth restored with the crown of (thin and uniform interface) and the results are reported in [Table 9-3] and [Figure 9-2].

Table 9-3: The peak values of von-Mises stress for the (thin and uniform interface) model

Component	**peak values of von-Mises stress**
Cement	15.61
Crown	240.6
Dentine	30.11
PDL	3.36
Spongy Bone	8.3
Trabecular Bone	34.91

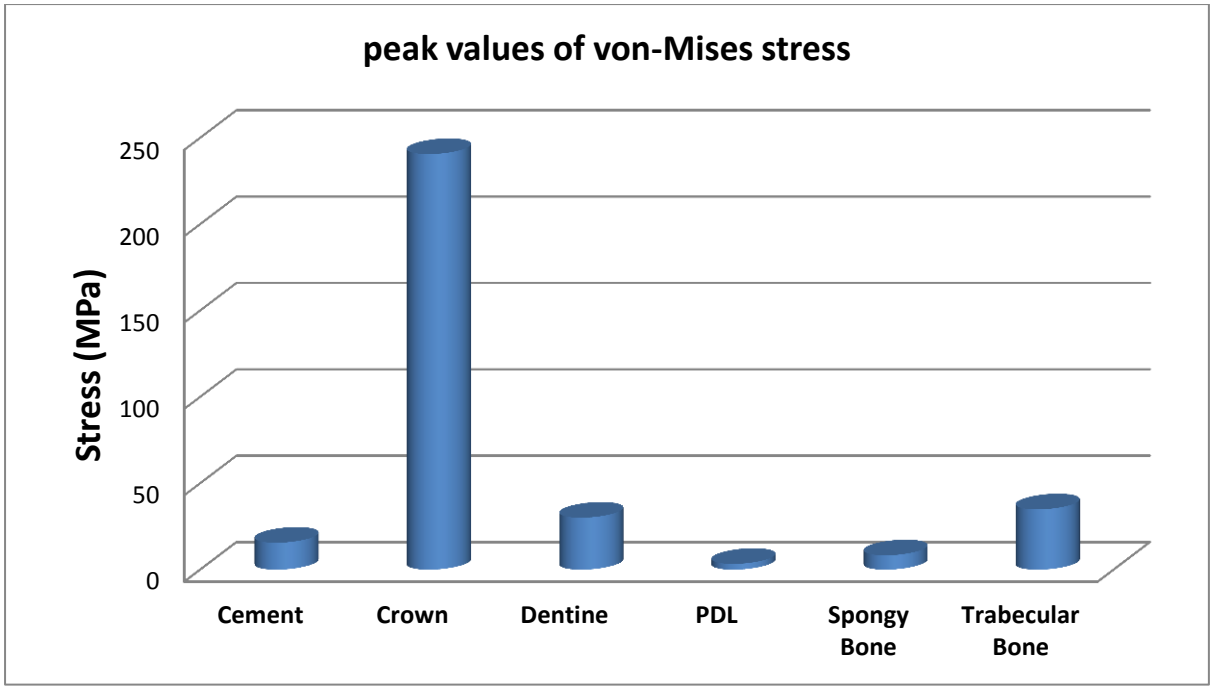

Figure 9-2: The peak values of von-Mises stress for the tooth restored with the thin and uniform interface crown

[Table 9-4] and [Figure 9-3] indicate the variation of the calculated maximum principal stress in the tooth restored by thin and uniform interface crown.

Table 9-4: The peak values of the maximum principal stress for the tooth restored with the (thin and uniform interface) crown

Component	**peak values maximum principal stress**
Cement	2.78
Crown	98.7
Dentine	2.24
PDL	2.69
Spongy Bone	7.37
Trabecular Bone	31.61

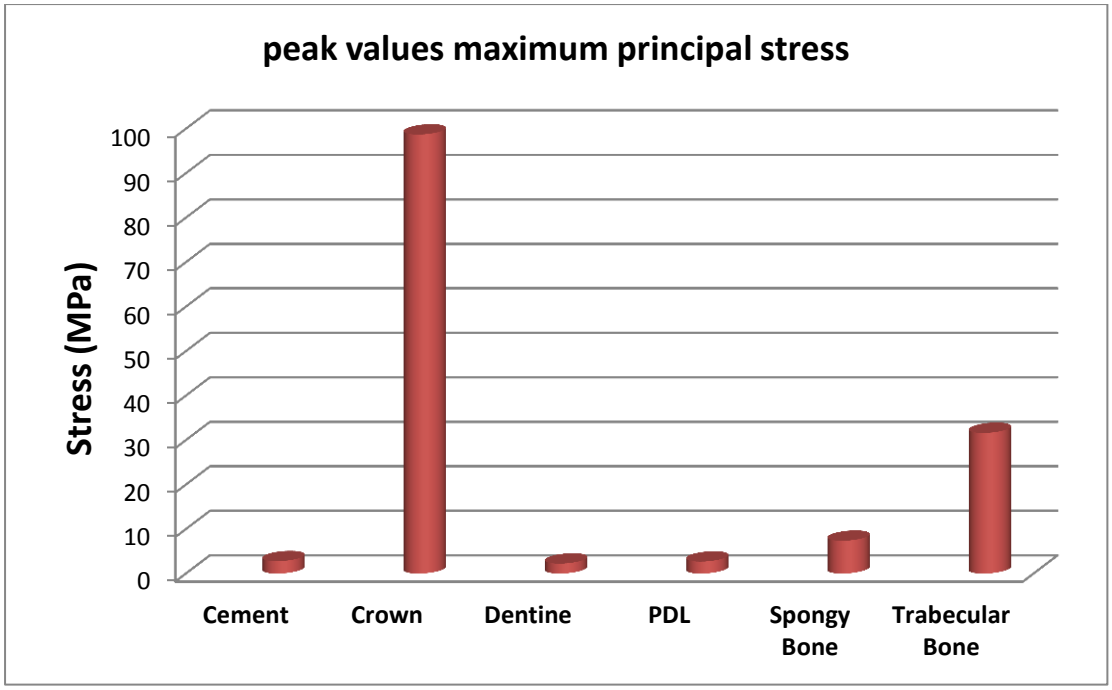

Figure 9-3: The peak values of the maximum principal stress for the tooth restored with the (thin and uniform interface) crown.

The von-Mises and the maximum principal stress values have been compared for each component of the (thin and uniform interface) model and shown in [Figure 9-4].

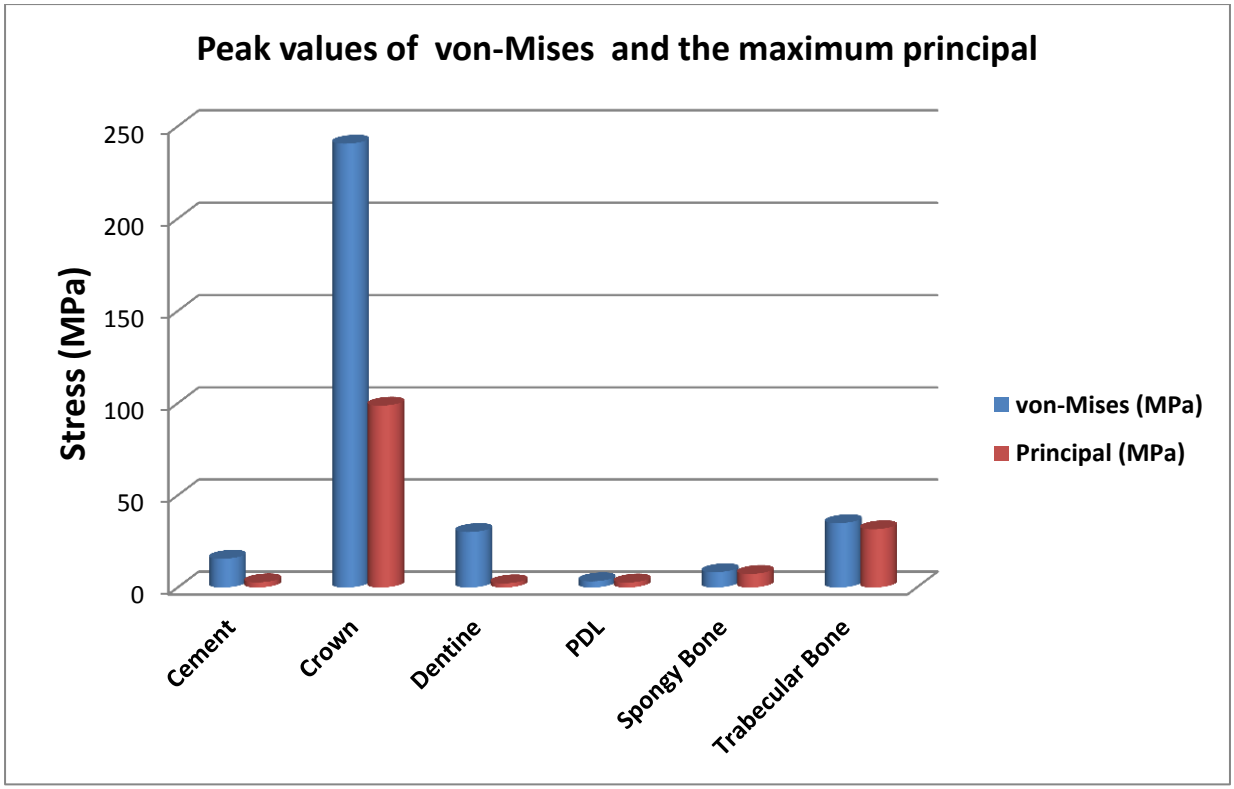

Figure 9-4: The peak values of von-Mises and the maximum principal stress for the tooth restored with the (thin and uniform interface) crown

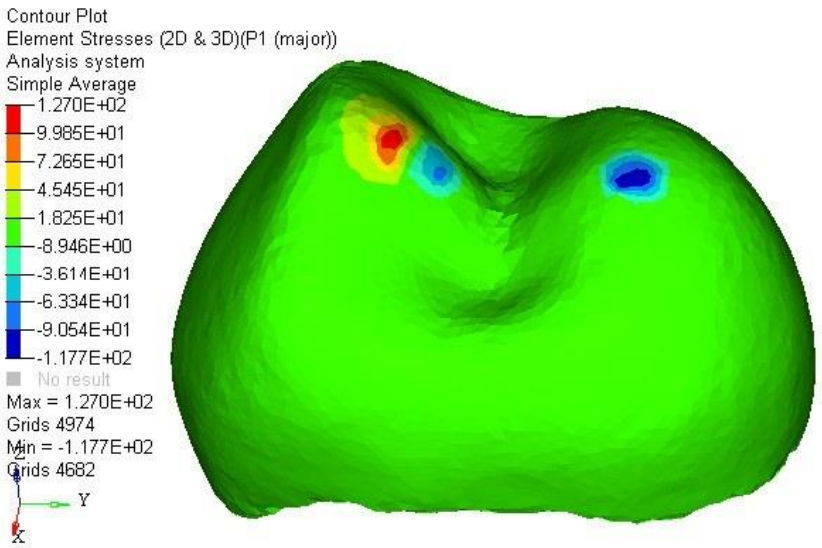

Figure 9-5: Max principal stress pattern in the crown of the (thin and uniform interface) model

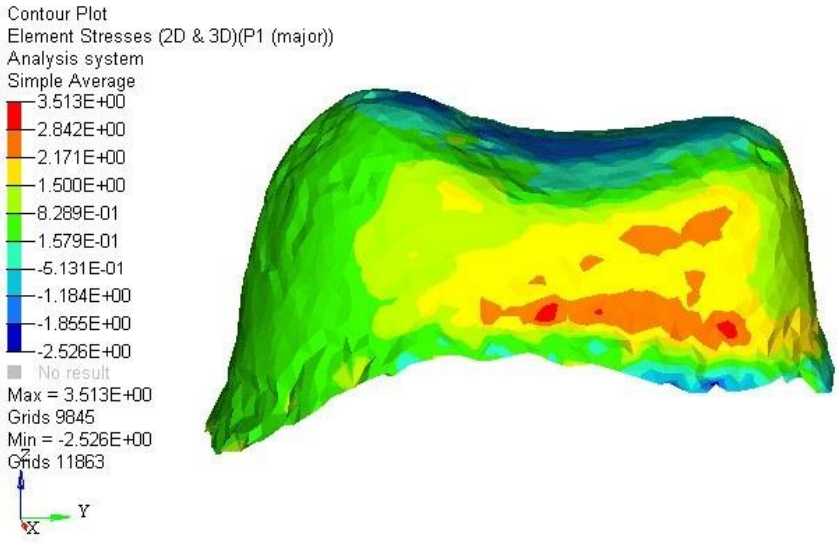

Figure 9-6: Max principal stress pattern in the cement of the (thin and uniform interface) model

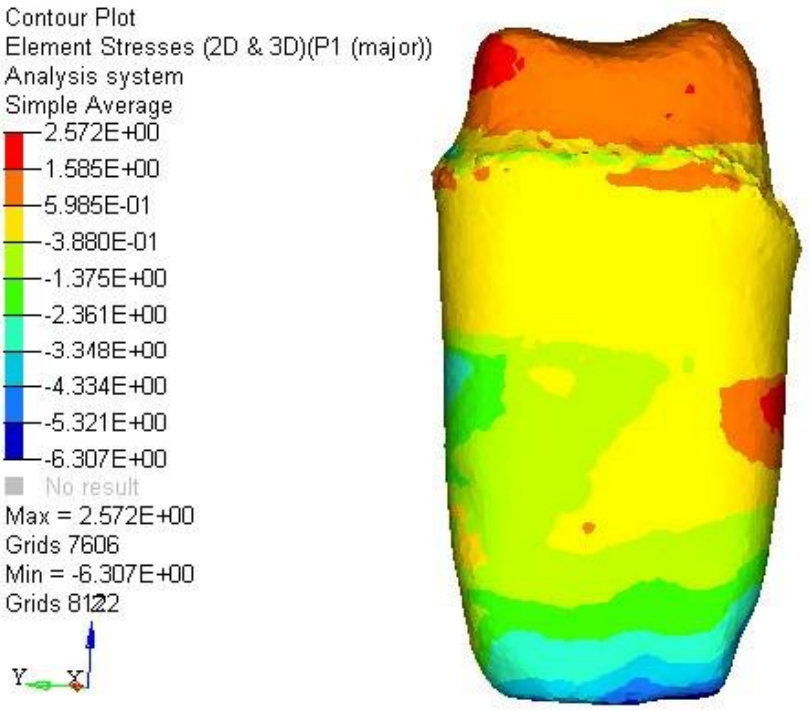

Figure 9-7: Max principal stress pattern in the dentin of the (thin and uniform interface) model

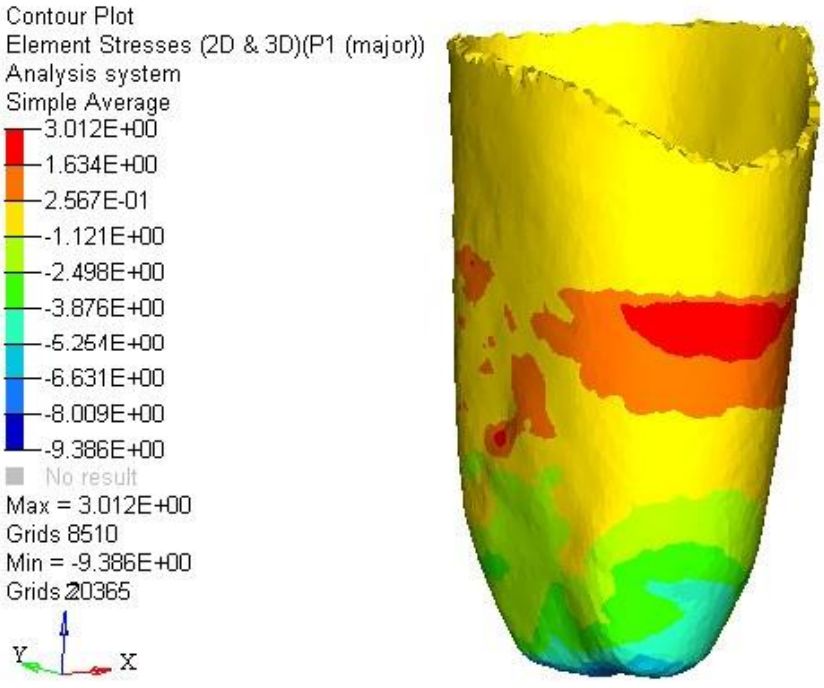

Figure 9-8: Max principal stress pattern in the PDL of the (thin and uniform interface) model

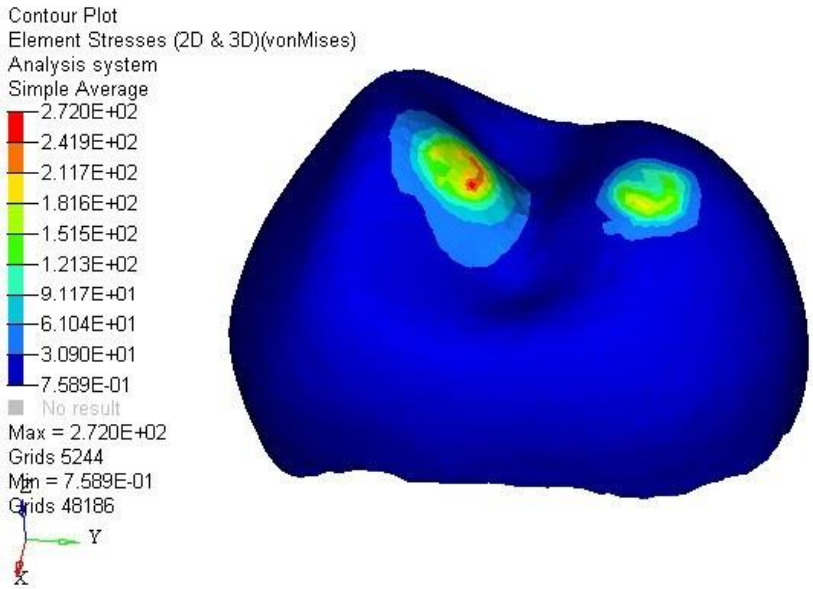

Figure 9-9: von Mises stress pattern in the crown of the (thin and uniform interface) model

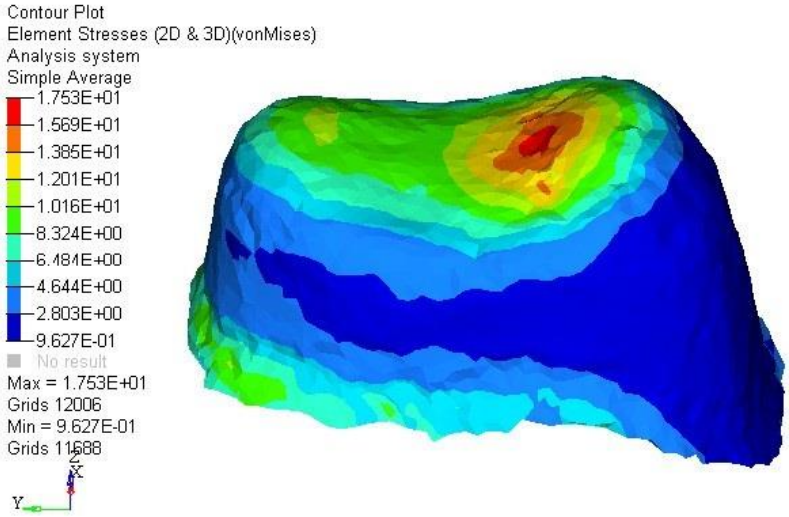

Figure 9-10 : von Mises stress pattern in the cement of the (thin and uniform interface) model

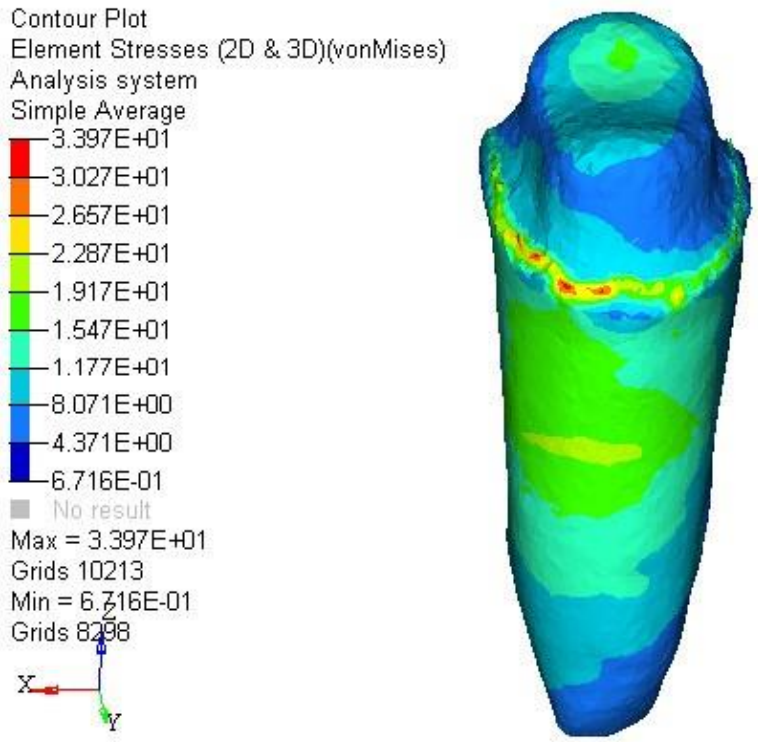

Figure 9-11: von Mises stress pattern in the dentine of the (thin and uniform interface) model

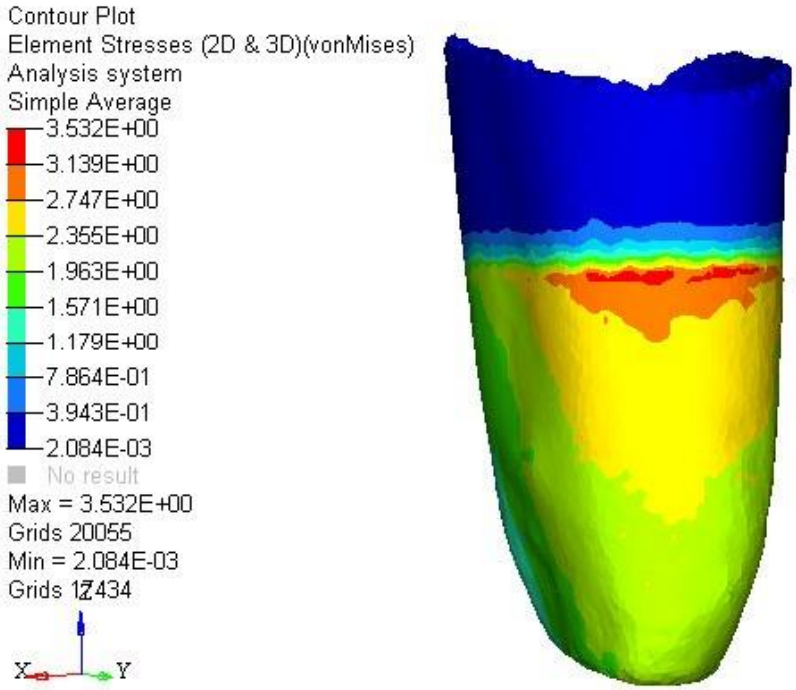

Figure 9-12: von Mises stress pattern in the PDL of the (thin and uniform interface) model

9.6.2 The stress values in the machined (thick and non-uniform interface) model

The peak values of the von Mises stress for the thick and non-uniform interface model components have been calculated and presented in [Table 9-5] and [Figure 9-13].

Table 9-5: The peak values of von-Mises stress for the tooth restored with the (thick and non-uniform interface) crown

Component	**peak values of von-Mises stress**
Cement	12.18
Crown	350.52
Dentine	25.99
PDL	3.44
Spongy Bone	8.3
Trabecular Bone	34.91

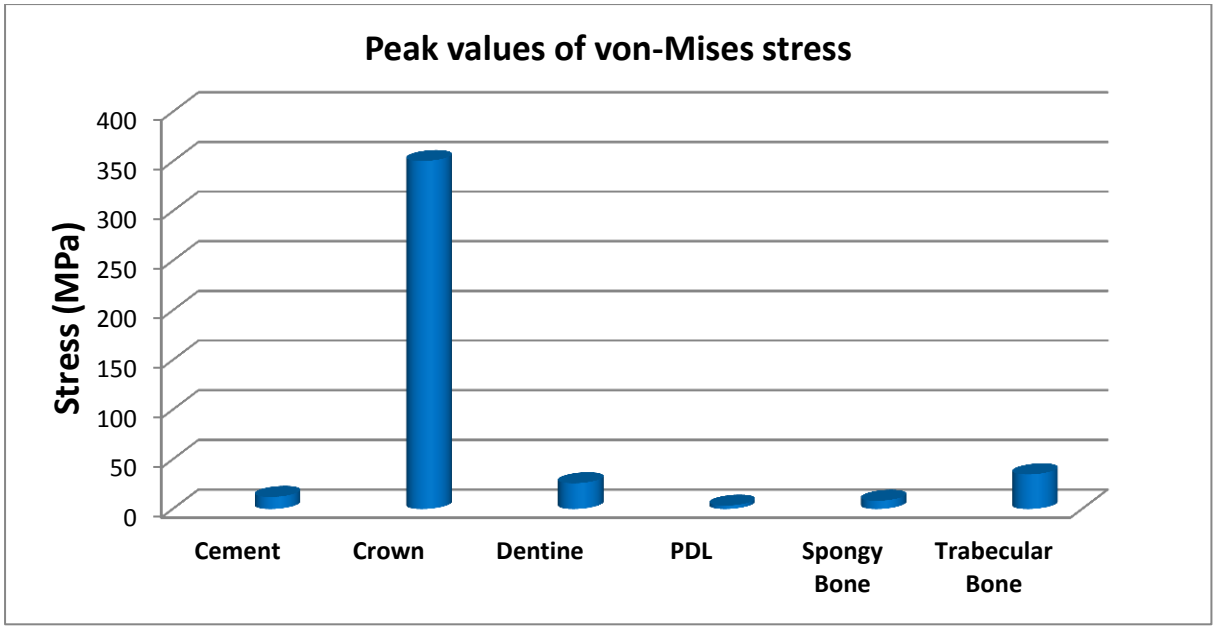

Figure 9-13: The peak values of von-Mises stress for the tooth restored with the (thick and non-uniform interface) crown

[Table 9-6] and [Figure 9-14] show the peak values of the maximum principal stress for the thick and non-uniform interface model components.

Table 9-6: The peak values of the maximum principal stress for the tooth restored with the (thick and non-uniform interface) crown

Component	**peak values of maximum principal stress**
Cement	2.92
Crown	140.18
Dentine	5.44
PDL	2.81
Spongy Bone	7.37
Trabecular Bone	31.61

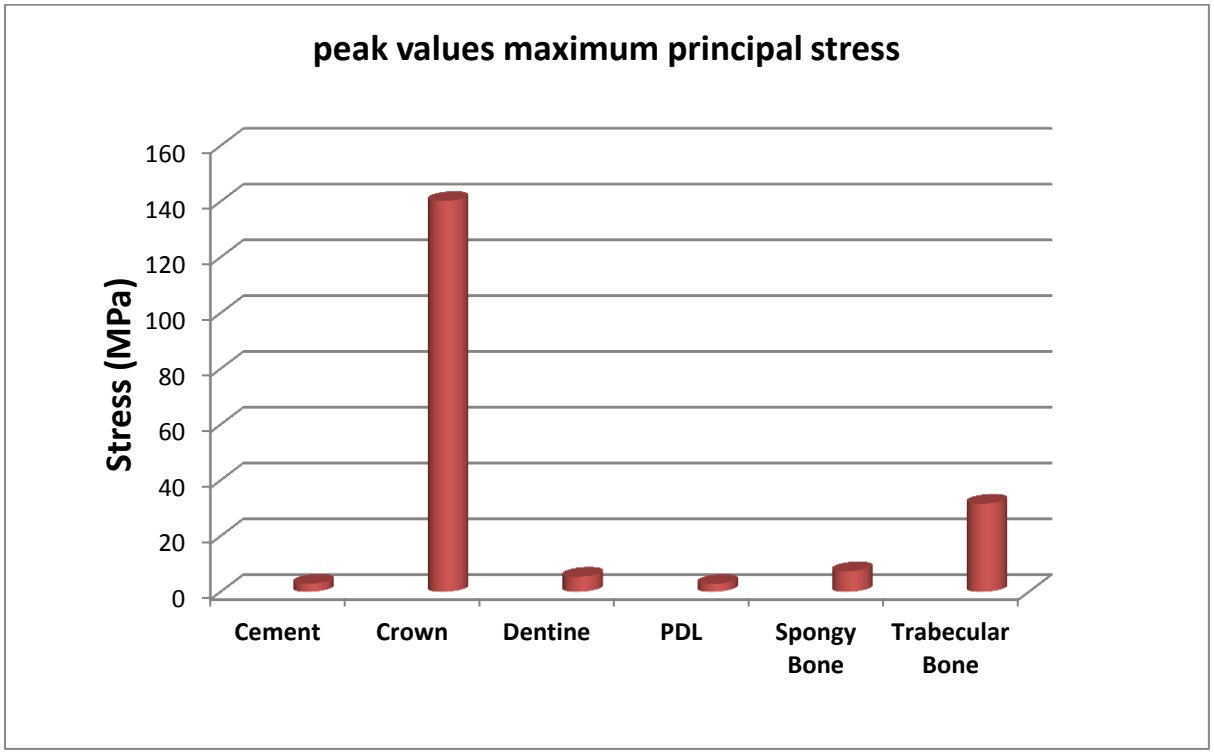

Figure 9-14: The peak values of the maximum principal stress for the tooth restored with the (thick and non-uniform interface) crown

A comparison between the peak values of von-Mises and the maximum principal stress for each component in the thick and non-uniform interface model is shown in [Figure 9-15]

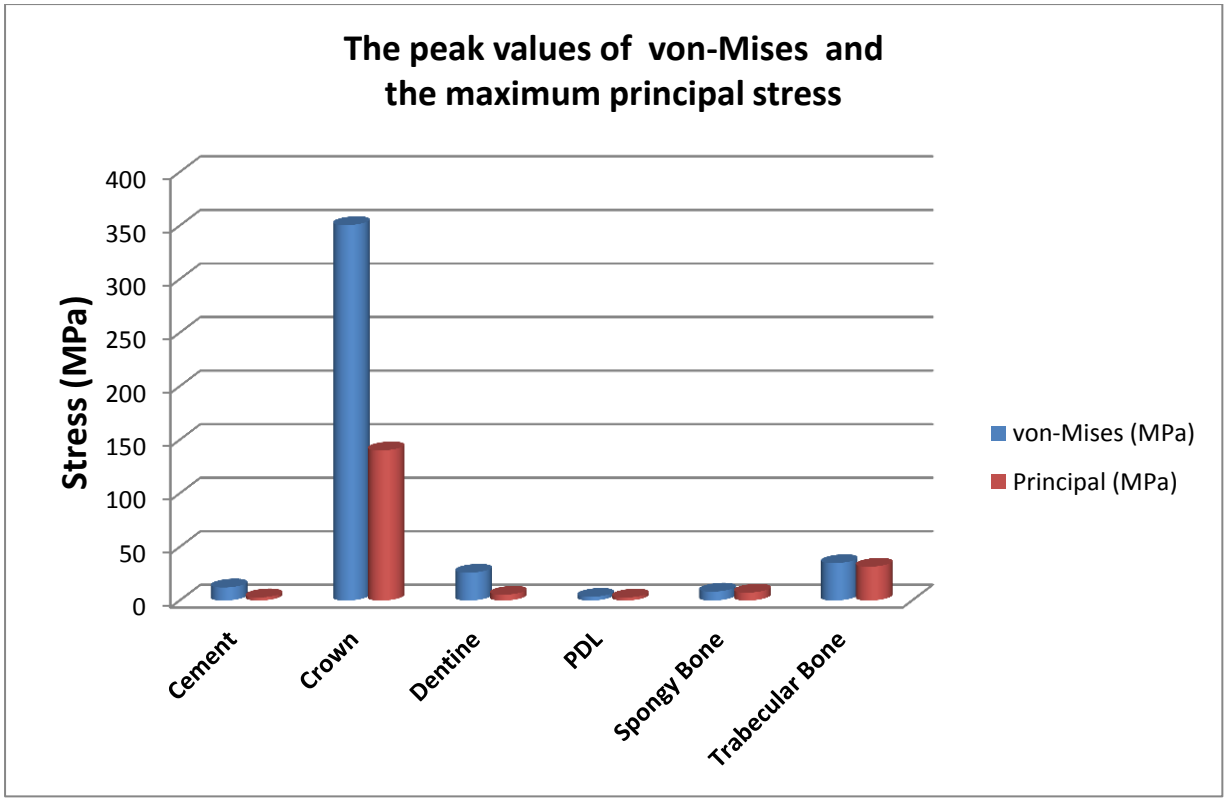

Figure 9-15: The peak values of von-Mises and the maximum principal stress for the tooth restored with the (thick and non-uniform interface) crown

The absolute values of the resulted von-Mises stress and the maximum principal stress in each component of the (thin and uniform interface) model were graphically compared with the von Mises stress and the maximum principal stress values in the corresponding components of the (thick and non-uniform interface) model respectively [Table 9-7 and 9-8] and][Figure 9-16 and 9-17].

The comparison between the components of the two models in respect to the peak values of von-Mises stress is shown in [Figure 9-16].

Table 9-7: The peak values of von Mises stress for both models

Component	thin and uniform interface	thick and non-uniform interface
Cement	15.61	12.18
Crown	240.6	350.52
Dentine	30.11	25.99
PDL	3.36	3.44
Spongy Bone	8.3	8.3
Trabecular Bone	34.91	34.91

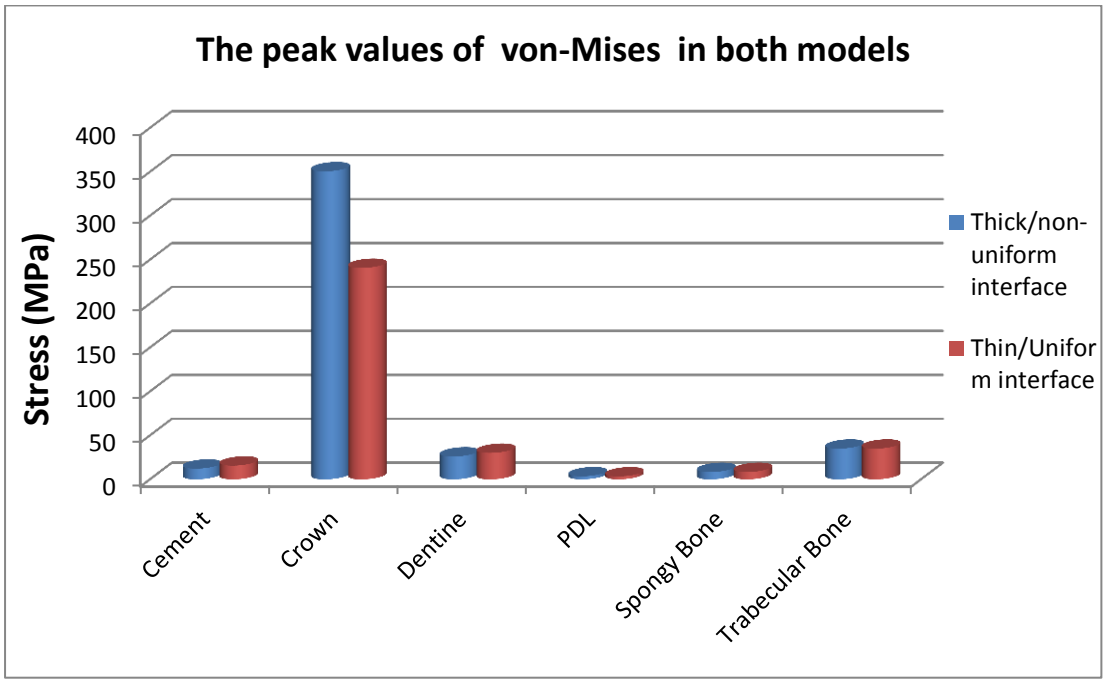

Figure 9-16: The peak values of von-Mises stress in the all components of both models

Table 9-8: The peak values of maximum principal stress for both models

Component	thin and uniform interface	thick and non-uniform interface
Cement	2.78	2.92
Crown	98.7	140.18
Dentine	2.24	5.44
PDL	2.69	2.81
Spongy Bone	7.37	7.37
Trabecular Bone	31.61	31.61

[Figure 9-17] shows the comparison in terms of the maximum principal stress for each component in both the models.

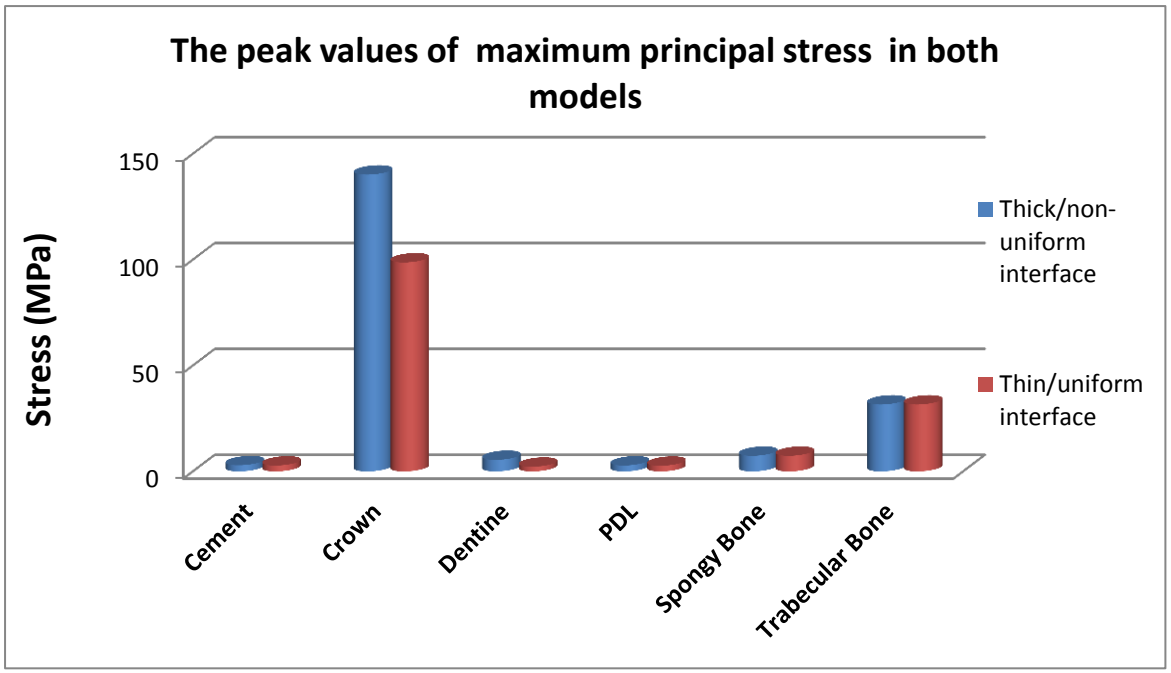

Figure 9-17: The peak values of the maximum principal stress in the all components of both models

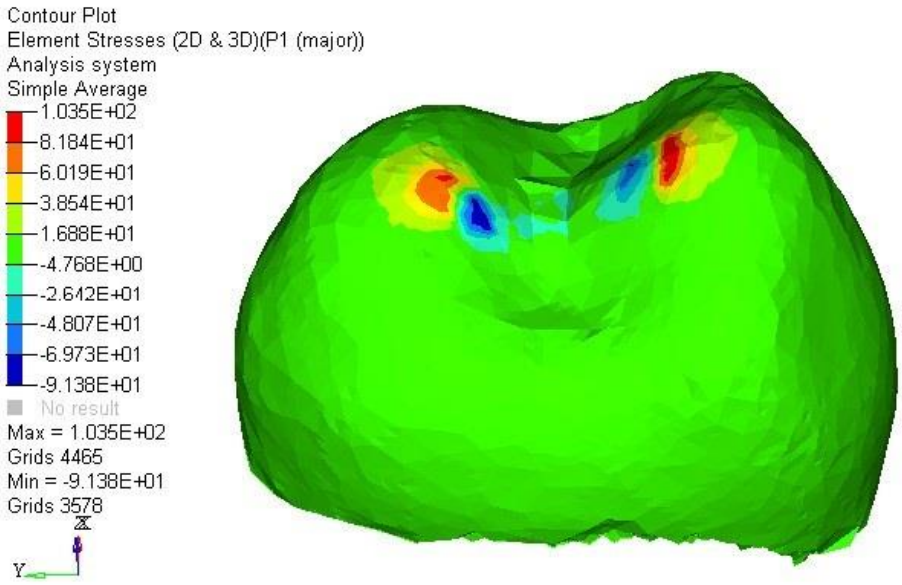

Figure 9-18: Max principal stress pattern in the crown of the (thick and non-uniform interface) model

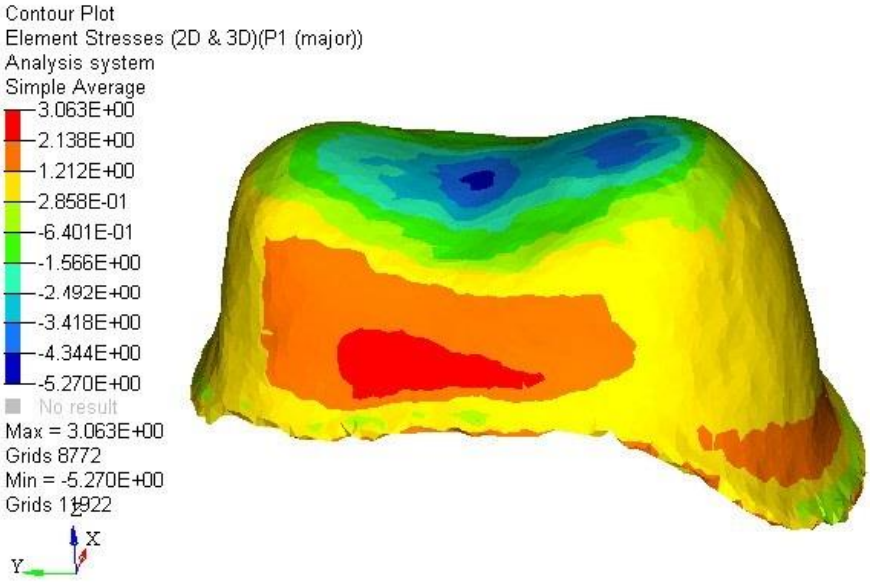

Figure 9-19: Max principal stress pattern in the cement of the (thick and non-uniform interface) model

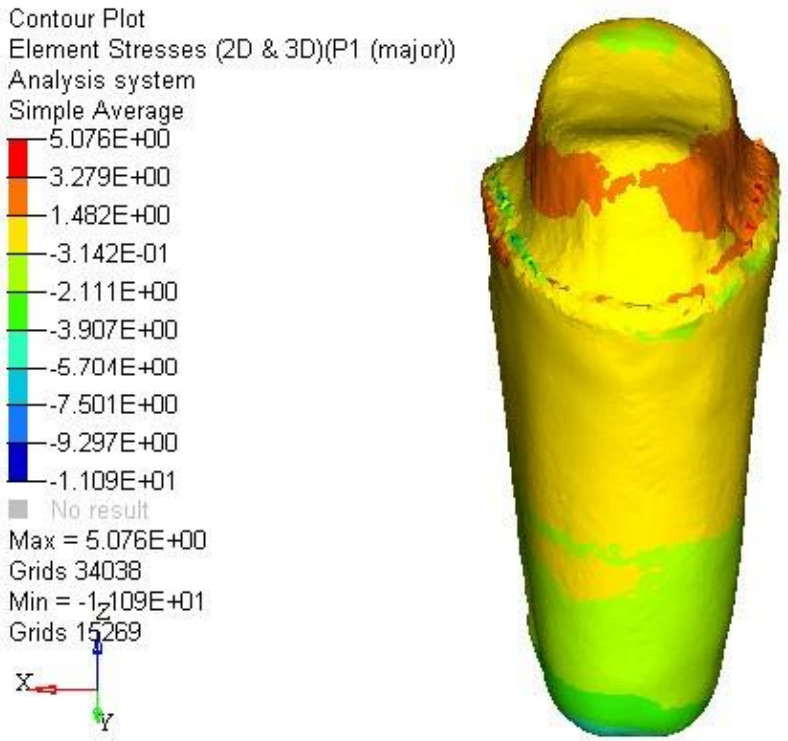

Figure 9-20: Max principal stress pattern in the dentine of the (thick and non-uniform interface) model

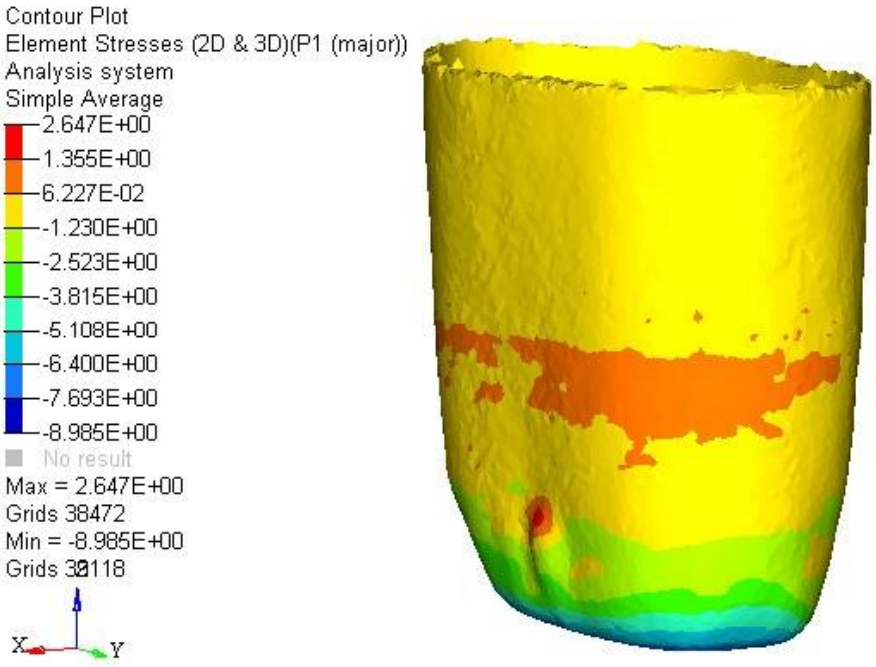

Figure 9-21: Max principal stress pattern in the PDL of the (thick and non-uniform interface) model

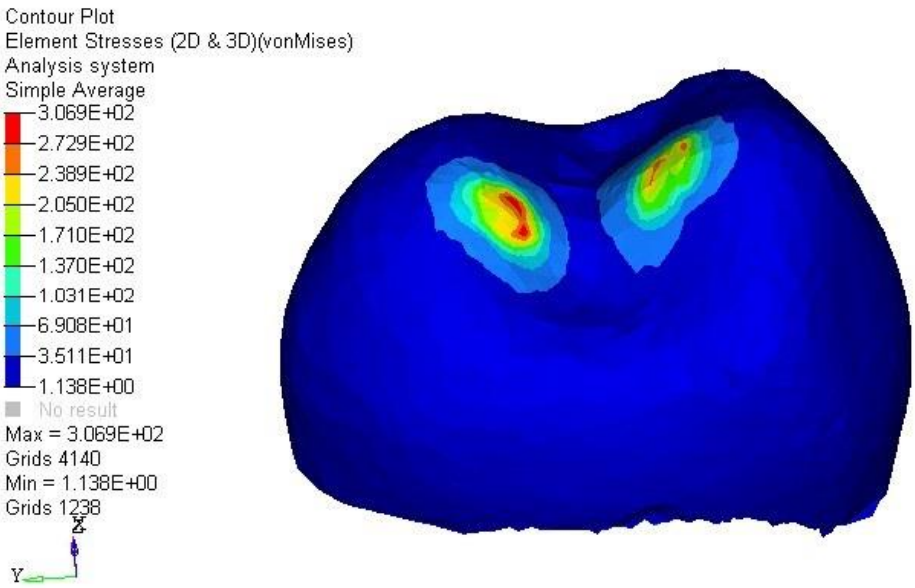

Figure 9-22: von Mises stress pattern in the crown of the (thick and non-uniform interface) model

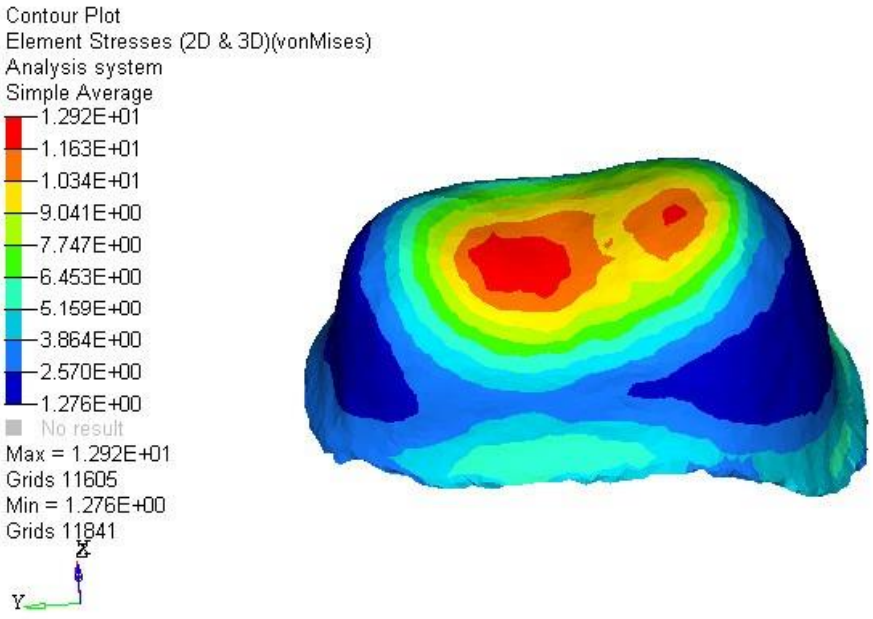

Figure 9-23: von Mises stress pattern in the cement of the (thick and non-uniform interface) model

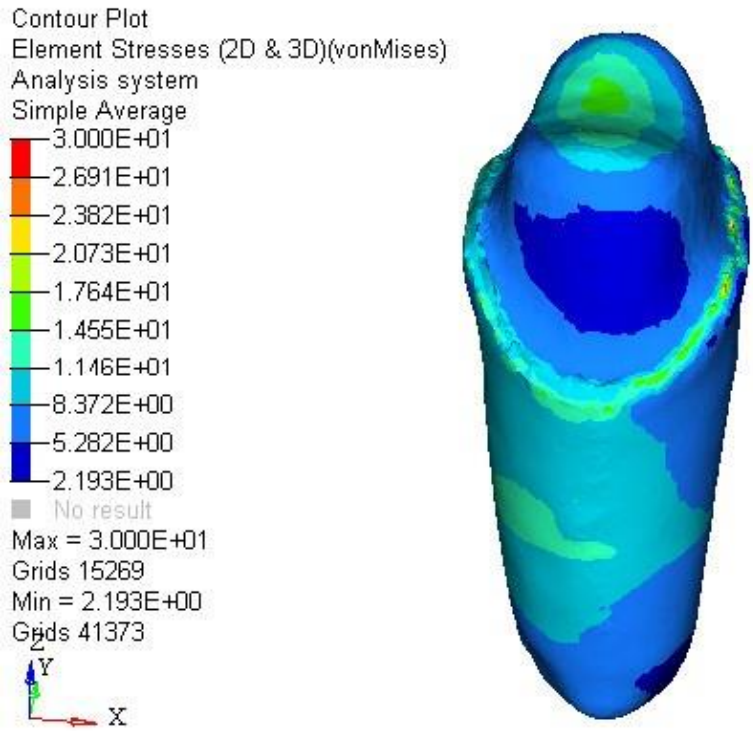

Figure 9-24: von Mises stress pattern in the dentine of the (thick and non-uniform interface) model

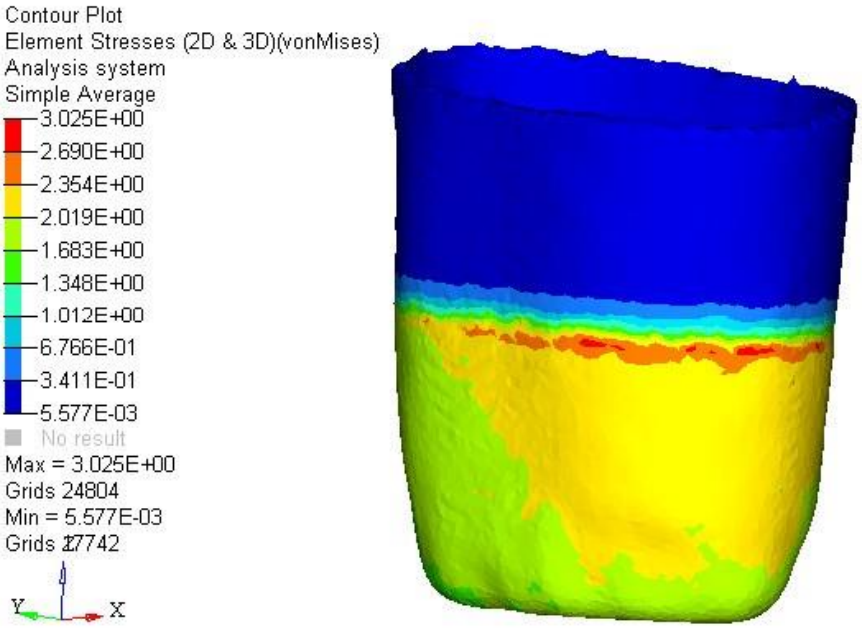

Figure 9-25: von Mises stress pattern in the PDL of the (thick and non-uniform interface) model

9.7 Discussion

A previous investigation reported in this thesis (Chapter 5) shows that different fabrication techniques show correspondingly different interface geometries. This finding raised the hypothesis that the stress state within the adhesively united ceramic crown-tooth complex may vary according to the nature of the internal interface geometry.

Thus, the aim of this investigation was to consider the effect of the internal interface geometries on the stress states within the crown-tooth complex and the supporting teeth. It is important to note that whilst two different fabrication techniques have been used to achieve two significantly different interface spaces ('pressed crown' with the most uniform and thinnest interface versus 'machined crown' with the thickets and least uniform interface) the focus of this investigation is on the nature of the interface and not the fabrication technique. In this particular study, the fabrication technique is a conduit to the creation of the interface geometry to be studied and care should be taken in not attributing the findings to the fabrication technique as this can give different results under different operational modes.

According to the data obtained for the stress state in the form of the maximum von-Mises and the maximum principal stress values, the ceramic crown component showed the highest stress values compared to the other components in both models.

In the (thick/non-uniform interface) model, the general trend of the maximum von-Mises and the maximum principal stress values was the same for the all components [Figure 9-13] and [Figure 9-14].

In the (thick/non-uniform interface) model all the components demonstrated slightly higher values for the calculated maximum von-Mises stress than the maximum principal stress values [Table 9-5] and [Table 9-6]. However, the differences of the von-Mises stress values compared with the maximum principal stress values in all the components except the crown were not a crucial difference [Figure 9-15].

The (thin/uniform interface) model behaved in a similar manner to the machined model [Figure 9-2] and [Figure 9-3] with all the components having shown a similar trend of the von-Mises and the principal stress values. Thus, the thickness of the cement interface does not affect the general stress trend of the von-Mises and the principal stresses across all the components.

The FE Analysis result showed that when the thickness of the interface is reduced as in the (thin/uniform interface)model, the crown component have demonstrated a lower level of stress values compared with a (thick/non-uniform interface) crown with higher interface thickness [Figure 9-16] and [Figure 9-17]. These results of high generated stresses in the crown due to the thick cement thickness were similar to the results of the study carried out by Thompson et al. (Thompson and Rekow, 2004). They have found that

increasing the film thickness of low elastic modulus cement (2-10 GPa) reduced the flexural strength of the full coverage crown ceramic restoration by increasing the generated stress within restoration structure. .

Moreover, the role of the thick cement film thickness on stress values (von-Mises) and the (principal stress) have been demonstrated prominently in the crown component of the (thick/non-uniform interface) model compared with the other components of the same model [Figure 9-13] and [Figure 9-14]. Increasing the cement thickness results in high stress value in the restoration framework is in accordance with the finding of Wimmer et al. study (Wimmer et al., 2014).

Generally, the crown and dentine components of the (thin and uniform interface) model showed lower levels in the two stress values compared with the identical components of the (thick and non-uniform interface) model [Figure 9-16] and [Figure 9-17] and in accordance with the finding of Liu et al. study. This discrepancy could be attributable to the high thickness of the cement that enables a high degree of crown flexure, thus, a larger tensile stress develops in the core (Liu et al., 2011).

The maximum tensile and compressive stresses (von-Mises) of the cement component of the (thick and non-uniform interface) model showed slightly lower stress values compared with the (thin and uniform interface) model [Figure 9-16]. These differences are probably due to the fact that the cement

interface of the (thin and uniform interface) model is too thin to dissipate the generated stress within cement layer appropriately. This finding is in accordance with the finding of the study by Proos et al. they have found that the thicker film of the cement interface led to lower stress in the cement layer but higher stress in the restoration (Proos et al., 2003).

The data has indicated that the difference in the stress values for the PDL component between both models was not that much different. The PDL component of the (thin and uniform interface) model was showed a maximum von-Mises stress value of [3.36 MPa] and maximum principal stress value of [2.69 MPa] compared with the PDL component of the (thick and non-uniform interface) model of [3.44MPa] and [2.81MPa] respectively.

According to the analysed data for the von-Mises stress and maximum principal stress values, the different cement interface thickness designs have an effect on the stress values of both the crown and the dentine components of both models. It does not, however, have any effect on the stress values of the Spongy bone and Trabecular bone component in both models [Figure 9-16 and 9-17]. This probably because the magnitude and effect of the load has been dissipated through the various structures and its intensity is reduced to the level where it no longer has a noticeable effect, which is in accordance with Shahrbaf et al. finding (Shahrbaf et al., 2013).

The (thin and uniform interface) model demonstrated less stress state in any individual layers in comparison with the (thick and non-uniform interface) model identical components. Although both models have different cement thickness, all the other FEA conditions were almost the same. It means that the (the thin and most uniform interface) crown model demonstrated a benign stress distribution compared with the (the thick and least uniform) interface crown model.

It can be said that the result of this investigation agrees with the result of the study carried out by Jager et al. who examined a stress state in crowns with three virtual uniform cement thicknesses. They found that the 140µm 'uniform' cement thickness could dissipate the generated stress more evenly than the 'non-uniform' cement thickness that varied from 25-140 µm. Although, high cement thickness was used in their study (140µm), the favourable stress distribution is probably attributed to the uniformity of the cement thickness (De Jager et al., 2005).

This result is in agreement with our present study, where the FEA results showed that the uniform cement thickness of the pressed model demonstrated a benign stress distribution pattern within the restored crown-tooth complex, although this was a thin interface thickness. Thus these two studies agree in that the uniformity of the cement thickness is the common factor in determining even stress distribution throughout the restored complex; and that this is the case regardless of the actual thickness of the interface. However, considering

the interface uniformity, none of FEA studies have used an actual uniform cement interface rather than considering the cement interface uniform virtually or using discs of ceramic with a uniform interface thickness instead of the crown. Thus, it was difficult to make a fair comparison of the results from the presented study with the result of another study as there are an insufficient body of the literature that covering similar aspects.

Based on the data from this investigation, the working null hypothesis that stated ’the different cement interface geometries would not affect the stress state of the adhesively cemented tooth crown complex’’ could be rejected.

9.8 Conclusions

Within the limitations of the presented study the following conclusions can be drown:

1. The crown-tooth complex with the thinner (and more uniform) interface space showed a more homogenous stress distribution compared to the tooth with a thicker (and less uniform) interface space.
2. Our results compared with those of De Jager et al, would suggest that the greater the uniformity of the interface thickness, regardless of the actual thickness value, will allow the tooth to perform better in terms of stress dissipation.
3. The stress distribution in the tooth components varied greatly between models and was affected by the cement interface thickness and cement interface uniformity.
4. The highest stress values have been seen in the crown component (at the loading points) of both assessed models regardless of the cement design and thickness.
5. The demonstrated stress state within the tooth components is affected by the interrelation of the cement thickness and uniformity.

   Thus the null hypothesis that ‘‘the geometry of the cement interface does not have any effect on the stress state of the adhesively cemented tooth crown complex’’ can be rejected.

General Discussion

10 General discussion

All-ceramic restorations can be considered as aesthetically superior to metal fused porcelain restorations. However, the ceramic shortcomings regarding their brittle nature and the low fracture strength have raised concerns about the longevity of this type of restoration (Anusavice, 2012).

The introduction of ceramics with a significantly greater amount of crystalline phase such as high-strength resin bonded silicate-based glass ceramic and non-silicate-based polycrystalline ceramic have led to high-strength ceramic restorations (Denry and Holloway, 2010, Thompson et al., 2011). However, the fracture strength of the ceramic microstructure is not the sole factor that determines its clinical performance. The actual integration of the crown with the tooth to create a ceramic crown-tooth complex is critical and determining the resistance to fracture. Parameters such as the crown design, its geometry, location of occlusal loads, cementation technique, modulus of elasticity of the cement, interface dimensions…etc. are all critical determinants and jointly will affect the overall durability of the restored tooth (Sobrinho et al., 1998, Pallis et al., 2004, AL-Makramani et al., 2008, Sorrentino et al., 2009).

By means of the finite element analysis, the effects of the elastic modulus of the cement materials as well as the tooth preparation designs on the stress distribution have been investigated by the study carried out by Shahrbaf et al. They have found that a desired stress distribution could be obtained when the

flat design of the ceramic crown cemented with a high elastic modulus cement, whereas the low elastic modulus is recommended for the anatomical preparation design of the ceramic crown (Shahrbaf et al., 2013).

It has been shown that in the non-uniform cement layer the stress development will vary and the failure incidence of the bond strength of the adhesive cement with the crown and the tooth might be increased (Mou et al., 2002, De Jager et al., 2005). The bonding surface can be affected by the non-uniform cement film thickness through increasing the maximum shear stress to values exceeding the bond strength of the cement layer to restoration and abutment surfaces. Thus, it is advisable to make the resin cement film thickness as uniform and as thin as possible(De Jager et al., 2005).

Due to an inability to create crowns with controlled interface geometries, these studies that examined the effect of the uniformity of the cement thickness were limited to the FE Analysis investigation of the virtual uniform cement or to use flat discs of ceramic rather than the actual crown design in the mechanical test.

The purpose of this study was to determine by means of mechanical fatigue testing and FEA the effect that the interface geometry (the thickness and uniformity) has on the fracture resistance of a tooth restored with a full-coverage adhesively cemented all-ceramic crown.

To expand the scope of the experiment and enable the comparison of a wider range of fabrication techniques comparison, the lithium disilicate glass ceramic has been selected. Using the lithium disilicate ceramic [IPS e.max® Pressed and IPS .max CAD], the two ceramic fabrication techniques [Pressed and machined] can be utilised.

To establish the nature of these apparently similar ceramics, an SEM investigation of the microstructure (post-fabrication and following acid-etch conditioning) was conducted. The results were based on comparing the images of the same SEM magnification power for both crown techniques simultaneously.

The SEM images, as shown in chapter 6, indicated a significant difference in the microstructure between pressed and machined lithium disilicate e.max ceramic crowns. The pressed lithium disilicate ceramic has shown a favourable length of the needle-shape crystals that should contribute in the toughening mechanism by increasing the energy that is required for the crack to propagate (Baran et al., 2001, Albakry et al., 2004a).

It was proved, that the fracture initiation site for the ceramic under the load is predominantly controlled by the density, severity and location of the critical flaws within the ceramic structure rather than its thickness (Thompson et al., 1994, Chinn, 2002, Guazzato et al., 2004b). It has been reported that failure of dental prosthesis is not coming as a result of the acute incidence of the overload

rather than the accumulation of stress that yield fatigue-related failure (McCabe et al., 1990a, Wiskott et al., 1994, Zhang et al., 2013).

A Frasaco tooth permanent upper right first premolar was prepared according to Ivoclar/Vivadent instruction for the monolithic e.max® crown in order to exclude the natural tooth variables. However, creating a hypothetically uniform interface required the development of a new technique for pressed ceramic crowns (vacuum-formed spacer technique [Isofolan® technique]). The developed fabrication technique has been described in chapter 5.

Isofolan® technique is based on creating a mould onto the preparation dye from a vacuum-formed polymer sheet with the aid of a Biostar machine (Isofolan® SCHEU DENTAL, GmbH, Germany). Thus, through the action of heat and pressure, the Isofolan® elastic foil sheet (Polyethylene low density PE-LD; size 0.1mm, SCHEU DENTAL, GmbH, Germany) was adapted to the external surface of the sample. The thin vacuum-formed Isofolan layer created a space corresponding to the space that would be created by the technician using the die spacer. Subsequent steps of the wax build up, wax lost technique and pressing the ceramic into the mould were followed the same route as in normal creation of a manual pressed ceramic crown

In order to eliminate the human technician variable during the manual pressed technique, a 3D wax printer (Solidscape® 3Z lab) has been used in this study. We postulated that the 3D wax printer would give us greater control over the

design of the interface parameters and enable the creation of a more uniform width interface. Moreover, to check the accuracy, and variability between systems, of the CAD/CAM milling machine in terms of the interface production, two CAD/CAM machine were involved; CEREC [CEREC® 3 inLab, SIRONA Dental Systems, GmbH] and Zirkonzahn® CAD/CAM system [Zirkonzahn®, Italy].

It is generally accepted that the internal and marginal fit are still of key importance for the long term success of all-ceramic crowns, whether conventionally or adhesively cemented (Sailer et al., 2007).

For the purpose of evaluating the different cement interface thickness that were created by the different ceramic crown fabricating techniques, a replica measuring technique was proposed. The technique consists of using a light body silicone impression material to replicate the space between the tooth and restoration. The measured dimension of the light body is used to evaluate the quality and nature of cement interface geometry (Laurent et al., 2008, Reich et al., 2011).

However, the replica technique has many disadvantages. It is a 2D system and can only be measured where it has been sectioned. Furthermore, it is not possible to standardize the position and the angulations of the measuring planes between samples, and that reduces the accuracy particularly when comparing between different samples. The study conducted by Qualtrough et al, showed

that it is just a measurement of the silicone that occupies the interface gap, and does not replicate the behaviour of the cement in the real clinical situation (Qualtrough et al., 1993). Accordingly, there was a need to develop a new measuring technique that enable characterizing the internal dimensions and geometry of the interface in an accurate, reproducible and repeatable manner.

It was well established, that the computer-aided methods for measuring the interface has a substantial impact in terms of the accuracy and the reliability of the measurement. Moreover, the computer-aided methods and due to their reproducible non-destructive nature it can provide valuable additional information about the measured specimen (Moldovan et al., 2011).

By using Mimics® software (Materialise Co., Ltd) a 3D novel method for measuring the interface dimensions was developed as an effective alternative technique to the replica technique. In this study, the assessment was performed by the combined use of micro CT scan images and Mimics® software. Measuring the cement interface using this methodology (radiopaque cement, micro-CT and 3D image modelling software) enabled a high accuracy and intra- (within the specimen) and inter- (within the various specimens) reproducible measurements to be taken. This method was performed by taking a measurement of the predefined nine points in the same cross sections for each sample. The measuring technique by Mimics® has been validated by means of a laser micrometer and it showed measurement accuracy up to 1 micron. The

invention and the validation of this measuring technique were described in chapter 5.

Although, there is a controversy on the accepted minimum and maximum adhesive cement dimensions. Studies showed a range of 50-100 μm and in other studies a range of 100-120 μm have been proposed as appropriate in terms of the longevity of the restoration. A study by Liu et al. has considered a thickness of 90μm as being optimal. However, an interface thickness of up to 160 μm might be tolerable (Molin et al., 1996, Krämer et al., 2000, Prakki et al., 2007, Liu et al., 2011, Reich et al., 2011).

The statistical analysis of the results obtained from the Mimics® measuring technique has indicated a significant difference between the various types of crown in terms of the interface thickness. The measurement of the cement thickness in the mesio-distal direction has revealed that the cement thickness of the vacuum-formed spacer [Isofolan®] group as shown in Table (5-8) showed the maximum thickness mean of (308μm), while the 3D printer group showed the minimum thickness mean of (44μm). Similarly, Table (5-12) shows that the maximum mean of the cement thickness measured in the bucco-lingual direction was showed by the vacuum-formed spacer [Isofolan®] group which was (330μm), while the minimum mean thickness was showed by the 3D printer group (54μm).

Obviously, it can be summarised from the outcome obtained regarding the minimum and the maximum thickness that the sample of the 3D printer technique is able to produce the thinnest thickness over the entire cement length among the other compared groups. Since, the vacuum-formed spacer [Isofolan®] sample has shown an extremely high cement thickness that is higher than the accepted standard of the recommended cement interface; it was decided to reject this technique from future studies of this project.

Moreover, the statistical analysis of the obtained data highlighted that the differences between the machined samples [CEREC® and Zirkonzahn®] was not significant. Therefore, the CEREC technique for the ceramic crown fabrication was selected as a representative for the machined fabrication technique in the further studies of this project.

The two pressed crown groups [manual pressed and the 3D wax printing/ceramic pressing] have shown the lowest standard deviation (SD) and (range) values compared with the other three groups in both directions [mesio-distally and bucco-lingually] [Table (5-8) and Table (5-12)]. Undoubtedly, the low SD means the gathered data is distributed very close to the mean. Thus, the results have pointed out a small discrepancy in the thickness of the cement throughout all the measured points in these two groups' samples. The cement thickness homogeneity of the pressed samples compared with the machined samples is consistent with Yeo et al. and Aboushelib et al. the findings (Yeo et

al., 2003, Aboushelib et al., 2012). Therefore, the thickness of the cement interface of the manual pressed and the 3D wax printing/ceramic pressing groups could be described as a thinnest and a most homogenous thickness compared with the other 3 groups (machined [CEREC®], machined [Zirkonzahn®] and the vacuum-formed spacer [Isofolan®]).

A 3D FE model of the restored natural tooth from a published study has been used after modifying the original non-uniform cement interface to be a uniform by using the FreeForm® and the haptic technology (SensAble Technologies, Inc.).

This system offers a sophisticated 3D visualization and a manual sculpture by the haptic phantom tool that enables modelling tooth components effectively.

Comparing the FE Analysis result of the stress values in the modified model's components with the original published study model's components revealed a non-significant difference in all the components except the crown component of the modified model. However, the stress state in the crown components of both models has not been negatively affected by modifying the interface geometry.

The possible reason of the undesirable stress value in the crown of the modified (uniform interface) model could be attributed to the limitation of the modelling software. A thickness of 180µm of the uniform cement thickness was the least thickness can be generated by the FreeForm® software. Moreover, during the step of generating the uniform cement layer, sharp corners were induced in the

inner surface of the crown component that acts as stress concentration area. However, the initial results of this study were encouraging for further investigations.

Dental ceramic structures are inherently vulnerable to cyclic mechanical fatigue. Moreover, the oral environment has all the necessary factors for the fatigue failure to occur in the dental ceramic restoration. It is well documented from the retrieved clinical data that the initiation and propagation of the cracks due to the fatigue effect of the masticatory force is supposed to be the common case for the clinical failure of the all-ceramic restoration (Zahran et al., 2008).

Furthermore, the effect of the cement interface geometry on the structural integrity of the ceramic restoration has been investigated in some studies. It has been suggested that the uniformity and the width of the interface space between the restoration and the tooth wall might determine the effect on the survivability of the prosthesis (De Jager et al., 2005, Wang et al., 2007).

In the study conducted in this investigation a mechanical fatigue testing was designed and aimed to evaluate the effect of the cement interface geometry on the structural integrity of the restored tooth-crown complex. Based on the findings mentioned in chapter 5, three fabricating techniques [3D wax printing/ ceramic pressing (thinnest and uniform interface cement), manual pressed (thin and most uniform interface cement) and machined (thick and least uniform interface cement)] were compared. Based on the different cement interface geometries that these crowns have, a null hypothesized was formulated, that all

the tested groups exhibit the same fatigue resistance to the cyclic fatigue loading of the chewing simulator. In this study, the cyclic fatigue loading with the most of the oral environment factors have been considered in order to compare the fatigue strength of the samples.

The fatigue life data in terms of the maximum number of the fatigue cycles to failure for a given load amount was statistically analysed to give a numerical value of the fatigue life. The results have indicated that there was a significant difference in the resistance to fatigue loading between the three groups.

Moreover, Weibull probability analysis and the α and β Weibull parameters indicate that the teeth restored with a 'manually-applied wax spacer and pressed-crown' that with (thin and most uniform interface cement), are best able to resist cyclic fatigue loading than the teeth restored with '3D wax printed/ceramic pressed crown' with (thinnest and uniform interface cement), and 'machined crown' (thick and least uniform interface cement).

Notwithstanding, the 3D printer/ ceramic pressed crown has a thinnest and uniform interface (mean 81µm ±26) compared with the other groups. However, the manual pressed crown survived more load cycles. The manual pressed crown showed an optimal or a standard interface thickness with most uniform interface geometry (mean 114µm ±19). The reasonable explanation for this variation is because, a standard thickness of (50-100µm) when combined with a high uniform degree of the cement interface geometry, leads to an even distribution of the generated stress under the external load.

Strength can be considered as an important mechanical property that has a high influence on the durability of ceramic-based dental restorations. Thus, measuring the fracture strength in order to evaluate the structural integrity of the ceramic restoration has been recommended by several studies(Attia and Kern, 2004, Sadighpour et al., 2006).

The complex structure modelling accuracy could be considered as the limitation factor of the earlier numerical analysis studies. However, the advancement in the digitizing tools such as [CT scan and MRI] has enabled to produce a more sophisticated 3D model with higher accuracy rather than 2D or crude and imperfect 3D model of the complex geometry object in the earlier studies. Recently, the image acquisition system using the micro CT scan is extensively applied as a tool for scanning the model for the 3D modelling purpose of the tooth and related structures (Plotino et al., 2006, Magne and Oganesyan, 2009).

By means of FE analysis, the role of the cement interface thickness on the stress state (von-Mises and maximum principal stress) of the restored tooth has been examined by some authors. Kamposiora et al. have examined cement interface thicknesses of [25 and 100μm]. The result demonstrated that the thinnest thickness showed the higher stress value. On the other hand, stress state in the restored tooth with the cement interfaces thicknesses of [50 and 150μm] have been evaluated by Wimmer et al. They have found that enlarging the cement thickness from 50 to 150μm led to increase the stress generation in the tooth structure components (Kamposiora et al., 1994, Wimmer et al., 2014).

In this project a 3D FE model of the restored tooth complex has been generated by the innovative methods that depend on the conjunction of the [micro CT, Mimics®, FreeForm® and Hypermesh®] software in order to evaluate the effect of the cement interface geometries on the stress distribution in terms of (von-Mises and maximum principal stress) of the restored tooth complex.

In this study, two ceramic fabrication techniques were involved that represented a uniform thin cement thickness and non-uniform thick thickness which are [pressed crowns] and [machined crowns] respectively.

The assumptions were made for the materials based on selecting the elastic modulus and poisson's ratio that in accordance with the existing literature. A static linear stress analysis was performed. The interface between the components was assumed as a perfectly united. Accordingly, no slip interface condition between the layers was assumed. The materials of the components were assumed to be as a homogenous, isotropic and display linear elastic behaviour. A static load of 300Naccording to the average load on the premolar was applied on the occlusal surface of the crown and the boundary condition was assumed at the most outer surface nodes of the cortical bone(Craig R, 2006).

According to the data obtained for the maximum von-Mises and the maximum principal stress values, the ceramic crown component manifested the highest stress values compared with the other components in both models. The general

trend of both types of the calculated stress values [maximum von-Mises and the maximum principal] was the same for the all components in both models.

The FE Analysis result showed that when the thickness of the interface is uniform within the accepted standard (50-100μm) as in the pressed model, the crown and the dentine components have demonstrated a lower level of von-Mises and the principal stress values compared with the crown with non-uniform higher cement thickness. This difference probably due to the fact that the high film thickness above the accepted standard of the cement interface allows for a high degree of crown flexure, which is in turn, result in large tensile stress development within the restoration, causing it to fracture. Whereas, a very thin cement thickness is unable to absorb the generated energy by the deformation and evenly distribute the generated stress within the components, which leads to an increase in the stress in the crown and tooth components, in accordance with Liu et al. finding (Liu et al., 2011). Thus these findings suggest that a thickness that is either too thick (>150 microns) or too thin (<50 microns) will lead to stress concentration and fracture of the ceramic crown.

According to the overall results of the FEA of this study, the pressed model (with a uniform and thin interface) demonstrated less stress state in any individual layers in comparison with the machined model (with non-uniform and thick interface) identical components. Thus, the pressed model showed the most benign stress state in comparison with the machined model.

In the FEA study by De Jager et al. a uniform high thickness of the interface (140µm) showed an even distribution of the stress compared with a non-uniform low thickness (25-140µm). According to our finding and based on the De Jager et al. finding, it can be concluded that regardless of the interface thickness, the interface uniformity is an important factor affecting the stress distribution with the tooth-crown complex.

Due to the errors in the fabricating of the crown, the interface space between the tooth prepared surface and the fitting surface of the crown is most often different from the desired. It is possible, thus, to find a cement thickness varying from 20 to 200 µm regard less the setup parameter of the thickness (Liu et al., 2011). In this project to standardize the setup parameters of the cement thickness, a zero value of the thickness was designed within the 3D wax printer/ceramic pressed and the CAD/CAM designing software as well as 12µm ±2µm for the manual pressed technique. Thus, the result data would be more comparable.

The samples with the zero thickness of the interface were used through all the investigations of this project. The cement thickness of both pressed crown samples has shown a most uniform and the thinnest thickness compared with the cement thickness of the machined crown sample that mentioned in chapter 5.

In the fatigue dynamic testing of this study, the pressed (thin/uniform interface) crown samples were show the highest Weibull modulus and the samples were survived the highest load cycles number comp compared with the machined (thick/non-uniform interface) samples. Similarly, FEA results indicated that the pressed (thin/uniform interface) crown sample has shown a least stress values in the crown and dentine components compared with the machined (thick/non-uniform interface) samples. Thus, the pressed crown model showed a most benign stress distribution than the machined model.

The FEA result has shown that the occlusal surface (at the loading points) of both models' is a more vulnerable area and where the fracture is likely to be initiated. Thus, the FEA result would be highly consistent with the mechanical testing result if the fracture analysis of the fatigue testing samples shows an occlusal crack driven failure in the tested crowns. However, it is very difficult to quantify precisely the moment and the path of the fracture in the brittle materials. Moreover, there were very few studies in the literature have been published considering the failure analysis of the fractured ceramic depending on the standardized approach of crack feature recognition (Quinn et al., 2005, Scherrer et al., 2007, Scherrer et al., 2008)

The mechanical fatigue testing as well as the FEA results have indicated that there is an effective relationship between the interface thickness and the structural integrity of the restored tooth complex. Moreover, these results

indicated as well, that the uniformity of the interface geometry is an important determinant of the structural integrity.

However, due to the assumptions required to undertake the FEA, these results cannot be extrapolated directly to the real clinical situation. Moreover, the static load analysis of the FEA result could not be directly correlated with the fatigue results of the mechanical fatigue testing.

Due to the study time limitation and a long time needed for generating the 3D FEA model of the 3D wax printed/ceramic pressed (thinnest/uniform interface) crown sample, it was not possible to involve the 3D wax printed/ceramic pressed crown in the FEA study. Thus, running an ideally *in vivo* test or involving the 3D wax printed/ceramic pressed crown sample in a fatigue behaviour analysis using a dynamic FEA would provide a clinically more reliable data.

General Conclusions

11 General Conclusions

The following points can be concluded from this study that help to address the research questions set out at the start of this project:

1. A uniform interface thickness (50-100μm) will enhance the structural integrity of the restored system by manifesting a benign distribution of the generated stress within the restored crown-tooth complex.
2. The manual pressed ceramic crown showed an interface thickness that was thin and more uniform than that of the 3D printed/ceramic pressed crown.
3. Setting the interface thickness as zero in the 3D wax printer software generated a very thin interface that reduced the overall structural integrity of the complex under fatigue load. This finding suggests that an increase of the interface thickness may results in a cement interface thickness that is within the accepted standard thickness and better able to resist fatigue loading.
4. The machined crown demonstrated a higher discrepancy and high thickness of the interface cement dimension, which correlated negatively with the reliability of the crown under the fatigue dynamic load. This suggests that the uniformity and thickness of the interface has a significant influence on the structural integrity of the tooth-crown complex.
5. The optimal coordination between the 3D modelling tools [the Micro-CT, Mimics® software and FreeForm® with haptic technology] can be effectively used for generating of an accurate and life-like 3D FE model.

6. The presented methodology to create an accurate anatomically-correct 3D FE model may be implemented for modelling accurately other dental or medical applications.
7. With the standard mechanical test, the FEA can be considered as an effective complementary tool for determine the stress distribution within the tooth components and for predicting the structural integrity of the restored tooth-crown complex. Thus, the FEA approach can be considered as a useful complementary analytical technique to evaluate the stress state in the complex geometry.
8. The new and novel technique for measuring the interface cement was validated up to 1 micron accuracy, which implies greater clinical reliability for this computational measurement technique in the future.

11.1 Clinical Relevance

1. In this study, the ceramic crown with a uniform cement thickness range from (50-100 μm) is more reliable under the load than ceramic crown with a uniform but less interface thickness or a non-uniform and greater thickness interface.
2. The manual pressed ceramic crown showed the most uniform and an acceptable cement thickness (50-100μm) compared with the machined and the 3D printed/ceramic pressed crown, which implies a great clinical reliability of this technique for the ceramic crown fabrication, in the hands of an expert ceramic technologist.

Further Studies

12 Further studies

The role of the interface geometry on the structural integrity of the ceramic tooth complex has been examined by this study by comparing five ceramic crown fabrication techniques. In order to decrease the bias, one type of resin composite cement [Variolink II, intro pack, Liechtenstein, Ivoclar/Vivadent] was used. It was found that the manual pressed ceramic crown showed the thin and most uniform interface thickness among the examined groups. Thus, the geometry of the interface in terms of overall dimensions and uniformity is a function of the fabrication technology. In order to evaluate the role of the types of cement on the interface geometry, the same study using one fabrication technique with several types of the cement is recommended as a further study to comprehensively estimate the possible variables affecting the interface geometry.

Furthermore, the interface measuring experiment has been performed using the 3D wax printer (Solidscape® 3Z lab) as it allows for greater control over the production of the interface geometry and enables the production of a uniform interface. For both the 3D wax printer, the interface parameter was set to zero thickness. However, the generated interface morphology correlated negatively with the structural integrity of the crown under the fatigue load. An increase in the cement interface thickness for the 3D printer sample in a future study could

produce an optimum thickness with a uniform geometry of the interface that increases the reliability of the crown under the load.

The reliability of the different ceramic crowns interface under a dynamic fatigue loading by the chewing simulator was compared. A 453N axial fatigue loading by a vertical indenter was applied in two occlusal points. However, in the real case the tooth is subjected to the load in several directions on several occlusal points. Using various load values in the chewing simulator that allow for a vertical and horizontal movement of the load and specimen would increase the reliability of the fatigue outcome.

Moreover, through the project the dentine substitute material AlphaDie® has been used to exclude the natural tooth variables. This material has a physical property (elastic modulus) close to the natural dentin and it is able to bond to the composite luting cement. However, it lacks the anisotropy of the dentin, which led to a different structural behaviour to that of dentin under a fatigue mechanical loading. Using natural tooth or materials closely matched to dentine properties but in the same structure of dentine would be the perfect replacement for the AlphaDie® in future studies. This, however, would have to be balanced against the increase in variability encountered between natural tooth samples and the possibility that these may have been damaged during functional use prior to extraction and during the extraction per se.

Designing an in vivo study that implements the concept of the uniform cement interface geometry under real oral conditions would contribute to generalise this idea as a means of enhancing the survival of the tooth that is adhesively restored with an all-ceramic crown.

References

13 References

.

ABO-HAMAR, S. E., HILLER, K. A., JUNG, H., FEDERLIN, M., FRIEDL, K. H. & SCHMALZ, G. 2005. Bond strength of a new universal self-adhesive resin luting cement to dentin and enamel. *Clinical oral investigations,* 9**,** 161-167.

ABOUSHELIB, M. N., DE JAGER, N., KLEVERLAAN, C. J. & FEILZER, A. J. 2007. Effect of loading method on the fracture mechanics of two layered all-ceramic restorative systems. *Dental Materials,* 23**,** 952-959.

ABOUSHELIB, M. N., ELMAHY, W. A. & GHAZY, M. H. 2012. Internal adaptation, marginal accuracy and microleakage of a pressable versus a machinable ceramic laminate veneers. *Journal of Dentistry,* 40**,** 670-677.

ABOUSHELIB, M. N., FEILZER, A. J., DE JAGER, N. & KLEVERLAAN, C. J. 2008 b. Prestresses in bilayered all-ceramic restorations. *Journal of Biomedical Materials Research Part B: Applied Biomaterials,* 87**,** 139-145.

ABOUSHELIB, M. N., KLEVERLAAN, C. J. & FEILZER, A. J. 2008 a. Microtensile Bond Strength of Different Components of Core Veneered All-Ceramic Restorations. Part 3: Double Veneer Technique. *Journal of prosthodontics,* 17**,** 9-13.

ADAIR, P. H. 1971. The chemical strengthening of dental porcelain. *Master Thesis, Australia;University of Sydney*.

ADDI, S., HEDAYATI-KHAMS, A., POYA, A. & SJÖGREN, G. 2002. Interface gap size of manually and CAD/CAM-manufactured ceramic inlays/onlays in vitro. *Journal of dentistry,* 30**,** 53-58.

ADDISON, O., MARQUIS, P. & FLEMING, G. 2007. Resin elasticity and the strengthening of all-ceramic restorations. *Journal of dental research,* 86**,** 519-523.

AL-MARZA, R., SHAHARBAF, S. & MARTIN, N. 2014a. Effect of Interface Geometry On The Integrity Of Ceramic Crowns. *IADR/PER CONGRESS , Dubrovnik, Croatia*.

AL-MARZA, R., SHAHARBAF, S. & MARTIN, N. 2013. A Novel Technique For Characterising The Interface Geometry of Crowns. *J Dent Res* 92 (Spec Iss B), 149, (BSODR/IADR).

AL-MARZA, R., SHAHARBAF, S. & MARTIN, N. 2014b. Validation of a novel technique for characterising the interface geometry of non-metallic crowns *BSSPD Annual Confernce*

AL-MAKRAMANI, B., RAZAK, A. & ABU-HASSAN, M. 2008. Evaluation of load at fracture of Procera AllCeram copings using different luting cements. *Journal of Prosthodontics,* 17**,** 120-124.

ALBAKRY, M., GUAZZATO, M. & SWAIN, M. V. 2003. Fracture toughness and hardness evaluation of three pressable all-ceramic dental materials. *Journal of dentistry,* 31**,** 181-188.

ALBAKRY, M., GUAZZATO, M. & SWAIN, M. V. 2004a. Influence of hot pressing on the microstructure and fracture toughness of two pressable dental glass–ceramics. *Journal of Biomedical Materials Research Part B: Applied Biomaterials,* 71**,** 99-107.

ALBAKRY, M., GUAZZATO, M. & VINCENT SWAIN, M. 2004b. Biaxial flexural strength and microstructure changes of two recycled pressable glass ceramics. *Journal of Prosthodontics,* 13**,** 141-149.

AMMAR, H. H., NGAN, P., CROUT, R. J., MUCINO, V. H. & MUKDADI, O. M. 2011. Three-dimensional modeling and finite element analysis in treatment planning for orthodontic tooth movement. *American Journal of Orthodontics and Dentofacial Orthopedics,* 139**,** e59-e71.

ANDREASEN, F., DAUGAARD-JENSEN, J. & MUNKSGAARD, E. 1991. Reinforcement of bonded crown fractured incisors with porcelain veneers. *Dental Traumatology,* 7**,** 78-83.

ANUSAVICE, K. J. 2012. Standardizing failure, success, and survival decisions in clinical studies of ceramic and metal–ceramic fixed dental prostheses. *Dental Materials,* 28**,** 102-111.

APPELDOORN, R. E., WILWERDING, T. M. & BARKMEIER, W. W. 1993. Bond strength of composite resin to porcelain with newer generation porcelain repair systems. *The Journal of Prosthetic Dentistry,* 70**,** 6-11.

References

AROLA, D., GALLES, L. & SARUBIN, M. 2001. A comparison of the mechanical behavior of posterior teeth with amalgam and composite MOD restorations. *Journal of dentistry,* 29**,** 63-73.

ASSIF, D., MARSHAK, B. L. & PILO, R. 1990. Cuspal flexure associated with amalgam restorations. *The Journal of Prosthetic Dentistry,* 63**,** 258-262.

ASSUNÇÃO, W. G., RICARDO BARÃO, V. A., TABATA, L. F., GOMES, É. A., DELBEN, J. A. & DOS SANTOS, P. H. 2009. Biomechanics studies in dentistry: bioengineering applied in oral implantology. *Journal of Craniofacial Surgery,* 20**,** 1173.

ASUNDI, A. & KISHEN, A. 2000. A strain gauge and photoelastic analysis of in vivo strain and in vitro stress distribution in human dental supporting structures. *Archives of Oral Biology,* 45**,** 543-550.

ATTAR, N., TAM, L. E. & MCCOMB, D. 2003. Mechanical and physical properties of contemporary dental luting agents. *The Journal of Prosthetic Dentistry,* 89**,** 127-134.

ATTIA, A. & KERN, M. 2004. Fracture strength of all-ceramic crowns luted using two bonding methods. *The Journal of prosthetic dentistry,* 91**,** 247-252.

AUSIELLO, P., RENGO, S., DAVIDSON, C. L. & WATTS, D. C. 2004. Stress distributions in adhesively cemented ceramic and resin-composite Class II inlay restorations: a 3D-FEA study. *Dental Materials,* 20**,** 862-872.

AYKOR, A. & OZEL, E. 2009. Five-year clinical evaluation of 300 teeth restored with porcelain laminate veneers using total-etch and a modified self-etch adhesive system. *Operative Dentistry,* 34**,** 516-523.

BALDASSARRI, M., ZHANG, Y., THOMPSON, V. P., REKOW, E. D. & STAPPERT, C. F. 2011. Reliability and failure modes of implant-supported zirconium-oxide fixed dental prostheses related to veneering techniques. *Journal of dentistry,* 39**,** 489-498.

BAN, S. 2008. Reliability and properties of core materials for all-ceramic dental restorations. *Japanese Dental Science Review,* 44**,** 3-21.

BARAN, G., BOBERICK, K. & MCCOOL, J. 2001. Fatigue of restorative materials. *Critical Reviews in Oral Biology & Medicine,* 12**,** 350-360.

BECHER, P. F. 1991. Microstructural design of toughened ceramics. *Journal of the American Ceramic Society,* 74**,** 255-269.

BERGMAN, M. A. 1999. The clinical performance of ceramic inlays: a review. *Australian dental journal,* 44**,** 157-168.

BERZINS, D., ABEY, S., COSTACHE, M., WILKIE, C. & ROBERTS, H. 2010. Resin-modified glass-ionomer setting reaction competition. *Journal of dental research,* 89**,** 82-86.

BESCHNIDT, S. & STRUB, J. 1999. Evaluation of the marginal accuracy of different all-ceramic crown systems after simulation in the artificial mouth. *Journal of oral rehabilitation,* 26**,** 582-593.

BESCHNIDT, S. & STRUB, J. 2001. Evaluation of the marginal accuracy of different all-ceramic crown systems after simulation in the artificial mouth. *Journal of oral rehabilitation,* 26**,** 582-593.

BEUER, F., AGGSTALLER, H., EDELHOFF, D., GERNET, W. & SORENSEN, J. 2009. Marginal and internal fits of fixed dental prostheses zirconia retainers. *Dental Materials,* 25**,** 94-102.

BEUER, F., SCHWEIGER, J. & EDELHOFF, D. 2008. Digital dentistry: an overview of recent developments for CAD/CAM generated restorations. *British Dental Journal,* 204**,** 505-511.

BINDL, A., LÜTHY, H. & MÖRMANN, W. H. 2006. Strength and fracture pattern of monolithic CAD/CAM-generated posterior crowns. *Dental Materials,* 22**,** 29-36.

BINDL, A. & MÖRMANN, W. 2005. Marginal and internal fit of all-ceramic CAD/CAM crown-copings on chamfer preparations. *Journal of oral rehabilitation,* 32**,** 441-447.

BINDL, A. & MÖRMANN, W. H. 2004. Survival rate of mono-ceramic and ceramic-core CAD/CAM-generated anterior crowns over 2–5 years. *European journal of oral sciences,* 112**,** 197-204.

BLATZ, M. B., OPPES, S., CHICHE, G., HOLST, S. & SADAN, A. 2008. Influence of cementation technique on fracture strength and leakage of alumina all-ceramic crowns after cyclic loading. *Quintessence international (Berlin, Germany: 1985),* 39**,** 23.

References

BLATZ, M. B., SADAN, A. & KERN, M. 2003. Resin-ceramic bonding: a review of the literature. *Journal of Prosthetic Dentistry,* 89**,** 268-274.

BOENING, K. W., WOLF, B. H., SCHMIDT, A. E., KÄSTNER, K. & WALTER, M. H. 2000. Clinical fit of Procera AllCeram crowns. *The Journal of prosthetic dentistry,* 84**,** 419-424.

BONA, Á. D., BORBA, M., BENETTI, P., DUAN, Y. & GRIGGS, J. A. 2013. Three-dimensional finite element modeling of all-ceramic restorations based on Micro-CT. *Journal of dentistry, Vol.41(5),p.412-419*.

BORCIC, J. & BRAUT, A. 2012. chapter 1/ Finite Element Analysis in Dental Medicine, [Finite Element Analysis - New Trends and Developments- book].

BOSCHIAN PEST, L., GUIDOTTI, S., PIETRABISSA, R. & GAGLIANI, M. 2006. Stress distribution in a post-restored tooth using the three-dimensional finite element method. *Journal of oral rehabilitation,* 33**,** 690-697.

BOUILLAGUET, S., TROESCH, S., WATAHA, J. C., KREJCI, I., MEYER, J. M. & PASHLEY, D. H. 2003. Microtensile bond strength between adhesive cements and root canal dentin. *Dental Materials,* 19**,** 199-205.

BOWLEY, J. F., ICHIM, I. P., KIESER, J. A. & SWAIN, M. V. 2013. FEA Evaluation of the Resistance Form of a Premolar Crown. *Journal of Prosthodontics,* 22**,** 304-312.

BRAGA, R. R., FERRACANE, J. L. & CONDON, J. R. 2002. Polymerization contraction stress in dual-cure cements and its effect on interfacial integrity of bonded inlays. *Journal of dentistry,* 30**,** 333-340.

BREMER, B. & GEURTSEN, W. 2001. Molar fracture resistance after adhesive restoration with ceramic inlays or resin-based composites. *American Journal of Dentistry,* 14**,** 216.

BROCHU, J. F. & EL-MOWAFY, O. 2002. Longevity and clinical performance of IPS-Empress ceramic restorations-a literature review. *Journal-Canadian Dental Association,* 68**,** 233-238.

BROSH, T., PORAT, N., VARDIMON, A. & PILO, R. 2011. Appropriateness of viscoelastic soft materials as in vitro simulators of the periodontal ligament. *Journal of Oral Rehabilitation,* 38**,** 929-939.

BURKE, F. 1995. The effect of variations in bonding procedure on fracture resistance of dentin-bonded all-ceramic crowns. *Quintessence international (Berlin, Germany: 1985),* 26**,** 293.

BURKE, F. 1999. Maximising the fracture resistance of dentine-bonded all-ceramic crowns. *Journal of dentistry,* 27**,** 169-173.

BURKE, F., FLEMING, G., NATHANSON, D. & MARQUIS, P. M. 2002. Are adhesive technologies needed to support ceramics? An assessment of the current evidence. *The journal of adhesive dentistry,* 4**,** 7.

BURKE, F., QUALTROUGH, A. & HALE, R. 1995. The dentine-bonded ceramic crown: an ideal restoration? *British dental journal,* 179**,** 58-63.

CASSON, A., GLYN JONES, J., YOUNGSON, C. & WOOD, D. 2001. The effect of luting media on the fracture resistance of a flame sprayed all-ceramic crown. *Journal of dentistry,* 29**,** 539-544.

CATTANEO, P., DALSTRA, M. & FRICH, L. 2001. A three-dimensional finite element model from computed tomography data: a semi-automated method. *Proceedings of the Institution of Mechanical Engineers, Part H: Journal of Engineering in Medicine,* 215**,** 203-212.

CHEN, H. Y., HICKEL, R., SETCOS, J. C. & KUNZELMANN, K.-H. 1999. Effects of surface finish and fatigue testing on the fracture strength of CAD-CAM and pressed-ceramic crowns. *The Journal of Prosthetic Dentistry,* 82**,** 468-475.

CHEN, J., LI, W., SWAIN, M. V., ALI DARENDELILER, M. & LI, Q. 2014. A periodontal ligament driven remodeling algorithm for orthodontic tooth movement. *Journal of biomechanics,* 47**,** 1689-1695.

CHENG, B., ZHAO, Y., WANG, H. & ZHANG, J. 2003. Three-dimensional finite element stress analysis of different designs of shape in all-ceramic crowns]. *Sichuan da xue xue bao. Yi xue ban= Journal of Sichuan University. Medical science edition,* 34**,** 265.

References

CHINN, R. E. 2002. *Ceramography: preparation and analysis of ceramic microstructures*, USA: ASM International®.

CHO, G. C., DONOVAN, T. E. & CHEE, W. 1998. Clinical experiences with bonded porcelain laminate veneers. *CDA,* 26**,** 121-129.

CHOI, K., CONDON, J. & FERRACANE, J. 2000. The effects of adhesive thickness on polymerization contraction stress of composite. *Journal of Dental Research,* 79**,** 812-817.

CHRISTENSEN, G. J. 2008. Will digital impressions eliminate the current problems with conventional impressions. *J Am Dent Assoc,* 139**,** 761-3.

COELHO, P., SILVA, N., BONFANTE, E., GUESS, P., REKOW, E. & THOMPSON, V. 2009. Fatigue testing of two porcelain–zirconia all-ceramic crown systems. *Dental Materials,* 25**,** 1122-1127.

COWIE, R. R. & BOKSMAN, L. 2007. A philosophical approach to selecting an impression technique. *Oral Health,* 97**,** 18.

CRAIG R, P. J., SAKAGUCHI R 2006. *Craig's Restorative Dental Materials*, 12th ed. Mosby; 2006.

CRANE, F. A. A., CHARLES, J. A. & FURNESS, J. 1997. *Selection and use of engineering materials,* Great Britain: Butterworth-Heinemann.

D'ARCANGELO, C., DE ANGELIS, F., VADINI, M. & D'AMARIO, M. 2011. Clinical evaluation on porcelain laminate veneers bonded with light-cured composite: results up to 7 years. *Clinical oral investigations***,** 1-9.

DATZMANN, G. 1996. CEREC Vitablocs Mark II machinable ceramic. *CAD/CIM in Aesthetic Dentistry. Cerec,* 10**,** 205-215.

DE GEE, A., FEILZER, A. & DAVIDSON, C. 1993. True linear polymerization shrinkage of unfilled resins and composites determined with a linometer. *Dental Materials,* 9**,** 11-14.

DE JAGER, N., DE KLER, M. & VAN DER ZEL, J. M. 2006. The influence of different core material on the FEA-determined stress distribution in dental crowns. *Dental Materials,* 22**,** 234-242.

DE JAGER, N., FEILZER, A. & DAVIDSON, C. 2000. The influence of surface roughness on porcelain strength. *Dental materials,* 16**,** 381-388.

DE JAGER, N., PALLAV, P. & FEILZER, A. J. 2005. The influence of design parameters on the FEA-determined stress distribution in CAD–CAM produced all-ceramic dental crowns. *Dental Materials,* 21**,** 242-251.

DE LA MACORRA, J. C. & PRADÍES, G. 2002. Conventional and adhesive luting cements. *Clinical oral investigations,* 6**,** 198-204.

DE SOUSA MUIANGA, M. I. 2009. *DATA CAPTURE STABILISING DEVICE.* Master Thesis, Johannesburg:Faculty of Health Sciences, University of the Witwatersrand.

DEJAK, B. & MLOTKOWSKI, A. 2008. Three-dimensional finite element analysis of strength and adhesion of composite resin versus ceramic inlays in molars. *The Journal of Prosthetic Dentistry,* 99**,** 131-140.

DEJAK, B. & MŁOTKOWSKI, A. 2013. The influence of ferrule effect and length of cast and FRC posts on the stresses in anterior teeth. *Dental Materials,* 29**,** e227-e237.

DELLA BONA, Á., BORBA, M., BENETTI, P., DUAN, Y. & GRIGGS, J. A. 2013. Three-dimensional finite element modelling of all-ceramic restorations based on micro-CT. *Journal of dentistry,* 41**,** 412-419.

DELLA BONA, A. & KELLY, J. R. 2008. The clinical success of all-ceramic restorations. *The Journal of the American Dental Association,* 139**,** 8S-13S.

DELONG, R. & DOUGLAS, W. H. 1991. An artificial oral environment for testing dental materials. *Biomedical Engineering, IEEE Transactions on,* 38**,** 339-345.

DENRY, I. 2013. How and when does fabrication damage adversely affect the clinical performance of ceramic restorations? *Dental Materials,* 29**,** 85-96.

DENRY, I. & HOLLOWAY, J. A. 2010. Ceramics for dental applications: a review. *Materials,* 3**,** 351-368.

DENRY, I. L. 1996. Recent advances in ceramics for dentistry. *Critical Reviews in Oral Biology & Medicine,* 7**,** 134-143.

References

DESAI, P. D. & DAS, U. K. 2011. Comparison of fracture resistance of teeth restored with ceramic inlay and resin composite: An in vitro study. *Indian Journal of Dental Research,* 22**,** 877.

DIAZ-ARNOLD, A. M., VARGAS, M. A. & HASELTON, D. R. 1999. Current status of luting agents for fixed prosthodontics. *The Journal of Prosthetic Dentistry,* 81**,** 135-141.

DONG, J., LUTHY, H., WOHLWEND, A. & SCHÄRER, P. 1992. Heat-pressed ceramics: technology and strength. *The International journal of prosthodontics,* 5**,** 9.

DRAUGHN, R. A. 1979. Compressive fatigue limits of composite restorative materials. *Journal of dental research,* 58**,** 1093-1096.

DRUMMOND, J. L. & BAPNA, M. S. 2003. Static and cyclic loading of fiber-reinforced dental resin. *Dental Materials,* 19**,** 226-231.

DUARTE, S., LOLATO, A. L., DE FREITAS, C. & DINELLI, W. 2005. SEM analysis of internal adaptation of adhesive restorations after contamination with saliva. *The journal of adhesive dentistry,* 7**,** 51.

DUMSHA, T. & GUTMANN, J. 1985. Clinical techniques for the placement of calcium hydroxide. *The Compendium of continuing education in dentistry,* 6**,** 482.

E.MAX, I. 2014 IPS e.max Cementation and Care. *available from,* http://www.ivoclarvivadent.us/en/ips-emax-cementation-and-care. *[26/7/2014]*.

EDELHOFF, D. & SORENSEN, J. A. 2002. Tooth structure removal associated with various preparation designs for anterior teeth. *The Journal of prosthetic dentistry,* 87**,** 503-509.

EDEN, G. & KACICZ, J. 1987. Dicor crown strength improvement due to bonding. *J Dent Res,* 66**,** 801.

EL-MOWAFY, O. 2001. The use of resin cements in restorative dentistry to overcome retention problems. *JOURNAL-CANADIAN DENTAL ASSOCIATION,* 67**,** 97-102.

ELGUINDY, J. F., MOSTAFA, D. H. & EL AGROUDI, M. A. 2010. Margin Assessment and Fracture Resistance of Adhesively Luted Ceramic Crowns. *Journal of American Science,* 6, 264-273.

ERASLAN, O., AYKENT, F., YÜCEL, M. T. & AKMAN, S. 2009. The finite element analysis of the effect of ferrule height on stress distribution at post-and-core-restored all-ceramic anterior crowns. *Clinical oral investigations,* 13**,** 223-227.

EREIFEJ, N., RODRIGUES, F. P., SILIKAS, N. & WATTS, D. C. 2011. Experimental and FE shear-bonding strength at core/veneer interfaces in bilayered ceramics. *Dental Materials,* 27**,** 590-597.

FARAH, J., CRAIG, R. G. & SIKARSKIE, D. L. 1973. Photoelastic and finite element stress analysis of a restored axisymmetric first molar. *Journal of Biomechanics,* 6**,** 511-520.

FASBINDER, D. J. 2006. Clinical performance of chairside CAD/CAM restorations. *The Journal of the American Dental Association,* 137**,** 22S-31S.

FAVA, L. & SAUNDERS, W. 1999. Calcium hydroxide pastes: classification and clinical indications. *International Endodontic Journal,* 32**,** 257-282.

FELDEN, A., SCHMALZ, G., FEDERLIN, M. & HILLER, K. A. 1998. Retrospective clinical investigation and survival analysis on ceramic inlays and partial ceramic crowns: results up to 7 years. *Clinical oral investigations,* 2**,** 161-167.

FELTON, D., KANOY, B., BAYNE, S. & WIRTHMAN, G. 1991. Effect of in vivo crown margin discrepancies on periodontal health. *The Journal of Prosthetic Dentistry,* 65**,** 357-364.

FILL, T. S., CAREY, J. P., TOOGOOD, R. W. & MAJOR, P. W. 2011. Experimentally determined mechanical properties of, and models for, the periodontal ligament: critical review of current literature. *Journal of dental biomechanics***,** Article ID 312980.

.

FLEMING, G. J. P. & ADDISON, O. 2009. Adhesive cementation and the strengthening of all-ceramic dental restorations. *Journal of Adhesion Science and Technology,* 23**,** 945-959.

FLEMING, G. J. P., DICKENS, M., THOMAS, L. J. & HARRIS, J. J. 2006. The in vitro failure of all-ceramic crowns and the connector area of fixed partial dentures using bilayered ceramic specimens: The influence of core to dentin thickness ratio. *Dental materials,* 22**,** 771-777.

FLEMING, G. J. P., NOLAN, L. & HARRIS, J. J. 2005. The in-vitro clinical failure of all-ceramic crowns and the connector area of fixed partial dentures: the influence of interfacial surface roughness. *Journal of dentistry,* 33**,** 405-412.

FRIEDMAN, M. 2001. Ask the experts. Porcelain veneers. *Journal of esthetic and restorative dentistry: official publication of the American Academy of Esthetic Dentistry...[et al.],* 13**,** 86.

FU, G., DENG, F., WANG, L. & REN, A. 2010. The three-dimension finite element analysis of stress in posterior tooth residual root restored with postcore crown. *Dental Traumatology,* 26**,** 64-69.

GEHRT, M., WOLFART, S., RAFAI, N., REICH, S. & EDELHOFF, D. 2013. Clinical results of lithium-disilicate crowns after up to 9 years of service. *Clinical oral investigations,* Vol.17(1),p.275-284.

GEMALMAZ, D., YORUC, B., OZCAN, M. & ALKUMRU, H. N. 1998. Effect of early water contact on solubility of glass ionomer luting cements. *The Journal of Prosthetic Dentistry,* 80**,** 474-478.

GENG, J.-P., TAN, K. B. & LIU, G.-R. 2001. Application of finite element analysis in implant dentistry: a review of the literature. *The Journal of Prosthetic Dentistry,* 85**,** 585-598.

GIANNETOPOULOS, S., VAN NOORT, R. & TSITROU, E. 2010. Evaluation of the marginal integrity of ceramic copings with different marginal angles using two different CAD/CAM systems. *Journal of dentistry,* 38**,** 980-986.

GIORDANO, I., RUSSELL, A., PELLETIER, L., CAMPBELL, S. & POBER, R. 1995. Flexural strength of an infused ceramic, glass ceramic, and feldspathic porcelain. *The Journal of prosthetic dentistry,* 73**,** 411-418.

GIORDANO II, R. A., PELLETIER, L., CAMPBELL, S. & POBER, R. 1995. Flexural strength of an infused ceramic, glass ceramic, and feldspathic porcelain. *The Journal of prosthetic dentistry,* 73**,** 411-418.

GLADYS, S., VAN MEERBEEK, B., BRAEM, M., LAMBRECHTS, P. & VANHERLE, G. 1997. Comparative physico-mechanical characterization of new hybrid restorative materials with conventional glass-ionomer and resin composite restorative materials. *Journal of dental research,* 76**,** 883-894.

GOEL, V. K., KHERA, S. C., GURUSAMI, S. & CHEN, R. 1992. Effect of cavity depth on stresses in a restored tooth. *The Journal of Prosthetic Dentistry,* 67**,** 174-183.

GOEL, V. K., KHERA, S. C., RALSTON, J. L. & CHANG, K. H. 1991. Stresses at the dentinoenamel junction of human teeth--A finite element investigation. *The Journal of Prosthetic Dentistry,* 66**,** 451-459.

GOEL, V. K., KHERA, S. C. & SINGH, K. 1990. Clinical implications of the response of enamel and dentin to masticatory loads. *The Journal of Prosthetic Dentistry,* 64**,** 446-454.

GOETZEN, N., NATT, G., MORLOCK, M. M. & TINCHERT, J. Numerical stress and reliability analysis of all-ceramic fixed-partial dentures. Proceedings of the 2003 Summer Bioengineering Conference, ASME, Key Biscayne, 2003. 869-870.

GONZAGA, C. C., CESAR, P. F., OKADA, C. Y., FREDERICCI, C., BENEDUCE NETO, F. & YOSHIMURA, H. N. 2008. Mechanical properties and porosity of dental glass-ceramics hot-pressed at different temperatures. *Materials Research,* 11**,** 301-306.

GROTEN, M., AXMANN, D., PRÖBSTER, L. & WEBER, H. 2000. Determination of the minimum number of marginal gap measurements required for practical in vitro testing. *The Journal of Prosthetic Dentistry,* 83**,** 40-49.

GUAZZATO, M., ALBAKRY, M., QUACH, L. & SWAIN, M. V. 2004a. Influence of grinding, sandblasting, polishing and heat treatment on the flexural strength of a glass-infiltrated alumina-reinforced dental ceramic. *Biomaterials,* 25**,** 2153-2160.

GUAZZATO, M., ALBAKRY, M., RINGER, S. P. & SWAIN, M. V. 2004b. Strength, fracture toughness and microstructure of a selection of all-ceramic materials. Part I. Pressable and alumina glass-infiltrated ceramics. *Dental Materials,* 20**,** 441-448.

HA, S.-R., KIM, S.-H., HAN, J.-S., YOO, S.-H., JEONG, S.-C., LEE, J.-B. & YEO, I.-S. 2013. The influence of various core designs on stress distribution in the veneered zirconia crown: a finite element analysis study. *The journal of advanced prosthodontics,* 5**,** 187-197.

HABELITZ, S., MARSHALL, S., MARSHALL, G. & BALOOCH, M. 2001. Mechanical properties of human dental enamel on the nanometre scale. *Archives of Oral Biology,* 46**,** 173-183.

HAMROCK, B. J., JACOBSON, B. O., SCHMID, S. R. & JACOBSON, B. 1999. *Fundamentals of machine elements*, WCB/McGraw-Hill Singapore, page 242-253.

.

HANNIG, C., WESTPHAL, C., BECKER, K. & ATTIN, T. 2005. Fracture resistance of endodontically treated maxillary premolars restored with CAD/CAM ceramic inlays. *The Journal of Prosthetic Dentistry,* 94**,** 342-349.

HARVEY, C. K. & KELLY, J. R. 1996. Contact damage as a failure mode during in vitro testing. *Journal of Prosthodontics,* 5**,** 95-100.

HASEGAWA, A., SHINYA, A., NAKASONE, Y., LASSILA, L. V. J. & VALLITTU, P. K. 2010. Development of 3D CAD/FEM analysis system for natural teeth and jaw bone constructed from X-ray CT images. *International journal of biomaterials,* vol(2010): Article ID 659802, 1-7.

HASELTON, D. R., DIAZ-ARNOLD, A. M. & HILLIS, S. L. 2000. Clinical assessment of high-strength all-ceramic crowns. *The Journal of prosthetic dentistry,* 83**,** 396-401.

HASSAN, M. A., ROGERS, R. J. & GERBER, A. G. 2011. Damping-controlled fluidelastic instability forces in multi-span tubes with loose supports. *Nuclear Engineering and Design,* 241**,** 2666-2673.

HAYASHI, M., SUGETA, A., TAKAHASHI, Y., IMAZATO, S. & EBISU, S. 2008. Static and fatigue fracture resistances of pulpless teeth restored with post–cores. *Dental Materials,* 24**,** 1178-1186.

HE, L. H. & SWAIN, M. V. 2007. Contact induced deformation of enamel. *Applied physics letters,* 90**,** 171916-171916-3.

HEINTZE, S., ALBRECHT, T., CAVALLERI, A. & STEINER, M. 2011. A new method to test the fracture probability of all-ceramic crowns with a dual-axis chewing simulator. *Dental Materials,* 27**,** e10-e19.

HICKEL, R. & MANHART, J. 2000. Longevity of restorations in posterior teeth and reasons for failure. *The journal of adhesive dentistry,* 3**,** 45-64.

HILL, E. & LOTT, J. 2011. A clinically focused discussion of luting materials. *Australian dental journal,* 56**,** 67-76.

HILL, E. E. 2007. Dental cements for definitive luting: a review and practical clinical considerations. *Dental Clinics of North America,* 51**,** 643-658.

HOJJATIE, B. & ANUSAVICE, K. 1990. Three-dimensional finite element analysis of glass-ceramic dental crowns. *Journal of biomechanics,* 23**,** 1157-1166.

IIZUKA, H., BRAUER, G., RUPP, N., OHASHI, M. & PAFFENBARGER, G. 1987. Forces fracturing cements at die interfaces and their dependence on film thickness. *Dental Materials,* 3**,** 187-193.

ISGRŅ, G., PALLAV, P., VAN DER ZEL, J. M. & FEILZER, A. J. 2003. The influence of the veneering porcelain and different surface treatments on the biaxial flexural strength of a heat-pressed ceramic. *The Journal of prosthetic dentistry,* 90**,** 465-473.

IVOCLAR/VIVADENT & PRODUCTS 2014. Ivoclar/ vivadent products; All-Ceramics Download Center, available from, http://www.ivoclarvivadent.co.uk/en/products/all-ceramics/all-ceramics-download-center.[26/07/2014].

IWERNER, G. C. 1998. Effects of Preparation and Luting System on All-Ceramic Computer.

JAECQUES, S., VAN OOSTERWYCK, H., MURARU, L., VAN CLEYNENBREUGEL, T., DE SMET, E., WEVERS, M., NAERT, I. & VANDER SLOTEN, J. 2004. Individualised, micro CT-based finite element modelling as a tool for biomechanical analysis related to tissue engineering of bone. *Biomaterials,* 25**,** 1683-1696.

JEDYNAKIEWICZ, N. & MARTIN, N. 2001. CEREC: science, research, and clinical application. *Compendium of continuing education in dentistry (Jamesburg, NJ: 1995),* 22**,** 7.

References

JENSEN, M., SHETH, J. & TOLLIVER, D. 1989. Etched-porcelain resin-bonded full-veneer crowns: in vitro fracture resistance. *Compendium (Newtown, Pa.),* 10**,** 336.

JIANG, W., BO, H., YONGCHUN, G. & LONGXING, N. 2010. Stress distribution in molars restored with inlays or onlays with or without endodontic treatment: a three-dimensional finite element analysis. *The Journal of Prosthetic Dentistry,* 103**,** 6-12.

JONGSMA, L. A., KLEVERLAAN, C. J., PALLAV, P. & FEILZER, A. J. 2012. Influence of polymerization mode and C-factor on cohesive strength of dual-cured resin cements. *Dental Materials*.

JUNG, M., LOMMEL, D. & KLIMEK, J. 2005. The imaging of root canal obturation using micro-CT. *International Endodontic Journal,* 38**,** 617-626.

KAMPOSIORA, P., PAPAVASILIOUS, G., BAYNE, S. C. & FELTON, D. A. 1994. Finite element analysis estimates of cement microfracture under complete veneer crowns. *The Journal of prosthetic dentistry,* 71**,** 435-441.

KARAKAYA, S., SENGUN, A. & ÖZER, F. 2005. Evaluation of internal adaptation in ceramic and composite resin inlays by silicon replica technique. *Journal of oral rehabilitation,* 32**,** 448-453.

KARATASLI, Ö., KURSOGLU, P., CAPA, N. & KAZAZOGLU, E. 2011. Comparison of the marginal fit of different coping materials and designs producted by computer aided manufacturing systems. *Dental materials journal,* Vol.30(1),p.97-102.

KASSEM, A. S., ATTA, O. & EL-MOWAFY, O. 2012. Fatigue resistance and microleakage of CAD/CAM ceramic and composite molar crowns. *Journal of Prosthodontics,* 21**,** 28-32.

KAWAI, N., LIN, J., YOUMARU, H., SHINYA, A. & SHINYA, A. 2012. Effects of three luting agents and cyclic impact loading on shear bond strengths to zirconia with tribochemical treatment. *Journal of Dental Sciences,* Vol.7(2),p.118-124.

KAYABAŞI, O., YÜZBASIOĞLU, E. & ERZINCANLI, F. 2006. Static, dynamic and fatigue behaviors of dental implant using finite element method. *Advances in engineering software,* 37**,** 649-658.

KELLY, J., GIORDANO, R., POBER, R. & CIMA, M. 1990. Fracture surface analysis of dental ceramics: clinically failed restorations. *The International journal of prosthodontics,* 3**,** 430.

KELLY, J., TESK, J. & SORENSEN, J. 1995. Failure of all-ceramic fixed partial dentures in vitro and in vivo: analysis and modeling. *Journal of Dental research,* 74**,** 1253-1258.

KELLY, J. R. 1999. Clinically relevant approach to failure testing of all-ceramic restorations. *The Journal of prosthetic dentistry,* 81**,** 652-661.

KELLY, J. R. 1995. Perspectives on strength. *Dental Materials,* 11**,** 103-110.

KELLY, J. R., CAMPBELL, S. D. & BOWEN, H. K. 1989. Fracture-surface analysis of dental ceramics. *The Journal of prosthetic dentistry,* 62**,** 536-541.

KELLY, J. R., NISHIMURA, I. & CAMPBELL, S. D. 1996. Ceramics in dentistry: historical roots and current perspectives. *The Journal of Prosthetic Dentistry,* 75**,** 18-32.

KIDD, E. A. M. & SMITH, B. G. N. 2003. *Pickard's manual of operative dentistry*, Oxford university press.

KINNEY, J., MARSHALL, S. & MARSHALL, G. 2003. The mechanical properties of human dentin: a critical review and re-evaluation of the dental literature. *Critical Reviews in Oral Biology & Medicine,* 14**,** 13-29.

KIOUS, A. R., ROBERTS, H. W. & BRACKETT, W. W. 2009. Film thicknesses of recently introduced luting cements. *The Journal of Prosthetic Dentistry,* 101**,** 189-192.

KLEIER, D., AVERBACH, R. & KAWULOK, T. 1985. Efficient calcium hydroxide placement within the root canal. *The Journal of Prosthetic Dentistry,* 53**,** 509.

KLEIN, C. A. 2009. Characteristic strength, Weibull modulus, and failure probability of fused silica glass. *Optical Engineering,* 48**,** 113401.

KO, C.-C., ROCHA, E. P. & LARSON, M. 2012. Past, Present and Future of Finite Element Analysis in Dentistry. *Biomedical Applications to Industrial Developments,* Finite Element Analysis - From Biomedical Applications to Industrial Developments, Dr.David Moratal (Ed.), ISBN: 978-953-51-0474-2, InTech, Available from:http://www.intechopen.com/books/finite-element-

analysis-from-biomedical-applications-to-industrial-developments/past-present-and-future-of-finite-element-analysis-in-dentistry**,** 1-25.

KOHORST, P., HERZOG, T. J., BORCHERS, L. & STIESCH-SCHOLZ, M. 2007. Load-bearing capacity of all-ceramic posterior four-unit fixed partial dentures with different zirconia frameworks. *European journal of oral sciences,* 115**,** 161-166.

KRÄMER, N. & FRANKENBERGER, R. 2005. Clinical performance of bonded leucite-reinforced glass ceramic inlays and onlays after eight years. *Dental Materials,* 21**,** 262-271.

KRÄMER, N., LOHBAUER, U. & FRANKENBERGER, R. 2000. Adhesive luting of indirect restorations. *American Journal of Dentistry,* vol.13(Spec No):60D-76D.

KUROE, T., ITOH, H., CAPUTO, A. A. & KONUMA, M. 2000. Biomechanics of cervical tooth structure lesions and their restoration. *Quintessence international (Berlin, Germany: 1985),* 31**,** 267.

KUSUMOTO, N., SOHMURA, T., YAMADA, S., WAKABAYASHI, K., NAKAMURA, T. & YATANI, H. 2006. Application of virtual reality force feedback haptic device for oral implant surgery. *Clinical oral implants research,* 17**,** 708-713.

LAUNEY, M. E. & RITCHIE, R. O. 2009. On the fracture toughness of advanced materials. *Advanced Materials,* 21**,** 2103-2110.

LAURENT, M., SCHEER, P., DEJOU, J. & LABORDE, G. 2008. Clinical evaluation of the marginal fit of cast crowns–validation of the silicone replica method. *Journal of oral rehabilitation,* 35**,** 116-122.

LAWN, B., BHOWMICK, S., BUSH, M. B., QASIM, T., REKOW, E. D. & ZHANG, Y. 2007. Failure Modes in Ceramic-Based Layer Structures: A Basis for Materials Design of Dental Crowns. *Journal of the American Ceramic Society,* 90**,** 1671-1683.

LAWN, B., DENG, Y., LLOYD, I., JANAL, M., REKOW, E. & THOMPSON, V. 2002. Materials design of ceramic-based layer structures for crowns. *Journal of dental research,* 81**,** 433-438.

LAWN, B. R., PAJARES, A., ZHANG, Y., DENG, Y., POLACK, M. A., LLOYD, I. K., REKOW, E. D. & THOMPSON, V. P. 2004. Materials design in the performance of all-ceramic crowns. *Biomaterials,* 25**,** 2885-2892.

LEE, J. J. W., KWON, J. Y., CHAI, H., LUCAS, P., THOMPSON, V. & LAWN, B. 2009. Fracture modes in human teeth. *Journal of dental research,* 88**,** 224-228.

LEEVAILOJ, C., PLATT, J. A., COCHRAN, M. A. & MOORE, B. K. 1998. In vitro study of fracture incidence and compressive fracture load of all-ceramic crowns cemented with resin-modified glass ionomer and other luting agents. *The Journal of Prosthetic Dentistry,* 80**,** 699-707.

LEWIS, G. 1993. A parametric finite element analysis study of the stresses in an endosseous implant. *Bio-medical materials and engineering,* 4**,** 495-502.

LIA, Z. C. & WHITE, S. N. 1999. Mechanical properties of dental luting cements. *The Journal of Prosthetic Dentistry,* 81**,** 597-609.

LIN, C. L., CHANG, C. H. & KO, C. C. 2001a. Multifactorial analysis of an MOD restored human premolar using auto-mesh finite element approach. *Journal of oral rehabilitation,* 28**,** 576-585.

LIN, S.-K., LEE, Y.-L. & LU, M.-W. 2001b. Evaluation of the staircase and the accelerated test methods for fatigue limit distributions. *International journal of fatigue,* 23**,** 75-83.

LIN, W. S., ERCOLI, C., FENG, C. & MORTON, D. 2012. The Effect of Core Material, Veneering Porcelain, and Fabrication Technique on the Biaxial Flexural Strength and Weibull Analysis of Selected Dental Ceramics. *Journal of Prosthodontics,* Vol.21(5),p.353-362.

LIU, B., LU, C., WU, Y., ZHANG, X., AROLA, D. & ZHANG, D. 2011. The Effects of Adhesive Type and Thickness on Stress Distribution in Molars Restored with All-Ceramic Crowns. *Journal of Prosthodontics,* 20**,** 35-44.

LIU, S. Y. & CHEN, I. 1991. Fatigue of Yttria-Stabilized Zirconia: I, Fatigue Damage, Fracture Origins, and Lifetime Prediction. *Journal of the American Ceramic Society,* 74**,** 1197-1205.

References

LOHBAUER, U., HORST, T., FRANKENBERGER, R., KRÄMER, N. & PETSCHELT, A. 2003. Flexural fatigue behavior of resin composite dental restoratives. *Dental Materials,* 19**,** 435-440.

LOHBAUER, U., PETSCHELT, A. & GREIL, P. 2002. Lifetime prediction of CAD/CAM dental ceramics. *Journal of biomedical materials research,* 63**,** 780-785.

LÜTHY, H., FILSER, F., LOEFFEL, O., SCHUMACHER, M., GAUCKLER, L. J. & HAMMERLE, C. H. 2005. Strength and reliability of four-unit all-ceramic posterior bridges. *Dental Materials,* 21**,** 930-937.

MA, L., GUESS, P. C. & ZHANG, Y. 2013. Load-bearing properties of minimal-invasive monolithic lithium disilicate and zirconia occlusal onlays: finite element and theoretical analyses. *Dental materials: official publication of the Academy of Dental Materials,* 29**,** 742-751.

MAGNE, P. 2007. Efficient 3D finite element analysis of dental restorative procedures using micro-CT data. *Dental Materials,* 23**,** 539-548.

MAGNE, P. 2010. Virtual prototyping of adhesively restored, endodontically treated molars. *The Journal of Prosthetic Dentistry,* 103**,** 343-351.

MAGNE, P. & BELSER, U. C. 2003. Porcelain versus composite inlays/onlays: effects of mechanical loads on stress distribution, adhesion, and crown flexure. *The International journal of periodontics & restorative dentistry,* 23**,** 543.

MAGNE, P., KWON, K. R., BELSER, U. C., HODGES, J. S. & DOUGLAS, W. H. 1999a. Crack propensity of porcelain laminate veneers: a simulated operatory evaluation. *The Journal of Prosthetic Dentistry,* 81**,** 327-334.

MAGNE, P. & OGANESYAN, T. 2009. CT scan-based finite element analysis of premolar cuspal deflection following operative procedures. *The International journal of periodontics & restorative dentistry,* 29**,** 361.

MAGNE, P. & TAN, D. T. 2008. Incisor compliance following operative procedures: a rapid 3-D finite element analysis using micro-CT data. *The journal of adhesive dentistry,* 10**,** 49.

MAGNE, P., VERSLUIS, A. & DOUGLAS, W. H. 1999b. Effect of luting composite shrinkage and thermal loads on the stress distribution in porcelain laminate veneers. *The Journal of Prosthetic Dentistry,* 81**,** 335-344.

MAHLER, D. & PEYTON, F. 1955. Photoelasticity as a research technique for analyzing stresses in dental structures. *Journal of dental research,* 34**,** 831-838.

MAIR, L., LANGFIELD, A., WALTON, R. & MANSOUR, Y. 2011. Correlation of shear strength, fatigue limit and fatigue life of six high impact denture resins. *Dental Materials,* 27**,** e64-e65.

MALAMENT, K., SOCRANSKY, S., THOMPSON, V. & REKOW, D. 2002. Survival of glass-ceramic materials and involved clinical risk: variables affecting long-term survival. *Practical procedures & aesthetic dentistry: PPAD***,** 5-11.

MALAMENT, K. A. & SOCRANSKY, S. S. 2001. Survival of Dicor glass-ceramic dental restorations over 16 years. Part III: effect of luting agent and tooth or tooth-substitute core structure. *The Journal of Prosthetic Dentistry,* 86**,** 511-519.

MANDAL, S., RAY, A. K. & RAY, A. K. 2004. Correlation between the mechanical properties and the microstructural behaviour of Al< sub> 2</sub> O< sub> 3</sub>–(Ag–Cu–Ti) brazed joints. *Materials Science and Engineering: A,* 383**,** 235-244.

MARQUARDT, P. & STRUB, J. R. 2006. Survival rates of IPS empress 2 all-ceramic crowns and fixed partial dentures: results of a 5-year prospective clinical study. *Quintessence international (Berlin, Germany: 1985),* 37**,** 253.

MARTIN, N. & JEDYNAKIEWICZ, N. 2000. Interface dimensions of CEREC-2 MOD inlays. *Dental materials,* 16**,** 68-74.

MARTIN, N. & JEDYNAKIEWICZ, N. 1998. Measurement of water sorption in dental composites. *Biomaterials,* 19**,** 77-83.

MARTIN, N., JEDYNAKIEWICZ, N. M. & FISHER, A. C. 2003. Hygroscopic expansion and solubility of composite restoratives. *Dental Materials,* 19**,** 77-86.

MARTÍNEZ FERNÁNDEZ, J., MUNOZ, A., DE ARELLANO LÓPEZ, A., VALERA FERIA, F., DOMINGUEZ-RODRIGUEZ, A. & SINGH, M. 2003. Microstructure–mechanical properties correlation in siliconized silicon carbide ceramics. *Acta Materialia,* 51**,** 3259-3275.

MCCABE, J., CARRICK, T., CHADWICK, R. & WALLS, A. 1990a. Alternative approaches to evaluating the fatigue characteristics of materials. *Dental Materials,* 6**,** 24-28.

MCCABE, J., WATTS, D., WILSON, H. & WORTHINGTON, H. 1990b. An investigation of test-house variability in the mechanical testing of dental materials and the statistical treatment of results. *Journal of dentistry,* 18**,** 90-97.

MCLAREN, E. A. 1998. All-ceramic alternatives to conventional metal-ceramic restorations. *Compendium,* 19**,** 307-25.

MCLAREN, E. A. & CAO, P. T. 2009. Ceramics in dentistry—part I: classes of materials. *Inside Dentistry,* 5**,** 94-103.

MCLAREN, E. A. & GIORDANO, R. 2005. Zirconia-based ceramics: material properties, esthetics, and layering techniques of a new veneering porcelain, VM9. *Quintessence Dent Technol,* 28**,** 99-111.

MCLAREN, E. A., GIORDANO, R., POBER, R. & ABOZENADA, B. 2003. Material testing and layering techniques of a new two-phase all-glass veneering porcelain for bonded porcelain and high-alumina frameworks. *Quintessence Dent Technol,* 26**,** 69-81.

MCLAREN, E. A. & WHITE, S. N. 2000. Survival of In-Ceram crowns in a private practice: a prospective clinical trial. *The Journal of Prosthetic Dentistry,* 83**,** 216-222.

MCLEAN, J. & VON FRAUNHOFER, J. 1971. The estimation of cement film thickness by an in vivo technique. *British dental journal,* 131**,** 107.

MEHL, A. & HICKEL, R. 1999. Current state of development and perspectives of machine-based production methods for dental restorations. *International Journal of Computerized Dentistry***,** 2(1):9-35.

MEYER, U., VOLLMER, D., RUNTE, C., BOURAUEL, C. & JOOS, U. 2001. Bone loading pattern around implants in average and atrophic edentulous maxillae: a finite-element analysis. *Journal of Cranio-Maxillofacial Surgery,* 29**,** 100-105.

MEYERS, M. A. & CHAWLA, K. K. 2009. *Mechanical behavior of materials*, Cambridge University: Press Cambridge.

MIYAZAKI, T., HOTTA, Y., KUNII, J., KURIYAMA, S. & TAMAKI, Y. 2009. A review of dental CAD/CAM: current status and future perspectives from 20 years of experience. *Dental materials journal,* 28**,** 44-56.

MOHAMMED, S. & DESAI, H. 2014. Basic Concepts of Finite Element Analysis and its Applications in Dentistry: An Overview. *Oral Hyg Health,* 2**,** 2332-0702.1000156.

MOLDOVAN, O., LUTHARDT, R. G., CORCODEL, N. & RUDOLPH, H. 2011. Three-dimensional fit of CAD/CAM-made zirconia copings. *Dental Materials,* Vol.27(12),p.1273-1278.

MOLIN, M. K., KARLSSON, S. L. & KRISTIANSEN, M. S. 1996. Influence of film thickness on joint bend strength of a ceramic/resin composite joint. *Dental Materials,* 12**,** 245-249.

MORENA, R., BEAUDREAU, G., LOCKWOOD, P., EVANS, A. & FAIRHURST, C. 1986. Fatigue of dental ceramics in a simulated oral environment. *Journal of Dental research,* 65**,** 993-997.

MÖRMANN, W., BRANDESTINI, M., LUTZ, F. & BARBAKOW, F. 1989. Chairside computer-aided direct ceramic inlays. *Quintessence international (Berlin, Germany: 1985),* 20**,** 329.

MÖRMANN, W. H. 2006. The evolution of the CEREC system. *The Journal of the American Dental Association,* 137**,** 7S.

MÖRMANN, W. H. 2002. An up to 5-year clinical evaluation of posterior In-Ceram CAD/CAM core crowns. *The International journal of prosthodontics,* 15**,** 451.

MOSCOVICH, H., ROETERS, F., VERDONSCHOT, N., DE KANTER, R. & CREUGERS, N. 1998. Effect of composite basing on the resistance to bulk fracture of industrial porcelain inlays. *Journal of dentistry,* 26**,** 183-189.

MOSHAVERINIA, A., ROOHPOUR, N., CHEE, W. W. L. & SCHRICKER, S. R. 2012. A review of polyelectrolyte modifications in conventional glass-ionomer dental cements. *J. Mater. Chem.,* 22**,** 2824-2833.

MOU, S. H., CHAI, T., WANG, J. S. & SHIAU, Y. Y. 2002. Influence of different convergence angles and tooth preparation heights on the internal adaptation of Cerec crowns. *The Journal of Prosthetic Dentistry,* 87**,** 248-255.

NAERT I, VAN DER DONCK A & L., B. 2005 Precision of fit and clinical evaluation of all-ceramic full restorations followed between 0.5 and 5 years. *J Oral Rehabil,* 32**,** 51-7.

NAKAMURA, T., DEI, N., KOJIMA, T. & WAKABAYASHI, K. 2003. Marginal and internal fit of Cerec 3 CAD/CAM all-ceramic crowns. *The International journal of prosthodontics,* 16**,** 244.

NAM, J., RAIGRODSKI, A. J. & HEINDL, H. 2008. Utilization of Multiple Restorative Materials in Full-Mouth Rehabilitation: A Clinical Report. *Journal of Esthetic and Restorative Dentistry,* 20**,** 251-263.

NELSON, W. B. 2009. *Accelerated testing: statistical models, test plans, and data analysis,* USA, A John Wiley & Sons, Inc.

NELSON, W. B. 2005. A bibliography of accelerated test plans. *Reliability, IEEE Transactions on,* 54**,** 194-197.

NIELSEN, R. B., ALYASSIN, A. M., PETERS, D. D., CARNES, D. L. & LANCASTER, J. 1995. Microcomputed tomography: an advanced system for detailed endodontic research. *Journal of Endodontics,* 21**,** 561-568.

NOROOZI, N., THOMSON, J. A., NOROOZI, N., SCHAFER, L. L. & HATZIKIRIAKOS, S. G. 2012. Viscoelastic behaviour and flow instabilities of biodegradable poly (ε-caprolactone) polyesters. *Rheologica acta,* 51**,** 179-192.

ODÉN, A., ANDERSSON, M., KRYSTEK-ONDRACEK, I. & MAGNUSSON, D. 1998. Five-year clinical evaluation of Procera AllCeram crowns. *The Journal of Prosthetic Dentistry,* 80**,** 450-456.

OHTANI, T., KUSUMOTO, N., WAKABAYASHI, K., YAMADA, S., NAKAMURA, T., KUMAZAWA, Y., YATANI, H. & SOHMURA, T. 2009. Application of haptic device to implant dentistry—accuracy verification of drilling into a pig bone. *Dental materials journal,* 28**,** 75-81.

OHYAMA, T., YOSHINARI, M. & ODA, Y. 1999. Effects of cyclic loading on the strength of all-ceramic materials. *The International journal of prosthodontics,* 12**,** 28.

OTTO, T. 2004. Computer-aided direct all-ceramic crowns: preliminary 1-year results of a prospective clinical study. *International Journal of Periodontics and Restorative Dentistry,* 24**,** 446-455.

OTTO, T. & DE NISCO, S. 2002. Computer-aided direct ceramic restorations: a 10-year prospective clinical study of Cerec CAD/CAM inlays and onlays. *Int J Prosthodont***,** 15(2):122-8.

PADIPATVUTHIKUL, P. & MAIR, L. H. 2008. Comparison of Shear Bond Strength, Fatigue Limit and Fatigue Life in resin-bonded metal to enamel bonds. *Dental Materials,* 24**,** 674-680.

PAGNIANO JR, R. P., SEGHI, R. R., ROSENSTIEL, S. F., WANG, R. & KATSUBE, N. 2005. The effect of a layer of resin luting agent on the biaxial flexure strength of two all-ceramic systems. *The Journal of Prosthetic Dentistry,* 93**,** 459-466.

PAGNIANO, R. P., SEGHI, R. R., ROSENSTIEL, S. F., WANG, R. & KATSUBE, N. 2005. The effect of a layer of resin luting agent on the biaxial flexure strength of two all-ceramic systems. *The Journal of prosthetic dentistry,* 93**,** 459-466.

PALAMARA, D., PALAMARA, J., TYAS, M. & MESSER, H. 2000. Strain patterns in cervical enamel of teeth subjected to occlusal loading. *Dental materials,* 16**,** 412-419.

PALLIS, K., GRIGGS, J. A., WOODY, R. D., GUILLEN, G. E. & MILLER, A. W. 2004. Fracture resistance of three all-ceramic restorative systems for posterior applications. *The Journal of Prosthetic Dentistry,* 91**,** 561-569.

PAMEIJER, C. H. 2012. A review of luting agents. *International Journal of Dentistry,* 2012.

PASHLEY, E. L., ZHANG, Y., E LOCKWOOD, P., RUEGGEBERG, F. A. & PASHLEY, D. H. 1998. Effects of HEMA on water evaporation from water–HEMA mixtures. *Dental Materials,* 14**,** 6-10.

PATRA, A. K., DEPAOLO, J. M., D'SOUZA, K. S., DETOLLA, D. & MEENAGHAN, M. A. 1998. Guidelines for analysis and redesign of dental implants. *Implant Dentistry,* 7**,** 355-368.

PEGORETTI, A., FAMBRI, L., ZAPPINI, G. & BIANCHETTI, M. 2002. Finite element analysis of a glass fibre reinforced composite endodontic post. *Biomaterials,* 23**,** 2667-2682.

PETERS, M. & POORT, H. 1983. Biomechanical stress analysis of the amalgam-tooth interface. *Journal of dental research,* 62**,** 358-362.

PEUMANS, M., VAN MEERBEEK, B., LAMBRECHTS, P. & VANHERLE, G. 2000. Porcelain veneers: a review of the literature. *Journal of dentistry,* 28**,** 163-177.

PIDDOCK, V. & QUALTROUGH, A. 1990. Dental ceramics—an update. *Journal of dentistry,* 18**,** 227-235.

PIEMJAI, M., MIYASAKA, K., IWASAKI, Y. & NAKABAYASHI, N. 2002. Comparison of microleakage of three acid-base luting cements versus one resin-bonded cement for Class V direct composite inlays. *The Journal of Prosthetic Dentistry,* 88**,** 598-603.

PIERRISNARD, L., BOHIN, F., RENAULT, P. & BARQUINS, M. 2002. Corono-radicular reconstruction of pulpless teeth: a mechanical study using finite element analysis. *The Journal of Prosthetic Dentistry,* 88**,** 442-448.

PIETRABISSA, R., QUAGLINI, V. & VILLA, T. 2002. Experimental Methods in Testing of Tissues and Implants*. *Meccanica,* 37**,** 477-488.

PILO, R., CARDASH, H. S., LEVIN, E. & ASSIF, D. 2002. Effect of core stiffness on the in vitro fracture of crowned, endodontically treated teeth. *The Journal of Prosthetic Dentistry,* 88**,** 302-306.

PIWOWARCZYK, A., LAUER, H. C. & SORENSEN, J. A. 2004. In vitro shear bond strength of cementing agents to fixed prosthodontic restorative materials. *The Journal of Prosthetic Dentistry,* 92**,** 265-273.

PIWOWARCZYK, A., OTTL, P. & LAUER, H. C. 2001. Laboratory strength of glass ionomer and zinc phosphate cements. *Journal of Prosthodontics,* 10**,** 140-147.

PLOTINO, G., GRANDE, N. M., PECCI, R., BEDINI, R., PAMEIJER, C. H. & SOMMA, F. 2006. Three-dimensional imaging using microcomputed tomography for studying tooth macromorphology. *J Am Dent Assoc,* 137**,** 1555-1561.

POPOWICS, T., RENSBERGER, J. & HERRING, S. 2001. The fracture behaviour of human and pig molar cusps. *Archives of Oral Biology,* 46**,** 1-12.

POSPIECH, P. 2002. All-ceramic crowns: bonding or cementing? *Clinical oral investigations,* 6**,** 189-197.

POTIKET, N., CHICHE, G. & FINGER, I. M. 2004. In vitro fracture strength of teeth restored with different all-ceramic crown systems. *The Journal of Prosthetic Dentistry,* 92**,** 491-495.

PRAKKI, A., CILLI, R., DA COSTA, A. U., DE PAIVA GONÇALVES, S. E., LIA MONDELLI, R. F. & PEREIRA, J. C. 2007. Effect of resin luting film thickness on fracture resistance of a ceramic cemented to dentin. *Journal of Prosthodontics,* 16**,** 172-178.

PRÖBSTER, L. 1996. Four year clinical study of glass-infiltrated, sintered alumina crowns. *Journal of oral rehabilitation,* 23**,** 147-151.

PRÖBSTER, L. 1993. Survival rate of In-Ceram restorations. *The International journal of prosthodontics,* 6**,** 259.

PRÖBSTER, L., GEIS-GERSTORFER, J., KIRCHNER, E. & KANJANTRA, P. 1997. In vitro evaluation of a glass–ceramic restorative material. *Journal of oral rehabilitation,* 24**,** 636-645.

PROOS, K. A., SWAIN, M. V., IRONSIDE, J. & STEVEN, G. P. 2003. Influence of cement on a restored crown of a first premolar using finite element analysis. *International Journal of Prosthodontics,* 16**,** 82-90.

PROOS, K. A., SWAIN, M. V., IRONSIDE, J. & STEVEN, G. P. 2002. Influence of margin design and taper abutment angle on a restored crown of a first premolar using finite element analysis. *The International journal of prosthodontics,* 16**,** 442-449.

QUALTROUGH, A. & PIDDOCK, V. 1997. Ceramics update. *Journal of dentistry,* 25**,** 91-95.

QUALTROUGH, A., PIDDOCK, V. & KYPREOU, V. 1993. A comparison of two in vitro methods for assessing the fitting accuracy of composite inlays. *British dental journal,* 174**,** 450-454.

QUINN, J., SUNDAR, V. & LLOYD, I. 2003. Influence of microstructure and chemistry on the fracture toughness of dental ceramics. *Dental Materials,* 19**,** 603-611.

QUINN, J. B., QUINN, G. D., KELLY, J. R. & SCHERRER, S. S. 2005. Fractographic analyses of three ceramic whole crown restoration failures. *Dental Materials,* 21**,** 920-929.

RAIGRODSKI, A. J. 2004. Contemporary materials and technologies for all-ceramic fixed partial dentures: a review of the literature. *The Journal of prosthetic dentistry,* 92**,** 557-562.

REEH, E. S., MESSER, H. H. & DOUGLAS, W. H. 1989. Reduction in tooth stiffness as a result of endodontic and restorative procedures. *Journal of Endodontics,* 15**,** 512-516.

REICH, S., UHLEN, S., GOZDOWSKI, S. & LOHBAUER, U. 2011. Measurement of cement thickness under lithium disilicate crowns using an impression material technique. *Clinical oral investigations,* 15**,** 521-526.

REICH, S., WICHMANN, M., NKENKE, E. & PROESCHEL, P. 2005. Clinical fit of all-ceramic three-unit fixed partial dentures, generated with three different CAD/CAM systems. *Eur J Oral Sci,* 113**,** 174-9.

REISS, B. & WALTHER, W. 2000. Clinical long-term results and 10-year Kaplan-Meier analysis of Cerec restorations. *International Journal of Computerized Dentistry,* 3: 9-23.

REKOW, D. & THOMPSON, V. P. 2007. Engineering long term clinical success of advanced ceramic prostheses. *Journal of Materials Science: Materials in Medicine,* 18**,** 47-56.

REKOW, E. D., HARSONO, M., JANAL, M., THOMPSON, V. P. & ZHANG, G. 2006. Factorial analysis of variables influencing stress in all-ceramic crowns. *Dental materials,* 22**,** 125-132.

RICE, R. 1996. Grain size and porosity dependence of ceramic fracture energy and toughness at 22 C. *Journal of materials science,* 31**,** 1969-1983.

RICE, R. W. 2002. Monolithic and composite ceramic machining flaw-microstructure-strength effects: model evaluation. *Journal of the European Ceramic Society,* 22**,** 1411-1424.

RIEGER, M., MAYBERRY, M. & BROSE, M. 1990. Finite element analysis of six endosseous implants. *The Journal of prosthetic dentistry,* 63**,** 671-676.

RIOS, H., MA, D., XIE, Y., GIANNOBILE, W., BONEWALD, L., CONWAY, S. & FENG, J. 2008. Periostin is essential for the integrity and function of the periodontal ligament during occlusal loading in mice. *Journal of periodontology,* 79**,** 1480-1490.

RITCHIE, R. 1988. Mechanisms of fatigue crack propagation in metals, ceramics and composites: role of crack tip shielding. *Materials Science and Engineering: A,* 103**,** 15-28.

RITCHIE, R. O. 1999. Mechanisms of fatigue-crack propagation in ductile and brittle solids. *International Journal of Fracture,* 100**,** 55-83.

RIZKALLA, A. & JONES, D. 2004. Mechanical properties of commercial high strength ceramic core materials. *Dental materials,* 20**,** 207-212.

ROBERSON, T., HEYMANN, H. O. & SWIFT, E. J. 2006. Sturdevant's art and science of operative dentistry. *USA: Mosby Inc.*

ROMBERG, O. & POPP, K. 1998. Fluid-damping controlled instability in tube bundles subjected to air cross-flow. *Flow, turbulence and combustion,* 61**,** 285-300.

ROMEED, S., FOK, S. & WILSON, N. 2006. A comparison of 2D and 3D finite element analysis of a restored tooth. *Journal of oral rehabilitation,* 33**,** 209-215.

ROSENSTIEL, S. F., LAND, M. F., FUJIMOTO, J. & COCKERILL, J. J. 2006. *Contemporary fixed prosthodontics*, USA: Mosby Inc.

ROSENTRITT, M., BEHR, M., GEBHARD, R. & HANDEL, G. 2006. Influence of stress simulation parameters on the fracture strength of all-ceramic fixed-partial dentures. *Dental Materials,* 22**,** 176-182.

SABBAGH, J., VREVEN, J. & LELOUP, G. 2002. Dynamic and static moduli of elasticity of resin-based materials. *Dental Materials,* 18**,** 64-71.

SADIGHPOUR, L., GERAMIPANAH, F. & RAEESI, B. 2006. In vitro mechanical tests for modern dental ceramics. *Journal of Dentistry of Tehran University of Medical Sciences,* Vol: 3, No.3, 143-152.

SAILER, I., FEHER, A., FILSER, F., GAUCKLER, L., LÜTHY, H. & HÄMMERLE, C. 2007. Five-year clinical results of zirconia frameworks for posterior fixed partial dentures. *The International journal of prosthodontics,* 20(4):383-8.

SAKAGUCHI, R., DOUGLAS, W., DELONG, R. & PINTADO, M. 1986. The wear of a posterior composite in an artificial mouth: a clinical correlation. *Dental Materials,* 2**,** 235-240.

SANCTUARY, C. S., WISKOTT, H. A., JUSTIZ, J., BOTSIS, J. & BELSER, U. C. 2005. In vitro time-dependent response of periodontal ligament to mechanical loading. *Journal of Applied Physiology,* 99**,** 2369-2378.

SANTIUSTE, C., RODRÍGUEZ-MILLÁN, M., GINER, E. & MIGUÉLEZ, H. 2014. The influence of anisotropy in numerical modeling of orthogonal cutting of cortical bone. *Composite Structures,* Vol.116,p.423-431.

SARAFIDOU, K., STIESCH, M., DITTMER, M. P., JÖRN, D., BORCHERS, L. & KOHORST, P. 2012. Load-bearing capacity of artificially aged zirconia fixed dental prostheses with heterogeneous abutment supports. *Clinical oral investigations,* 16**,** 961-968.

SCHAEFER, O., WATTS, D. C., SIGUSCH, B. W., KUEPPER, H. & GUENTSCH, A. 2012. Marginal and internal fit of pressed lithium disilicate partial crowns in vitro: a three-dimensional analysis of accuracy and reproducibility. *Dental Materials,* 28**,** 320-326.

SCHERRER, S. S., DE RIJK, W. G., BELSER, U. C. & MEYER, J. M. 1994. Effect of cement film thickness on the fracture resistance of a machinable glass-ceramic. *Dental Materials,* 10**,** 172-177.

SCHERRER, S. S., QUINN, G. D. & QUINN, J. B. 2008. Fractographic failure analysis of a Procera® AllCeram crown using stereo and scanning electron microscopy. *dental materials,* 24**,** 1107-1113.

SCHERRER, S. S., QUINN, J. B., QUINN, G. D. & WISKOTT, H. A. 2007. Fractographic ceramic failure analysis using the replica technique. *dental materials,* 23**,** 1397-1404.

SCHMALZ, G., FEDERLIN, M. & REICH, E. 1995. Effect of dimension of luting space and luting composite on marginal adaptation of a class II ceramic inlay. *The Journal of Prosthetic Dentistry,* 73**,** 392-399.

SEGAL, B. S. 2001. Retrospective assessment of 546 all-ceramic anterior and posterior crowns in a general practice. *The Journal of Prosthetic Dentistry,* 85**,** 544-550.

SEGHI, R., DAHER, T. & CAPUTO, A. 1990. Relative flexural strength of dental restorative ceramics. *Dental Materials,* 6**,** 181-184.

SHAHRBAF, S., VANNOORT, R., MIRZAKOUCHAKI, B., GHASSEMIEH, E. & MARTIN, N. 2013. Effect of the crown design and interface lute parameters on the stress-state of a machined crown–tooth system: a finite element analysis. *Dental Materials,* 29**,** e123-e131.

SHEARER, B., GOUGH, M. B. & SETCHELL, D. J. 1996. Influence of marginal configuration and porcelain addition on the fit of In-Ceram crowns. *Biomaterials,* 17**,** 1891-1895.

SHEN, J. Z. & KOSMAC, T. 2013. *Advanced Ceramics for Dentistry*, USA: Butterworth-Heinemann, Elsevier Inc.

SHETTY, P., HEGDE, A. M. & RAI, K. 2010. Finite Element Method–An Effective Research Tool for Dentistry. *Journal of Clinical Pediatric Dentistry,* 34**,** 281-285.

SHILLINGBURG, H. T., HOBO, S., WHITSETT, L. D., JACOBI, R. & BRACKETT, S. 2012. *Fundamentals of fixed prosthodontics*, FOURTH EDITION, Quintessence Publishing Co, Inc.

SHINOHARA, N., MINESAKI, Y., MUKOYOSHI, N., MORIYAMA, H. & JIMI, T. 1989. [The effect of the cementing material on the strength of the all ceramic crown]. *Nihon Hotetsu Shika Gakkai zasshi,* 33**,** 416-421.

SILVA, N., BONFANTE, E., RAFFERTY, B., ZAVANELLI, R., REKOW, E., THOMPSON, V. & COELHO, P. 2011. Modified Y-TZP core design improves all-ceramic crown reliability. *Journal of dental research,* 90**,** 104-108.

References

SILVA, N. R. F. A., DE SOUZA, G. M., COELHO, P. G., STAPPERT, C. F. J., CLARK, E. A., REKOW, E. D. & THOMPSON, V. P. 2008. Effect of water storage time and composite cement thickness on fatigue of a glass-ceramic trilayer system. *Journal of Biomedical Materials Research Part B: Applied Biomaterials,* 84**,** 117-123.

SINDEL, J., PETSCHELT, A., GRELLNER, F., DIERKEN, C. & GREIL, P. 1998. Evaluation of subsurface damage in CAD/CAM machined dental ceramics. *Journal of Materials Science: Materials in Medicine,* 9**,** 291-295.

SJÖGREN, G., LANTTO, R. & TILLBERG, A. 1999. Clinical evaluation of all-ceramic crowns (Dicor) in general practice. *The Journal of Prosthetic Dentistry,* 81**,** 277-284.

SOARES, C. J., VERSLUIS, A., VALDIVIA, A. D. C. M., BICALHO, A. A., VERÍSSIMO, C., BARRETO, B. C. F. & ROSCOE, M. G. 2012. Finite Element Analysis in Dentistry - Improving the Quality of Oral Health Care, Finite Element Analysis - From Biomedical Applications to Industrial Developments. (BOOK) InTech Poblisher Inc. : chapter (2); p.25-56 , Availablefrom: http://www.intechopen.com/books/finite-element-analysis-from-biomedical-applications-to-industrial-developments/finite-element-analysis-in-dentistry-improving-the-quality-of-oral-health-care.

SOARES, P. V., SANTOS-FILHO, P. C. F., QUEIROZ, E. C., ARAÚJO, T. C., CAMPOS, R. E., ARAÚJO, C. A. & SOARES, C. J. 2008. Fracture resistance and stress distribution in endodontically treated maxillary premolars restored with composite resin. *Journal of Prosthodontics,* 17**,** 114-119.

SOBRINHO, L. C., CATTELL, M. & KNOWLES, J. 1998. Fracture strength of all-ceramic crowns. *Journal of Materials Science: Materials in Medicine,* 9**,** 555-559.

SÖDERHOLM, K.-J. 2012. Fracture of Dental Materials. [Book]- Applied Fracture Mechanics: InTech Inc. , Chapter - 4 , p. 109-142 .

SORENSEN, J., KANG, S. & AVERA, S. 1991. Porcelain-composite interface microleakage with various porcelain surface treatments. *Dental Materials,* 7**,** 118-123.

SORRENTINO, R., GALASSO, L., TETÈ, S., DE SIMONE, G. & ZARONE, F. 2009. Clinical Evaluation of 209 All-Ceramic Single Crowns Cemented on Natural and Implant-Supported Abutments with Different Luting Agents: A 6-Year Retrospective Study. *Clinical Implant Dentistry and Related Research,* Vol.14(2),p.184-197.

SPEARS, I., VAN NOORT, R., CROMPTON, R., CARDEW, G. & HOWARD, I. 1993. The effects of enamel anisotropy on the distribution of stress in a tooth. *Journal of dental research,* 72**,** 1526-1531.

SPOHR, A., BORGES, G. & PLATT, J. 2013. Thickness of immediate dentin sealing materials and its effect on the fracture load of a reinforced all-ceramic crown. *European Journal of Dentistry,* Vol.7(4),p.474-483.

ST-GEORGES, A. J., STURDEVANT, J. R., SWIFT, E. J. & THOMPSON, J. Y. 2003. Fracture resistance of prepared teeth restored with bonded inlay restorations. *The Journal of Prosthetic Dentistry,* 89**,** 551-557.

STOKES, A. & HOOD, J. 1993. Impact fracture characteristics of intact and crowned human central incisors. *Journal of oral rehabilitation,* 20**,** 89-95.

STURDEVANT, J. R., BAYNE, S. C. & HEYMANN, H. O. 1999. Margin Gap Size of Ceramic Inlays Using Second-Generation CAD/CAM Equipment. *Journal of Esthetic and Restorative Dentistry,* 11**,** 206-214.

SUMER, E. & DEGER, Y. 2011. Contemporary Permanent Luting Agents Used in Dentistry: A Literature Review. *Int Dent Res,* 1**,** 26-31.

SÜMER, E. & DEGER, Y. 2011. Contemporary permanent luting agents used in dentistry: A literature review. *Int Dent Res,* 1**,** 26-31.

SUN, X., WITZEL, E. A., BIAN, H. & KANG, S. 2008. 3-D finite element simulation for ultrasonic propagation in tooth. *Journal of dentistry,* 36**,** 546-553.

SUNDH, A., MOLIN, M. & SJÖGREN, G. 2005. Fracture resistance of yttrium oxide partially-stabilized zirconia all-ceramic bridges after veneering and mechanical fatigue testing. *Dental materials,* 21**,** 476-482.

References

SUZUKI, C., MIURA, H., OKADA, D. & KOMADA, W. 2008. Investigation of stress distribution in roots restored with different crown materials and luting agents. *Dental materials journal,* 27**,** 229-236.

TAJIMA, K., CHEN, K.-K., TAKAHASHI, N., NODA, N., NAGAMATSU, Y. & KAKIGAWA, H. 2009. Three-dimensional finite element modeling from CT images of tooth and its validation. *Dental materials journal,* 28**,** 219-226.

TAN, P. L. B. & DUNNE, J. T. 2004. An esthetic comparison of a metal ceramic crown and cast metal abutment with an all-ceramic crown and zirconia abutment: A clinical report. *The Journal of prosthetic dentistry,* 91**,** 215-218.

THOMASON, J. 2013. On the application of Weibull analysis to experimentally determined single fibre strength distributions. *Composites Science and Technology,* 77**,** 74-80.

THOMPSON, J., ANUSAVICE, K., NAMAN, A. & MORRIS, H. 1994. Fracture surface characterization of clinically failed all-ceramic crowns. *Journal of dental research,* 73**,** 1824-1832.

THOMPSON, J. Y., STONER, B. R., PIASCIK, J. R. & SMITH, R. 2011. Adhesion/cementation to zirconia and other non-silicate ceramics: Where are we now? *Dental Materials,* 27**,** 71-82.

THOMPSON, V. P. & REKOW, D. E. 2004. Dental ceramics and the molar crown testing ground. *Journal of Applied Oral Science,* 12(sp. issue):p. 26-36.

THONGTHAMMACHAT, S., MOORE, B. K., BARCO II, M. T., HOVIJITRA, S., BROWN, D. T. & ANDRES, C. J. 2002. Dimensional accuracy of dental casts: influence of tray material, impression material, and time. *Journal of Prosthodontics,* 11**,** 98-108.

TIAN, K. V., NAGY, P. M., CHASS, G. A., FEJERDY, P., NICHOLSON, J. W., CSIZMADIA, I. G. & DOBÓ-NAGY, C. 2012. Qualitative assessment of microstructure and Hertzian indentation failure in biocompatible glass ionomer cements. *Journal of Materials Science: Materials in Medicine,* Vol.23(3),p.677-685.

TINSCHERT, J., ZWEZ, D., MARX, R. & ANUSAVICE, K. 2000. Structural reliability of alumina-, feldspar-, leucite-, mica-and zirconia-based ceramics. *Journal of Dentistry,* 28**,** 529-535.

TOKSAVUL, S. & TOMAN, M. 2007. A short-term clinical evaluation of IPS Empress 2 crowns. *The International journal of prosthodontics,* 20(2):168-172.

TOMS, S. R. & EBERHARDT, A. W. 2003. A nonlinear finite element analysis of the periodontal ligament under orthodontic tooth loading. *American journal of orthodontics and dentofacial orthopedics,* 123**,** 657-665.

TSITROU, E. A., HELVATJOGLU-ANTONIADES, M. & VAN NOORT, R. 2010. A preliminary evaluation of the structural integrity and fracture mode of minimally prepared resin bonded CAD/CAM crowns. *Journal of dentistry,* 38**,** 16-22.

TSITROU, E. A., NORTHEAST, S. E. & VAN NOORT, R. 2007. Evaluation of the marginal fit of three margin designs of resin composite crowns using CAD/CAM. *Journal of dentistry,* 35**,** 68-73.

TWIGGS, S. W., MACKERT, J. R., OXFORD, A. L., ERGLE, J. W. & LOCKWOOD, P. E. 2005. Isothermal phase transformations of a dental porcelain. *Dental materials,* 21**,** 580-585.

VAN DIJKEN, J., HÖGLUND-ÅBERG, C. & OLOFSSON, A. 1998. Fired ceramic inlays: a 6-year follow up. *Journal of dentistry,* 26**,** 219-225.

VAN DIJKEN, J. W. V., HASSELROT, L., ÖRMIN, A. & OLOFSSON, A. L. 2001. Restorations with extensive dentin/enamel-bonded ceramic coverage. A 5-year follow-up. *European Journal of Oral Sciences,* 109**,** 222-229.

VAN NOORT, R. 2007. *Introduction to dental materials*, Mosby Inc.

VAN OOSTERWYCK, H., DUYCK, J., VANDER SLOTEN, J., VAN DER PERRE, G., DE COOMANS, M., LIEVEN, S. & PUERS, R. 1998. The influence of bone mechanical properties and implant fixation upon bone loading around oral implants. *Clinical oral implants research,* 9**,** 407-418.

VARGAS, M. A., BERGERON, C. & DIAZ-ARNOLD, A. 2011. Cementing all-ceramic restorations Recommendations for success. *The Journal of the American Dental Association,* 142**,** 20S-24S.

VERSLUIS, A. & TANTBIROJN, D. 2009. Relationship between shrinkage and stress. *Dental computing and applications: advanced techniques for clinical dentistry,* " In Clinical Technologies: Concepts, Methodologies, Tools and Applications, page 1374-1392 , available from: http://www.igi-global.com/chapter/relationship-between-shrinkage-stress/53654**,** .

VERSLUIS, A., TANTBIROJN, D., PINTADO, M. R., DELONG, R. & DOUGLAS, W. H. 2004. Residual shrinkage stress distributions in molars after composite restoration. *Dental Materials,* 20**,** 554-564.

VERSLUIS, A. & VERSLUIS-TANTBIROJN, D. 2011. Filling Cavities Or Restoring Teeth? *Journal of the Tennessee Dental Association,* 91(2)36-43.

VIVADENT. & IVOCLAR. 2009. IPS e. max Lithium Disilicate: The Future of All-Ceramic Dentistry—Material Science, Practical Applications, Keys to Success. *Amherst, NY: Ivoclar Vivadent***,** 1-15.

WAGH, A., SINGH, J. & POEPPEL, R. 1993. Dependence of ceramic fracture properties on porosity. *Journal of materials science,* 28**,** 3589-3593.

WAGNER, J., HILLER, K. A. & SCHMALZ, G. 2003. Long-term clinical performance and longevity of gold alloy vs ceramic partial crowns. *Clinical Oral Investigations,* 7**,** 80-85.

WAKABAYASHI, N., ONA, M., SUZUKI, T. & IGARASHI, Y. 2008. Nonlinear finite element analyses: advances and challenges in dental applications. *Journal of dentistry,* 36**,** 463-471.

WALTER, M., WOLF, B., WOLF, A. & BOENING, K. 2006. Six-year clinical performance of all-ceramic crowns with alumina cores. *The International journal of prosthodontics,* 19(2):162-3.

WALTON, T. R. 2002. An up to 15-year longitudinal study of 515 metal-ceramic FPDs: Part 1. Outcome. *The International journal of prosthodontics,* 15(5):439-445.

WANG, W. C., MCDONALD, A., PETRIE, A. & SETCHELL, D. 2007. Interface dimensions of CEREC-3 MOD onlays. *The European journal of prosthodontics and restorative dentistry,* 15(4):183-189.

WEBBER, R., SCHWIEBERT, K. & CATHEY, G. 1981. A technique for placement of calcium hydroxide in the root canal system. *The Journal of the American Dental Association,* 103**,** 417-421.

WHITE, S., MIKLUS, V., MCLAREN, E., LANG, L. & CAPUTO, A. 2005. Flexural strength of a layered zirconia and porcelain dental all-ceramic system. *The Journal of prosthetic dentistry,* 94**,** 125-131.

WHITE, S. & YU, Z. 1993a. Physical properties of fixed prosthodontic, resin composite luting agents. *The International journal of prosthodontics,* 6(4):384-389.

WHITE, S. N. & YU, Z. 1993b. Compressive and diametral tensile strengths of current adhesive luting agents. *The Journal of Prosthetic Dentistry,* 69**,** 568-572.

WILLIAMS, R., BIBB, R., EGGBEER, D. & COLLIS, J. 2006. Use of CAD/CAM technology to fabricate a removable partial denture framework. *The Journal of prosthetic dentistry,* 96**,** 96-99.

WIMMER, T., ERDELT, K. J., RAITH, S., SCHNEIDER, J. M., STAWARCZYK, B. & BEUER, F. 2014. Effects of Differing Thickness and Mechanical Properties of Cement on the Stress Levels and Distributions in a Three-Unit Zirconia Fixed Prosthesis by FEA. *Journal of Prosthodontics,* Vol.23(5),p.358-366.

WISKOTT, H. W., NICHOLLS, J. & BELSER, U. 1994. Stress fatigue: Basic principles and prosthodontic implications. *The International journal of prosthodontics,* 8**,** 105-116.

WOLF, D., POWERS, J. & O'KEEFE, K. 1993. Bond strength of composite to etched and sandblasted porcelain. *American Journal of Dentistry,* 6(3):155-158.

WOLFART, S., LUDWIG, K., UPHAUS, A. & KERN, M. 2007. Fracture strength of all-ceramic posterior inlay-retained fixed partial dentures. *Dental materials,* 23**,** 1513-1520.

WOLFART, S., WEGNER, S. M., AL-HALABI, A. & KERN, M. 2003. Clinical evaluation of marginal fit of a new experimental all-ceramic system before and after cementation. *The International journal of prosthodontics,* 16**,** 587.

References

XU, H., SMITH, D., JAHANMIR, S., ROMBERG, E., KELLY, J., THOMPSON, V. & REKOW, E. 1998. Indentation damage and mechanical properties of human enamel and dentin. *Journal of dental research,* 77**,** 472-480.

YAMANEL, K., ÇAGLAR, A., GÜLSAHI, K. & ÖZDEN, U. A. 2009. Effects of different ceramic and composite materials on stress distribution in inlay and onlay cavities: 3-D finite element analysis. *Dental materials journal,* 28**,** 661-670.

YANG, H. S., LANG, L. A., MOLINA, A. & FELTON, D. A. 2001. The effects of dowel design and load direction on dowel-and-core restorations. *The Journal of Prosthetic Dentistry,* 85**,** 558-567.

YEO, I. S., YANG, J. H. & LEE, J. B. 2003. In vitro marginal fit of three all-ceramic crown systems. *The Journal of prosthetic dentistry,* 90**,** 459-464.

YETTRAM, A., WRIGHT, K. & PICKARD, H. 1976. Finite element stress analysis of the crowns of normal and restored teeth. *Journal of dental research,* 55**,** 1004-1011.

YILDIRIM, M., FISCHER, H., MARX, R. & EDELHOFF, D. 2003. In vivo fracture resistance of implant-supported all-ceramic restorations. *The Journal of prosthetic dentistry,* 90**,** 325-331.

YILDIZ, C., VANLıOĞLU, B. A., EVREN, B., ULUDAMAR, A. & KULAK-OZKAN, Y. 2013. Fracture Resistance of Manually and CAD/CAM Manufactured Ceramic Onlays. *Journal of Prosthodontics,* 22**,** 537-542.

YILMAZ, H., AYDIN, C. & GUL, B. E. 2007. Flexural strength and fracture toughness of dental core ceramics. *The Journal of prosthetic dentistry,* 98**,** 120-128.

YOSHIDA, K., MORIMOTO, N., TSUO, Y. & ATSUTA, M. 2004. Flexural fatigue behavior of machinable and light-activated hybrid composites for esthetic restorations. *Journal of Biomedical Materials Research Part B: Applied Biomaterials,* 70**,** 218-222.

YUNMAO, X. J. L. W. L. & JUKUN, Z. J. S. 2008. Microdiffraction Measurements of Natural Tooth by High Resolution X-ray Diffraction Equipment. *Journal of Biomedical Engineering,* 25(1):65-68.

ZAHRAN, M., EL-MOWAFY, O., TAM, L., WATSON, P. A. & FINER, Y. 2008. Fracture Strength and Fatigue Resistance of All-Ceramic Molar Crowns Manufactured with CAD/CAM Technology. *Journal of Prosthodontics,* 17**,** 370-377.

ZARONE, F., APICELLA, D., SORRENTINO, R., FERRO, V., AVERSA, R. & APICELLA, A. 2005a. Influence of tooth preparation design on the stress distribution in maxillary central incisors restored by means of alumina porcelain veneers: a 3D-finite element analysis. *Dental Materials,* 21**,** 1178-1188.

ZARONE, F., SORRENTINO, R., VACCARO, F., RUSSO, S. & SIMONE, G. 2005b. Retrospective Clinical Evaluation of 86 Procera AllCeram™ Anterior Single Crowns on Natural and Implant-Supported Abutments. *Clinical Implant Dentistry and Related Research,* 7**,** s95-s102.

ZHANG, Y., SAILER, I. & LAWN, B. R. 2013. Fatigue of dental ceramics. *Journal of dentistry,* 41**,** 1135-1147.

ZHAO, J., PLATT, J. A. & XIE, D. 2009. Characterization of a novel light-cured star-shape poly (acrylic acid)-composed glass-ionomer cement: fluoride release, water sorption, shrinkage, and hygroscopic expansion. *European journal of oral sciences,* 117**,** 755-765.

ZIDAN, O. & FERGUSON, G. C. 2003. The retention of complete crowns prepared with three different tapers and luted with four different cements. *The Journal of Prosthetic Dentistry,* 89**,** 565-571.

ZORZIN, J., PETSCHELT, A., EBERT, J. & LOHBAUER, U. 2012. pH neutralization and influence on mechanical strength in self-adhesive resin luting agents. *Dental Materials,* Vol.28(6),p.672-679.